

# Otto S. Wolfbeis: List of Major Publications (with Graphical Abstracts)

**ORCID:** <https://orcid.org/0000-0002-6124-2842>  
**Google Scholar:** <https://scholar.google.com/citations?hl=en&user=pJlFf1IAAAA>  
**ResearchGate:** [https://www.researchgate.net/profile/Otto\\_Wolfbeis](https://www.researchgate.net/profile/Otto_Wolfbeis)  
**ResearcherID:** [www.researcherID.com/rid/D-2855-2009](http://www.researcherID.com/rid/D-2855-2009)  
**Publons:** <https://publons.com/researcher/1702959/otto-s-wolfbeis/>  
**Wikipedia:** [https://en.wikipedia.org/wiki/Otto\\_S.\\_Wolfbeis](https://en.wikipedia.org/wiki/Otto_S._Wolfbeis)  
**Figures of merit (Google.Scholar; as per 19-Nov-2021):**

	All	Since 2016
Citations	~ 47,500	~ 16,500
h-index	113	56

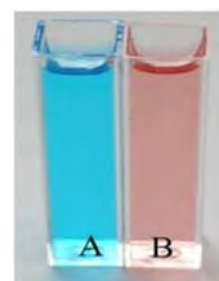
**Web:** <https://www.uni-regensburg.de/chemistry-pharmacy/analytical-chemistry/former-members/retired-professors/index.html>



## 610. *Topical Review: Fluorescent Chameleon Labels for Bioconjugation and Imaging of Proteins, Nucleic Acids, Biogenic Amines and Surface Amino Groups. A Review.* O. S. Wolfbeis; *Methods & Appl. Fluorescence* (2021), vol. 9, paper number 042001. DOI:

10.1088/2050-6120/ac1a0a. Journal IF: 3.1.

**Abstract:** Chameleon labels (ChLs) possess the unique property of changing (visible) color and fluorescence on binding to amino groups of biomolecules. Some ChLs react with primary aliphatic amino groups such as those in lysine or with amino groups artificially introduced into polynucleic acids or saccharides, while others also react with secondary amino groups. Under controlled circumstances, the reactions are fairly specific. The review is subdivided into the following sections: (1) An introduction and classification of fluorescent labels; (2) pyrylium labels that undergo shortwave color changes upon labelling, typically from blue to red; (3) cyanine type of labels (that also undergo shortwave color changes, typically from green to blue); (4) various other (less common) ChLs; (5) hemocyanine labels that undergo longwave color changes, typically from yellow to purple; (6) the application of various ChLs to labeling of proteins and amino-modified saccharides and oligonucleotides; (7) applications in fluorometric assays and sensing; (8) in fluorescence imaging of biomolecules; (9) in studies on affinity interactions (receptor-ligand binding); (10) in surface and interface chemistry; and (11) in chromatography, electrophoresis and isotachopheresis of biomolecules. This review cites 108 references.

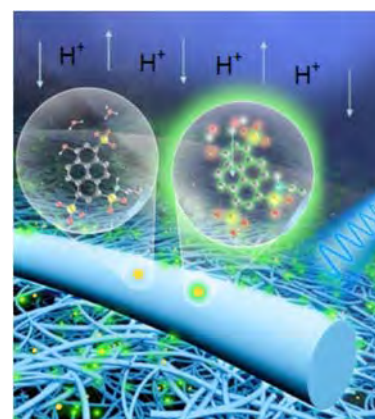


Colors of solutions of label Py-1 (A) and of Py-1-stained human serum albumin (B).

## 609. *Review: Optical Sensing and Imaging of pH Values: Spectroscopies, Materials and Applications.* A. Steinegger, O. S. Wolfbeis, S. M. Borisov; *Chem. Reviews* (2020) 120(22) 12357 - 12489. DOI: 10.1021/acs.chemrev.0c00451. Journal IF:

54.3.

**Abstract:** This is the first comprehensive review on methods and materials for use in optical sensing of pH values, and on applications of such sensors. The Review starts with an introduction that contains subsections on the definition of the pH value, a brief look back on optical methods for sensing of pH, on the effects of ionic strength on pH values and pKa values, on the selectivity, sensitivity, precision, dynamic ranges and temperature dependence of such sensors. Commonly used optical sensing schemes are covered in a next main chapter, with subsections on methods based on absorptiometry, reflectometry, luminescence, refractive index, surface plasmon resonance, photonic crystals, turbidity, mechanical displacement, interferometry and solvatochromism. This is followed by sections on absorptiometric and luminescent molecular probes for use pH in sensors. Further large sections cover polymeric hosts and supports, and methods for immobilization of indicator dyes. Further and more specific sections summarize the state of the art in materials with dual functionality (indicator and host), nanomaterials, sensors based on upconversion and 2-photon absorption, multiparameter sensors, imaging, and sensors for extreme pH values. A chapter on the many sensing formats has subsections on planar, fiber optic, evanescent wave, refractive index, surface plasmon resonance and holography based sensor designs, and on distributed sensing. Another section summarizes selected applications in areas such as medicine, biology, oceanography, bioprocess monitoring, corrosion studies, on the use of pH sensors as transducers in biosensors and chemical sensors, and their integration into flow-injection analyzers, microfluidic devices and lab-on-a-chip systems. An extra section is devoted to current challenges, with subsections on challenges of general nature and those of specific nature. A concluding chapter gives an outlook on potential future trends and perspectives.



## 608. *Review: Non-Invasive Electrochemical Sensors and Biosensors Targeting Salivary Biomarkers.* V. Mani, T. Beduk, W. Khushaim, A. E. Ceylan, S. Timu, O. S. Wolfbeis, K. N. Salama; *Trends Anal. Chem. (TrACH)* (2021), 135, paper # 116164. DOI: 10.1016/j.trac.2020.116164. Journal IF: 9.8.

**Abstract:** The analysis of salivary markers has grown into a promising non-invasive route for easy, safe, and pain-free biomedical monitoring and has the potential to change the existing way of clinical diagnosis, management, and treatment. Therefore, the interest in saliva as a diagnostic fluid has advanced rapidly in recent years. Advancements in sensing technology, the arrival of novel materials, and the innovative electrode fabrication methods, and accuracy in sampling have recently made significant progress in this field and strongly establishing saliva as a potential alternative fluid resource for traditional blood analysis. The attractive features of saliva analysis are the ease and convenience, samples can be collected readily and more frequently, with less stress on the patient, without piercing the body. In addition, salivary sensing can be easily coupled with in-vitro, in-situ, and POC diagnostic sensors. Saliva contains wide

varieties of biomarkers that are useful to detect chronic and infectious diseases. Early-stage detection of cancer, diabetes, Alzheimer's, neurodegenerative diseases, infectious diseases and chronic stress disorders are possible by detecting their corresponding biomarkers levels in saliva.

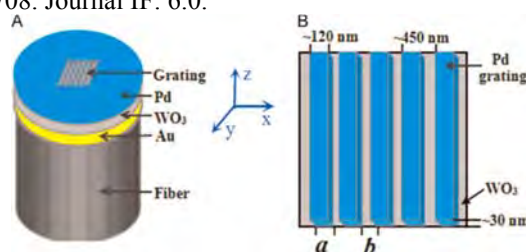
Besides, it is a most appropriate biological fluid for scientific investigations concerning drug abuse ethics. Sialochemistry has promising applicability in toxicology and forensic medicine for analyzing and detecting user drug addiction and alcohol abuse by simply mapping the saliva data. This will enable authorities to make quick decisions on criminal cases, and compare salivary data with blood data to provide more accurate and timely judgments. Electrochemical sensors are the most suitable analytical method for simple, fast and cost-effective analysis of saliva biomarkers in POC. This review, with 520 refs., discusses the scope of electroanalytical techniques in monitoring salivary analytes, broadly divided into three sections; (1) The salivary analytes, their correlation with blood, and their electrochemical detection approaches are presented. (2) The acute and chronic diseases that can be detected by electrochemical salivary analysis are discussed. (3) The salivary drug analysis is discussed. Finally, the technical advancements in making advanced electrochemical sensors and biosensors are discussed.

The table shows representative analytes and their relevant concentration ranges in saliva and blood.

Analyte	Conc. in Saliva	Conc. in Blood
Glucose	70 – 88 $\mu\text{M}$	3.9 – 7.1 mM
Creatinine	5.3 – 18 $\mu\text{M}$	74 – 107 $\mu\text{M}$
Urea	6.5 – 11 mM	2.5 to 7.1 mM
Uric acid	199 – 240 $\mu\text{M}$	202 – 428 $\mu\text{M}$ (men) 143 – 363 $\mu\text{M}$ (women)
Nitrite	130 - 220 $\mu\text{M}$	50 – 100 nM
pH value	6.2 – 7.6	7.1 – 7.5
Lactate	0.1 – 2.5 mM	0.5 – 2.2 mM (venous) 0.1 – 1.6 mM (arterial)
Potassium	2.6 – 18.5 mM	3.6 - 5.2 mM

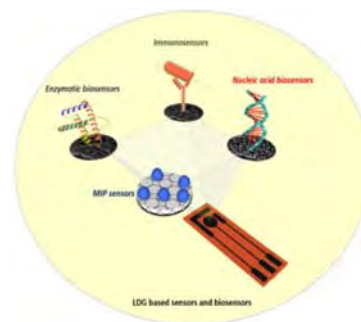
**607. Review: Fiber Optic Chemical Sensors and Biosensors (2015-2019): A Review.** X.-D. Wang, O. S. Wolfbeis, *Anal. Chem. (Wash.)*, (2020), 92, 397-430. DOI: 10.1021/acs.analchem.9b04708. Journal IF: 6.0.

This review covers work on fiber optic chemical sensors and biosensors (FOCS) published in the time between October 2015 and October 2019 and is written in continuation of previous reviews. The focus is on chemical sensors and biosensors for defined chemical, environmental, or biochemical species, on spectroscopic detection schemes, and on new materials for analyte recognition and signal transduction. The figure on the right shows a schematic of a fast-response fiber optical sensor for hydrogen. The tip of the fiber carries a nanostructured Pd-grating and layers of gold and  $\text{WO}_3$  that change color and optical reflectivity upon exposure to a few ppm of hydrogen gas. From H. Yan et al.; *Opt. Commun.* (2016).



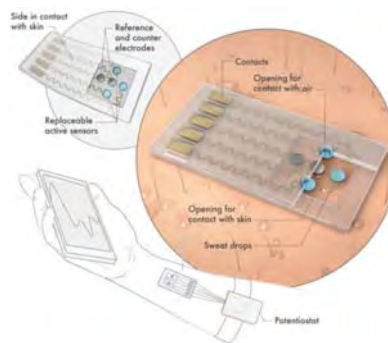
**606. Review: Electrochemical Sensors and Biosensors Using Laser-Derived Graphene: A Comprehensive Review.** A. A. Lahcen, S. Rauf, T. Beduk, C. Durmus, A. Aljedaibi, S. Timur, H. N. Alshareef, A. Amine, O. S. Wolfbeis, K. N. Salama; *Biosensors & Bioelectronics* (2020) 168, 112565. DOI: 10.1016/j.bios.2020.112565. Journal IF: 10.3.

**Abstract:** Laser-derived graphene (LDG) technology is gaining attention as a novel platform for electrochemical sensors and biosensors. Compared to established methods for graphene synthesis, LDG provides many advantages such as cost-effectiveness, fast electron mobility, mask free and green synthesis, good electrical conductivity, porosity, mechanical stability and large surface area. This review discusses, in a critical way, recent advancements in this field. First, we focus on the fabrication and doping of LDG platforms using different strategies. Next, the techniques for the modification of LDG sensors using nanomaterials, conducting polymers, biological receptors and artificial receptors are presented. We then describe the advances achieved for various LDG sensing and biosensing schemes and their applications in the fields of environmental monitoring, food safety, and clinical diagnosis..



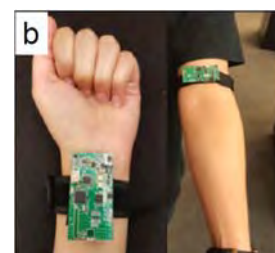
**605. A MXene-Based Wearable Biosensor System for High-Performance In-Vitro Perspiration Analysis.** Y. Lei, W. Zhao, Y. Zhang, Q. Jiang, J. He, A. J. Baeumner, O. S. Wolfbeis, Z. L. Wang, K. N. Salama, H. N. Alshareef, *Small* (2019) 1191190. DOI: 10.1002/smll.201901190. Journal IF: 9.6.

**Abstract:** Wearable electrochemical biosensors for sweat analysis present a promising means for noninvasive biomarker monitoring. A stretchable, wearable, and modular multifunctional biosensor is developed, incorporating a novel MXene/Prussian blue ( $\text{Ti}_3\text{C}_2\text{T}_x/\text{PB}$ ) composite designed for durable and sensitive detection of biomarkers (e.g., glucose and lactate) in sweat. Furthermore, an implemented solid-liquid-air three-phase interface design leads to superior sensor performance and stability. Typical electrochemical sensitivities of  $35.3 \mu\text{A mm}^{-1} \text{cm}^{-2}$  for glucose and  $11.4 \mu\text{A mm}^{-1} \text{cm}^{-2}$  for lactate are achieved using artificial sweat. During in vitro perspiration monitoring of human subjects, the signals (glucose and lactate level) can be measured simultaneously with high sensitivity and good repeatability. This approach represents an important step toward the realization of ultrasensitive enzymatic wearable biosensors for personalized health monitoring.



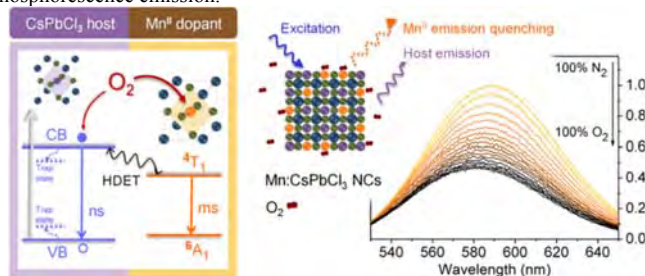
**604. KAUSTat: A Wireless, Wearable, Open-Source Potentiostat for Electrochemical Measurements.** R. Ahmad, S. G. Surya, J. B. Sales, H. Mkaouar, S. Y. C. Catunda, D. R. Belfort, Y. Lei, Z. L. Wang, A. J. Baeumner, O. S. Wolfbeis, H. N. Alshareef, K. N. Salama. *2019 IEEE Sensors (Montreal, Canada; 27-30 Oct. 2019)*, pp. 1-4. DOI: 10.1109/SENSOR43011.2019.8956815.

**Abstract:** Potentiostats used in laboratories are heavy, non-portable, and expensive. To fill this void, we introduce KAUSTat, a wireless, wearable, open-source potentiostat. The KAUSTat device interfaces with a smartphone to generate cyclic voltammetry curves using a Bluetooth Low Energy (BLE) protocol. Experiments with buffer and hexacyanoferrate solutions were conducted to assess the efficiency of the device. The results generated by KAUSTat are in agreement with those of the commercial potentiostat Emstat. Considering wireless and wearable features of KAUSTat, it represents a convenient portable device for on-site sensing with low-power requirements.



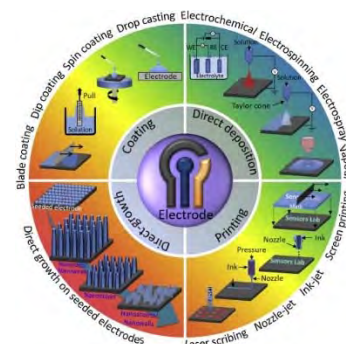
**602. Mn(II)-Doped Cesium Lead Chloride Perovskite Nanocrystals: Demonstration of Oxygen Sensing Capability Based on Luminescent Dopants and Host-Dopant Energy Transfer.** F. Lin, F. Li, Z. Lai, Z. Cai, Y. Wang, O. S. Wolfbeis, X. Chen. *ACS Appl. Mat. Interfaces* (2018), 10, 23335-23343. DOI: 10.1021/acscami.8b06329. Journal IF: 8.5.

**Abstract:** We demonstrate the O<sub>2</sub> sensing capability of Mn(II)-doped CsPbCl<sub>3</sub> nanocrystals (Mn:CsPbCl<sub>3</sub> NCs) and reveal the role of O<sub>2</sub> on the optical de-excitation of such perovskite nanocrystals (PNCs). By adjusting the amount and distribution of Mn(II) dopants, as well as the host-dopant energy transfer (HDET) process in PNCs, we highlight that O<sub>2</sub> can reversibly quench the Mn(II) emission due to their temporarily disturbance to the ligand field of near-surface dopants in PNCs. In the phosphorescence mode, the PL of the NCs is quenched by 53% on going from 0 to 100% of O<sub>2</sub>. The Stern-Volmer plot is linear in the 0-12% O<sub>2</sub> concentration range. High sensing reversibility and rapid signal response are also achieved. In our perception, the mechanism study makes these PNCs well suited as optical probes for O<sub>2</sub>, and it is enlightening to explore more possibilities of the inherent O<sub>2</sub> sensing based on semiconductor doped-NCs (not restricted to Mn-doped PNCs) with phosphorescence emission.



**601. Review: Deposition of Nanomaterials: A Crucial Step in Biosensor Fabrication.** R. Ahmad, O. S. Wolfbeis Y.-B. Hahn, H. Alshareef, L. Torsi, K. N. Salama. *Materials Today Comm.*, (2018), 17, 289-321. DOI: 10.1016/j.mtcomm.2018.09.024. Journal IF: 9.9.

**Abstract:** Biosensor development includes the deposition of nanomaterials onto a sensor surface. This is a crucial step for obtaining improved performance. Various methods have been used to create a successful matrix of nanomaterials that warrant proper contact between the material and sensor surface. The purpose of nanomaterial deposition is to provide a high surface area to improve the performance of biosensors by supporting the stable immobilization of enzymes in a more significant quantity as well as enhancing the catalytic or bioaffinity features. In this review (with 431 refs.), we summarize the methods used for nanomaterial deposition onto an electrode surface for efficient biosensor fabrication. An optimized nanomaterial deposition method is also crucial for the mechanical stability and fabrication reproducibility of electrodes when designing a suitable biosensing device. In addition, we discuss the challenges faced during biosensor application as well as prospects for superior deposition methods.



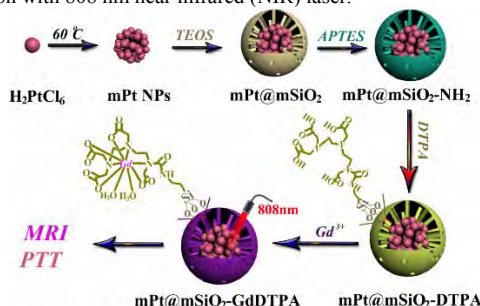
**599. Double-Mesoporous Core-Shell Nanosystems Based on Platinum Nanoparticles Functionalized with Lanthanide Complexes for In-vivo Magnetic Resonance Imaging and Photothermal Therapy.** L. Zhao, X. Ge, G. Yan, X. Wang, P. Hu, L. Shi, O. S. Wolfbeis, H. Zhang, L. Sun; *Nanoscale* (2017), 9(41), 16012-16023. DOI: 10.1039/C7NR04983H. Journal IF: 7.4.

**Abstract:** A double-mesoporous nanosystem was synthesized for treating as well as imaging cancer cells by using a simple and mild method. The mesoporous platinum (Pt) nanoparticles acting as core show excellent photothermal effect under illumination with 808 nm near infrared (NIR) laser.

The mesoporous silica linked with lanthanide (Gd) complex acting as shell display potential applications as contrast agents for magnetic resonance imaging (MRI). The final mPt@mSiO<sub>2</sub>-GdDTPA nanosystems are biocompatible, both in vitro and in vivo, as demonstrated by the thiazolyl tetrazolium assay and histological and serum biochemistry analysis. The mPt@mSiO<sub>2</sub>-GdDTPA nanosystems exhibit excellent photothermal therapy effect on HeLa cells and tumor-bearing mice. As theranostic agents, the nanosystems display higher r1 value than the medical contrast agent gadovist and were successfully applied to in vivo MRI for Kunming mice.

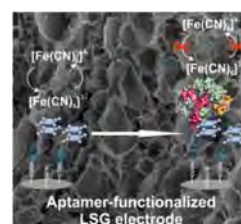
Therefore, the first systematic study on photothermal effect of nanosystems based on mesoporous Pt nanoparticles does encourage the potential applications of metal nanoparticles and hybrid nanocomposites for cancer bioimaging and therapy.

The graph on the right shows a schematic of the synthesis of a meso-Pt@mSiO<sub>2</sub>-GdDTPA nanosystem, and its application in in-vivo magnetic resonance imaging (MRI) and photothermal therapy (PTT)



**598. Laser-Scribed Graphene Electrodes for Aptamer-Based Biosensing.** C. Fenzl, P. Nayak, T. Hirsch, O. S. Wolfbeis, H. N. Alshareef, A. J. Baeumner; *ACS Sensors* (2017), 2, 616-620. DOI: 10.1021/acssensors.7b00066. Journal IF: 7.7.

**Abstract:** Graphene as a transducer material has produced some of the best-performing sensing approaches to date opening the door toward integrated miniaturized all-carbon point-of-care devices. Addressing this opportunity, laser-scribed graphene (LSG) electrodes are demonstrated here as highly sensitive and reliable biosensor transducers in blood serum analysis. These flexible electrodes with large electrochemical surface were fabricated using a direct-write laser process on polyimide foils. A universal immobilization approach is established by anchoring 1-pyrenebutyric acid to LSG and subsequently covalently attaching an aptamer against the coagulation factor thrombin as an exemplary bioreceptor to the carboxy groups. The resulting biosensor displays an extremely low detection limit of 1 pM in buffer, and of 5 pM in serum.

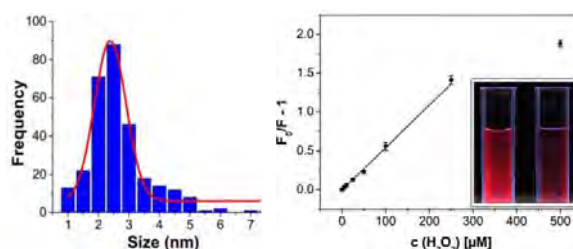


**597. Europium-doped GdVO4 Nanocrystals as a Luminescent Probe for Hydrogen Peroxide and for Enzymatic Sensing of Glucose.** V. Muhr, M. Buchner, T. Hirsch, D. J. Jovanović, S. D. Dolić, M. D. Dramićanin, O. S. Wolfbeis;



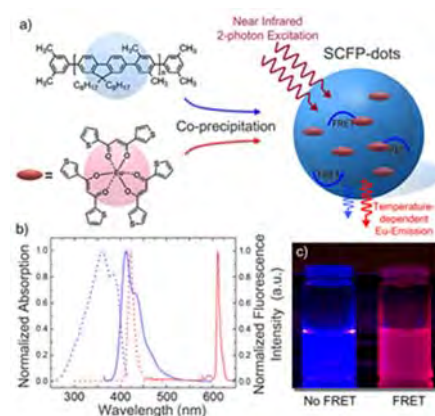
**Sensors Actuat., B: Chemical (2017), 241, 349-356.** DOI: 10.1016/j.snb.2016.10.090. Journal IF: 6.4.

**Abstract.** The authors describe the preparation of  $\text{Eu}^{3+}$ -doped  $\text{GdVO}_4$  nanocrystals (NCs) by precipitation of the  $\text{Gd}^{3+}(\text{Eu}^{3+})$ -citrate complex which was then converted to the respective vanadate by dialysis. The fractions of  $\text{Eu}^{3+}$  ranged from 5 to 100 mol%. The NCs were characterized by XRD, TEM, ICP-OES and dynamic light scattering which revealed that they possess superior colloidal stability in aqueous solutions in that no precipitation can be observed even after several months. The NCs display red and largely red-shifted fluorescence (peaking at 618 nm) on photoexcitation at around 300 nm. Fluorescence is strongly quenched by hydrogen peroxide. It is also shown that the fraction of doping with  $\text{Eu}^{3+}$  strongly affects quenchability. Most efficient quenching by  $\text{H}_2\text{O}_2$  is observed if the NCs are doped with 50% of  $\text{Eu}^{3+}$ . The findings were exploited to develop a fluorometric assay for  $\text{H}_2\text{O}_2$  that works in the 5 to 250  $\mu\text{M}$  concentration range, with a limit of detection as low as 1.6  $\mu\text{M}$  (at a signal-to-noise ratio of 3). The probe was further employed to design a highly sensitive enzymatic assay for glucose via measurement of the quantity of  $\text{H}_2\text{O}_2$  formed as a result of the catalytic action of glucose oxidase.



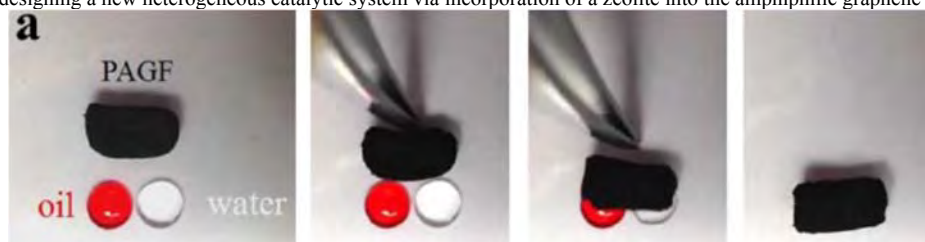
**596. Two-Photon Excitation Temperature Nanosensors Based on a Conjugated Fluorescent Polymer Doped with a Europium Probe.** X.-D. Wang, R. J. Meier, M. Schaeferling, S. Bange, J. M. Lupton, M. Sperber, J. Wegener, V. Ondrus, U. Beifuss, U. Henne, C. Klein, O. S. Wolfbeis; *Adv. Opt. Mat.* (2016), 4, 1854-1859. DOI: 10.1002/adom.201600601. Journal IF: 6.8.

**Abstract.** A strongly fluorescent organic semiconducting polymer doped with a highly temperature dependent europium(III) complex was converted into a nanosized material that is capable of optically sensing temperature (T) in the range from 0 to 50 °C via two-photon excitation at 720 nm. The nanosensors were prepared from a blue-fluorescent polyfluorene that acts as both a light-harvesting antenna (to capture two-photon energy) and an energy donor in a FRET system. The photonic energy absorbed by the polymer is transferred to the T-sensitive red-luminescent europium complex contained in the nanoparticles. The close spatial proximity of the donor and the acceptor warrants efficient FRET. A poly(ethylene glycol)-co-poly(propylene oxide) block copolymer was also added to render the particles biocompatible. We show that T can be calculated from (a) the intensity of the luminescence of the europium complex, (b) the ratio of the intensities of the red and blue luminescence, or (c) the T-dependent luminescence lifetime of the Eu(III) complex.



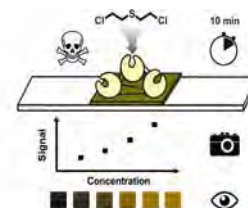
**595. A Phytic Acid-Induced Super-Amphiphilic Multifunctional 3D Graphene Foam.** X. Song, Y. Chen, M. Rong, Z. Xie, T. Zhao, Y. Wang, X. Chen, O. S. Wolfbeis; *Angew. Chem. Intl. Ed.* (2016), 55, 3936-3941. DOI: 10.1002/anie.201511064. Journal IF: 11.8.

**Abstract.** It is generally believed that 3D graphenes are monoliths with strongly hydrophobic surfaces. Here, we demonstrate the preparation of a 3D superamphiphilic (i.e., a highly hydrophilic and oleophilic) graphene assembly in a single-step using phytic acid acting as a gelator and as a dopant. The product shows both hydrophilic and oleophilic intelligence, which overcomes the drawbacks of presently known hydrophobic 3D graphene assemblies. The utility of the new material was demonstrated by designing a new heterogeneous catalytic system via incorporation of a zeolite into the amphiphilic graphene scaffold. This multifunctional bulk network enables high-performance epoxidation of alkene without addition of a co-solvent or stirring. Besides, the bulk amphiphilic catalyst can be conveniently recovered and steadily reused, thereby providing a clean catalytic process with simplified work-up. The Figures shows photos of the side-by-side simultaneous adsorption (from left to right) of water and oil by the phytic acid-graphene foam (PAGF) presented here.



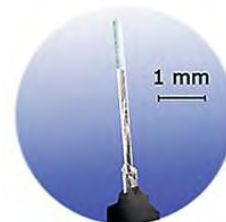
**594. Enzyme Based Test Stripes for Visual or Photographic Detection and Quantitation of Gaseous Sulfur Mustard.** S. Bidmanova, M. S. Steiner, M. Stepan, K. Vymazalova, M. A. Gruber, A. Duerkop, J. Damborsky, Z. Prokop, O. S. Wolfbeis; *Anal. Chem. (Wash.)* (2016), 88, 6044-6049. DOI: 10.1021/acs.analchem.6b01272. Journal IF: 5.9.

**Abstract.** The article describes a test stripe for rapid detection of sulfur mustard (SM) by either visual read-out, or RGB-based digital photography. The detection scheme is based on the use of the enzyme haloalkane dehalogenase that hydrolyzes SM to form protons. The decrease in local pH value is indicated by a pH sensitive dye contained in the stripe whose color changes from blue to yellow.



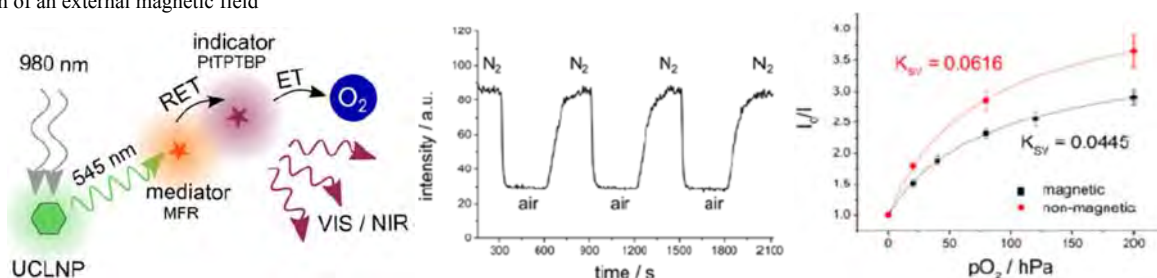
593. **Review: Fiber Optic Chemical Sensors and Biosensors (2013 – 2015).** X.-D. Wang, O. S. Wolfbeis, *Anal. Chem. (Wash.)*, (2016), 88, 203-227. DOI: 10.1021/acs.analchem.5b04298. Journal IF: 5.8

**Abstract.** High-quality optical fibers can be produced now at a low cost and large quantity, and this has rapidly promoted the development of fiber optic (chemical) sensors. After over 30 years of innovation, fiber optic sensing technology has become more mature and popular because of acceptable costs, compact instrumentation, high accuracy and the capability of performing measurements at inaccessible sites, over large distances, in strong magnetic fields and in harsh environment. However, the technology is proceeding quickly in terms of innovation, and respective applications have been found in highly diversified fields. This review covers respective work published in the time period between December 2012 and November 2015, and is written in continuation of previous reviews.



592. **Composite Particles with Magnetic Properties, Near-Infrared Excitation, and Far-Red Emission for Luminescence-Based Oxygen Sensing.** E. Scheucher, S. Wilhelm, O. S. Wolfbeis, T. Hirsch, T. Mayr, *Microsyst. Nanoeng.* (2016), vol. 1, 15026. DOI: 10.1038/micronano.2015.26. Open access.

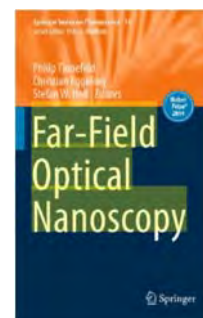
**Abstract:** Oxygen sensing, magnetic and upconversion luminescence properties are combined in multi-functional composite particles prepared herein by a simple mixing, baking and grinding procedure. Upconverting nanocrystals are used as an excitation source and an oxygen indicator with far-red emission. The composite particles are excited with near infrared laser light (980 nm). The visible upconversion emission is converted into an oxygen concentration-dependent far-red emission (< 750 nm) using an inert mediator dye and a platinumated benzoporphyrin dye. This concept combines the advantages of NIR excitation and far red emissive indicator dyes, offering minimized auto-fluorescence and enhanced membrane permeability. Additional functionality is obtained by incorporating magnetic nanoparticles into the composite particles, which enables easy manipulation and separation of the particles by the application of an external magnetic field



591. **Book Series Editor: Far-Field Optical Nanoscopy.** P. Tinnefeld, C. Eggeling, S. W. Hell (eds.). *Springer Series on Fluorescence*, vol. 14, 2015 (O. S. Wolfbeis, Series Ed.); 298 pp. ISBN: 978-3-662-45546-3 (print); 978-3-662-45547-0 (on-line).

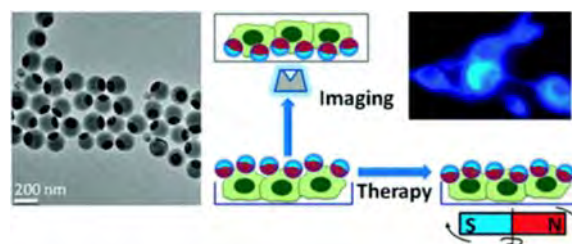
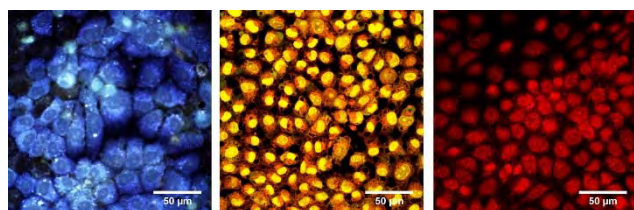
Also contains chapters written by the 2014 Nobel Prize awardees S. W. Hell and W. E. Moerner.

**Abstract:** This book describes developments in the field of super-resolution fluorescence microscopy or nanoscopy. In 11 chapters, distinguished scientists and leaders in their respective fields describe different nanoscopy approaches, various labeling technologies, and concrete applications. The topics covered include the principles and applications of the most popular nanoscopy techniques STED and PALM/STORM, along with advances brought about by fluorescent proteins and organic dyes optimized for fluorescence nanoscopy. Furthermore, the photophysics of fluorescent labels is addressed, specifically for improving their photoswitching capabilities. Important applications are also discussed, such as the tracking and counting of molecules to determine acting forces in cells, and quantitative cellular imaging, respectively, as well as the mapping of chemical reaction centers at the nano-scale.



590. **Review: An Overview of Nanoparticles Commonly Used in Fluorescent Bioimaging.** O. S. Wolfbeis, *Chem. Soc. Rev.* (2015), 44, 4743-4768. DOI: 10.1039/c4cs00392f. Open access. Journal IF: 33.4.

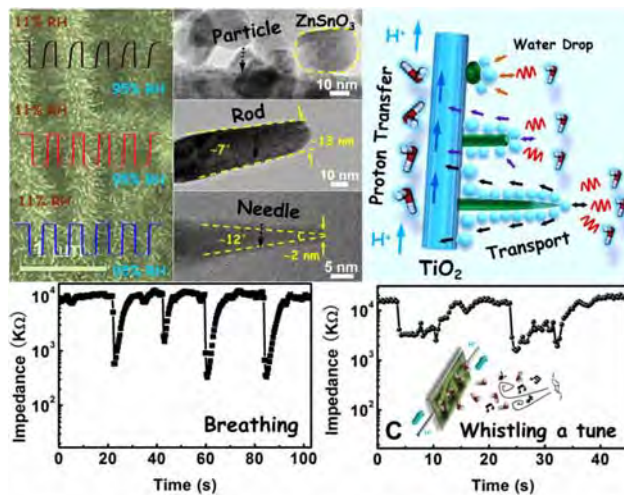
**Abstract:** The article gives an overview on the various kinds of nanoparticles (NPs) that are widely used for purposes of fluorescent imaging, mainly of cells and tissue. Following an introduction and a discussion of merits of fluorescent NPs compared to molecular fluorophores, labels and probes, the article assesses the kinds and specific features of nanomaterials often used in bioimaging. These include fluorescently doped silicas and sol-gels, hydrophilic polymers (hydrogels), hydrophobic organic polymers, semiconducting polymer dots, quantum dots, carbon dots, other carbonaceous nanomaterials, upconversion NPs, noble metal NPs (mainly gold and silver), various others nanomaterials, and dendrimers. Another section covers coatings and methods for surface modification of NPs. Next, examples are given on the use of nanoparticles in (a) plain fluorescence imaging of cells, (b) targeted imaging, (c) imaging of chemical species, and (d) imaging temperature. A final section covers aspects of multimodal imaging (for example fluorescence/nmr), imaging combined with drug and gene delivery, or imaging combined with therapy or diagnosis. A *Supporting Information* gives specific examples for materials and methods used in imaging, sensing, multimodal imaging and theranostics such as imaging combined with drug delivery or photodynamic therapy. The article contains 270 references in the main part, and 157 references in the *Supporting Information*. The graph on the left shows cell images obtained by using carbon dots, and how the wavelength of excitation affects the color of luminescence. The graph on the right shows blue fluorescent nanobeads made from poly(styrene-*b*-allyl alcohol) and labeled with pyrene. They possess a magnetic core and can be applied to fluorescent imaging of imaging cancer cells (top) and, simultaneously, to magnetically induced heat lysis of cell membranes.





**589. Rational Tailoring of ZnSnO<sub>3</sub>-TiO<sub>2</sub> Heterojunctions with Bioinspired Surface Wettability for High-Performance Humidity Nanosensors.** Z. Zhang, J. Huang, B. Dong, Q. Yuan, Y. He, O. S. Wolfbeis. *Nanoscale* (2015), 7, 4149-4155. DOI: 10.1039/c4nr07559e. Journal IF: 7.4

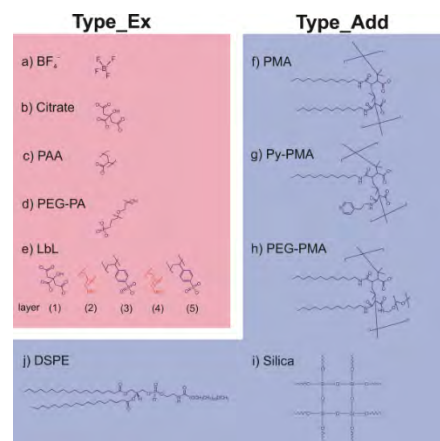
**Abstract:** We have developed a novel kind of branched heterostructures by hydrothermal growth of the ZnSnO<sub>3</sub> nanostructures on TiO<sub>2</sub> electrospun nanofibers, and demonstrate enhanced sensing of relative humidity (RH) through sequential tailoring ZnSnO<sub>3</sub> nanostructures inspired by the cactus. Combining with the first-principles calculations, it is deduced that the quantity of adsorbed water molecules can be increased on the ZnSnO<sub>3</sub>-TiO<sub>2</sub> heterojunction surface by reducing the surface potential barrier. The bioinspired ZnSnO<sub>3</sub> nanoneedles, acting like branches on the heterostructures, can further boost their adsorption abilities for water molecules via a water-collection process. The adsorbed water molecules at the tips of the ZnSnO<sub>3</sub> nanoneedles quickly desorb at a lower humidity environment due to the small area of the tips (1.5 to 2.5 nm). Thus, the optimal ZnSnO<sub>3</sub>-TiO<sub>2</sub> heterostructures exhibit fast response and recovery times (of ~2.5 s and ~3 s, respectively). Its good sensitivity may enable it to detect tiny fluctuations in the RH surrounding any high-precision instrumentation.



**588. Water Dispersible Upconverting Nanoparticles: Effects of Surface Modification on Luminescence and Colloidal Stability.** S. Wilhelm, M. Kaiser, C. Würth, J. Heiland, C. Carrillo-Carrion, V. Muhr, O. S. Wolfbeis, W. J. Parak, U. Resch-Genger, T. Hirsch, *Nanoscale* (2015), 7, 1403-1410. DOI: 10.1039/c4nr05954a. Journal IF: 7.4

We present a systematic study on the effect of surface ligands on the luminescence properties and colloidal stability of  $\beta$ -NaYF<sub>4</sub>:Yb,Er upconversion nanoparticles (UCNPs), comparing nine different surface coatings to render these UCNPs water-dispersible and bioconjugatable. A prerequisite for this study was a large-scale synthetic method that yields ~2 g per batch of monodisperse oleate-capped UCNPs providing identical core particles. These ~23-nm sized UCNPs display an upconversion quantum yield of ~0.35% when dispersed in cyclohexane and excited with a power density of 150 W cm<sup>-2</sup>. A comparison of the colloidal stability and luminescence properties of these UCNPs, subsequently surface-modified with ligand exchange or encapsulation protocols, revealed that the ratio of the green (545 nm) and red (658 nm) emission bands determined at a constant excitation power density depends on the surface chemistry. We demonstrate that the brightness of the upconverted luminescence is strongly affected by the type of surface modification, i.e., ligand exchange or encapsulation, yet hardly by the chemical nature of the ligand.

The *Scheme at the right* gives an overview of strategies for surface modification of oleate-coated UCNPs. The modifications can be classified into two categories: (a) - (e) ligand exchange methods (type\_Ex); (f) - (j): addition of an amphiphilic layer or silica coating (type\_Add).



**587. Review: Luminescent Sensing and Imaging of Oxygen: Fierce Competition to the Clark Electrode.** O. S. Wolfbeis, *Bioessays* (2015) 37(8), 921-928. DOI: 10.1002/bies.201500002. Journal IF: 4.7. Open access.

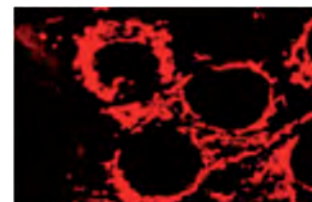
**Abstract:** Luminescence-based sensing schemes for oxygen have experienced a fast growth and are in the process of replacing the Clark electrode in many fields. Unlike electrodes, sensing is not limited to point measurements via fiber optic microsensors, but includes additional features such as planar sensing, imaging and intracellular assays using nanosized sensor particles. This essay discusses, in layman's terms, (a) the common solid-state sensor approaches based on the use of indicator dyes and host polymers; (b) fiber optic and planar sensing schemes as well as nanoparticle-based intracellular sensing; and (c) common spectroscopies. Optical sensors also are capable of multiple simultaneous sensing (such as O<sub>2</sub> and temperature). Sensors for O<sub>2</sub> are produced nowadays in large quantities. Fields of application include plant and animal physiology, clinical chemistry, marine sciences, the chemical industry and process biotechnology.



Optoelectronic system containing an RSB port (left) and a fiber connector (right) for fiber optic decay time-based sensing of O<sub>2</sub>.



Schematic of the state of the art in imaging O<sub>2</sub>. Left: PC with software and for display. Center: Handheld portable instrument for lifetime imaging. Red film: Sensor membrane incorporating a quenchable luminescent probe for O<sub>2</sub> to be placed on the object of interest (a bioreactor, or skin, or an aircraft, etc.; symbolized by a cube)



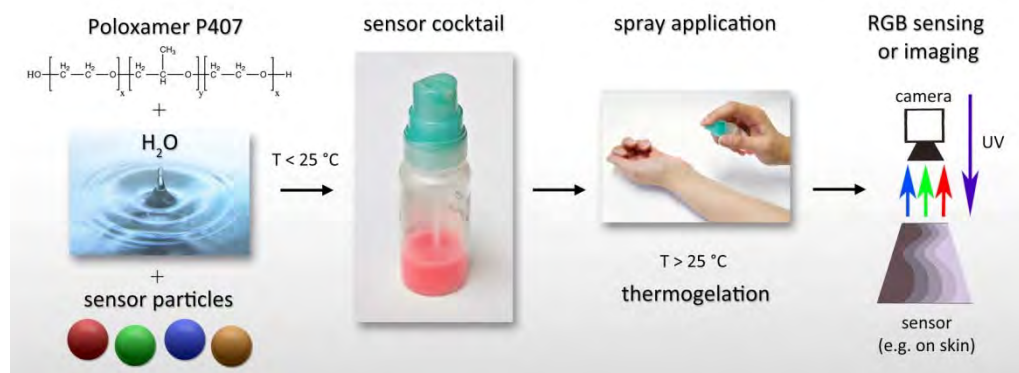
Imaging of mitochondrial O<sub>2</sub> in cells using sensor NPs. Pictures are comparable to those obtained with a mitotracker but luminescence intensity depends on local pO<sub>2</sub>

**586. A Water-sprayable, Thermogelating and Biocompatible Polymer Host for Use in Fluorescent Chemical Sensing and Imaging of Oxygen, pH Values and Temperature.** X. Wang, R. J. Meier, C. Schmittlein, S. Schreml, M. Schäferling, O. S. Wolfbeis; *Sensors & Actuat., B: Chem.* (2015), 221, 37-44. DOI: 10.1016/j.snb.2015.05.082. journal IF: 4.1.

**Abstract:** We report on the use of a sprayable and thermogelating biomaterial (Pluronic™; a.k.a. Pluronic™) in optical imaging of pH values, local oxygen and temperature (T). The material is highly biocompatible and easy to handle. We also show that the material is well permeable to oxygen (thus making it a good choice for use in oxygen sensors), and is stable in liquid solution and at elevated T. We demonstrate its applicability in optical sensors for oxygen, pH values and T. This was accomplished by incorporating appropriate luminescent probes in various kinds of microparticles (which act as hosts for the probes and prevent dye leaching and aggregation), and then dispersing the microparticles in the thermogelating polymer. The resulting sensor gels were deposited on the surface of interest via spraying at T's of <20 °C. At these T's, the gels adhere well to the target, even on uneven surfaces such as skin, wounds, and

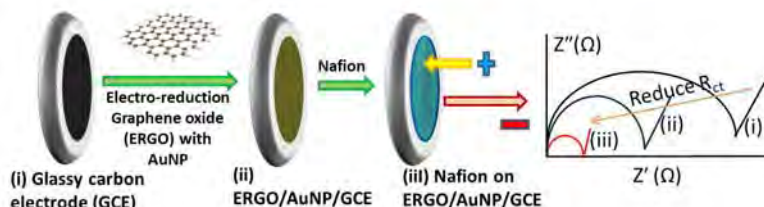
bacterial cultures.

If T is risen to above 25 °C, the gels form a thin and soft but solid sensing layer which, however, can be removed from surface of interest by cooling and wiping it off, or by washing with water. Sprayable thermogelating sensors present obvious advantages over other sensors by not causing damage to the surface of interest. In our perception, the sensing materials also have wide further applicability in sensors for other species including clinically relevant gases, enzyme substrates (such as glucose or lactate) and ions



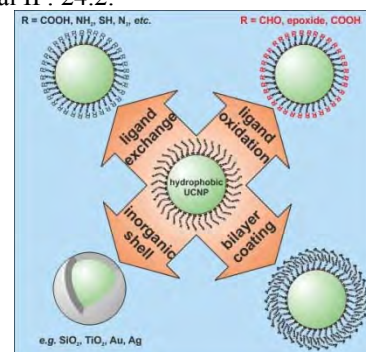
**585. Review: Nanomaterial-based Electrochemical Sensing of Neurological Drugs and Neurotransmitters.** B. J. Sanghavi, O. S. Wolfbeis, T. Hirsch, N. S. Swami; *Microchim. Acta* (2015), 182, 1-41. DOI: 10.1007/s00604-014-1308-4. Open access.

Journal IF: 3.7. **Abstract:** Nanomaterial-modified detection systems represent a chief driver towards the adoption of electrochemical methods, since nanomaterials enable functional tunability, ability to self-assemble, and novel electrical, optical and catalytic properties that emerge at this scale. This results in tremendous gains in terms of sensitivity, selectivity and versatility. We review the electrochemical methods and mechanisms that may be applied in the detection of neurological drugs. We focus on understanding how specific nano-sized modifiers may be applied to influence the electron transfer event to result in gains in sensitivity, selectivity and versatility of the detection system. Specific sections are dedicated to electrodes based on the carbon materials, supporting electrolytes, and on electrochemical detection paradigms for neurological drugs and neurotransmitters. We finally discuss emerging trends and future challenges such as the development of strategies for simultaneous detection of multiple targets with high spatial and temporal resolutions, the integration of microfluidic strategies for analyte preconcentration, the real-time monitoring of neurotransmitter secretions from active cell cultures under electro- and chemotactic cues, aptamer-based biosensors, and the miniaturization of the sensing system for detection in small sample volumes and for enabling cost savings due to manufacturing scale-up. The Supp. Information includes a list of the key properties of the analytes, viz.  $pK_a$  values, half-life of drugs and their electro-chemical mechanisms. It also defines analytical figures of merit of the drugs and neurotransmitters. The review contains 198 references in the main manuscript and 207 references in the Supp. Information.



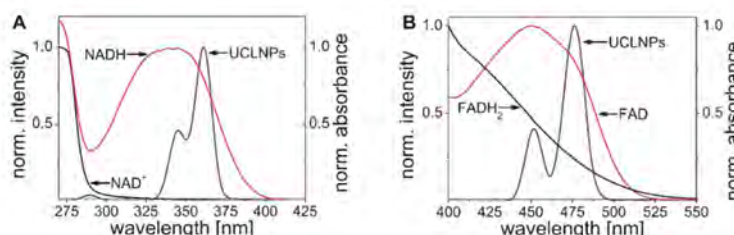
**584. Review: Upconversion Nanoparticles: From Hydrophobic to Hydrophilic Surfaces.** V. Muhr, S. Wilhelm, T. Hirsch, O. S. Wolfbeis; *Acc. Chem. Res.* (2014), 47, 3481–3493. DOI: 10.1021/ar500253g. Journal IF: 24.2.

**Abstract:** Photon upconverting nanoparticles (UCNPs) have emerged as a promising new class of nanomaterials due to their capability of converting near-IR light into visible luminescence. Unfortunately, most methods for preparing UCNPs yield hydrophobic materials, but water-dispersibility is needed in the We additionally address the need for (a) a better control of particle size and homogeneity during synthesis, (b) more reproducible methods for surface loading and/or modification, (c) synthetic methods yielding higher yields of UCNPs, (d) materials displaying higher quantum yields in water solution without the need for tedious surface modifications), (e) improved methods for work-up (including the suppression of aggregation), (f) new methods for surface characterization, and (g) more affordable reagents for use in surface modification. It is noted that most synthetic research in the area is of the trial-and-error kind, presumably due to the lack of an understanding of the mechanisms causing current limitations. Finally, all particles are discussed in terms of their biocompatibility (as far as data are available) which is quintessential in terms of imaging, the largest field of application. The article contains 98 references.



**583. Spectrally Matched Upconverting Luminescent Nanoparticles for Monitoring Enzymatic Reactions.** S. Wilhelm, M. del Barrio, J. Heiland, S. F. Himmelstoss, J. Galbán, O. S. Wolfbeis, T. Hirsch; *ACS Appl. Mat. Interf.* (2014), 6, 15427-15433. DOI: 10.1021/am5038643. Journal IF: 5.0.

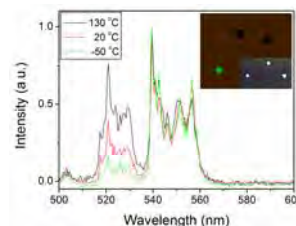
**Abstract:** We report on upconverting luminescent nanoparticles (UCLNPs) that are spectrally tuned such that their emission matches the absorption bands of the two most important species associated with enzymatic redox reactions. The core-shell UCLNPs consist of a hexagonal NaYF<sub>4</sub> core doped with Yb(III) and Tm(III) ions, and a shell of undoped hexagonal NaYF<sub>4</sub>. Upon 980-nm excitation, they display emission bands peaking at 360 nm and 475 nm which is a perfect match to the absorption bands of the enzyme cosubstrate NADH and the coenzyme FAD, respectively. By exploiting these spectral overlaps, we have designed fluorescent detection schemes for NADH and FAD that are based on the modulation of the emission intensities of UCLNPs by FAD and NADH via an inner filter effect. The Figures below show the normalized upconversion luminescence spectra of hydrophilic hexagonal NaYF<sub>4</sub>:Yb,Tm@NaYF<sub>4</sub> core-shell particles dispersed in MES buffer, and the overlap with the absorption bands of NADH (left) and FAD (right)





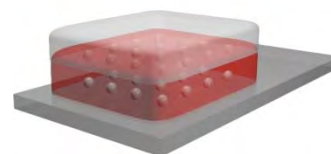
**582. Size Dependence of the Upconverted Luminescence of NaYF<sub>4</sub>:Er,Yb Microspheres for Use in Ratiometric Thermometry.** B. Dong, R. N. Hua, B. S. Cao, Z. P. Li, Y. Y. He, O. S. Wolfbeis; *PhysChemChemPhys* (2014) 16, 20009-20012. DOI: 10.1039/C4CP01966K. Journal IF: 4.2.

**Abstract:** We report on the size dependence of the upconversion luminescence of temperature (*T*)-sensitive particles of the type NaYF<sub>4</sub>:Er,Yb with a size between 0.7 and 2 μm that have been prepared by a poly(acrylic acid)-assisted hydrothermal process. It is found that the fluorescence intensity ratio of their green upconversion emissions (with peaks at 521 and 539 nm) is strongly size-dependent at *T*'s between 223 and 403 K. If the size of the spheres is increased from 0.7 to 1.6 μm, the slope of the sensitivity to *T* strongly decreases. This effect is mainly attributed to the larger specific surface area of the smaller spheres where relatively more Er(III) ions are located at the surface. It also shows that sensing *T* by this method is prone to error unless particles sizes are well controlled. The Figure shows the upconversion emission spectra at 223 K, 293 K and 403 K.



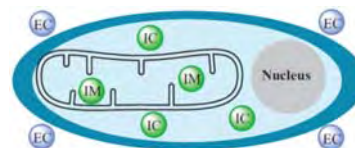
**581. Photonic Crystal Based Sensing and Imaging of Potassium Ions.** C. Fenzl, M. Kirchinger, T. Hirsch, O. S. Wolfbeis, *Chemosensors (Basel)* (2014), 2, 207-218. DOI: 10.3390/chemosensors2030207. Journal IF: 2.9. *Open access.*

**Abstract:** We report on a method for selective optical sensing and imaging of potassium ion using a sandwich assembly composed of layers of photonic crystals and an ion-selective membrane. This represents a new scheme for sensing ions in that an ionic strength-sensitive photonic crystal hydrogel layer is combined with a K<sup>+</sup>-selective membrane. The latter consists of plasticized poly(vinyl chloride) doped with the the K<sup>+</sup>-carrier valinomycin. The film has a red color if immersed into plain water, but appears green in 5 mM KCl and purple at KCl concentrations of 100 mM or higher. This 3D PhC sensor responds to K<sup>+</sup> ions in the 1 to 50 mM concentration range (which includes the K<sup>+</sup> concentration range encountered in blood) and shows high selectivity over ammonium and sodium ions. Sensors films were also imaged with a digital camera by exploiting the RGB technique. The Figure gives a cross-section of the sensor layer. A microscope glass slide forms the bottom. It is first covered with a wet polyacrylamide film containing polystyrene nanoparticles. The top layer consists of a potassium-selective plasticized PVC membrane firmly attached to the PAA film. The sample containing K<sup>+</sup> ions is placed on the top layer.



**580. Targetable Phosphorescent Oxygen Nanosensors for the Assessment of Tumor Mitochondrial Dysfunction by Monitoring Respiratory Activity.** X. Wang, H. Peng, L. Yang, F. You, F. Teng, L. Hou, O. S. Wolfbeis; *Angew. Chem. Intl. Ed.*, (2014) 53, 12471-12475. DOI: 10.1002/anie.201405048. Journal IF: 11.3.

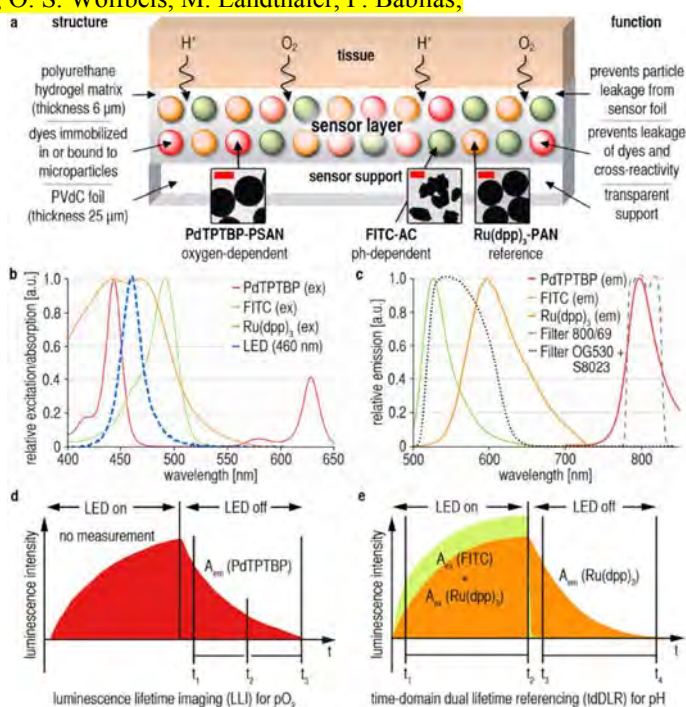
**Abstract:** Most oxygen sensing strategies merely report extracellular (*ec*-) or intracellular (*ic*-) oxygen rather than intra-mitochondrial (*im*-) oxygen. The latter is much desired however, particularly in diagnosis of subtle mitochondrial dysfunction. We are presenting a method to assess tumor mitochondrial dysfunction (by comparison to healthy cells) by using three kinds of luminescent nanosensors for oxygen. Targeted sensing is accomplished by proper modification of the surface of the polystyrene nanoparticles with either silica (for *ec*-oxygen), polylysine (*ic*-oxygen), or triphenylphosphonium groups (for *im*-oxygen). This strategy enables targeted placement of the nanoprobes so that they can respond to *ec*-, *ic*-, and *im*-oxygen, respectively. Time-resolved luminescence is applied to determine the respective oxygen consumption rates (OCRs) under varying respiratory conditions. The results demonstrate that mitochondria in tumor cells are distinctly less active than those of healthy cells, which is interpreted in terms of both restrained glucose utilization and physically impaired mitochondria in tumor cells. The figure shows a schematic of the placement of the 3 targetable nanosensors inside a cell.



**579. Luminescent Dual Sensors Reveal Extracellular pH-Gradients and Hypoxia on Chronic Wounds that Disrupt Epidermal Repair.** S. Schreml, R. J. Meier, M. Kirschbaum, O. S. Wolfbeis, M. Landthaler, P. Babilas; *Theranostics* (2014), 4, 721-735. DOI: 10.7150/thno.9052. Journal IF: 7.8. *Open Access.*

**Abstract:** We are presenting a method to simultaneously image extracellular wound pH and oxygenation in-vivo. It is based on hydrogel-based biocompatible luminescent dual sensor foils doped with pH-responsive and oxygen-responsive microparticles, respectively. The sensor foils were placed on wounds, and fluorescence images were acquired by two kinds of lifetime imaging (td-DLR and LLI). The pH-gradients were identified as governors of cell proliferation. Simultaneous imaging of oxygen also revealed marked hypoxia, albeit with no correlating gradient in oxygen partial pressure. pH-gradients in chronic wounds of humans are predominantly generated via centrifugally increasing pH-regulatory expression of Na<sup>+</sup>/H<sup>+</sup>-exchanger-1. The study has implications in terms of cell science where spatial variations of pH play key roles, e.g. in tumor growth. The article includes 3 supplementary movies.

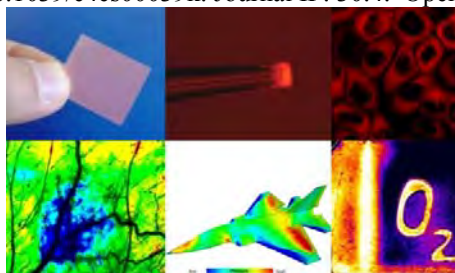
The Fig. shows how dual maging is performed. (A) Sensor foil scheme with (i) oxygen-dependent Pd(II)-meso-tetraphenyl-tetrazobenzoporphyrin in poly(styrene-co-acrylonitrile) particles (Pd-TPTBP-PSAN), (ii) pH-sensitive fluorescein bound to aminocellulose particles (FITC-AC), and (iii) the pH-independent reference dye Ru(dpp)<sub>3</sub> in oxygen-impermeable polyacrylonitrile particles. The particles are embedded in a polyurethane hydrogel matrix on a poly(vinylidene chloride) (PVdC) support. The insets show transmission electron microscopic pictures. (B,C) Excitation spectra and emission (em) spectra of the sensor particles using a 460-nm light emitting diode. (D,E) Detection schemes for pO<sub>2</sub> (by luminescence lifetime imaging) and pH (via time-domain dual lifetime referencing).





**578. Review: Optical Methods for Sensing and Imaging Oxygen: Materials, Spectroscopies and Applications.** X. Wang, O. S. Wolfbeis; *Chem. Soc. Rev.* (2014), 43, 3666-3761. DOI: 10.1039/c4cs00039k. Journal IF: 30.4. Open access.

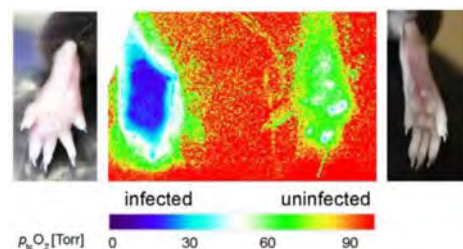
**Abstract:** We review the current state of optical methods for sensing oxygen. These have become a powerful alternative to electrochemical detection and are in the process of replacing the Clark electrode in many fields. The article (with 693 refs.) is divided into main sections on direct spectroscopic sensing of oxygen, on absorptiometric and luminescent probes, on polymeric matrices and supports, on additives and related materials, on spectroscopic schemes for read-out and imaging, and on sensing formats (such as waveguide sensing, sensor arrays, multiple sensors and nanosensors). We finally discuss future trends and applications and summarize the properties of the most often used indicator probes and polymers. A Supporting Information (with 385 refs.) gives a selection of applications of such sensors in medicine, biology, marine and geosciences, in intracellular sensing, aerodynamics, industry and biotechnology, among others.



**576. Hypoxia in *Leishmania major* Skin Lesions Impairs the NO-Dependent Leishmanicidal Activity of Macrophages.** A. Mahnke, R. J. Meier, V. Schatz, J. Hofmann, K. Castiglione, U. Schleicher, O. S. Wolfbeis, C. Bogdan, J. Jantsch; *J. Invest. Dermatol.* (2014), 134, 2339-2346. DOI: 10.1038/jid.2014.121. journal IF: 5.5.

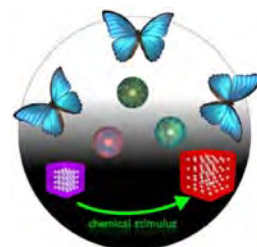
**Abstract:** We analyzed the oxygen levels found in leishmanial skin lesions and their effect on the NOS2-dependent leishmanicidal activity of macrophages. Mice were infected with *Leishm. major* in the footpad and cutaneous oxygen tensions ( $pO_2$ ) were assessed with optical sensors. Macrophages were analyzed for their leishmanicidal activity and NO release under different atmospheric  $pO_2$ . When L.-lesions reached their maximum size, the tissue  $pO_2$  was low. Macrophages activated under these conditions failed to produce sufficient amounts of NO in order to clear *L. major*. Killing was restored when the macrophages were re-oxygenated or exposed to a NO-donor. It is concluded that the low oxygen levels found at sites of *L. major* infection impair the NOS2-dependent leishmanicidal activity of macrophages. Oxygen may be an underestimated local factor participating in the persistence of *Leishmania*.

For a *Commentary* on this article (entitled *The Virtues of Oxygenation: Low Tissue Oxygen Adversely Affects the Killing of Leishmania*), see: L. M. Das, K. Q. Lu, *J. Invest. Dermatol.* (2014) 134, 2303-2305; DOI: 10.1038/jid.2014.232; [www.nature.com/jid/journal/v134/n9/abs/jid2014232a.html](http://www.nature.com/jid/journal/v134/n9/abs/jid2014232a.html)



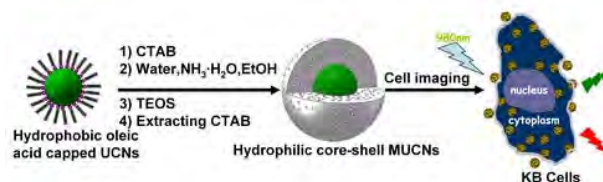
**575. Review: Photonic Crystals for Chemical Sensing and Biosensing.** C. Fenzl, T. Hirsch, O. S. Wolfbeis; *Angew. Chem. Intl. Ed.* (2014) 53, 3318-3335. DOI: 10.1002/anie.201307828. Journal IF: 11.3.

**Abstract:** This review covers the photonic crystal (PhC) technology as used for purposes of sensing of mainly chemical and biochemical parameters, with a particular focus on the materials applied. Specific sections cover (a) a lead-in into natural and synthetic photonic nano-architectures, (b) the various kinds of structures of PhCs, (c) reflection and diffraction in PhCs, (d) aspects of sensing based on mechanical, thermal, optical, electrical, magnetic and purely chemical stimuli, (e) aspects of biosensing based on biomolecules incorporated into PhCs, and (f) current trends and limitations of such sensors. Contains 215 references.



**574. Direct Formation of Mesoporous Upconverting Nanoparticles for Bioimaging of Living Cells.** T. Liu, L. Sun, Y. Qiu, J. Liu, F. Li, L. Shi, O. S. Wolfbeis; *Microchim. Acta* (2014), 181, 775-782. DOI: 10.1007/s00604-013-1073-9. journal IF: 3.7.

**Abstract:** We describe a single-step method for the synthesis of mesoporous upconverting nanoprobe (MUCNs) of the type  $NaYF_4:Yb,Er@mSiO_2$ , with the mesoporous and assisted by CTAB which serve as both phase transfer assistant agents and pore-generating templates. With effective emission upon 980-nm light excitation and low cytotoxicity according to the thiazolyltetrazolium assay, the MUCNs can be applied to image human nasopharyngeal epidermal carcinoma cells in-vitro via laser scanning upconversion luminescence microscopy. silica directly encapsulating the hydrophobic upconversion nanoparticles



**572. Tyrosine-Specific Sequential Labeling of Proteins.** G. B. Cserép, A. Herner, O. S. Wolfbeis, P. Kele; *Bioorg. Med. Chem. Lett.* (2013), 23, 5776-5778. DOI: 10.1016/j.bmcl.2013.09.002. journal IF: 2.3.

**Abstract:** We report (a) on the synthesis of a long-wavelength fluorescent coumarin containing an azido group, (b) the synthesis of two linkers containing an allyloxy acetate and an alkyne function, respectively, and (c) the selective modification of tyrosine in human serum albumin by a sequential method involving Pd(II)-catalyzed modification of the tyrosine hydroxy group with an alkyne linker group, this followed by an azide-alkyne click reaction with the coumarin. The method is likely to be applicable to various kinds of azido-modified fluorophores, and the Pd(II)-catalyzed modification of the tyrosine hydroxy group also may be used to introduce other kinds of tags. With these reagents, fluorescent modulation of Tyr-containing proteins and peptides becomes possible either directly or in a sequential manner.

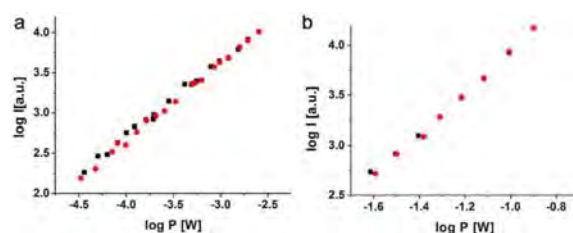
**570. Editorial: Probes, Sensors, Labels: Why is Real Progress Slow?** O. S. Wolfbeis; *Angew. Chem. Intl. Ed.* (2013), 52, 9864-9865. DOI: 10.1002/anie.201305915. Journal IF: 13.7.

This *Editorial* takes a critical look at recent progress in the development of molecular probes, sensors, and labels. The lack of true sensors is obvious, and one may ask why we still have so few sensors for continuous(!) monitoring of at least the most significant healthcare parameters (such as glucose) or environmental parameters such as heavy metal ions.

**569. Imaging of Cellular Oxygen via Two-Photon Excitation of Fluorescent Sensor Nanoparticles.** X. Wang, D. E. Achatz, C. Hupf, Sperber, J. Wegener, S. Bange, J. M. Lupton, O. S. Wolfbeis; *Sensors & Actuat., B (Chem.)* (2013), 188, 257-262. DOI: 10.1016/j.snb.2013.06.087. journal IF: 3.8.

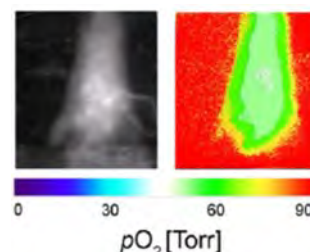
**Abstract:** Polystyrene nanoparticles (PSNPs) with an average size of 85 nm and loaded with an oxygen-quenchable luminescent ruthenium complex were used to image oxygen inside cells following 2-photon excitation (2-PE). The ruthenium probe possesses a large 2-photon absorption cross-section, and 2-PE is achieved by irradiation in the near infrared with fs-pulsed laser systems.

The luminescence of the dye-loaded PSNPs is strongly quenched by oxygen, and Stern-Volmer plots are linear for both conventional 1-PE and for 2-PE. The particles are readily taken up by mammalian cells (MCF-7), presumably via membrane mediated pathways. The 2-PE is considered to be advantageous over conventional imaging techniques because it works in the near-infrared where background absorption and luminescence of biomatter is much weaker than at excitation wavelengths of <600 nm. The Fig. shows double-logarithmic plots of laser power versus emission intensity of the oxygen probe Ru(dpp). Plot (a): excitation via single-photon absorption; the slope is 0.95. Plot (b): excitation via 2-PE (slope 2.04).



**568. Ratiometric Luminescence 2D In-vivo Imaging and Monitoring of Mouse Skin Oxygenation.** J. Hofmann, R. J. Meier, A. Mahnke, V. Schatz, F. Brackmann, R. Trollmann, C. Bogdan, G. Liebsch, X. Wang, O. S. Wolfbeis, J. Jantsch; *Meth. Appl. Fluoresc. (London)* (2013) 1, 045002. DOI: 10.1088/2050-6120/1/4/045002. journal IF: 2.3.

**Abstract:** Tissue oxygenation plays a critical role in the pathogenesis of various diseases, but non-invasive, robust and user-friendly methods for its measurement in vivo still need to be established. Here, we are presenting an in vivo oxygen-detection system that uses ratiometric luminescence imaging (RLI) as a readout scheme to determine the skin oxygen tension of mouse hind footpads via side-by-side comparison with more established techniques including luminescence-lifetime imaging using planar sensor films and the polarographic electrode as the gold standard. We also demonstrate that this technology allows the detection of changes in mouse skin tissue oxygenation induced by subjecting mice to systemic hypoxia. The data demonstrate oxygen imaging based on RLI to be a most useful tool for reliably and easily analyzing and monitoring skin tissue oxygenation in vivo. This technology will advance our understanding of local regulation of skin tissue oxygenation in various disease conditions.



**567. Review: Luminescent Probes and Sensors for Temperature.** X. Wang, R. J. Meier, O. S. Wolfbeis; *Chem. Soc. Rev.* (2013), 42, 7834-7869. DOI: 10.1039/c3cs60102a. Open access. Journal IF: 24.9.

**Abstract:** Temperature ( $T$ ) is the most fundamental parameter in science. Respective sensors also are widely used in daily life. Besides conventional thermometers, optical sensors are considered to be attractive alternatives in sensing and on-line monitoring of  $T$ . This review focuses on all kinds of luminescent probes and sensors for measurement of  $T$  and summarizes the recent progress in their design and application formats. In the introduction, we cover the significance of optical probes for  $T$ , the origin of their  $T$ -dependent spectra, and the various detection modes. This is followed by a survey on (a) molecular probes, (b) nanomaterials, and (c) bulk materials for sensing  $T$ , a discussion of polymeric matrices for immobilizing probes and an overview on the various application formats of  $T$ -sensors. The review closes with a discussion on the prospects, challenges, and new directions in the design of new probes and sensors. 248 references.



**566. Ultra-Small, Highly Stable, and Membrane-Impermeable Fluorescent Nanosensors for Oxygen.** X. Wang, J. A. Stolwijk, M. Sperber, R. J. Meier, J. Wegener, O. S. Wolfbeis; *Meth. Appl. Fluoresc. (IOP Publ.; London)* (2013), 1, 035002 (7 pp). DOI: 10.1088/2050-6120/1/3/035002.

**Abstract:** We report on the preparation of ultra-small fluorescent nanosensors for oxygen via a one-pot approach. The nanoparticles have a hydrophobic core capable of firmly hosting hydrophobic luminescent oxygen probes. Their surface is composed of a dense and long-chain poly(ethylene glycol) shell, which renders them cell-membrane impermeable but yet highly sensitive to oxygen, and also highly stable in aqueous solutions and cell culture media. These features make them potentially suitable for sensing oxygen in extracellular fluids such as blood, interstitial and brain fluid, in (micro) bioreactors and micro- or nanoscale fluidic devices. Four kinds of nanosensors are presented, whose excitation spectra cover a wide spectral range (395 – 630 nm), thus matching many common laser lines, and with emission maxima ranging from 565 to 800 nm, thereby minimizing interference from background luminescence of biomatter. The unquenched lifetimes are on the order of 5.8 – 234  $\mu$ s, which – in turn – enables lifetime imaging and background separation via time-gated methods. The Figure below shows (on the left) the architecture of the ultra-small oxygen-sensitive nanoparticles (NPs) and the chemical structures of the oxygen indicators. Figure (D) shows photographic pictures of oxygen nanosensors in aqueous solutions under ambient light; (E) shows the same cuvettes under UV light. From



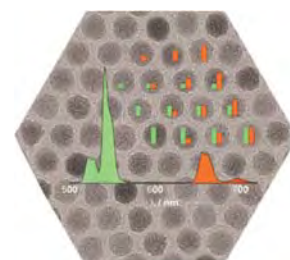
left to right: Ir-NPs, Ru-NPs, Pt-NPs and Pd-NPs, respectively.



**565. Review: Photon-Upconverting Nanoparticles for Optical Encoding and Multiplexing of Cells, Biomolecules and Microspheres.** H.-H. Gorris, O. S. Wolfbeis; *Angew. Chem. Int. Ed.* (2013), 52, 3584-3600. DOI: 10.1002/anie.201208196.

Journal IF: 13.4.

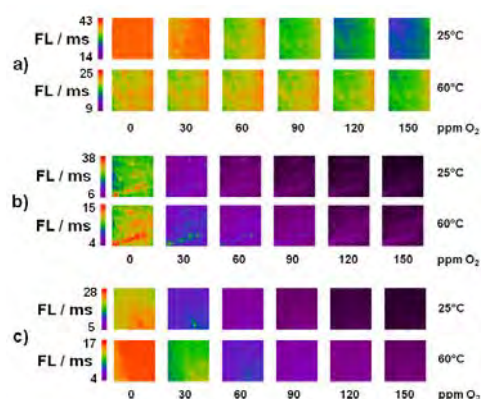
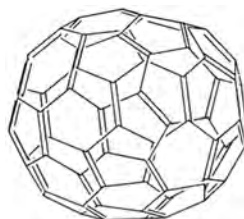
**Abstract:** Photon upconverting nanoparticles (UCNPs) can emit visible light under near-infrared excitation (anti-Stokes emission). This unique optical property precludes background fluorescence and light scattering by biological materials. The emission of multiple and narrow emission lines is an additional hallmark of UCNPs that opens new avenues for optical encoding. Distinct emission signatures can be obtained if the multiple emission of UCNPs is tuned by their dopant composition or by surface modification with dyes. Tuning only one of the multiple emission lines and using another one as a constant reference signal enables the design of ratiometric codes that are resistant to fluctuations in absolute signal intensities. Combining several UCNPs, each displaying a distinct set of emission lines, expands the coding capacity exponentially and lays the foundation for highly multiplexed analyte detection. The review highlights the potential of UCNPs for labeling and encoding biomolecules, microspheres, and of whole cells.



**564. Sensing and Imaging of Oxygen with Parts per Billion Limits of Detection and Based on the Quenching of the Delayed Fluorescence of <sup>13</sup>C<sub>70</sub> Fullerene in Polymer Hosts.** S. Kochmann, C. Baleizão, M. N. Berberan-Santos, O. S. Wolfbeis; *Anal. Chem.* (2013), 85, 1300-1304. DOI: 10.1021/ac303486f. Journal IF: 5.9.

**Abstract:** The method for sensing trace oxygen in the gas phase is based on the extreme efficiency of the quenching of the thermally activated delayed fluorescence of isotopically enriched (85%) carbon-13 fullerene C<sub>70</sub> (<sup>13</sup>C<sub>70</sub>). The fullerene was dissolved in polymer matrices of varying oxygen permeability, viz. polystyrene (PS), ethyl cellulose (EC), and an organically modified silica gel ("ormosil"). The sensor films (5 – 10 μm thick), on photoexcitation at 470 nm, display a strong delayed photoluminescence with peaks between 670 and 700 nm.

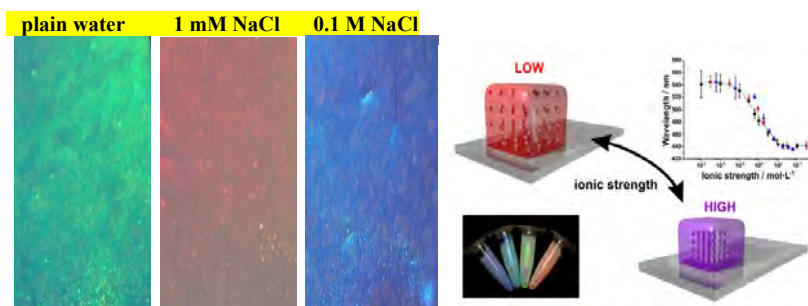
Quenching by oxygen was studied at 25 °C and 60 °C, and at levels from zero to 150 ppmv of oxygen in nitrogen gas. The rapid lifetime determination (RLD) method was applied to determine oxygen-dependent decay times and to perform fluorescence lifetime imaging of oxygen. The oxygen sensors reported here are the most sensitive ones described so far. The color figure shows images based on decay time measurements of C<sub>70</sub> in PS, EC and ormosil at various temperatures at



**563. Optical Sensing of Ionic Strength Using Photonic Crystals in a Hydrogel Matrix.** Ch. Fenzl, Th. Hirsch, O. S. Wolfbeis; *ACS Appl. Mat. Interfaces* (2013), 5, 173-178. DOI: 10.1021/am302355g. Journal IF: 6.7.

**Abstract:** Monodisperse, highly neg. charged, crosslinked polystyrene nanoparticles with a diam. between 80 to 120 nm have been incorporated into a polyacrylamide hydrogel where they display an iridescent color that conventionally is attributed to the so-called photonic crystal effect. The film is red in plain water but turns to green in the presence of 1 mM soln. of an electrolyte, and to purple in 100 mM solns. of electrolytes. See the Figure.

Quantitative reflection spectroscopy resulted in plots of reflected light wavelength vs. ionic strength (IS) that are almost linear in the logarithmic concentration range from 5•10<sup>-5</sup> to 10<sup>-2</sup> mol•L<sup>-1</sup>. Such films are capable of monitoring the IS of aqueous solutions in the pH range from 5 to 9. In addition to visual and instrumental readout, the sensor films can be analyzed with a digital camera at fixed angle. The digital images were separated into their red, green and blue (RGB) channels and analyzed. The red channel was found to be best suited for determination of IS and resulted in calibration plots that are comparable if not better than those obtained by reflectometry.



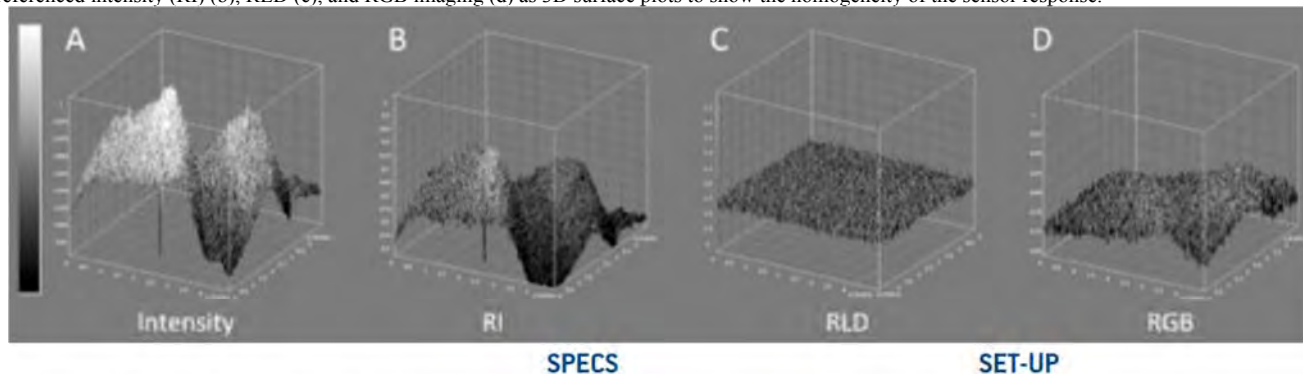
**562. Referenced Luminescent Sensing and Imaging with Digital Color Cameras: A Comparative Study.** L. H.

Fischer, R. J. Meier, M. Schaeferling, O. S. Wolfbeis; *Sensors Actuat. B (Chemical)* (2013), 177, 500-506. DOI:

10.1016/j.snb.2012.11.041. journal IF: 3.9.

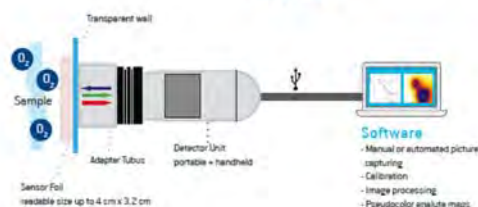
**Abstract:** We have performed a comparative study on different imaging techniques for optical chemical sensors with the aim to assess the utility of red-green-blue (RGB) color cameras for quantitative analysis. A luminescent film for sensing barometric pressure (via quenching by oxygen) was used as a model system and calibrated by four fluorescence imaging methods including intensity imaging, referenced intensity imaging, lifetime imaging, and RGB based imaging using a customary digital color camera. The results are compared with respect to standard deviations, lateral signal homogeneity, and resolution. The imaging methods were applied to the sensor film under identical experimental conditions in order to warrant comparable results.

The figure shows images of a sensor film at 100 mbar air pressure at 25° with inhomogeneous illumination. The results are shown for intensity (a), referenced intensity (RI) (b), RLD (c), and RGB imaging (d) as 3D surface plots to show the homogeneity of the sensor response.



The graph on the right shows a schematic of a typical commercially instrument for imaging of oxygen (A1), pH values (A2) or carbon dioxide (A3), for example in seawater or in plants or on skin.

A1 O <sub>2</sub>	D-100% O <sub>2</sub>
A2 pH	2.5 - 4.5 5.5 - 7.5
A3 CO <sub>2</sub>	0 - 1 1 - 25 %

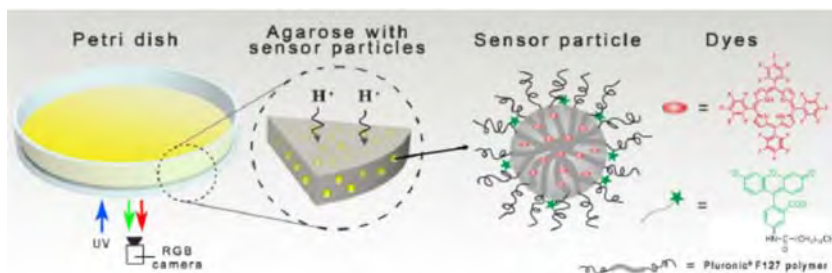


**561. Fluorescent pH-Sensitive Nanoparticles in an Agarose Matrix for Imaging of Bacterial Growth and Metabolism.**

X. Wang, R. J. Meier, O. S. Wolfbeis; *Angew. Chem. Int. Ed.* (2013), 52, 406-409. DOI: 10.1002/anie.201205715. Journal

IF: 13.4.

**Abstract:** We report on novel nanosensors for fluorescent imaging of physiological pH values. Features include (a) very small diameters (12 nm); (b) biocompatibility due to the use of a hydrogel kind of material [a commercial poly(ethylene glycol)-co-poly-ethyleneoxide], non-covalent immobilization (based on strong hydrophobic interactions), and (c) lack of toxicity. Such nanosensors, if incorporated into an agar film, enable continuous monitoring of the pH value of bacterial cultures, and thus of their growth.



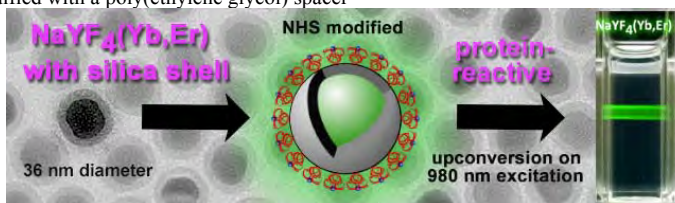
**560. Multicolor Upconversion Nanoparticles for Protein Conjugation.** S. Wilhelm, T. Hirsch, W. M. Patterson, E.

Scheucher, T. Mayr, O. S. Wolfbeis; *Theranostics* (2013), 3, 239-248. DOI: 10.7150/thno.5113. Open access. Journal IF:

8.0.

**Abstract:** We describe the preparation of protein-conjugatable, monodisperse, lanthanide-doped hexagonal-phase NaYF<sub>4</sub> upconverting luminescent nanoparticles. Their core was coated with a silica shell which then was modified with a poly(ethylene glycol) spacer

and N-hydroxysuccinimide ester groups. The particles were characterized by transmission electron microscopy, Raman, X-ray diffraction, and dynamic light scattering. NHS functionalization renders them highly reactive towards proteins. The protein-reactive UCLNPs and their conjugates to streptavidin and bovine serum albumin display multi-color emissions upon 980-nm continuous wave laser excitation. Surface plasmon resonance studies were carried out to prove bioconjugation and to compare the affinity of the particles for proteins immobilized on a thin gold film.

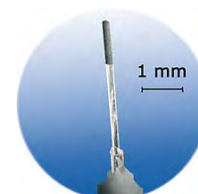


**559. Review: Fiber Optic Chemical Sensors and Biosensors (2008 – 2012).** X. Wang, O.

S. Wolfbeis; *Anal. Chem. (Wash.)* (2013), 85, 487-508. DOI: 10.1021/ac303159b. Journal IF:

5.9.

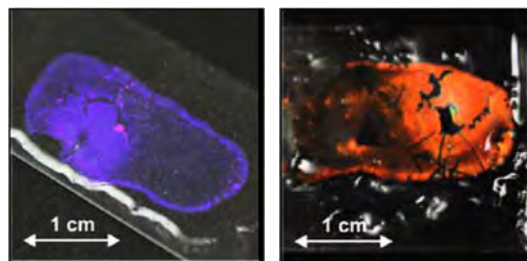
**Abstract:** Fiber optics enable direct optical spectroscopy (from the IR to the UV; in absorption, emission and plasmonic resonance) to be performed at inaccessible sites, over large distances, in strong magnetic fields and in harsh environment. If equipped with chem. responsive coatings, they also enable species to be sensed that are not directly amenable to optical spectroscopy. This article reviews the progress made in the past 5 years and also reports on recent trends.





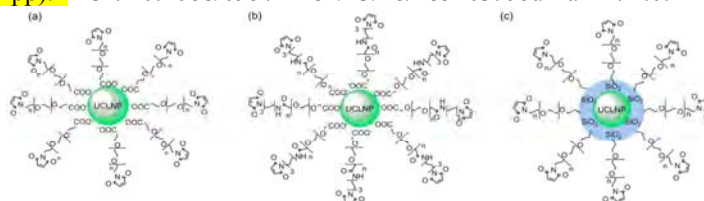
**558. Photonic Crystal Based Sensor for Organic Solvents and for Solvent-Water Mixtures.** Ch. Fenzl, Th. Hirsch, O. S. Wolfbeis; *Sensors (Basel)* **2012**, *12*, 16954-16963 (Special Issue on *State-of-the-Art Sensors Technology in Germany*, 2012). DOI: 10.3390/s121216954. Open access. IF 2.2.

**Abstract:** Monodisperse polystyrene nanoparticles with a diameter of 173 nm were incorporated into a polydimethylsiloxane matrix where they display an iridescent color that can be attributed to the photonic crystal effect. The film is violet in plain water, but turns to red in the presence of the non-polar solvent n-hexane. Several solvents were studied. The films are capable of monitoring the water content of ethanol/water mixtures, where only 1% of water leads to a shift of the peak wavelength of reflected light by 5 nm. The method also can be applied to determine, both visually and instrumentally, the fraction of methanol in ethanol/methanol mixtures. Here, a fraction of 1% of methanol results in a wavelength shift of 2 nm. The reflected wavelength is not influenced by temperature changes nor impeded by photobleaching. The signal changes are fully reversible, and response times are <1 s.



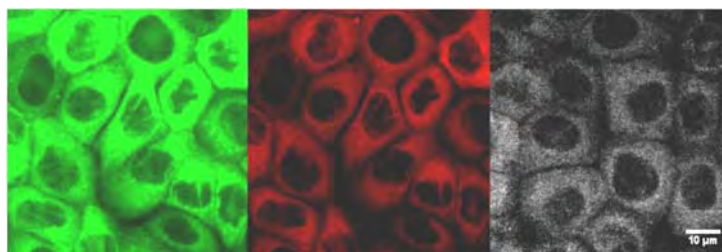
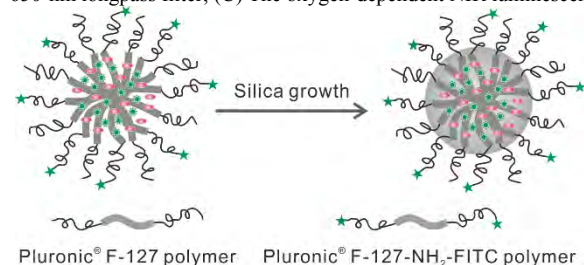
**557. Maleimide Activation of Photon-Upconverting Nanoparticles for Bioconjugation.** R. B. Liebherr, T. Soukka, O. S. Wolfbeis, H. H. Gorris; *Nanotechnol.* (2012), *23*, 485103 (7 pp). DOI: 10.1088/0957-4484/23/48/485103. Journal IF: 4.0.

**Abstract:** Oleic acid-coated UCLNPs obtained by solvothermal synthesis were functionalized with hydrophilic PEG and thiol-reactive maleimides either by ligand exchange or by silanization and covalent attachment. Three types of maleimide-functionalized UCLNPs (with and without silica shell) were characterized by transmission electron microscopy, dynamic light scattering and Raman spectroscopy. Ligand exchange of oleic acid by maleimide-PEG-COOH yielded UCLNPs that did not aggregate, were colloidally stable, and reacted readily with proteins. Such labels are required for background-free imaging.



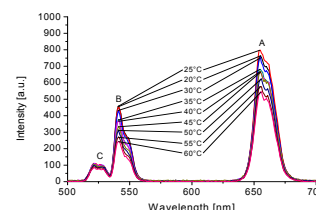
**556. Ultra-Small, Highly Stable and Sensitive Dual Nanosensors for Imaging Intracellular Oxygen and pH in Cytosol.** X. Wang, J. A. Stolwijk, T. Lang, M. Sperber, R. J. Meier, J. Wegener, O. S. Wolfbeis; *J. Am. Chem. Soc.* (2012), *134*, 17011-17014. DOI: 10.1021/ja308830e. Journal IF: 9.9. Article featured in *JACS Spotlights (J. Am. Chem. Soc.*

(2012), *134*, 18151-18152). **Abstract:** We report on the first dual nanosensors for imaging of pH values and oxygen partial pressure in cells. The sensors have a unique nanostructure in that a soft core structure is rigidized with a silane reagent, while poly(ethylene glycol) chains form an outer shell. Lipophilic oxygen-sensitive probes and reference dyes are encapsulated inside the hydrophobic core, while a pH-sensitive probe is covalently attached to the poly(ethylene glycol) end-group on the shell. The core/shell structure renders the nanosensors well dispersed and highly stable in various kinds of aqueous media. Their average size is 12 nm, and they respond to both pH values and oxygen in the physiological range. They do not pass cell-membranes, but can be internalized into the cellular cytosol by electroporation, upon which they enable sensing and imaging of pH values and oxygen with high spatial resolution. The *Figure* shows confocal laser scanning microscopy images of the nanosensors internalized into normal rat kidney cells via electroporation. (A) The green luminescence of the pH-dependent signal of the nanosensors as seen with a 520-nm bandpass filter; (B) The red luminescence as seen with a 650-nm longpass filter; (C) The oxygen-dependent NIR luminescence (black/white) of the nanoparticles.



**555. Photon Upconverting Nanoparticles for Luminescent Sensing of Temperature.** A. Sedlmeier, D. E. Achatz, L. H. Fischer, H. H. Gorris, O. S. Wolfbeis; *Nanoscale* (2012), *4*, 7090-7096. DOI: 10.1039/c2nr32314a. Journal IF: 5.9.

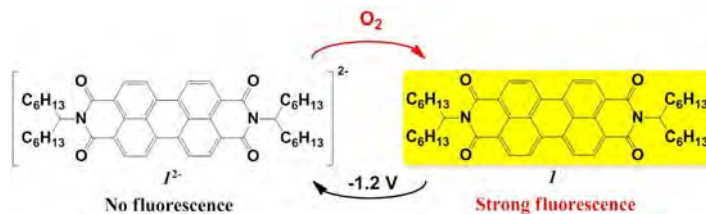
**Abstract:** Nanoparticles displaying photon upconversion have advantages like the low background fluorescence of biological specimen due to near infrared (NIR) excitation and the presence of two or more emission bands. The ratio of these intensities of the main bands of upconverted emission of hexagonal NaYF<sub>4</sub> nanoparticles doped with Yb<sup>3+</sup> as the sensitizer and with Er<sup>3+</sup>, Ho<sup>3+</sup>, or Tm<sup>3+</sup> as the activators yields robust data for the determination of temperature in the "physiological" range (20 – 60°C). Resolutions of <±1 °C can be achieved with particles consisting of a doped core and an inactive shell.



**553. Efficient Fluorescence Turn-On Sensing of Dissolved Oxygen by Electrochemical Switching.** I. Shin, T. Hirsch, B. Ehrl, D. Jang, J. Hong, O. S. Wolfbeis; *Anal. Chem. (Wash.)*, (2012), *84*, 9163-9168. DOI: 10.1021/ac301830a. Journal IF: 5.9.

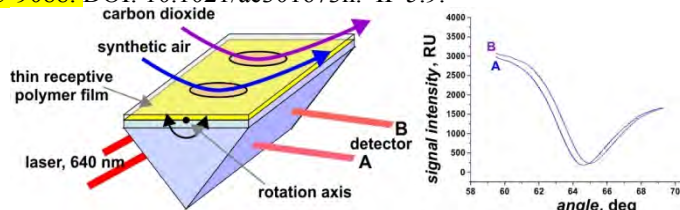
**Abstract:** We report on a novel method for sensing oxygen that is based on the use of a perylene diimide dye (PDD) which is electro-chemically reduced to its non-fluorescent dianion form (PDD<sup>2-</sup>).

In the presence of oxygen, the dianion is oxidized to its initial form via an electron transfer reaction with oxygen upon which fluorescence is recovered. As a result, the fluorescence intensity of the dianion solution increases upon the addition of oxygen gas. Results demonstrate that high sensitivity is obtained when the emission intensity reaches its maximum by the addition of 2.4% (v/v) oxygen gas. In addition, by using electrochemical reduction, oxygen determination becomes regenerative, and no significant degradation is observed over several turnovers. The limit of detection is 0.14% oxygen in argon gas.



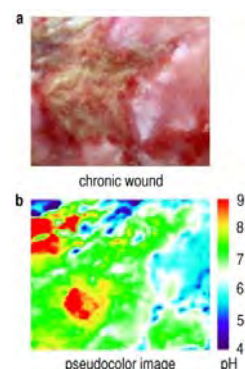
**552. Surface Plasmon Resonance Sensor for Dissolved and Gaseous Carbon Dioxide.** T. Lang, T. Hirsch, C. Fenzl, F. Brandl, O. S. Wolfbeis; *Anal. Chem. (Wash.)* (2012), 84, 9085-9088. DOI: 10.1021/ac301673n. IF 5.9.

**Abstract:** We describe a novel kind of sensor for carbon dioxide. It is based on surface plasmon resonance (SPR) and a polymer blend that is capable of fully reversibly binding CO<sub>2</sub>. The interaction results in a change in the polarity and refractive index that can be detected via SPR. The sensor responds with high specificity. The method is simple, and the method – unlike previous ones – enables continuous sensing over extended periods of time. It can be applied to sense both dissolved and gaseous carbon dioxide.



**551. Sprayable pH Sensor and its Use for Photographic Wound Imaging in-vivo.** S. Schreml, R. J. Meier, J. Cattani, D. Flittner, S. Gehmert, O. S. Wolfbeis, M. Landthaler, P. Babilas; *Exptl. Dermatol.* (2012), 21, 942–970. DOI: 10.1111/exd.12042. IF 4.4.

**Abstract:** Non-invasive luminescence imaging is of great interest for studying biological parameters (such as oxygen and pH) in cutaneous wound healing. Recently, we developed the first method for 2D luminescence imaging of pH in vivo on humans, and a method for one-stop-shop visualization of oxygen and pH using the RGB read-out of commercial cameras. Both methods make use of semitransparent sensor foils. Here, we describe a sprayable ratiometric luminescent pH sensor, which combines properties of both these methods and is suitable for in vivo use. Fluorescein isothiocyanate (FITC) was used as the pH indicator, and the ruthenium(II) complex Ru(dpp) as the reference dye. A digital (RGB) photo of the spray on the tissue is then taken, and the signals of the green fluorescent pH indicator are stored in the green channel, while that of the reference dye are stored in the red channel. Images are processed by ratioing the intensities of the two channels to result in pseudo-color pH maps of tissue surfaces, e.g. wounds.

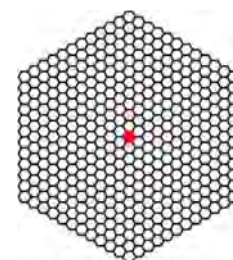


**550. Referenced Dual Pressure and Temperature Sensitive Paint for Color Camera Read-out.** L. H. Fischer, C. Karakus, R. J. Meier, O. S. Wolfbeis, E. Holder, M. Schaeferling; *Chemistry – Eur. J.* (2012) 18, 15706-15713. DOI: 10.1002/chem.201201358. Journal IF: 5.9.

**Abstract:** We are presenting the first fluorescent material for referenced simultaneous RGB imaging of barometric pressure (oxygen partial pressure) and temperature (*T*). The dually sensitive coating contains two Pt(II) complexes acting as indicator for pressure (oxygen) and *T*, and a blue emitting reference dye, respectively. They are incorporated in polymer nanoparticles dispersed in a polyurethane hydrogel which is spread onto a solid support. The luminescence of the pressure probe (PtTFPP) matches the red channel of a RGB color camera, while that of the *T* probe matches the green channel. The blue-emitting reference dye (9,10-diphenyl-anthracene), in turn, matches the blue channel. In contrast to other dually sensitive materials, this new coating allows for simultaneous imaging of both indicator signals and the reference signal in one RGB color picture without having to separate the signals with additional optical filters. All dyes can be excited with a 405-nm LED and display good photostability under continuous illumination. Barometric pressure was determined with a resolution of 22 mbar, and *T* with a resolution of 4.3 °C. The formulae related to the probes and polymers (PAN, PVDCAN, PS, PVP) used are given below.

**549. Review: Graphenes in Chemical Sensors and Biosensors.** S. Kochmann, Th. Hirsch, O.S. Wolfbeis; *Trends Anal. Chem.* (2012), 39, 87-113. DOI: 10.1016/j.trac.2012.06.004). Journal IF: 6.3.

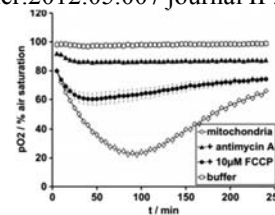
**Abstract:** This review covers the current state of the art of using graphenes in electrochemical and optical chemical sensors and biosensors. We first discuss the types of graphenes, graphene oxides, and the like, and also give a definition for each. This is followed by a section on the use of nonmodified materials ("plain graphenes") in mainly electrochemical and optical chemical sensors and (bio)sensors. The next section summarizes the various kinds of sensors based on composite materials containing graphenes, with subsections on electro-chemical, field effect transistor-based, fluorescent, chemi-luminescent and colorimetric sensors. It is shown that the use of graphenes alone or in composite form can improve the performance of chemical sensors and biosensors, in particular with respect to the dynamic ranges, lower limits of detection, selectivity and size of instrumentation. The review is based on ~270 references from the time period between 2007 and 2012.





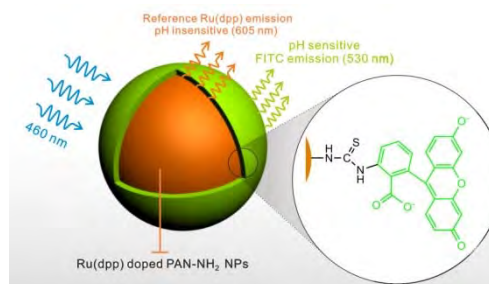
**548. Long Time Monitoring of the Respiratory Activity of Isolated Mitochondria.** A. Heller, L. H. Fischer, O. S. Wolfbeis, A. Goepferich, *Exptl Cell Research* (2012), 318(14), 1667-1672. DOI: 10.1016/j.yexcr.2012.05.007 journal IF: 3.6.

**Abstract:** We have investigated the ability of optical oxygen sensors incorporated in a microplate to det. the respiratory activity of cell fractions. Different cell fractions were monitored, in particular to evaluate the long term functionality of isolated mitochondria. It is possible to continuously sense respiratory activity of isolated mitochondria over time. We found that they are functional for three hours but stop respiring at a crit. limit of 20% air satn. in the system. Furthermore, inhibition and enhancement of respiratory activity were detected. In conclusion, oxygen sensors are a powerful tool to evaluate the functionality of isolated mitochondria. The Figure shows the inhibition of mitochondrial respiration with antimycin A (black triangles) and FCCP (carbonyl cyanide 4-(trifluoromethoxy)phenylhydrazone (black circles).



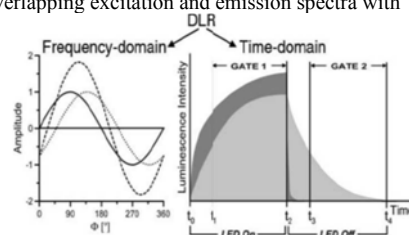
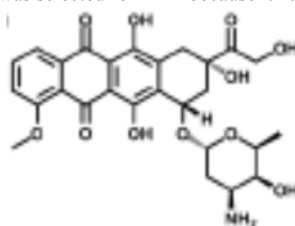
**547. Fluorophore-Doped Polymer Nanomaterial for Referenced Imaging of pH and Temperature with Sub-Micrometer Resolution.** X. Wang, R. J. Meier, O. S. Wolfbeis; *Adv. Funct. Mat.* (2012), 22, 4202-4207. DOI: 10.1002/adfm.201200813. Journal IF: 8.5.

**Abstract:** We report on a new kind of pH and temperature (*T*)-sensitive material. It is composed of dye-doped polymer nanoparticles incorporated into a thin film of a polyurethane hydrogel. The new pH/*T*-sensitive nanoparticles were obtained by post-staining oxygen-impermeable amino-functionalized polyacrylonitrile nanoparticles with a long-lifetime reference dye. Staining is followed by covalently linking fluorescein isothiocyanate onto the surface of the nanoparticle. The sensor material has distinct features: (a) It enables imaging of pH via time domain dual-lifetime referencing (td-DLR); (b) effects of *T* on pH sensing may be compensated for; (c) *T* can simultaneously be visualized via rapid lifetime imaging; (d) It offers superior spatial resolution due to the use of nanosized sensor particles.



**546. Dual Lifetime Referenced Fluorometry for the Determination of Doxorubicin in Urine.** F. Martínez Ferreras, O. S. Wolfbeis, H. H. Gorris, *Anal. Chim. Acta* 729 (2012), 62-66. DOI: 10.1016/j.aca.2012.03.050. journal IF: 4.3.

**Abstract:** Dual Lifetime Referencing (DLR) is introduced as a rapid method for measuring the concentration of a fluorescent analyte in solution. This new self-referenced approach is particularly useful for the determination of fluorescent drugs of medical importance such as doxorubicin. The long-lived reference dye ruthenium(II)tris-(4,7-diphenyl-1,10-phenanthroline) was selected for DLR because it has overlapping excitation and emission spectra with doxorubicin. Frequency-domain and time-domain DLR were applied and their performances were compared. Both modes of DLR yielded similar analytical ranges and limits of detection (~400 nM). The limit of detection may be further decreased by using a stronger excitation light source. The developed DLR methods were evaluated determining spiked samples of doxorubicin in human urine. The standard addition technique was applied in order to overcome the matrix effect. Excellent recovery rates (~98 %) were obtained.

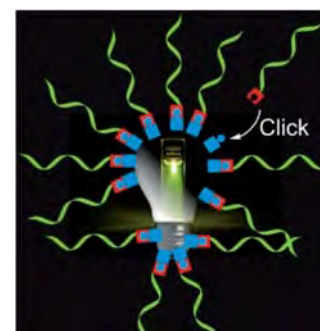


**545. The Activity Ratio of <sup>228</sup>Th to <sup>228</sup>Ra in Bone Tissue of Recently Deceased Humans: A New Dating Method in Forensic Examinations.** B. Zinka, R. Kandlbinder, R. Schupfner, G. Haas, O. S. Wolfbeis, M. Graw; *Anthropol. Anzeiger (= J. Biol. Clin. Anthropology)* (2012), 69, 147-157. DOI: 10.1127/0003-5548/2012/0127.

**Abstract:** Reliable determination of time since death in human skeletons or single bones often is limited by methodical difficulties. Determination of the specific activity ratio of natural radionuclides, in particular of <sup>232</sup>Th (Thorium), <sup>228</sup>Th and <sup>228</sup>Ra (Radium) seems to be a new appropriate method to calculate the post mortem interval. These radionuclides are incorporated by any human being, mainly from food. So with an individual's death the uptake of radionuclides ends. But the decay of <sup>232</sup>Th produces <sup>228</sup>Ra and <sup>228</sup>Th due to its decay series, whereas <sup>228</sup>Th is continuously built up in the human's bones. Thus, it can be concluded that in all deceased humans at different times after death different activity ratios of <sup>228</sup>Th to <sup>228</sup>Ra will develop in bone. According to this fact it should be possible to calculate time since death of an individual by first analysing the specific activities of <sup>228</sup>Th and <sup>228</sup>Ra in bones of deceased and then determining the <sup>228</sup>Th/<sup>228</sup>Ra activity ratio, which can be assigned to a certain post-mortem interval.

**544. DNA "Nanolamps": Clicked DNA Conjugates with Photon Upconverting Nanoparticles as Highly Emissive Biomaterials.** M. M. Rubner, D. E. Achatz, H. S. Mader, J. A. Stolwijk, J. Wegener, G. S. Harms, O. S. Wolfbeis, H.-A. Wagenknecht; *ChemPlusChem* (2012), 77, 129-134. DOI: 10.1002/cplu.201100055. Journal IF: 3.3.

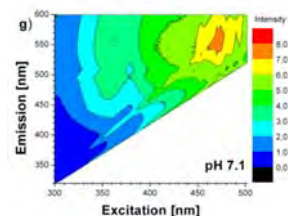
**Abstract:** Upconverting nanoparticles (UCNPs) display visible luminescence when excited in the near-infrared (NIR) region but have no biorecognition capabilities. However, functionalization of their surface with azido groups renders them conjugatable to ethynyl-modified oligonucleotides in a bioorthogonal fashion. Single-stranded DNA was covalently attached to the surface of UCNPs by click chemistry and purified by size exclusion chromatography (SEC) at elevated temperature. Covalent attachment was evidenced by diffuse reflectance infrared Fourier transform (DRIFT) spectroscopy. DNA conjugation makes the particle soluble in water and enables it to recognize its counterstrand. Such UCNPs are capable of nonspecifically crossing cell membranes. Confocal microscopy reveals the high potential of the bright UCNPs for live cell imaging in the NIR, where the UCNP-DNA conjugates can be considered to act as a kind of nano-sized lamp. Furthermore, cross-linking of those DNA nanolamps yields highly emissive aggregates.



**543. The pH Dependence of the Total Fluorescence of Graphite Oxide.** S. Kochmann, T. Hirsch, O. S. Wolfbeis; *J. Fluoresc.* (2012), 22, 849-855. DOI: 10.1007/s10895-011-1019-8.

Journal IF: 2.1.

**Abstract:** Graphite oxide was characterized by pH dependent excitation-emission matrices in the spectral range from 300 to 500 nm in excitation, and from 320 to 600 nm in emission which reveal the presence of two pH steps. These are assigned to the presence of carboxy groups and phenolic hydroxy groups, respectively. Fluorescence is strongest at 470 nm excitation and at 555 nm emission. The fluorescence intensity is a function of pH but not of temperature, and is not quenched by oxygen.



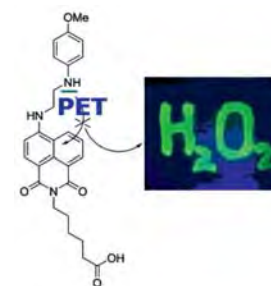
**542. 2-Volume Book: Fluorescent Proteins vol. I: From Understanding to Design. Vol. II: Application of Fluorescent Protein Technology.** G. Jung (ed.); *Springer Series on Fluorescence*, vol. 12, 2011 (O. S. Wolfbeis, Series Ed.). ISBNs: 978-3-642-23371-5 and 978-3-642-23376-0. DOI: 10.1007/978-3-642-23372-2F. See: [www.springer.com/series/4243](http://www.springer.com/series/4243).

**Contents:** \* Fluorescent Proteins: Nature's Colorful Gifts for Live Cell Imaging (by J. Wiedenmann, C. D'Angelo, G. U. Nienhaus); \* Green Fluorescent Protein Photodynamics as a Tool for Fluorescence Correlative Studies and Applications (by G. Chirico, M. Collini, L. D'Alfonso, M. Caccia, S. Carlo Daglio, B. Campanini); \* The Proton Sensitivity of Fluorescent Proteins: Towards Intracellular pH Indicators (by R. Bizzarri); \* Green Fluorescent Protein-Based Chloride Ion Sensors for In Vivo Imaging (by P. Bregestovski, D. Arosio); \* Fluorescent Genetically Encoded Calcium Indicators and Their In Vivo Application (by T. Gensch, D. Kaschuba); \* Action Potentials in Heart Cells (by L. Kaestner, Q. Tian, P. Lipp); \* Probing Structure and Dynamics of the Cell Membrane with Single Fluorescent Proteins (by A. Pezzarossa, S. Fenz, T. Schmidt); \* Fluorescence Correlation and Cross-Correlation Spectroscopy Using Fluorescent Proteins for Measurements of Biomolecular Processes in Living Organisms (by Y. H. Foo, V. Korzh, T. Wohland); \* Investigating the Life Cycle of HIV with Fluorescent Proteins (by V. Baumgaertel, S. Ivanchenko, B. Mueller, D. C. Lamb).



**541. A New Fluorescent PET Probe for Hydrogen Peroxide, and its Use in Enzymatic Assays for L-Lactate and D-Glucose.** D. B. M. Groegel, M. Link, A. Duerkop, O. S. Wolfbeis; *ChemBioChem* (2011), 12, 2779-2785. DOI: 10.1002/cbic.201100561. IF 3.9.

**Abstract:** The probe is based on the yellow fluorophore 4-amino-1,8-naphthalimide that is coupled to p-anisidine (as a redox-active group) to form a probe that is based on photoinduced electron transfer (PET). The preparation of the probe (to which we refer as HP Green) was accomplished in four steps. Its fluorescence is independent of pH in the physiological range and quenched due to a PET process that occurs between the p-anisidine redox moiety and the naphthalimide luminophore. If the p-anisidine group is oxidized by HP, PET is suppressed and fluorescence intensity is strongly increased. Addition of horseradish peroxidase (HRP) enhances the oxidation of HP Green and further improves the detection limit of HP. The use of HRP and HP Green enables the determination of HP with a limit of detection (LOD) as low as 64 nM. HP Green also enables sensitive enzymatic assays of L-lactate and D-glucose using the respective oxidases.



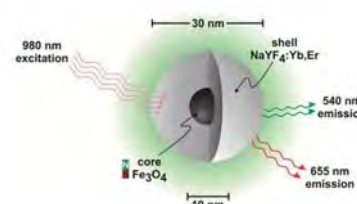
**540. Book edited: Lanthanide Luminescence: Photophysical, Analytical and Biological Aspects.** P. Hänninen, H. Härmä (eds.); *Springer Series on Fluorescence*, vol. 7, (2011) (O. S. Wolfbeis; Series Ed.); 385 pp. ISBN: 978-3-642-21022-8. DOI: 10.1007/978-3-642-21023-5.

**Cover Text:** Lanthanides have fascinated scientists for more than two centuries now, and ever since efficient separation techniques were established some 50 years ago, they have found their way into industrial exploitation and to everyday life. Numerous applications are based on their unique luminescent properties. This volume presents established knowledge about the photophysical basics of lanthanide probes and materials, and describes instrumentation-related aspects including chemical and physical sensors. The uses of lanthanides in bioanalysis and medicine are outlined, such as assays for in vitro diagnostics and research. All chapters were compiled by renowned scientists with a broad audience in mind, providing both beginners in the field and advanced researchers with comprehensive information on the given subject.



**539. Magnetic Nanosensor Particles with Luminescence Upconversion Capability.** S. Wilhelm, T. Hirsch, E. Scheucher, T. Mayr, O. S. Wolfbeis; *Angew. Chem. Intl. Ed.* (2011), 50(37), A59-A62. DOI: 10.1002/ange.201105813. Journal IF: 12.7.

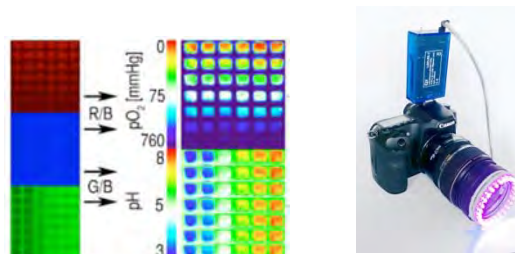
**Abstract:** Nanoparticles made of magnetite and with an average size of 10 nm have been used as seed crystals to further grow, on their surface, a layer of upconverting material consisting of Yb,Er-doped hexagonal NaYF<sub>4</sub>. The resulting multifunctional upconverting and magnetic nanoparticles represent a novel material for potential use in magnetic resonance imaging, as "nanolamps", and in bioimaging. Such particles may also form the basis for a new generation of optical immunosensors or gene sensors that can be separated from complex biomatter by magnetic force and where fluorescent signals can be generated using a 980-nm diode laser whose light easily penetrates most tissue.



**538. Simultaneous Photographing of Oxygen and pH in-vivo Using Sensor Films.** R. J. Meier, S. Schreml, X. Wang, M. Landthaler, P. Babilas, O. S. Wolfbeis; *Angew. Chem. Int. Ed.* (2011), 50, 10893-10896. DOI: 10.1002/anie.201104530 journal IF: 12.7.

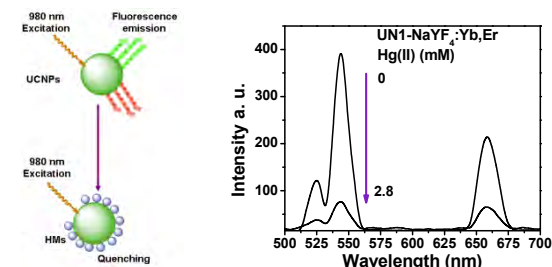


**Abstract:** We are presenting a method for real-time and simultaneous visualization of oxygen and pH in vivo using the RGB option of commercial digital cameras. Luminophores were used with emission peaks that correspond to the RGB channels of the camera. To create a 2D sensor, micro-particles were loaded (a) with an oxygen-sensitive platinum(II) complex whose data are stored in the red channel, (b) fluorescein isothiocyanate (the pH probe; data stored in the green channel), and (c) diphenyl-anthracene (as reference dye; data stored in the blue channel) and placed in a biocompatible hydrogel matrix. The sensor was characterized in vitro, and used to image oxygen and pH in human wounds. The novel imaging technique presented herein can be adapted to visualize various important chemical parameters, and may simplify imaging to a large extent.



**537. Quenching of the Luminescence of Upconverting Luminescent Nanoparticles by Heavy Metal Ions.** S. M. Saleh, R. Ali, O. S. Wolfbeis; *Chem. – Eur. J.* (2011), 17, 14611-14617. DOI: 10.1002/chem.201101860. Journal IF: 5.5.

**Abstract:** The red and green luminescence of upconverting luminescent nanoparticles (photoexcited with a 980-nm diode laser) is dynamically and statically quenched by heavy metal ions (in particular by Hg(II) ions), and by bromide and iodide. Quantitative quenching studies are presented. The efficiency of quenching is different for the two main emission bands.



**536. Brightly Fluorescent Purple and Blue Labels for Amines and Proteins.** M. Link, P. Kele, D. E. Achatz, O. S. Wolfbeis; *Bioorg. Med. Chem. Lett.* (2011), 21, 5538-5542. DOI: 10.1016/j.bmcl.2011.06.133. IF 2.6.

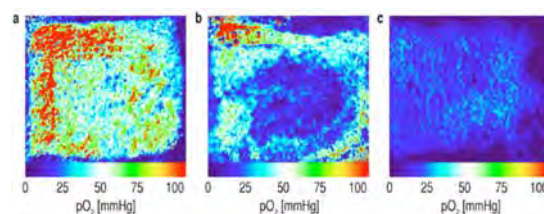
**Abstract:** Fluorescent labels for amino acids and proteins were obtained that display excellent temporal and photo-stability as shown below for solutions of a purple and a blue (nonreactive) dye (compounds 3 and 8) that were stored in aqueous solution on a desk for more than 1 year.



**535. Two-Dimensional Luminescence Imaging of Physiological Wound Oxygenation.** S. Schreml, R. J. Meier, O. S. Wolfbeis, T. Maisch, R.-M. Szeimies, M. Landthaler, J. Regensburger, F. Santarelli, I. Klimant, P. Babilas; *Exp. Dermatol.* (2011), 20, 550-554. DOI: 10.1111/j.1600-0625.2011.01263.x. Journal IF: 4.2.

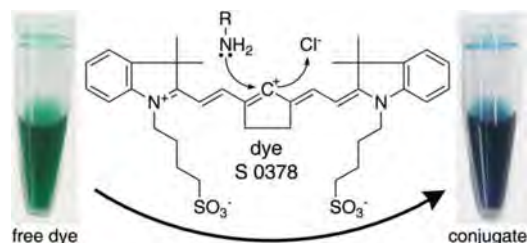
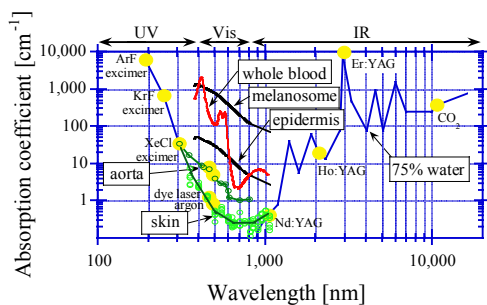
**Abstract:** We have studied the distribution of pO<sub>2</sub> during physiological wound healing. Split-thickness skin graft donor sites (n = 12) served as standardized wound models. Wound surface pO<sub>2</sub> was measured at 1, 6, and 14 days after split-skin harvesting using 2-dimensional luminescence lifetime imaging (2D-LLI) of Pd(II)-meso-tetraphenyl-benzoporphyrin in poly(styrene-co-acrylonitrile) particles on transparent foils. In another experiment, we removed the stratum corneum (SC) on the volar forearm (n = 10) by tape strippings to study the impact of the SC on the epidermal oxygen barrier. Split-skin donor site pO<sub>2</sub> significantly decreased during the time course of physiological healing.

**Figures:** (a) One day after skin graft harvesting, where vast areas lack an epidermal oxygen barrier. (b) After 6 days, large areas within the donor site wounds are re-epithelialized; (c) 14 days p.o.; most of the wound is re-epithelialized.



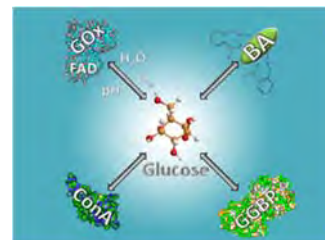
**534. Long-Wavelength Absorbing and Fluorescent Chameleon Labels for Proteins, Peptides and Amines.** H. H. Gorris, S. M. Saleh, D. B. M. Groegel, S. Ernst, K. Reiner, H. Mustroph, O. S. Wolfbeis; *Bioconj. Chem.* (2011), 22, 1433-1437. DOI: /10.1021/bc200192k. Journal IF: 5.0.

**Abstract:** Long-wavelength absorbing labels that change their color and fluorescence upon conjugation to proteins and other biomolecules provide two critical advantages over the wealth of conventional amine-reactive labels. At first, the progress of the labeling reaction can be monitored continuously either visually or by spectrometry without prior purification. Then, the labeled biomolecule can be interrogated with red or near-infrared light (i.e. above 600 nm), which minimizes background interference in biological samples (see the figure at the left). These unique characteristics are met by a group of long-wavelength absorbing cyanine dyes carrying a reactive chloro substituent for nucleophilic substitution with primary amines, which is accompanied by a color change from green to blue. In addition to this so-called chameleon effect, the dyes exhibit a change in fluorescence. Despite their structural similarity, the reactivity of the dyes differs strongly. The fastest labeling kinetics is observed with dye S 0378 as its five-membered ring affords a stabilizing effect on the intermediate carbocation during an SN1-type of nucleophilic substitution. The reaction mechanism of the amine-reactive cyanine dyes provides a blueprint for the design of future long-wavelength absorbing chameleon dyes.



**533. Review. Optical Methods for Sensing Glucose.** M. S. Steiner, A. Duerkop, O. S. Wolfbeis; *Chem. Soc. Rev.* (2011), 40, 4805-4839. DOI: 10.1039/c1cs15063d. Journal IF: 26.6.

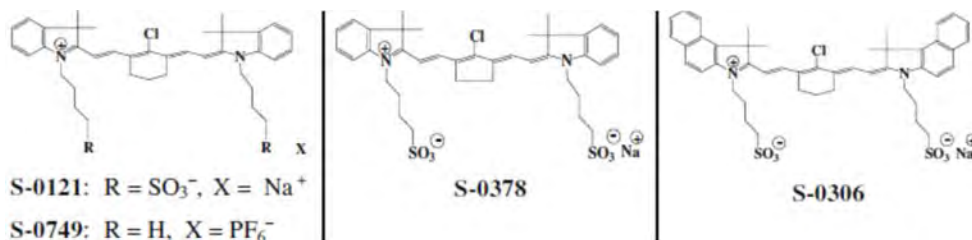
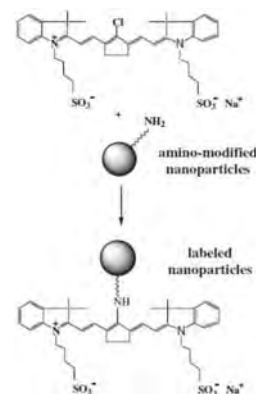
**Abstract:** This review covers the present state of the art in optical sensing of glucose. Following an introduction into the significance of (continuous) sensing of glucose and a brief look back, we discuss methods based on (a) monitoring the optical properties of intrinsically fluorescent or labeled enzymes, their co-enzymes and co-substrates; (b) the measurement of the products of enzymatic oxidation of glucose by glucose oxidase; (c) the use of synthetic boronic acids (BA); (d) the use of Concanavalin A; and (e), the application of other glucose-binding proteins. We finally present an assessment of the various methods.



**532. New Silica and Polystyrene Nanoparticles Labeled with Longwave Absorbing and Fluorescent Chameleon Dyes.** S. M. Saleh, R. Ali, O. S. Wolfbeis; *Microchim Acta* (2011), 174, 429-434. DOI: 10.1007/s00604-011-0627-y. journal IF: 2.6.

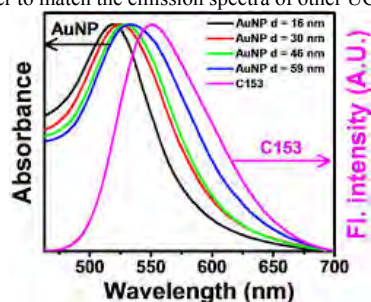
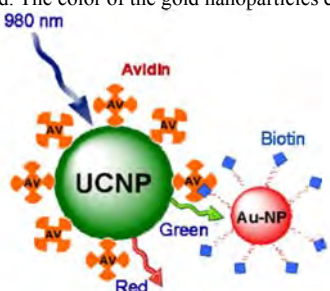
**Abstract:** We are presenting new fluorescent nanoparticles (NPs) made from silica or polystyrene. Such NPs are potentially useful for purposes of cellular imaging and sensing. The NPs were surface-modified with amino groups, and longwave absorbing and emitting dyes were then conjugated, via their reactive chloro atoms, to the NPs. The reactions proceed at temperatures of around 65 °C and in predominantly aqueous solution, and are accompanied by a color change from typically green to blue. By analogy to other labels giving this effect, we refer to such dyes as chameleon labels. All NPs were characterized in terms of size, by absorption and emission spectroscopy, thermogravimetry and zeta potentials. The chameleon effect also was used to detect the presence of minute quantities of amino groups on the surface of NPs, both by absorptimetry and, with particular sensitivity, by fluorescence.

Shown below (↓) are hemical structures of representative reactive labels.



**531. Detection of Biotin-Avidin Affinity Binding by Exploiting a Self-Referenced System Composed of Upconverting Nanoparticles and Gold Nanoparticles.** S. M. Saleh, R. Ali, T. Hirsch, O. S. Wolfbeis; *J. Nanoparticle Res.* (2011), 13, 4603-4611. DOI: 10.1007/s11051-011-0424-x. IF 3.3.

**Abstract:** We describe an affinity system based on the interaction of two types of nanoparticles. The first consists of upconverting luminescent NaYF<sub>4</sub>:Yb,Er nanoparticles (UCLNPs) with a size of 40 – 100 nm, absorbing light in the infrared and showing luminescence at 521, 543 and at 657 nm. The second consists of (red) gold nanoparticles (Au-NPs) with a size of about 50 nm and capable of absorbing the green luminescence of the UCNPs. The UCNPs were coated with silica and then labeled with avidin, while the AuNPs were coated with biotin. The two kinds of NPs represent a self referenced bioaffinity system that is applicable to biosensing in biological samples. In the presence of avidin-modified UCNPs, the biotinylated Au-NPs can be detected in the range from 12 to 250 µg·mL<sup>-1</sup> by ratioing the intensity of the red (analyte-independent) emission to that of the green (analyte-dependent) emission band. The color of the gold nanoparticles can be adjusted via their charge in order to match the emission spectra of other UCLNPs.





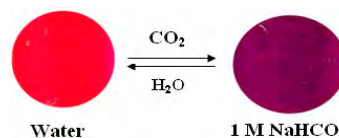
**530. Review. Fluorescent Sensing, Biosensing, and Screening Using Upconverting Nanoparticles.** D. E. Achatz, A. Reham, O. S. Wolfbeis; *Topics Curr. Chem.* (2011), 300, 29-50. DOI: 10.1007/128 2010 98. Journal IF: 4.3.

**Abstract:** Upconverting nanoparticles (UCNPs) display the unique property of converting near-infrared light (with wavelengths of typically 800 to 1000 nm) into visible luminescence. The main classes of materials are discussed. We also review the state of the art of using UCNPs (a) to label biomolecules such as antibodies and (synthetic) oligomers for use in affinity assay and flow assays; (b) to act as nanolamps whose emission intensity is modulated by chemical indicators, thus leading to a novel kind of chemical sensors; and (c), in FRET-based chemical sensors and biosensors.



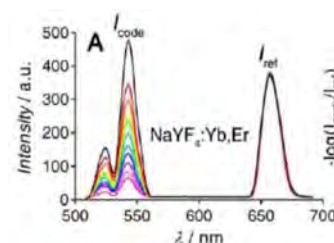
**529. Optical Sensing Scheme for Carbon Dioxide Using a Solvatochromic Probe.** R. Ali, T. Lang, S. M. Saleh, R. J. Meier, O. S. Wolfbeis; *Anal. Chem.* (2011), 82, 2846-2851. DOI: 10.1021/ac200298j. Journal IF: 5.8.

**Abstract:** The sensing scheme – unlike previous ones that are based on the use of pH indicator probes – is making use of solvatochromic probe Nile Red (NR). Dissolved in a matrix of ethyl cellulose, it can report the polarity of its microenvironment that is modulated by an additive (a hydrophobic amidine) which – in turn – is capable of reversibly binding carbon dioxide. The spectra of NR undergo a strong solvatochromic shift both in color (from brick-red to magenta) and in fluorescence (from orange to red) if the respective sensor layer is exposed to gaseous CO<sub>2</sub> (gCO<sub>2</sub>) or dissolved CO<sub>2</sub> (dCO<sub>2</sub>). Both visual and instrumental readout are possible. The detection limits are around 0.23% for gCO<sub>2</sub> and 1.53 hPa for dCO<sub>2</sub>. The response time is in the order of 10 min in the forward direction, and 3 min in the reverse direction for gCO<sub>2</sub>. The optical response also can be quantified using a digital camera by extracting the spectral information contained in the blue and green color channels (in reflectometry), or in the green and red channels (in fluorescence), resp.. Pseudo-color pictures also enable RGB imaging of the spatial distribution of pCO<sub>2</sub>.



**528. Tuning the Dual Emission of Photon-Upconverting Nanoparticles for Ratiometric Multiplexed Encoding.** H.-H. Gorris, R. Ali, S. M. Saleh, O. S. Wolfbeis; *Adv. Mater.* (2011) 23, 1652-1655. DOI: 10.1002/adma.201004697. Journal IF: 10.9.

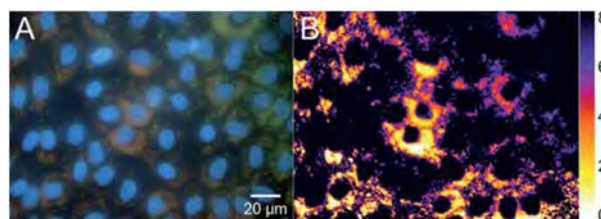
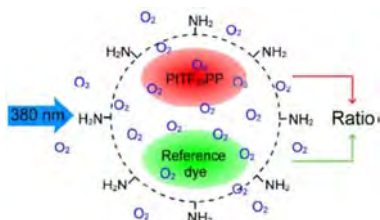
**Abstract:** Commercially available longwave dyes were immobilized in different concentrations on the surface of upconverting luminescent nanoparticles in order to selectively tune one of the dual emission bands ( $I_{code}$ ). The second emission band ( $I_{ref}$ ), by contrast, serves as an internal reference to obtain ratiometric codes. Combining UCNPs with distinct emission bands expands the coding capacity exponentially.



**527. Self-Referenced RGB Colour Imaging of Intracellular Oxygen.** X. D. Wang, H. H. Gorris, J. A. Stolwijk, R. J. Meier, D. B. M. Groegel, J. Wegener, O. S. Wolfbeis; *Chem. Sci. (Cambridge)* (2011) 2, 901-906. DOI: 10.1039/c0sc00610f. Journal IF: 7.5.

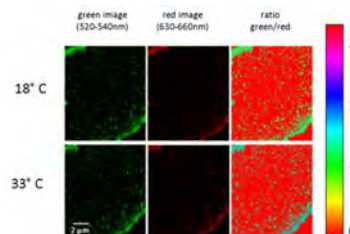
**Abstract:** The nanosensors contain two luminophores matching the red and the green channels of red-green-blue (RGB) color cameras. The red emission of the

oxygen probe is quenched by oxygen, while the (constant) blue-green emission of the second fluorophore serves as a reference. The dyes are incorporated into polystyrene particles for in-sensing of oxygen. The image on the right shows (A) a conventional photographic picture, and (B), the ratioed picture in pseudo-colors that reflects the concentration of oxygen (in ppm) according to the calibration bar (right).



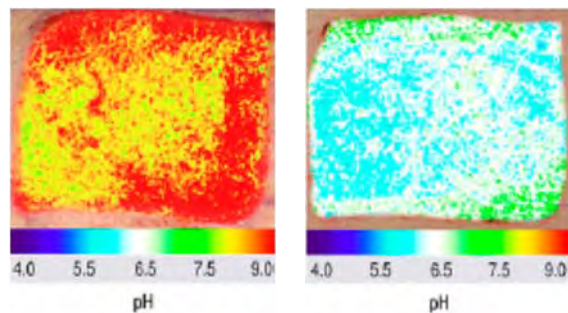
**526. Highlight Article. Upconversion Nanoparticles for Nanoscale Thermometry.** L. H. Fischer, G. S. Harms, O. S. Wolfbeis; *Angew. Chem. Intl. Ed.* (2011) 50, 4546-4548. DOI: 10.1002/anie.201006835. Journal IF: 12.7.

**Abstract:** Lanthanide ion-doped nanoparticles display a strongly temperature-dependent luminescence that can be used to sense temperature in sub-μm dimensions, for example in cells or nanofluidics. Unlike molecular probes, the use of such nanoparticles with their anti-Stokes emission is not interfered by background luminescence, and the excitation wavelengths (> 700 nm) are hardly absorbed by cells.



**522. 2D Luminescence Imaging of Wound pH.** S. Schreml, R. J. Meier, O. S. Wolfbeis, M. Landthaler, R.-M. Szeimies, P. Babilas; *Proc. Natl. Acad. Sci. USA* (2011) 108, 2432-2437. DOI: 10.1073/pnas.1006945108. Journal IF: 9.8.

**Abstract:** We are presenting a luminescent sensor for 2D, high-resolution imaging of pH *in vivo*. The sensing scheme is based on luminescence imaging of fluorescein and a ruthenium phenanthroline complex. To create a biocompatible 2D sensor, these dyes were bound to or incorporated in microparticles (aminocellulose, poly-acrylonitrile) and particles were immobilized in polyurethane hydrogel on transparent foils. We demonstrate sensor precision and validity by conducting *in vitro* and *in vivo* experiments, and show the versatility in imaging pH during physiological and chronic cutaneous wound healing in humans. Implementation of this technique may open new vistas in wound healing, tumor biology and other biomedical fields. The graphs show images of the pH of an acute wound (left) and 14 days *p. o.* (right).



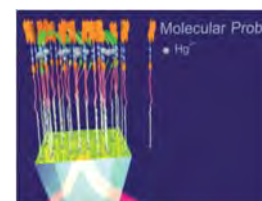
**Advanced Fluorescence Reporters in Chemistry and Biology III: Applications to Sensing and Imaging.** A. P. Demchenko (ed.); *Springer Series on Fluorescence*, vol. 10, 2011, (O. S. Wolfbeis, Series Ed.); 352 pp. ISBN: 978-3-642-18034-7.

**Contents:** \*Interfacial behavior of fluorescent dyes. Power and weakness of nanoscopic description; \*Fluorescence probing of physicochemical characteristics of the room temperature ionic liquids; \*Fluorescence spectroscopy in polymer science; \*Fluorescence probing in structurally anisotropic materials. From liquid crystals to macromolecules, micelles and lipid bilayers; \*Optimized dyes for protein and nucleic acid detection; \*Functional nucleic acids for fluorescence based biosensing applications; \*Covalent labeling of biomolecules in living cells; \*Tetracysteine and bipartite tags for biarsenical organic fluorophores; \*Labeling of oligohistidine-tagged proteins; \*In vivo imaging of vascular targets using near-infrared fluorescent probes; \*Whole-body imaging of hematopoietic and cancer cells using near infrared probes. Also see: [www.springer.com/series/4243](http://www.springer.com/series/4243).



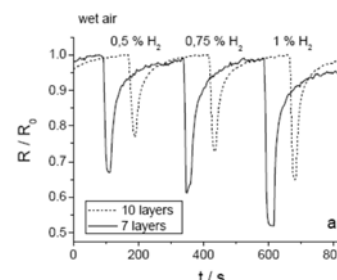
**521. Selective Picomolar Detection of Mercury(II) in Water Using Optical Sensors.** C. Diez-Gil, R. Martinez, I. Ratera, T. Hirsch, A. Espinosa, A. Tarraga, P. Molina, O. S. Wolfbeis, J. Veciana; *Chem. Comm.* (2011), 47, 1842-1844. DOI: 10.1039/C0CC04860G. Open access. Journal IF: 5.8.

**Abstract:** The rational design of a functionalized self-assembled monolayer on a gold surface containing a 2,3-diaza-1,3-butadiene receptor unit enables highly sensitive and selective detection of mercury (II) concentrations on aqueous media on the picomolar range, meliorating on three orders of magnitude the EPA mercury (II) detection limit on potable water.



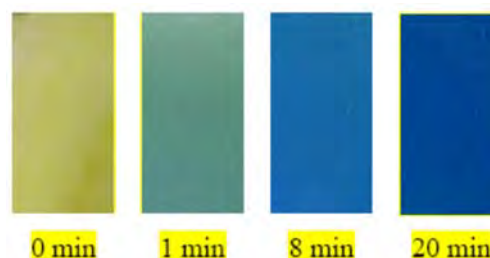
**520. Hydrogen Sensor Based on a Graphene-Palladium Nanocomposite.** U. Lange, T. Hirsch, V. M. Mirsky, O. S. Wolfbeis; *Electrochim. Acta* (2010), 56, 3707-3712. DOI: 10.1016/j.electacta.2010.10.078. Journal IF: 3.6.

**Abstract:** We describe a sensor for detecting hydrogen at levels from 0.5 to 1% in synthetic air. Pure graphene is poorly sensitive to hydrogen, but incorporation of PdNPs increases its sensitivity by more than an order of magnitude. The effects of hydrogen, nitrogen dioxide and humidity were studied. The sensor regeneration was accelerated essentially in humid air. The sensitivity of the nanocomposite depends on the number of bilayers of graphene-PdNPs prepared via layer-by-layer deposition on gold electrodes. The material was characterized by absorption spectroscopy, scanning electron and Raman spectroscopy, and surface plasmon resonance. Cyclic voltammetry demonstrated the presence of electrocatalytic centers in the palladium-decorated graphene.



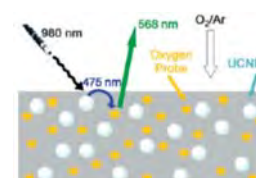
**519. Irreversible Sensing of Oxygen Ingress.** S. Wilhelm, O. S. Wolfbeis; *Sensors Actuat. B* (2010), 153, 199-204. DOI: 10.1016/j.snb.2010.10.037. IF 3.4.

**Abstract:** Absorption-based opto-chemical sensors for oxygen are presented that consist of leuco dyes (leuco indigo and leuco thioindigo) incorporated into two kinds of polymer matrices. An irreversible and visible color change (to red or blue) is caused by a chromogenic chemistry involving the oxidation of the (virtually colorless) leuco dyes by molecular oxygen. The moderately gas permeable copolymer poly(styrene-co-acrylonitrile) and a highly oxygen-permeable polyurethane hydrogel, respectively, are used in order to increase the effective dynamic range for visualizing and detecting oxygen. We describe the preparation and properties of four different types of such oxygen sensors that are obtained by dip-coating a gas impermeable foil made from poly(ethylene terephthalate) with a sensor layer composed of leuco dye and polymer. The figure shows the color changes that occur with a typical film on exposing it to air.



**518. Luminescent Sensing of Oxygen Using a Quenchable Probe Along with Upconverting Nanoparticles.** D. E. Achatz, R. J. Meier, L. H. Fischer, O. S. Wolfbeis; *Angew. Chem. Intl. Ed.* (2011), 50, 260-263. DOI: 10.1002/anie.201004902. IF 12.7.

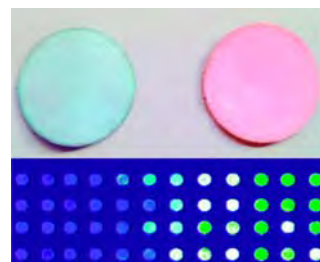
**Abstract:** We are presenting the first sensor for oxygen that can be excited with NIR light. It makes use of upconverting nanoparticles of the type NaYF<sub>4</sub>: Yb, Tm that are photo-excited with a 980-nm laser and whose visible luminescence is used to photoexcite a quenchable iridium probe for oxygen, thereby overcoming the lack of NIR-excitable probes for oxygen. The components and materials used are readily available, and merits of working at such long excitation wavelength include the complete absence of luminescence background that can be strong in many samples to be analyzed. A new type of ratiometric readout also is demonstrated.





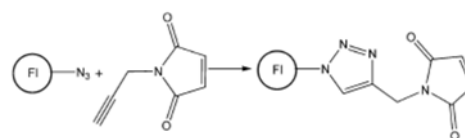
**515. Chromogenic Sensing of Biogenic Amines Using a Chameleon Probe and the Red-Green-Blue Readout of Digital Camera Images.** M. S. Steiner, R. J. Meier, A. Duerkop, O. S. Wolfbeis; *Anal. Chem.* (2010), 82, 8402-8405. DOI: 10.1021/ac102029j. Journal IF: 5.2.

**Abstract:** We report on sensing spots containing an amine reactive chromogenic probe and a green fluorescent (amine insensitive) reference dye incorporated in a hydrogel matrix on a solid support. Such spots enable the direct determination of primary amines and, especially, biogenic amines (BA). A distinct color change from blue to red occurs on dipping the test spots into a pH 9.0 sample containing primary amines. BAs can be determined in the concentration range from 0.01 to 10 mM within 15 min, enabling rapid, qualitative, and semiquantitative evaluation. In the "photographic" approach, the typically 4-7.5-fold increase in fluorescence intensity of the probe at 620 nm along with the constant green fluorescence at 515 nm of a reference dye are used for quantitation of BAs. The sensing spots are photoexcited with high-power 505 nm light-emitting diodes (LEDs) in a black box. A digital picture is acquired with a commercially available digital camera, and the color information is extracted via red-green-blue (RGB) readout. The ratio of the intensities of the red channel and the green (reference) channel yields pseudocolor pictures and calibration plots.



**514. Click Chemistry Based Method for the Preparation of Maleimide-Type Thiol-Reactive Labels.** M. Link, X. Li, J. Kleim, O. S. Wolfbeis; *Eur. J. Org. Chem.* (2010), 6922-6927. DOI: 10.1002/ejoc.201001085. Journal IF: 3.1.

**Abstract:** The so-called click reaction is shown to allow the efficient introduction of the maleimido group into azido-modified benzoxazines by reacting them with an alkyne-modified maleimide to yield thiol-reactive fluorescent labels 5-7. The reaction proceeds under mild conditions and provides a new strategy to introduce the maleimide group into fluoro-phores. Conceivably, it may be extended to radioactive, electro-active, isotopic, or spin labels.



**513. Opto-Chemical Micro-Capillary Clocks.** S. Wilhelm, O. S. Wolfbeis; *Microchim. Acta* (2010), 171, 211-216. DOI: 10.1007/s00604-010-0456-4. Journal IF: 2.6. **Abstract:** Opto-chemical capillary clocks are presented that are based on the measurement of a colored segment in a microchannel. Color is created by a chromogenic chemistry involving the oxidation of a virtually colorless leuco-dye. Poly(ethylene glycol) (PEG) is used as a solvent, and indigo and thioindigo (in their reduced leuco forms) act as oxygen-sensitive dyes. The clock is started by removing one seal at the end of the capillary. A visible color change occurs as air diffuses into the microchannel due to an irreversible color reaction. The length of the colored segment is proportional to the time elapsed. PEGs of different average molar mass affect the diffusion rate of oxygen in the microchannel and thereby affect the rate of the migration of the color front. Both temperature and relative humidity exert a strong effect. Six types of such clocks are described that enable times to be determined in the range from 1 day to 6 months, possibly of decades.



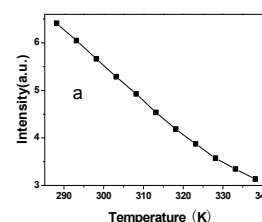
**512. Review. Upconverting Luminescent Nanoparticles for Use in Bioconjugation and Bioimaging.** H. S. Mader, P. Kele, S. M. Saleh, O. S. Wolfbeis; *Curr. Opin. Chem. Biol.* (2010), 14, 582-596. DOI: 10.1016/j.cbpa.2010.08.014. Journal IF: 8.3.

**Abstract:** Upconverting luminescent nanoparticles (UCNPs) display the unique property of emitting visible light following photoexcitation with near-infrared laser light. This results in features such as virtually zero auto-fluorescence of (biological) matter and easy separation of the emission peaks from stray light. Other features include rather narrow emission bands, very high chemical stability, the lack of bleaching, and the absence of blinking effects. This article reviews the work performed in the past few years with UCNPs in terms of surface modifications, bioconjugation, and optical (cellular) imaging.



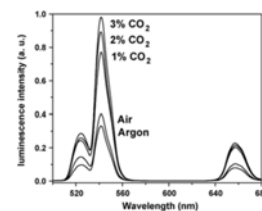
**511. Temperature-Sensitive Luminescent Nanoparticles and Films Based on a Terbium(III) Complex Probe.** L. Sun, J. Yu, H. Peng, J. Z. Zhang, L. Shi, O. S. Wolfbeis; *J. Phys. Chem. C* (2010), 114, 12642-12648. DOI: 10.1021/jp1028323. Journal IF: 4.2.

**Abstract:** The terbium-tris[(2-hydroxy-benzoyl)-2-aminoethyl]amine complex (Tb-THBA) with its high color purity, long luminescence lifetime and high quantum yield has been found to be a viable indicator for optical sensing of temperature ( $T$ ). Both its luminescence intensity and lifetime strongly depend on  $T$  in the range from 15 to 65 °C. When photoexcited at 341 nm, it displays typical Tb<sup>3+</sup> ion emission bands with the strongest peak at 546 nm and a typical decay time of 1.15 ms at 15 °C. The probe is shown to be an excellent for sensing  $T$ , as demonstrated in two kinds of optical sensor membranes.



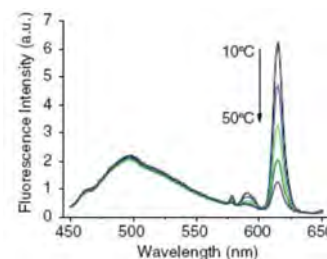
**510. Upconverting Nanoparticle Based Optical Sensor for Carbon Dioxide.** R. Ali, S. M. Saleh, R. J. Meier, H. A. Azab, I. Elgawad, O. S. Wolfbeis; *Sensors Actuat. B (Chemical)* (2010), 150, 126-131. DOI: 10.1016/j.snb.2010.07.031. IF 3.1.

**Abstract:** We demonstrate a novel optical sensor for carbon dioxide in concentrations between 0 and 3%. The sensing scheme is based on the optical interrogation of a 12- $\mu\text{m}$  polystyrene (PS) film containing upconverting nanoparticles (UCNPs; 40 – 100 nm in size) of the type  $\text{NaYF}_4:\text{Yb,Er}$ , and the longwave absorption pH probe bromothymol blue (BTB) in its anionic (blue) form. PS is chosen as a matrix because it displays permeation selectivity for  $\text{CO}_2$  and rejects protons. The color of BTB in the PS matrix depends on the partial pressure of  $\text{CO}_2$  gas. The UCNPs are photoexcited with a 980-nm laser diode to give a green (542 nm) and a red (657 nm) emission whose intensity is screened off (depending on whether BTB is present in its blue or yellow form) due to an inner filter effect.



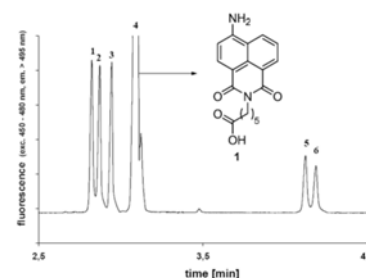
**509. Ratiometric Fluorescent Nanoparticles for Sensing Temperature.** H. Peng, S. Huang, O. S. Wolfbeis; *J. Nanoparticle Res.* (2010), 12, 2729-2733. DOI: 10.1007/s11051-010-0046-8. Journal IF: 2.5.

**Abstract:** Nanoparticles made from a poly(methyl methacrylate)-co-1,2-bis(trimethoxysilyl)decane composite and containing a red-luminescent europium(III) complex were prepared by the encapsulation-precipitation method. By introducing a green-emitting naphthalimide reference dye, the NPs display both a green and a red fluorescence under single-wavelength excitation. The ratio of fluorescence intensities is highly temperature dependent in the 25 - 45  $^{\circ}\text{C}$  range, with a sensitivity of  $-4.0\%$  per  $^{\circ}\text{C}$ . Given their small size (20 – 30 nm) and biocompatibility (due to the presence of an outer layer of silica), such NPs are useful *T* sensors for cellular sensing and imaging.



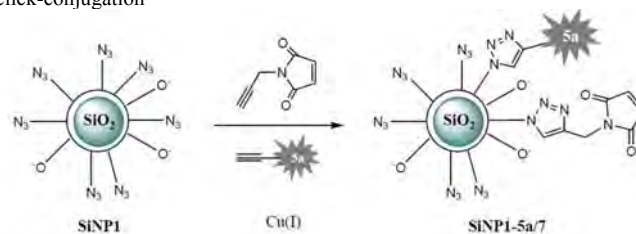
**508. A New Weakly Basic Fluorescent Label for Use in Isoelectric Focusing and Chip Electrophoresis.** P. Schulze, M. Link, M. Schulze, S. Thuermann, O. S. Wolfbeis, D. Belder; *Electrophoresis* (2010), 31, 2749-2753. DOI: 10.1002/elps.201000007. IF 3.1.

**Abstract:** We present a amino-reactive fluorescence marker (referred to as UR-431) that is well suited for electrophoretic techniques. The pH independent fluorescence intensity of the fluorophore makes UR-431 very interesting for electrophoretic applications such as isoelectric focusing. The absorption maximum of the yellow daylight chromophore is 431 nm, whereas fluorescence emission is observed at 537 nm (quantum yield 10%). The on-chip detection limit of labeled lysine is 12 nM. An important feature of the new label is that it effects only a subtle change of the pI value of proteins compared to common anionic labels, e.g. fluorescein isothiocyanate. This was studied by comparing isoelectric properties of native proteins and labeled proteins in capillary isoelectric focusing. UR-431 was also applied to sensitive detection of amines and peptides in MCE.



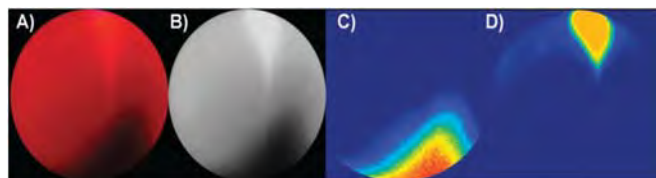
**507. Colloidal Silica Nanoparticles for Use in Click Chemistry-Based Conjugations and Fluorescent Affinity Assays.** D. E. Achatz, F. J. Heiligtag, X. Li, M. Link, O. S. Wolfbeis; *Sensors Actuat. B (Chemical)* (2010), 150, 211-219. DOI: 10.1016/j.snb.2010.07.014. IF 3.1.

**Abstract:** Silica nanoparticles (SiNPs) with an average diameter of 25 nm were prepared by a one-pot method that involves the formation of a silica core that is subsequently covered with a shell functionalized with either azido groups or alkyne groups for use in copper(I)-catalyzed click reactions. Respective triethoxysilane reagents are presented. The SiNPs were (a) rendered fluorescent by click-conjugation to fluorophores of various colors, and (b) made bioconjugatable by introducing maleimide groups (that covalently bind thiols) and biotin (a widely used bioaffinity reagent that binds streptavidin). Particles were characterized by transmission electron microscopy, infrared spectroscopy, fluorescence, and light scattering. The fluorescently labeled SiNPs carrying maleimido groups were conjugated to the thiol group of bovine serum albumin (BSA) labeled with a fluorophore, and fluorescence resonance energy transfer was shown to occur between the labeled SiNPs and the labeled BSA. This is considered to represent a new approach towards nanoparticlebased fluorescent bioassays.



**506. Review: Multiple Fluorescent Chemical Sensing and Imaging.** M. I. J. Stich, L. H. Fischer, O. S. Wolfbeis; *Chem. Soc. Rev.* (2010), 39, 3102-3114. DOI: 10.1039/b909635n. Journal IF: 20.1.

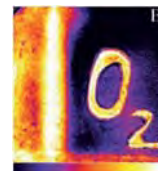
**Abstract:** Optical sensors, unlike most others, enable multiple sensing of (bio) chemical species by making use of probes whose signals can be differentiated by spectral and/or temporal resolution. Multiple sensors are of substantial interest for continuous monitoring of chemical parameters in complex samples. Such sensors enable non-invasive, non-toxic and online detection. We are discussing here the state of the art in terms of spectroscopic principles, materials (mainly indicator probes and polymers), and are giving selected examples for dual and triple sensors (such as combined sensing of  $\text{O}_2/\text{CO}_2$ ,  $\text{pH}/\text{O}_2$ ,  $\text{pH}/\text{temperature}$ ,  $\text{O}_2/\text{T}$ ,  $\text{O}_2/\text{T}/\text{pH}$ ,  $\text{O}_2/\text{T}/\text{glucose}$  and the like).





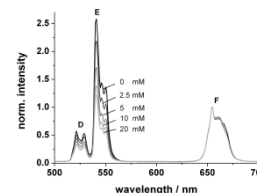
**505. Photographing Oxygen Distribution.** X. Wang, R. J. Meier, M. Link, O. S. Wolfbeis; *Angew. Chem. Int. Ed.* (2010), 49, 4907-4909. DOI: 10.1002/anie.201001305. Journal IF: 11.8.

**Abstract:** The spatial distribution of oxygen can be imaged with a conventional digital camera by making use of a specially designed sensor film containing a quenchable red-fluorescent probe for oxygen along with a green-emitting reference fluorophore. It exploits the RGB option of digital photography and this has resulted in a simple method for quantitative sensing and imaging of this important species.



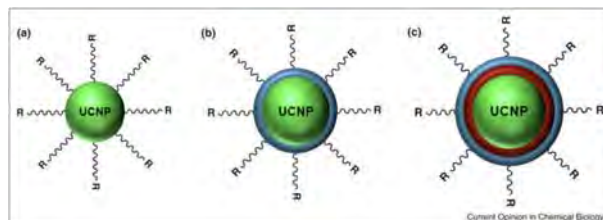
**504. Optical Ammonia Sensor Based on Upconverting Luminescent Nanoparticles.** H. S. Mader, O. S. Wolfbeis; *Anal. Chem.* (2010), 82, 5002-5004. DOI: 10.1021/ac1007283. Journal IF: 5.2.

**Abstract:** The sensor exploits the phenomenon of upconversion luminescence and is based on (a) the use of upconverting nanoparticles (UCNPs) of the NaYF<sub>4</sub>:Yb,Er type that can be excited with 980 nm laser light to give a green and red luminescence and (b) the pH probe phenol red immobilized in a polystyrene matrix. Exposure of the sensor film to ammonia causes a strong increase in the 560 nm absorption of the pH probe which, in turn, causes the green emission of the UCNPs to be screened off. The red emission of the UCNPs, in contrast, remains unaffected by ammonia and can serve as a reference signal. Due to the use of 980 nm as the excitation light source, the optical signal obtained is completely free of background visible luminescence of the sample and of scattered light. This is advantageous in the case of sensing ammonia in complex matrices.



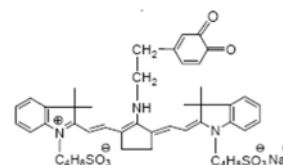
**503. Surface-Modified Upconverting Microparticles and Nanoparticles for Use in Click Chemistries.** H. S. Mader, M. Link, D. E. Achatz, K. Uhlmann, X. Li, O. S. Wolfbeis; *Chem. - Eur. J.* (2010), 16, 5416-5424. DOI: 10.1002/chem.201000117. Journal IF: 5.4.

**Abstract:** We report on a method for modifying the surface of upconverting particles such that they become amenable to click chemistry. Respective reagents are presented and used in both kinds of particles, either directly or in combination with tetraethoxysilane. The particles were labeled, via the click reaction, (a) with fluorophores to yield materials that have emission colors that depend on the wavelength of excitation; (b) with maleimido groups (so to obtain labels for thiols), and (c) with biotin (so to make them useful for affinity studies based on the biotin-streptavidin system). Such particle may be used in numerous areas including upconversion imaging, biolabeling, derivatization, encoding, and security.



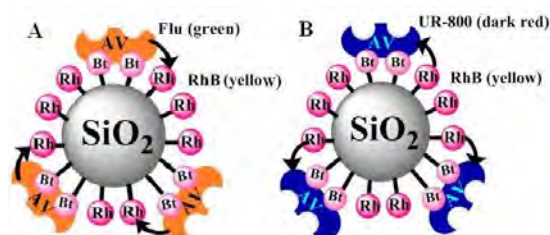
**502. A Near-Infrared Fluorescent Probe for Monitoring Tyrosinase Activity.** X. Li, W. Shi, S. Chen, J. Jia, H. Ma, O. S. Wolfbeis; *Chem. Comm.* (2010), 2560-2562. DOI: 10.1039/c001225d. Journal IF: 5.5.

**Abstract:** We report on the first NIR fluorescent probe for monitoring tyrosinase activity. Upon reaction with tyrosinase, the tyramine moiety of the probe was oxidized into o-quinone, which leads to quenching via intramolecular electron transfer from the cyanine skeleton to the quinone unit.



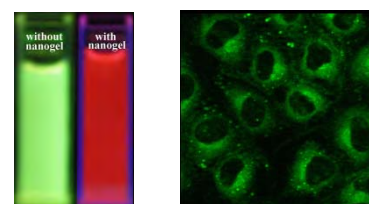
**501. Novel Multicolor Fluorescently Labeled Silica Nanoparticles for Interface Fluorescence Resonance Energy Transfer.** S. M. Saleh, R. Mueller, H. M. Mader, A. Duerkop, O. S. Wolfbeis; *Anal. Bioanal. Chem.* (2010) 398, 1615-1623. DOI: 10.1007/s00216-010-3758-9. Journal IF: 3.5.

**Abstract:** Fluorescent silica nanoparticles (SiNPs) were prepared by covalent attachment of fluorophores to the amino-modified surface of SiNPs with a typical diameter of 15 nm. The SiNPs are intended for use in novel kinds of fluorescence resonance energy transfer (FRET) based affinity assays at the interface between nanoparticle and sample solution. Various labels were employed to obtain a set of SiNPs with excitation maxima ranging from 337 to 659 nm, and emission maxima ranging from 436 nm to the near infrared (710 nm). The surface of the fluorescent SiNPs was bio-tinylated, and binding of labeled avidin to the surface was studied via fluorescence resonance energy transfer (FRET) in two model cases. In the first, FRET occurs from the biotinylated fluorescent SiNP (the donor) to the labeled avidin (the acceptor). In the second, FRET occurs in the other direction.



**500. A Nanogel for Ratiometric Fluorescent Sensing of Intracellular pH Values.** H. Peng, J. A. Stolwijk, L. Sun, J. Wegener, O. S. Wolfbeis; *Angew. Chem. Int. Ed.* (2010), 49, 4246-4249. DOI: 10.1002/anie.200906926. Journal IF: 11.8.

**Abstract:** We are reporting on the first ratiometric fluorescent nanogel (NG) for sensing pH. It can be easily prepared and made pH-responsive via addition of a pH probe and a (ratiometric) FRET system. It has been used to ratiometric imaging of pH inside cells.

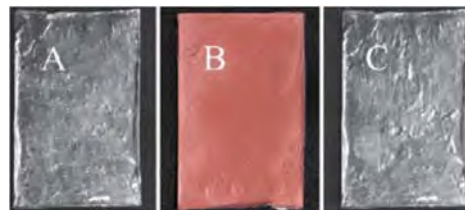


**497. Dual Sensing of pO<sub>2</sub> and Temperature Using a Water-Based and Sprayable Fluorescent Paint.** L. H. Fischer, S. M. Borisov, M. Schaeferling, I. Klimant, O. S. Wolfbeis; *Analyst* (2010) 135, 1224-1229. DOI: 10.1039/b927255k. Journal IF: 3.8.

**Abstract:** Core-shell particles (NPs) composed of a polystyrene core and a poly(vinyl pyrrolidone) shell were dyed with a luminescent platinum(II) porphyrin probe for oxygen. In parallel, microparticles were dyed with a luminescent iridium(II) complex acting as a probe for temperature (T). The particles were

deposited (by spraying) on a surface to enable continuous imaging of the distribution of oxygen (and thus of barometric pressure) and  $T$ . Unlike in most previous paints of this kind, a binder polymer is not needed and water can be used as a dispersant. This makes the paint environmentally friendly and reduces costs in terms of occupational health and disposal.

Both indicator probes can be excited at 405 nm using LEDs or diode lasers, whilst their emission maxima are spectrally separated by about 130 nm. Thus, two independent optical signals are obtained that allow for fluorescent imaging of barometric pressure (in fact oxygen partial pressure) and of  $T$ , but also to correct the oxygen signal for effects of  $T$ . The paint was calibrated at air pressures ranging from 50 mbar to 2000 mbar and at  $T$ 's between 1 °C and 50 °C. The images show the aluminum foil before and after coating and washing. (A) Before spraying it with the PS/PVP particles; (B) after spraying it with the red paint (dyed with PtTFPP), and (C) after removing the red paint with water.

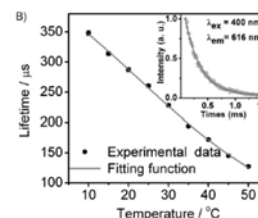
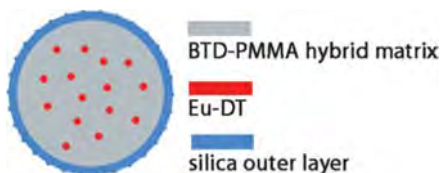


#### 496. Luminescent Europium(III) Nanoparticles for Sensing and Imaging of Temperature in the Physiological Range.

H. Peng, M. I. J. Stich, J. Yu, L. Sun, L. H. Fischer, O. S. Wolfbeis; *Adv. Mat.* (2010), 22, 716-719. DOI:

10.1002/adma.200901614. Journal IF: 8.4.

**Abstract:** Lanthanide-based nano-particles with a diameter of 20–30 nm are introduced for use in luminescent sensing and imaging of physiological temperatures. They are characterized by (i) visible-light photo-excitation, (ii) line-like emission (which facilitates multicolor (dual) sensing), (iii) inert-ness to external perturbations as a result of encapsulation of the europium probe into a biocompatible protective nanoshell, (iv) high photostability, (v) a dynamic range that covers  $T$ 's encountered in medicine, (cellular) biology, and biotechnology, and (vi) good resolution (typically  $\pm 0.3$  °C).

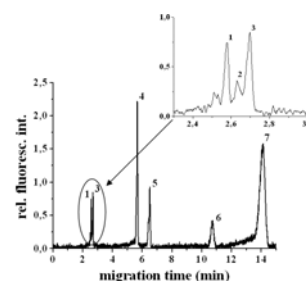


#### 493. Determination of Biogenic Amines by Capillary Electrophoresis Using a Chameleon Type of Fluorescent Stain.

M. S. Steiner, R. Meier, A. Duerkop, O. S. Wolfbeis; *Microchim. Acta* (2009) 167, 259-266. DOI: 10.1007/s00604-

009-0247-y. Journal IF: 2.6.

**Abstract:** A method was developed for the determination of biogenic amines (BAs) via micellar electrokinetic chromatography along with laser induced fluorescence detection using the amino-reactive chameleon stain Py-1. A labeling protocol was established for seven primary BAs by optimizing the reaction conditions in terms of the amount of reagents, reaction temperature, reaction time and solvent. Derivatization was accomplished within 30 min and is visible by the naked eye because it is accompanied by a color change from blue to red. Separation of the labeled BAs was achieved within 15 min with a background buffer of pH 2.5 containing phosphate, Tween®80, and methanol.

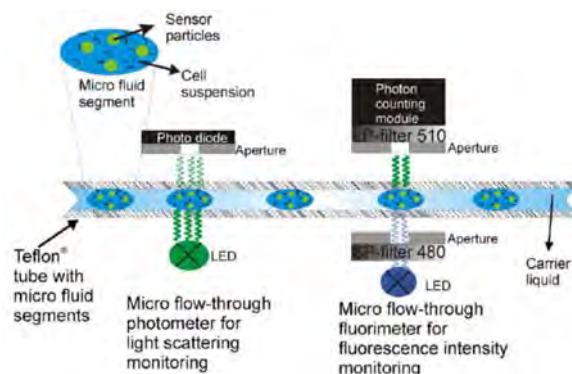


#### 492. Highly Resolved Dose-Response Functions for Drug-Modulated Bacteria Cultivation Obtained by Fluorometric and Photometric Flow-Through Sensing in Microsegmented Flow.

A. Funfak, R. Hartung, J. Cao, K. Martin, K.-H. Wiesmüller, O. S. Wolfbeis, J. M. Koehler; *Sens. Act. B: Chem.* (2009), 142, 66–72. DOI: 10.1016/j.snb.2009.07.017. Journal

IF: 3.1.

**Abstract:** The microfluid segmental technique was applied to the investigation of dose-response relationships of cell cultures. The concentration-dependent response of an *Escherichia coli* culture was studied with respect to the effectors of 2,4-dinitrophenol and an antibacterial peptide amide (KKVVFVKVFK-NH<sub>2</sub>). Large sequences with up to 250 micro fluid segments containing gradually varying concentrations of the effectors were generated using a microfluidic arrangement. The response of the cell culture was followed by a double sensor system. A twin arrangement of a micro flow-through photometer and a micro flow-through fluorometer was used along with the application of pH-sensitive polymer sensor particles. This experimental setup allows a detailed determination of drug-related changes in fluorescence intensity by the bacterial culture and of the sensor particles as a function of time. The segmented flow technique for multi-parameter drug screening provides new insights into the biological response cultivated at the nanoliter scale.

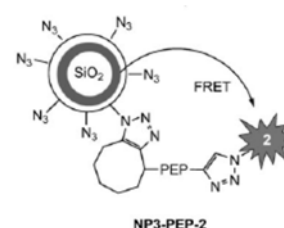


#### 491. Probing the Activity of Matrix Metalloproteinase II Using a Sequentially Click-Labeled Silica Nanoparticle FRET Probe.

D. E. Achatz, G. Mezö, P. Kele, O. S. Wolfbeis; *ChemBioChem* (2009), 10, 2316-1320. DOI:

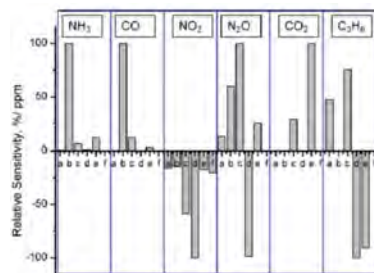
10.1002/cbic.200900261. Journal IF: 3.3.

**Abstract:** Fluorescent core-shell silica nanoparticles (SiNPs) bearing a fluorescently labeled substrate for the tumor marker protease MMP-2 were prepared. FRET from the SiNP to the label is observed but suppressed once the substrate is hydrolyzed by the enzyme. The reaction rate is a direct parameter for determining the activity of MMP-2.



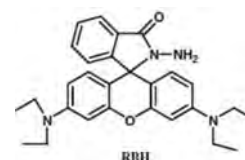
**490. Gas Sensing Properties of Electrically Conductive Copper(I) Compounds at Elevated Temperatures.** B. Wolpert, O. S. Wolfbeis, V. M. Mirsky; *Sens. Actuat. B* (2009), 142B, 446-450. DOI: 10.1016/j.snb.2008.06.047. Journal IF: 3.1.

**Abstract:** The electrical conductance at 240 °C of a number of copper(I) compounds including halides, tellurides, phosphides, and of NiO was studied with respect to its response to ammonia, nitrogen dioxide, nitrous oxide, carbon monoxide, carbon dioxide, and propane. Analytical sensitivity and kinetic parameters were compared quantitatively. The high diversity of sensitivity patterns makes these compounds promising candidates for use in sensor arrays. Principal component analysis of the data obtained with a virtual sensor array enabled highly selective sensing of five of the six analytes studied using only two principle components.



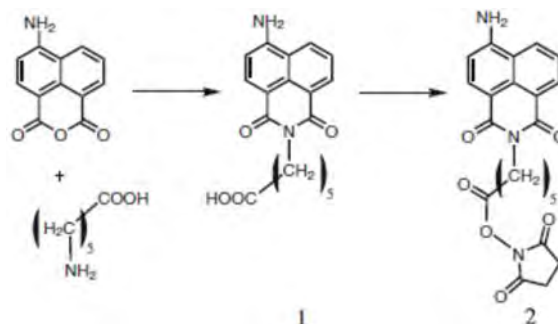
**489. A Fluorescent Probe for Diacetyl Detection.** X. Li, A. Duerkop, O. S. Wolfbeis; *J. Fluoresc.* (2009), 19, 601-606. DOI: 10.1007/s10895-008-0450-y. Journal IF: 1.8.

**Abstract:** A water-soluble fluorescent probe, rhodamine B hydrazide (RBH), was prepared and its properties for recognition of diacetyl were studied. The method employs the reaction of diacetyl with RBH, a colorless and nonfluorescent rhodamine B spiro form derivative to give a pink-colored fluorescent substance. In weakly acidic media, RBH reacts more selectively with diacetyl than with other carbonyls, causing a large increase in fluorescence intensity and thereby providing an easy assay for the determination of diacetyl.



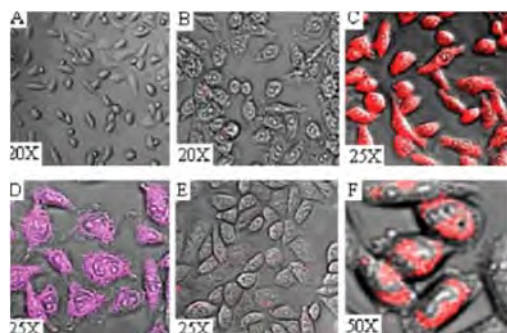
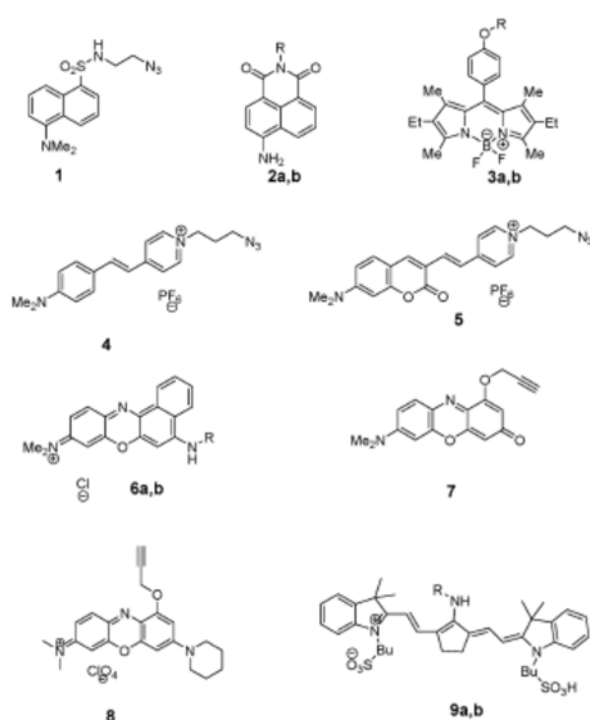
**488. New Diode Laser Excitable and Green Fluorescent Label, and its Application to Detection of Bovine Serum Albumin via Microchip Electrophoresis.** M. Link, P. Schulze, D. Belder, O. S. Wolfbeis; *Microchim Acta* (2009), 166, 183-188. DOI: 10.1007/s00604-009-0169-8. Journal IF: 2.6.

**Abstract:** A novel amino-reactive fluorescent label is presented that is based on a yellow daylight chromophore and fluorophore. Its absorption band is wide and peaks at 431 nm in water solution, thus well matching the lines of either the 375-nm and the 431-nm diode lasers and of many frequency-variable dye lasers. When conjugated to bovine serum albumin (BSA), the fluorescence peaks at 501 nm with a quantum yield of 0.21. Its large Stokes' shift of 70 nm facilitates the discrimination of undesired excitation light which is particularly important for sensitive detection in miniaturized separation techniques such as microchip capillary electrophoresis (MCE). Unlike several other fluorophores, the fluorescence intensity of the new label is independent of pH over a broad range (3 to 9). The applicability of the label is demonstrated by labeling the amino acid lysine and the 66 kD protein BSA, and by separating BSA from the free label via MCE within 90 s. The limit of detection is in the order of 12 nM at an optically active path length of 20 μm.



**487. Clickable Fluorophores for Biological Labeling – With or Without Copper.** P. Kele, X. Li, M. Link, K. Nagy, A. Herner, K. Lőrincz, S. Beni, O. S. Wolfbeis; *Org. Biomol. Chem.* (2009), 7, 3486-3490. DOI: 10.1039/b907741c. Journal IF: 3.6.

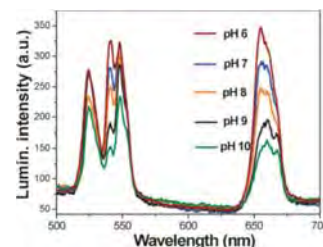
**Abstract:** We describe a set of new clickable fluorophores that virtually cover the whole visible spectrum reaching the near infra-red regime. The dyes are capable of participating in classical copper catalyzed 1,3-dipolar cycloaddition reactions with the counteracting function. We also have prepared dyes containing a cyclooctyne moiety, an alkyne derivative that enables copper free clicking to azides. The suitability of these dyes for fluorescent labeling of biomolecules is presented by examples on model frameworks representing major biopolymer building blocks. The versatility of these dyes is presented in cell labeling experiments as well as by labeling the azide modified surface glycans of CHO-cells either by copper catalyzed or copper-free click reaction. These dyes are expected to have a large variety of applications in (bio)orthogonal labeling schemes both in vivo and in vitro. The figure on the right shows formulas of the clicke reagents. R is -CH<sub>2</sub>-CH<sub>2</sub>-N<sub>3</sub> in compounds (a), and -CH<sub>2</sub>=CH in case of compounds (b).





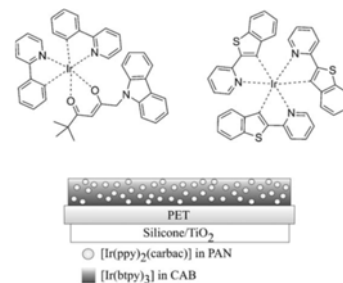
**486. pH Sensor Based on Upconverting Luminescent Lanthanide Nanorods.** L. Sun, H. Peng, M. I. J. Stich, D. E. Achatz, O. S. Wolfbeis; *Chem. Comm.* (2009), 33, 5000-5002. DOI: 10.1039/b907822c. Journal IF: 5.5.

*Abstract:* The pH sensor exploits the phenomenon of upconversion luminescence and is based on a hydrogel matrix containing (a) nanorods of the NaYF<sub>4</sub>:Er,Yb type that can be excited with 980-nm laser light to give a green and red (dual) emission, and (b) a longwave absorbing pH probe that causes a pH-dependent inner filter effect.



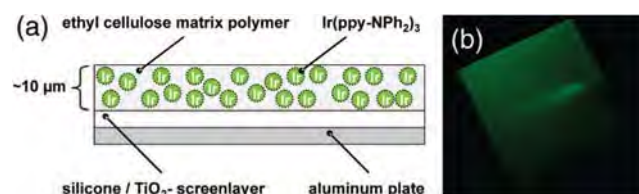
**485. Red and Green Emitting Iridium(III) Complexes for a Dual Barometric and Temperature Sensitive Paint.** L. H. Fischer, M. I. J. Stich, O. S. Wolfbeis, N. Tian, E. Holder, M. Schaeferling; *Chemistry – Eur. J.* (2009), 15, 10857-10863. DOI: 10.1002/chem.200901511. Journal IF: 5.5.

*Abstract:* A dually luminescent paint for measurement of barometric pressure (BP) and temperature (*T*) is presented. The green-emitting iridium(III) complex Ir-(ppy)(carbac) was applied as a novel probe for *T* along with the red-emitting complex [Ir-(btpy)] which functions as a probe for BP (in fact for oxygen). The two iridium complexes were dissolved in two different polymer materials to achieve optimal responses. The effects of *T* on the response of the oxygen probe can be corrected for by simultaneous optical determination of *T*. The signals of the probes for *T* and BP can be separated by optical filters due to the ~75 nm difference in their emission maxima. The dual sensor is applicable to luminescence lifetime imaging of *T* and barometric pressure.



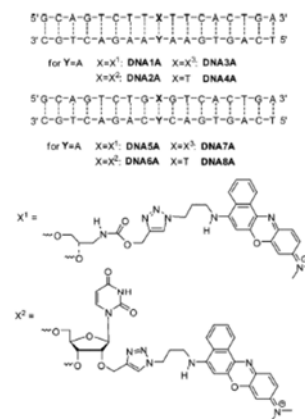
**483. Exceptional Oxygen Sensing Capabilities and Triplet State Properties of Ir(ppy-NPh<sub>2</sub>)<sub>3</sub>.** C. Mak, D. Pentlechner, M. I. J. Stich, O. S. Wolfbeis, W.-K. Chan, H. Yersin; *Chem. Mat.* (2009), 21, 2173-2175. DOI: 10.1021/cm9003678. Journal IF: 5.1.

*Abstract:* The oxygen sensing capabilities of a new highly fluorescent iridium complex display favorable sensing properties for oxygen which is due to a relatively long emission lifetime, a high luminescence quantum yield, and a good solubility in organic solvents and in organic polymers. Dissolved in ethyl cellulose, the complex displays high sensitivity to changes of oxygen partial pressure even at air pressures as high as 1500 ~mbar. The sensor material may be used in fiber optic sensors, in micro-plates, and – if cast onto the surfaces of aircraft models as a thin film; see Fig. (a) – for imaging of air pressure distributions on surfaces. Fig. (b) shows how quenching is suppressed (luminescence lights up) if nitrogen gas is blown over the sensor layer.



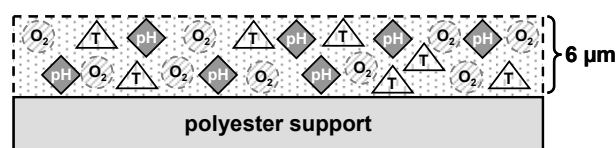
**481. Comparison of a Nucleosidic vs. Non-Nucleosidic Postsynthetic "Click" Modification of DNA with Base-Labile Fluorescent Probes.** S. Berndt, N. Herzig, P. Kele, D. Lachmann, X. Li, O. S. Wolfbeis, H.-A. Wagenknecht; *Bioconj. Chem.* (2009), 20, 558-564. DOI: 10.1021/bc8004864. Journal IF: 4.4.

*Abstract:* Two azides (bearing a phenoxazinium and a coumarin fluorophore, respectively) were applied in postsynthetic click-type bioconjugation and coupled to oligonucleotides modified with alkyne groups. The modified duplexes were investigated by UV/vis absorption spectroscopy and fluorescence spectroscopy in order to study the different optical properties of the two chromophores and to evaluate their potential for bioanalytical applications. The sequence-selective fluorescence quenching of the phenoxazinium label differs only slightly and does not depend on the type of modification. The significant Stokes shift of ~100 nm and the good quantum yields make the coumarin chromophore a powerful fluorescent label for nucleic acids.



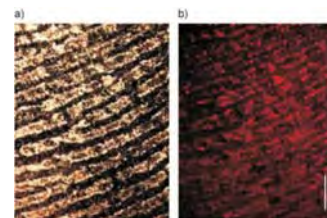
**480. Multicolor Fluorescent and Permeation-Selective Microbeads Enable Simultaneous Sensing of pH, Oxygen and Temperature.** M. I. J. Stich, M. Schaeferling, O. S. Wolfbeis; *Adv. Mater.* (2009), 21, 2216-2220. DOI: 10.1002/adma.200803575. Journal IF: 8.4.

*Abstract:* Several types of sensing microspheres, each consisting of a smart combination of a polymer and a specific indicator probe, are used to sense the 3 parameter simultaneously. The spectral information obtained from the beads can be clearly identified by either spectral or temporal resolution. All probes can be photoexcited at the same wavelength (405 nm). The sensor beads are incorporated into a sensor matrix (a hydrogel) in varying ratios, thus allowing the intensity of the single signals to be easily adjusted by proper variation of the ratio of beads. Two kinds of triple sensors are being presented. In the first, the optical signals of the three kinds of beads are being distinguished using different emission filters along with time-resolved spectroscopy. In the second type, the highly different decay times of the probes are exploited to separate overlapping signals.



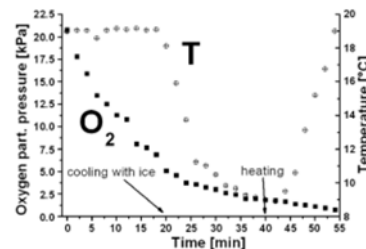
**479. Highlight Article: Nanoparticle-Enhanced Fluorescent Imaging of Latent Finger-prints Reveals Drug Abuse.** O. S. Wolfbeis; *Angew. Chem. Intl. Ed.* (2009), 48, 2268-2269. DOI: 10.1002/anie.200805765. Journal IF: 10.3.

**Abstract:** A Highlight Article on two recent papers by Russell et al. where the authors have combined three kinds of high technology: (1) magnetic nanoparticles, (2) fluorescence imaging, and (3) immunoassay, so to produce a method that has a high potential not only for the detection of various kinds of drugs, but also for the detection of other species such as chemicals formed in explosions.



**478. Method for Simultaneous Luminescence Sensing of Two Species Using Optical Probes of Different Decay Time, and its Application to an Enzymatic Reaction at Varying Temperature.** S. Nagl, M. I. J. Stich, M. Schaeferling, O. S. Wolfbeis; *Anal. Bioanal. Chem.* (2009), 393, 1199-1207. DOI: 10.1007/s00216-008-2467-0. Journal IF: 3.9.

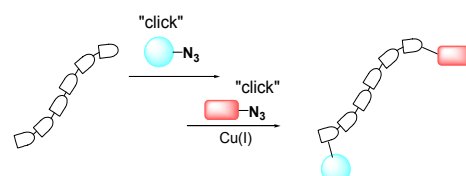
**Abstract:** We present a scheme (referred to as DLD) for optical sensing of two species simultaneously and even at identical excitation and emission wavelengths of two probes provided (a) their decay times are different enough to enable two time windows to be recorded, and (b) the emission of the shorter-lived probe decays to below the detectable limit while that of the other still can be measured. DLD is demonstrated to work by sensing oxygen and temperature independently. The scheme was applied to monitor the consumption of oxygen in the glucose oxidase-catalyzed oxidation of glucose at varying  $T$ s. The schemes on the right show the differences between the widely used DLR method and the (new) DLD method for dual sensing.



**476. Dual Labeling of Biomolecules by Click Chemistry: a Sequential**

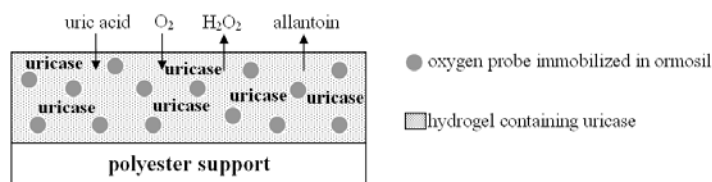
**Approach.** P. Kele, G. Mezö, D. Achatz, O. S. Wolfbeis; *Angew. Chem. Intl. Ed.* (2009) 48, 344-347. DOI: 10.1002/anie.200804514. Journal IF: 10.8.

**Abstract:** Dual labeling of model compounds was carried out using both copper-free and copper-mediated click chemistry in sequential manner. This method can be used to introduce two labels into biological targets or nanoparticles, thus quickly converting them into e.g. FRET systems.



**474. Fully Reversible Optical Uric Acid Biosensor Using Oxygen Transduction.** P. Schrenkhammer, O. S. Wolfbeis; *Biosens. Bioelectron.* (2008) 24, 1000-1005. DOI: 10.1016/j.bios.2008.08.007. Journal IF: 5.1.

**Abstract:** An optical biosensor is presented for continuous determination of uric acid. The scheme is based on the measurement of the consumption of oxygen during the oxidation of uric acid that is catalyzed by the enzyme uricase. The enzyme is immobilized in a polyurethane hydrogel next to a metal-organic probe whose fluorescence is quenched by oxygen. The consumption of oxygen was followed via changes of luminescence intensity and can be related to the concentration of uric acid. Analytical ranges (0 to 2 mM), the response times (80 - 100 s), reproducibility, and long term stability were investigated.



**473. Journal Volume Edited: Methods and Applications of Fluorescence.** O. S. Wolfbeis (ed.) *J. Fluoresc.* (2008), 18, 599-760 (Proc. of the 10<sup>th</sup> Conf. on Methods and Applic. of Fluorescence (MAF-10); Salzburg, 2007). DOI:

10.1007/s10895-008-0380-8. Contains the following papers: (1) **Translational and Rotational Motions of Albumin Sensed by a Non-Covalent Associated Porphyrin Under Physiological and Acidic Conditions: A Fluorescence Correlation Spectroscopy and Time Resolved Anisotropy Study** (by S. M. Andrade, Silvia M. B. Costa, Antonie J. W. G. Visser) (2) **Single Molecule Fluorescence of Native and Refolded Peridinin-Chlorophyll-Protein Complexes** (by S. Wörmke, S. Mackowski, C. Bräuchle); (3) **Fluorescent Microcrystals Obtained from Coumarin 6 Using the Reprecipitation Method** (by S. Fery-Forgues; R. El-Ayoubi; Jean-François Lamère); (4) **Low-Temperature Spectral Dynamics of Single TDI Molecules in n-Alkane Matrices** (by S. Mackowski; S. Wörmke, C. Bräuchle); (5) **Effect of Temperature and Oxygen on Luminescence Spectra and Polarization of Divinylbenzoxazolybiphenyl Thin Films** (by A. V. Kukhta, E. E. Kolesnik, N. A. Galinovskii); (6) **Disabling Photoinduced Electron Transfer in 4,4-Difluoro-8-(4'-hydroxyphenyl)-1,3,5,7-tetramethyl-4-bora-3a,4a-diaza-s-indacene by Phosphorylation** (by M. Jacob, A. Schmitt, G. Jung); (7) **Spectroscopic Study of Benzanthrone 3-N-Derivatives as New Hydrophobic Fluorescent Probes for Biomolecules** (by E. M. Kirilova, I. Kalnina, I. Meirovics); (8) **Sensitized Luminescence of Trivalent Lanthanide Complexes Eu(III)/Quinaldinic Acid and Eu(III)/1,4-Dihydro-Oxochinoline-3-Carboxylic Acid** (by A. S. Ndao, A. Buzády, I. Hornyák); (9) **Flow-Injection Chemiluminescence Determination of Aspartic Acid in Tea Leaves Using Tris(2,2'-bipyridyl) Ruthenium(II)-Ce(IV) System** (by Sang H. Lee; Chi W. Jeon, Saikh M. Wabaidur); (10) **Characterization of Interaction Between Bergenin and Human Serum Albumin in Membrane Mimetic Environments** (by Yaheng Zhang, Lijun Dong, Xingguo Chen); (11) **Probing the Interaction of Trans-resveratrol with Bovine Serum Albumin: A Fluorescence Quenching Study with Tachiya Model** (by J. B. Xiao, X. Q. Chen, M. Tachiya); (12) **On Mechanism of Intermediate-Sized Circular DNA Compaction Mediated by Spermine: Contribution of Fluorescence Lifetime Correlation Spectroscopy** (by J. Humpolíčková, M. Štěpánek, M. Hof); (13) **Preparation, Characterization and Photophysical Properties of Highly Luminescent Terbium Complexes Incorporated into SiO<sub>2</sub>/Polymer Hybrid Material** (by Li Xu, Yu-Fei Ma, Min-Yu Tan); (14) **Europium Luminescent Polymeric Microspheres Fabricated by Spray Drying Process** (by Priscilla P. Luz; Ana M. Pires, Osvaldo A. Serra); (15) **Interaction between Pazufloxacin and DNA Mediated by Copper(II) Ions** (by Guoliang Zhang, Xuchun Fu, Guoping Wang); (16) **A Fluorescence Emission, FT-IR and UV-VIS Absorption Study of the Some Uranium(VI) Schiff Bases Complexes** (by Th. Măluțan, A. Pui, Doina Humelnicu); (17) **Spectroscopic Properties and Conformational Stability of Concholepas concholepas Hemocyanin** (by Krassimira Idakieva, Peter Nikolov, Valery L. Shnyrov); (18) **Interaction among Cadmium Sulfide Nanoparticles, Acridine Orange, and Deoxyribonucleic Acid in Fluorescence Spectra and a Method for Deoxyribonucleic Acid Determination** (by Jie Mao, Shoujun Lai, Weisheng Liu); (19) **Cellular Uptake of Fluorescent Labelled Biotin-Streptavidin Microspheres** (by M. Bradley, L. Alexander, R. M. Sanchez-Martin); (20) **pH Fluorescent Probes: Chlorinated Fluoresceins** (by Feng-Yan Ge, Li-Gong Chen); (21) **Molecular Switching in the Near Infrared (NIR) to Visible/NIR f-f emission with a Functional-Lanthanide Complexes** (by Ga-Lai Law, Ka-Leung Wong, Kok-Wai Cheah); (22) **Thermodynamic Studies on the Interaction of Dioxopromethazine to  $\beta$ -Cyclodextrin and Bovine Serum Albumin** (by Hua-Xin Zhang, Xing Huang, Min Zhang).

#### 472. Transcutaneous pO<sub>2</sub> Imaging During Tourniquet-Induced Forearm Ischemia Using Planar Optical Oxygen

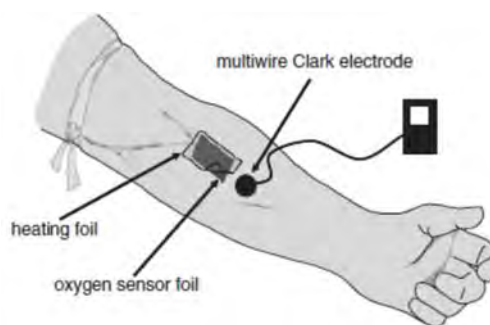
**Sensors.** P. Babilas, P. Lamby, L. Prantl, S. Schreml, E. M. Jung, G. Liebsch, O. S. Wolfbeis, M. Landthaler, R. M. Szeimies, C. Abels, *Skin Res. Technol.* (2008), 14, 304–311. DOI: 10.1111/j.1600-0846.2008.00295.x.

**Background:** Oxygen-dependent quenching of luminescence using transparent planar sensor foils was shown to overcome the limitations of the polarographic electrode technique in an animal model. This method was then transferred to a clinical setting to measure the transcutaneous pO<sub>2</sub> (ptcO<sub>2</sub>).

**Methods:** In six healthy subjects, a cuff on the upper arm was occluded up to 20mmHg above systolic pressure and released after 8 min. PtcO<sub>2</sub> was measured at the lower arm every 30 s before, during, and up to 20 min after cuff occlusion (at 40 °C skin temperature) using luminescence lifetime imaging (LLI) of platinum(II)-octaethylporphyrin immobilized in a polystyrene matrix. For validation, the polarographic Clark electrode technique was applied in close proximity, and measurements were conducted simultaneously.

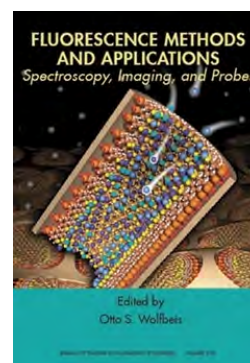
**Results:** PtcO<sub>2</sub> measurements before and at the end of ischemic and reperfusion phases did not differ significantly using the Clark electrode vs. LLI. At both the initial ischemic and the reperfusion phases, the Clark electrode measured a faster decrease or increase, respectively, in ptcO<sub>2</sub> because of the oxygen consumption occurring in the Clark method.

**Conclusion:** The method provides accurate and reproducible ptcO<sub>2</sub> values under changing microcirculatory conditions. The lack of oxygen consumption during measurement allows both a more realistic estimation of ptcO<sub>2</sub> than compared with the gold standard and permanent use in regions with critical oxygen supply.



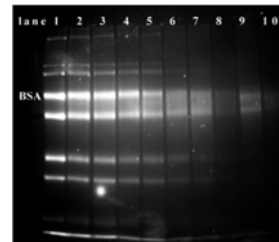
#### 471. Journal Volume Edited: Fluorescence Methods and Applications: Spectroscopy, Imaging, and Probes. O. S. Wolfbeis (ed.). Special Issue of the *Ann. New York Acad. Sci.* (2008), vol. 1130, pp. 1-328. DOI: 10.1196/annals.1430.057. Journal IF: 4.7.

This volume features papers on new spectroscopic methods and techniques, the development and application of fluorescent probes, and new techniques and applications of fluorescence imaging. Specific areas include the following: fluorescence lifetime, fluorescence (in vivo) imaging, time resolved fluorescence, luminescence anisotropy, fluorescent (NMIR) labels, luminescent lanthanides, fluorescent sensors and probes, fluorescence microscopy, FRET, fluorescent nanoparticles and dots, high throughput screening, fluorescent bioassays, luminescence based DNA technologies, FISH and immunohistochemistry, luminescence on metal surfaces, fluorescent proteins, upconversion, multiphoton fluorescence, confocal techniques, near field and far field techniques, single photon counting, fluorescence correlation spectroscopy (FCS), and flow cytometry.



#### 470. SDS-PAGE of Proteins Using a Chameleon-Type of Fluorescent Pre-Stain. R. J. Meier, M. S. Steiner, A. Duerkop, O. S. Wolfbeis; *Anal. Chem.* (2008) 80, 6274-6279. DOI: 10.1021/ac800581v. Journal IF: 5.3.

**Abstract:** A prestaining method for protein SDS-PAGE was developed using the fluorogenic amino-reactive label Py-1. This resulted in one of the fastest and most sensitive protocols available. The label Py-1 is blue and virtually nonfluorescent but turns to red and becomes strongly fluorescent once it is conjugated to the amino group of a protein. LODs as low as 16 pg of protein which is better than the best (commercial) poststains and comparable to the best (commercial) pre-stains. In addition, prestaining requires marginal amounts of staining solution. The change in electrophoretic mobility and band broadening is at a low level because Py-1 causes a mass shift of 288 Da per bound molecule only. By virtue of the small mass shift it causes, this stain is compatible with protein detection via MS.



#### 468. Multiplex Bacterial Growth Monitoring in 24-Well Microplates Using a Dual Optical Sensor for Dissolved Oxygen and pH. A. S. Kocincová, S. Nagl, S. Arain, C. Krause, S. M. Borisov, M. Arnold, O. S. Wolfbeis; *Biotechnol. Bioeng.*, (2008) 100, 430-438. DOI: 10.1002/bit.21793. Journal IF: 3.0.

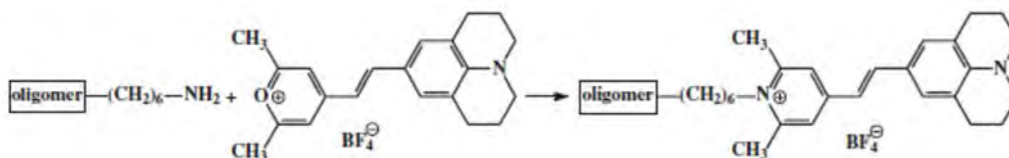
**Abstract:** Simultaneous optical monitoring of oxygen and pH during bacterial cultivation in 24-well microplates is presented using an integrated dual sensor for dissolved oxygen and pH values. The dual sensor is based on oxygen-sensitive organosilica microparticles and pH-sensitive microbeads from a polymethacrylate derivative embedded into a polyurethane hydrogel. The readout is based on a phase-domain fluorescence lifetime-based method referred to as modified frequency domain dual lifetime referencing using a commercially available detector system for 24-well microplates. The sensor was used for monitoring the growth of *Pseudomonas putida* bacterial cultures. The method is suitable for parallelized, miniaturized bioprocessing, and cell-based high-throughput screening applications.



#### 467. Probing DNA Hybridization in Homogeneous Solution and at Interfaces via Measurement of the Intrinsic Fluorescence Decay Time of a Label. B. K. Hoefelschweiger, O. S. Wolfbeis; *J. Fluoresc.* (2008), 18, 413-421. DOI: 10.1007/s10895-007-0281-2. journal IF: 2.6

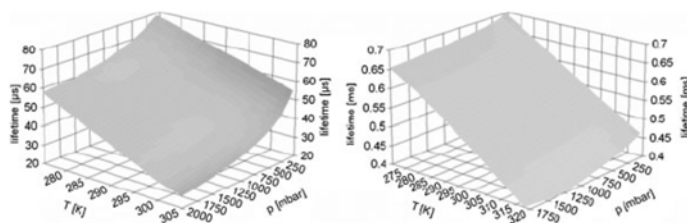
**Abstract:** The hybridization of DNA oligomers including molecular beacons can be detected by measurement of either the decay time or the intensity of a single fluorescent pyrylium label attached to the end of the respective oligonucleotide (see below). The method works both in solution and solid phase and can distinguish between fully complementary and mismatch sequences as demonstrated for a 15-mer oligonucleotide and a 25-mer molecular beacon. The fluorescence lifetime method is advantageous in (a) requiring a single label (and therefore a single labeling step) only; and (b), being based on measurement of a self-referenced magnitude that is hardly affected by parameters such as fluctuations in light intensity that make measurement of intensity more prone to interferences.





**466. Dual Luminescent Sensor Material for Simultaneous Imaging of Barometric Pressure and Temperature on Surfaces.** M. I. J. Stich, S. Nagl, O. S. Wolfbeis, U. Henne, M. Schaeferling; *Adv. Funct. Mat.* (2008) 18, 1399-1406. DOI: 10.1002/adfm.200701199. Journal IF: 7.0

**Abstract:** A composite material is presented for simultaneous luminescent sensing of air pressure and temperature ( $T$ ) on surfaces. The sensor consists of a fluorinated platinum porphyrin complex as the oxygen-sensitive probe, and a highly  $T$ -sensitive europium complex acting as a probe for  $T$ . The signals are separated via the different luminescence lifetimes of the indicators by making use of a new 4-window technique that enables time-resolved determination of 2 decay times.

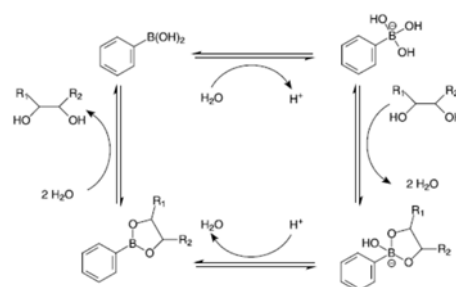


**465. Biannual Review: Fiber Optic Chemical Sensors and Biosensors (2006-2007).** O. S. Wolfbeis; *Anal. Chem. (Wash.)* (2008), 80, 4269-4283. DOI: 10.1021/ac800473b. journal IF: 5.7.

**Abstract:** This review covers the time period from January 2006 to January 2008 and is written in continuation of previous reviews (1-3). Data were electronically searched in SciFinder and MedLine. Additionally, references from (sensor) journals were collected by the author over the past 2 years. The number of citations in this review is limited, and a stringent selection had to be made therefore. Priority was given to fiber-optic sensors (FOS) of defined chemical, environmental, or biochemical significance and to new schemes.

**464. Review: Boronic Acid Based Probes for Microdetermination of Saccharides and Glycosylated Biomolecules.** H. S. Mader, O. S. Wolfbeis; *Microchim. Acta* (2008), 162, 1-34. DOI: 10.1007/s00604-008-0947-8. Journal IF: 1.9.

**Abstract:** This review covers the progress made in the development of fluorescent probes for saccharides and glycosylated biomolecules. Such probes are supposed to work at physiological pH and at room temperature, and preferably have fast responses. The modes of interactions between probe and saccharides are discussed, not the least with the aim to assist in the design of more selective probes for which there is a substantial need. Contains sections on - Unspecific saccharide probes; - Probes for specific determination of glucose; - Probes incorporated into hydrogels and polymers for use in continuous sensing; - Probes for sugar acids and their derivatives; - Probes for determination of glycoproteins; - Boronic acids for probing nucleosides; - Non-fluorescent probes based on boronic acids.



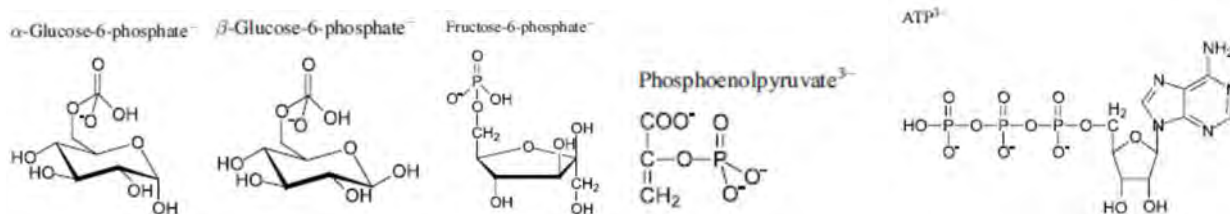
**463. Dual Fluorescence Sensor for Trace Oxygen and Temperature with Unmatched Range and Sensitivity,** C. Baleizão, S. Nagl, M. Schaeferling, M. N. Berberan-Santos, O. S. Wolfbeis; *Anal. Chem.* (2008), 80, 6449-6457. DOI: 10.1021/ac801034p. Journal IF: 5.6.

**Abstract:** An optical dual sensor for oxygen and temperature ( $T$ ) is presented which is highly oxygen sensitive and covers a broad  $T$  range. It contains two luminescent compounds incorporated into polymer films. Ruthenium tris(1,10-phenanthroline) has a highly  $T$ -dependent luminescence and is incorporated in poly(acrylonitrile) to avoid cross-sensitivity to oxygen. Fullerene  $C_{70}$  was used as the oxygen-sensitive probe owing to its intense thermally activated delayed fluorescence (TADF) at elevated  $T$ 's that is extremely oxygen sensitive. The cross-sensitivity of  $C_{70}$  to  $T$  is accounted for by means of the  $T$  sensor.  $C_{70}$  is incorporated into a highly oxygen permeable polymer, either ethyl cellulose (EC) or organosilica (OS). The two luminescent probes have different emission spectra and decay times and their emissions can be discriminated using both parameters. Spatially resolved sensing is achieved by means of fluorescence lifetime imaging. The dual sensor covers the temp. range from 0 and 120 °C, and detection limits for oxygen are in the low ppbv range. These ranges outperform all dual oxygen and  $T$  sensors reported so far.

$C_{70}/EC$ (6 $\mu\text{m}$ ) or $C_{70}/OS$ (12 $\mu\text{m}$ )
$Ru(\text{phen})_3/PAN$ (6 $\mu\text{m}$ )
polyester support
silicone / $TiO_2$ layer (80 $\mu\text{m}$ )

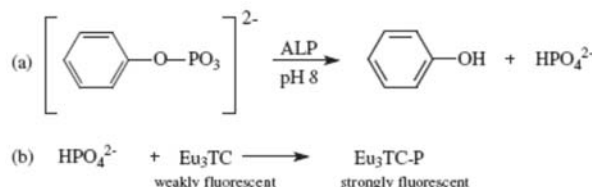
**461. Review: Fluorescent Probes for Microdetermination of Inorganic Phosphates and Biophosphates.** C. Spangler, M. Schaeferling, O. S. Wolfbeis; *Microchimica Acta* (2008), 161, 1-39. DOI: 10.1007/s00604-007-0897-6. Journal IF: 1.6.

**Abstract:** This review covers the progress made in the development of fluorescent probes for inorganic and organic phosphates that are of significance in biosciences. Such probes need to work at physiological pH and at room temperature. The various modes of interactions between probe and phosphate species are discussed, not the least with the aim to assist in the design of more selective probes for which there is a substantial need. Formulae for typical bioorganic phosphates, for which fluorescent probes are known, are given below.



**460. Time-Resolved Fluorescence-Based Assay for the Determination of Alkaline Phosphatase Activity, and Application to the Screening of its Inhibitors.** P. Schrenkhammer, I. C. Rosnizeck, A. Duerkop, O. S. Wolfbeis, M. Schaeferling, J. Biomol. Screen. (2008), 13, 9-16. DOI: 10.1177/1087057107312031. Journal IF: 2.8.

**Abstract:** A single-step end point method is presented for detn. of the activity of the enzyme alk. phosphatase (ALP) using the effect of enhancement of fluorescence of the easily accessible europium(III)-tetracycline 3:1 complex (EuTC). Its luminescence, peaking at 616 nm if excited at 405 nm, is enhanced by a factor of 2.5 in the presence of phosphate. Phenyl phosphate was used as a substrate that is enzymically hydrolyzed to form phenol and phosphate. The latter coordinates to EuTC and enhances its luminescence intensity as a result of the displacement of water from the inner coordination sphere of the central metal. The assay is performed in a time-resolved (gated) mode, which is shown to yield larger signal changes than steady-state measurement of fluorescence. The limit of detection for ALP is 4 mmol/L. Based on this scheme, a model assay for theophylline as inhibitor for ALP was developed with a linear range from 14 to 68 mmol/L of theophylline.



**459. Review: Optical Biosensors.** S. M. Borisov, O. S. Wolfbeis; Chem. Rev. (2008), 108, 423-461. DOI: 10.1021/cr068105t. Journal IF: 32.8.

**Contents:** 1. Introduction and Scope; 2. General Remarks (including Definition of Biosensors, Classification of Biosensors; General Aspects of Signal Generation, Immobilization of Biomolecules, and Sample Handling); Frequently Used Spectroscopies and Internal Referencing); 3. Enzymatic Biosensors; 4. Immunosensors (with Subsections on Immunosensor Formats Direct Immunosensors, Competitive Immunosensors, Sandwich Immunosensors, Displacement Immunosensors and a Comparative Study on Immunosensor Formats, Immobilization of Antibodies on Sensor Surfaces and Nonspecific Protein Binding, Specific Immunosensors for Proteins and Antibodies, for Toxins, for Drugs, for Bacteria, for Pesticides, and Multianalyte Immunosensors); 5. Biosensors Based on Ligand-Receptor Interactions (such as for Saccharides and Glycoproteins, for Inorganic Ions, for Gaseous Species, and for Toxins); 6. Nucleic Acid Biosensors (including Single DNA Sensors on Solid Supports and on Fiber-Optics, DNA Arrays, Molecular Beacons in DNA Sensors, Liposome-Based DNA Assays, Aptamer-Based DNA Sensing); 7. Whole-Cell Biosensors (with subsections on Catalytic Whole-Cell Biosensors, External Stimuli-Based Cellular Biosensors, Genetically Engineered Whole-Cell Biosensors); 8. Solid Supports for Use in Optical Biosensors.

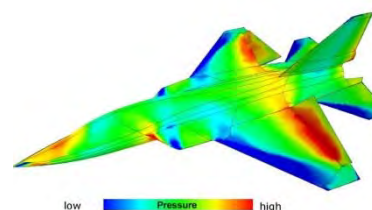
**458. Review: Sensor Paints.** O. S. Wolfbeis; Adv. Mat. (2008), 20, 3759-3763. DOI: 10.1002/adma.200702276. Journal IF: 8.2.

**Abstract:** Fluorescence microscopy is widely used for chemical imaging of intrinsically fluorescent chemical species, such as chlorophylls, or nonfluorescent species (e.g., DNA) that have been labeled appropriately or to which a relevant molecular probe has been added. However, there are numerous analytes that neither have an intrinsic luminescence nor can be rendered luminescent with the help of labels or probes. Such parameters include oxygen, pH, CO<sub>2</sub>, ammonia, and glucose. There are also numerous applications where the 2D distribution of a chemical or physical parameter is of interest. The use of a "sensor paint" is ideal in such situations. The state of this new technology is discussed herein with emphasis on current and future trends, for example, the use of pressure- and temperature-sensitive paints; known technological limitations are also discussed. These "paints" respond to a (bio)chemical parameter with a change in their optical properties. The object of interest is painted and the color or fluorescence of the paint is monitored by optical imaging. This technique enables monitoring of physical and chemical parameters over relatively large areas and in real time. In a typical application, the object of interest is painted and the fluorescence of the paint is monitored by methods of optical imaging. This technique represents a simple but exciting new technology to monitor (bio)chemical and physical parameters over relatively large areas and in real time.



**457b. Book Chapter: Fluorescence Sensing and Imaging Using Pressure-Sensitive Paints and Temperature-Sensitive Paints.** M. I. J. Stich, O. S. Wolfbeis; in: Standardization and Quality Assurance in Fluorescence, vol. 1, U. Resch-Genger (ed.), Springer Berlin – Heidelberg (2008), pp. 429-461; ISBN 978-3-540-75206-6. DOI 10.1007/978-3-540-75207-3.

**Abstract:** Barometric-pressure-sensitive paints (PSPs) and temperature-sensitive paints (TSPs) are widely used in aerodynamic research and wind tunnel testing. Both systems are based on the incorporation of the respective indicators into a matrix polymer (often referred to as the "binder") to be cast on the area of interest. Spatially resolved distributions of oxygen partial pressure (pO<sub>2</sub>) and T can be instantly visualized by making use of respective paints and appropriate techniques of fluorescence imaging. This chapter summarizes state of the art in probes and polymers for use in PSPs and TSPs. Fluorescence spectroscopic methods for the interrogation of the paints are described along with the components and respective experimental setups. Finally, we discuss the advantages and drawbacks of various systems and methods, along with their utility in fields of applications such as measurement of barometric pressure on aircrafts.



**457a. Book: Fluorescence of Supermolecules, Polymers, and Nanosystems.** Springer Series on Fluorescence, vol. 4; M. N. Berberan-Santos (ed.), (O. S. Wolfbeis, Series Editor) Springer, Berlin – Heidelberg (2008). ISBN 978-3-540-73927-2. DOI: 10.1007/978-3-540-73928-9.

Contents:

*History and Fundamental Aspects*

\* Early History of Solution Fluorescence: The Lignum nephriticum of Nicolás Monardes (by A.U.Acuña · F.Amat-Guerri);  
\* From Well-Known to Underrated Applications of Fluorescence (by B.Valeur); \* Principles of Directed Electronic Energy Transfer (by D.L.Andrews · R.G.Crisp); \* Luminescence Decays with Underlying Distributions of Rate Constants: General Properties and Selected Cases (by M.N.Berberan-Santos · E.N.Bodunov · B.Valeur); \* Fluorescence as the Choice Method for Single-Molecule Detection (by M.Orrit).

*Molecular and Supramolecular Systems*

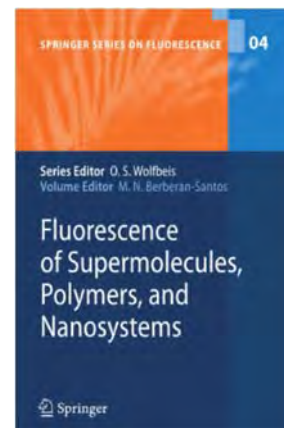
\* Water-soluble Fluorescent Chemosensors: in Tune with Protons (by A.J.Parola · J.C.Lima · C.Lodeiro · F.Pina); \* The Fluorescence of Fullerenes (by S. Nascimento · C. Baleizão · M.N.Berberan-Santos).

*Polymers, Semiconductors, Model Membranes and Cells*

\* Resonance Energy Transfer in Polymer Interfaces (by J.P.S.Farinha · J.M.G.Martinho); \* Defocused Imaging in Wide-field Fluorescence Microscopy (by H. Uji-i · A. Deres · B. Muls · S. Melnikov · J. Enderlein · J. Hofkens); \* Dynamics of Excited States and Charge Photogeneration in Organic Semiconductor Materials (by K. G. Jespersen · Y. Zaushitsyn · S. Westenhoff · T. Pullerits · A. Yartsev · O. Inganäs · V. Sundström); \* Resonance Energy Transfer in Biophysics: Formalisms and Application to Membrane Model Systems (by L.M.S.Loura · M.Prieto); \* Measuring Diffusion in a Living Cell Using Fluorescence Correlation Spectroscopy. A Closer Look at Anomalous Diffusion Using HIV-1 Integrase and its Interactions as a Probe (by J.Vercammen · G.Maertens · Y.Engelborghs); \* Pushing the Complexity of Model Bilayers: Novel Prospects for Membrane Biophysics (by N.Kahya · D.Merkle · P.Schwille).

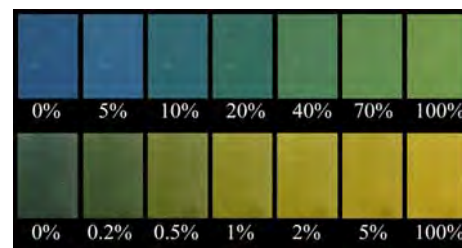
*Nanotubes, Microparticles and Nanoparticles*

\* Photoluminescence Properties of Carbon Nanotubes (by B.Zhou · Y.Lin · B.A.Harruff · Y.-P.Sun); \* Fluorescence Correlation Spectroscopic Studies of a Single Lipopolyamine–DNA Nanoparticle (by N.Adjimatera · A. Benda · I.S. Blagbrough · M. Langner, M.Hof · T.Kral); \* Morphology-Dependent Resonance Emission from Individual Micron-Sized Particles (by T. A. Smith · A. J. Trevitt · P. J. Wearne · E. J. Bieske, L.J. McKimmie · D.K.Bird); \* New Plastic Microparticles and Nanoparticles for Fluorescent Sensing and Encoding (S.M. Borisov · T. Mayr · A. A. Karasyov · I. Klimant · P. Chojnacki, C. Moser · S. Nagl · M. Schaeferling · M. I. Stich · A. S. Kocincova · O.S.Wolfbeis)



**456. Optical Carbon Dioxide Sensors Based on Silicone Encapsulated Room Temperature Ionic Liquids, S. M. Borisov, M. Ch. Orschulik, I. Klimant, O. S. Wolfbeis; *Chem. Mat.* (2008), 19, 6187-6194. DOI: 10.1021/cm7019312. Journal IF: 5.1.**

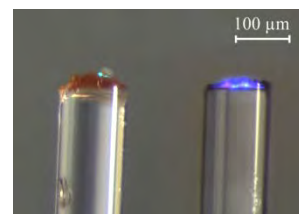
*Abstract:* The new optical CO<sub>2</sub> sensor is based on an emulsions of room-temperature ionic liquid (RTIL) in a silicone matrix. The pH indicators thymol blue, bromothymol blue and 8-hydroxy-pyrene-1,3,6-trisulfonate along with a reference fluorophore were dissolved in the RTIL. Sodium phosphate was used as a base in place of quaternary ammonium hydroxides. The sensitivity of the material can be fine-tuned by varying the pK<sub>a</sub> of the indicator. The picture shows photographic images of the two types of sensor foils (upper row and lower row) at varying of carbon dioxide levels in the test gas (at 20 °C, 100% relative humidity, at barometric pressure).



**454. Fiber Optic Microsensors for Simultaneous Sensing of Oxygen and pH, and of Oxygen and Temperature. A. S. Kocincova, S. M. Borisov, C. Krause, O. S. Wolfbeis; *Anal. Chem.* (2007), 79, 8486-8493. DOI: 10.1021/ac070514h. Journal IF: 5.7.**

*Abstract:* Fiber optic micro-sensors have been developed with a tip diameter of ~140 μm that is covered with sensor compositions based on luminescent microbeads that respond to the respective parameters by a change in the decay time and/or intensity of their luminescence. The use of microbeads enables the ratio of the signals to be easily varied, reduces the risk of fluorescence energy transfer between indicator dyes, and reduces the adverse effect of singlet oxygen that is produced in the oxygen-sensitive beads. Measurements were performed in the frequency domain. Information on DO and T is obtained by using two sets of excitation and emission filters and by working at different modulation frequencies. The microsensor for DO/pH relies on a modified dual luminophore referencing scheme at two modulation frequencies and where only one excitation source is used.

The picture at the right shows images of the microsensors of type SC-1 (left) and of type SC-2 (right) during excitation with a 505-nm and a 470-nm LEDs, respectively. The left-side sensor tip (O<sub>2</sub>/T) displays a green color that results from the green LED along with the red fluorescence of the dual sensor. The right-hand sensor tip (pH/O<sub>2</sub>) displays the blue color of the 470-nm LED and a some red and green luminescence that results from the dual sensor.



**452. Book Chapter: New Plastic Microparticles and Nanoparticles for Fluorescent Sensing and Encoding. S. M. Borisov, T. Mayr, A. A. Karasyov, I. Klimant, P. Chojnacki, C. Moser, S. Nagl, M. Schaeferling, M. I. Stich, A. S. Kocincova, O. S. Wolfbeis; in: *Springer Series on Fluorescence*, vol. 4: *Fluorescence of Supermolecules, Polymers, and Nanosystems* (M. N. Berberan, ed.), pp. 431-463 (2007). DOI: 10.1007/4243\_2007\_013.**

Contents:

- 1 Materials and Methods for Making Polymer Beads (with subsections on polymers and dyes)
- 2 Chemical Sensing with Addressable Micro- and Nanospheres
- 3 Dyed Polymer Microparticles and Their Use in Sensor Layers
- 4 Luminescence Lifetime Encoded Microbeads as Carriers for Multiplexed Bioassays
- 5 Dyed Polymer Microparticles and Their Use in Pressure-Sensitive and Temperature-Sensitive Paints (PSPs and TSPs)
- 6 Phosphorescent Polymeric Nanospheres as Labels for Homogeneous Protein Assays and Protein Arrays Using Luminescence Lifetime Imaging

**451. Development of an Optical pH Sensor for Early Detection of Danger of Corrosion in Steel-Reinforced Concrete**



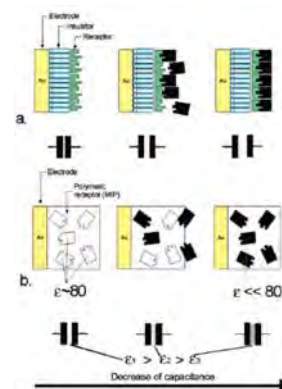
**Structures** (= Entwicklung eines optischen pH-Sensors zur Früherkennung korrosionsgefährdender Zustände in Stahlbeton); N. Dantan, M. Hoehse, A. A. Karasyov, O. S. Wolfbeis; *Technisches Messen* (2007), 74, 211-216. DOI: 10.1524/teme.2007.74.4.211 In German. Web: [https://www.researchgate.net/publication/245404656\\_Development\\_of\\_an\\_Optical\\_pH\\_Sensor\\_for\\_Early\\_Detection\\_of\\_Danger\\_of\\_Corrosion\\_in\\_Steel-Reinforced\\_Concrete\\_Structures](https://www.researchgate.net/publication/245404656_Development_of_an_Optical_pH_Sensor_for_Early_Detection_of_Danger_of_Corrosion_in_Steel-Reinforced_Concrete_Structures) [accessed Nov 20, 2020].

**Abstract:** The decrease of the pH value of cement-bound matrix in steel-reinforced structures due to chemical attacks damages corrosion protective layers and results in serious deteriorations of the structures. To date commercially available systems for monitoring the pH value in steel-reinforced concrete structures do not meet all technical requirements. Hence a concrete-embeddable fiber optic pH sensor was developed. It uses Thymol Blue as the indicator dye, and Amberlite XAD4 as the solid support. The sensing membrane is coated with TiO<sub>2</sub> particles (acting as an optical isolation) and placed at the end of a PMMA optical fiber additionally protected with a steel tube.



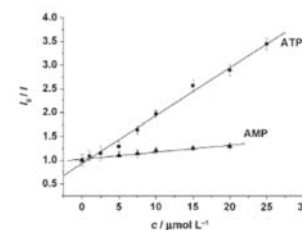
**450. Capacitive Detection in Ultrathin Chemosensors Prepared by Molecularly Imprinted Grafting Photopolymerization.** T. L. Delaney, D. Zimin, M. Rahm, D. Weiss, O. S. Wolfbeis, V. M. Mirsky; *Anal. Chem.* (2007), 79, 3220-3225. DOI: 10.1021/ac062143v. Journal IF: 5.7.

**Abstract:** The usual applications of capacitive detection in chemo- and biosensors are based on changes in effective thickness of insulating layers due to adsorption of analyte onto receptors. Ultrathin chemosensors based on molecularly imprinted polymerization enable a realization of another capacitive approach that exploits changes in electrical capacitance due to modification of the dielectric constant of the polymer. Such chemosensors were prepared by photografted molecularly imprinted polymerization on the surface of gold electrodes. An adsorbed layer of hydrophobic photo-initiator (benzophenone) provided grafted polymerization on the surface of the alkanethiol-modified gold electrode. The chemosensors were characterized by cyclic voltammetry, impedance spectroscopy, and scanning electron and atomic force microscopy. Binding of analyte was detected by measurements of electrical capacitance. The results indicate a decrease of the dielectric constant of the polymer layer due to analyte binding up to 20%. The figure symbolizes that signals of capacitive sensors can be caused by (a) changes in the thickness of the total insulating layer, and (b) by changes of the dielectric constant of the insulating layer.



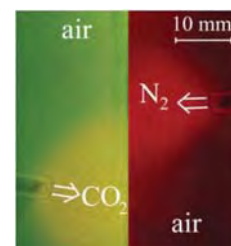
**449. Europium Tetracycline as a Luminescent Probe for Nucleoside Phosphates, and its Application to the Determination of Kinase Activity.** M. Schaeferling, O. S. Wolfbeis; *Chem. – Eur. J.* (2007), 13, 4342-4349. DOI: 10.1002/chem.200601509. Journal IF: 5.0.

**Abstract:** We have studied the effect of a series of adenosine (ATP, ADP, AMP, cAMP) and guanosine (GTP, GDP) phospho-esters, and of pyrophosphate (PP) on the fluorescence emission of the europium tetracycline (EuTC) complex. These compounds have strongly different quenching effects on the luminescence emission of EuTC. The triphosphates ATP and GTP behave as strong quenchers in reducing the fluorescence intensity of EuTC to 25% of its initial value by formation of a ternary 1:1:1 complex. All other phosphates showed a weak quenching effect. The applicability of this fluorescent probe to the determination of the activity of phosphorylation enzymes is demonstrated by means of creatine kinase as a model for non-membranebound kinases. In contrast to other methods, this approach does not require the use of radioactively labeled ATP substrates, additional enzymes, or of rather complex immunoassays.



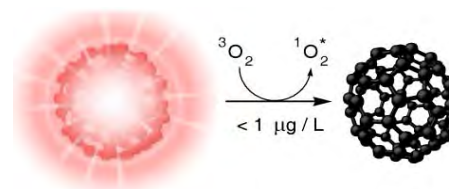
**448. Highlight Article. Optical Multiple Chemical Sensing: Status and Current Challenges.** S. Nagl, O. S. Wolfbeis; *Analyst* (2007), 132, 507-511. DOI: 10.1039/b702753b. Journal IF: 3.2.

**Abstract:** Recent advances of dually sensing devices are highlighted with a focus on fluorescence-based methods and the biologically and clinically important analytes oxygen, pH, carbon dioxide and temperature. Indicator chemistries such as permeation-selective microbeads and nanoparticles allow the production of microscopically homogeneous sensor layers. The use of combinations of spectral discriminations along with time-resolved monitoring schemes based on luminescence lifetime or intensity-lifetime ratios enables all-optical real-time multi-analyte determination.



**447. Optical Sensing and Imaging of Trace Oxygen with Record Response.** S. Nagl, C. Baleizão, S. M. Borisov, M. Schaeferling, M. N. Berberan-Santos, O. S. Wolfbeis; *Angew. Chem. Intl. Ed.* (2007), 46, 2317-2319. DOI: 10.1002/anie.200603754. Journal IF: 10.3.

**Abstract:** Ultratrace quantities of oxygen can be determined over a temperature range of more than 100 °C by exploiting the extremely efficient quenching of the delayed fluorescence of fullerene C70 incorporated into organosilica or ethyl cellulose.



**Book Series Edited: Springer Series on Chemical Sensors and Biosensors.** O. S. Wolfbeis (Series Ed.); 2003 – 2007.

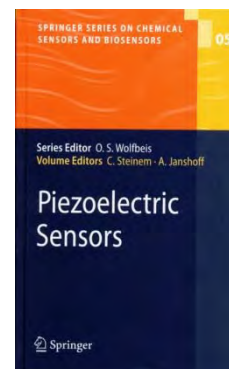
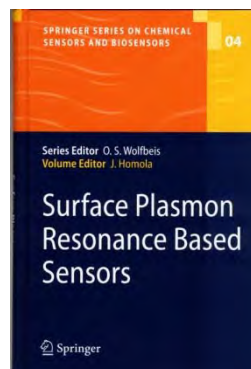
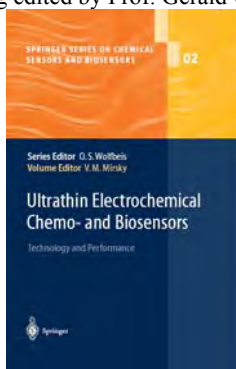
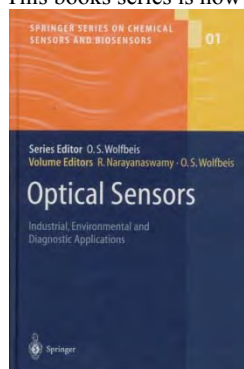
Vol. 1. **Optical Sensors for Industrial, Environmental and Clinical Applications**, R. Narayanaswamy, O. S. Wolfbeis (eds.), 2003. ISBN 3-540-40888-X.

Vol. 2. **Ultrathin Electrochemical Chemo- and Biosensors**; V. M. Mirsky (ed.) *Springer Series on Chemical Sensors and Biosensors*, vol. 2 (2004); ISBN: 978-3-642-05961-2 (Print) 978-3-662-05204-4 (Online).

Vol. 3. **Frontiers in Optical Fiber Sensing: Novel Principles and Techniques**; G. Orellana, M. C. Moreno-Bondi (eds.), *Springer Series on Chemical Sensors and Biosensors*, vol. 3 (2005); ISBN: 978-3-540-27756-9 (Print) 978-3-540-27757-6 (Online).

Vol. 4. **Surface Plasmon Resonance Based Chemical Sensing and Biosensing**; J. Homola (ed.), 2006, *Springer Series on Chemical Sensors and Biosensors*, vol. 4 (2006), ISBN: 978-3-540-33918-2 (Print) 978-3-540-33919-9 (Online).

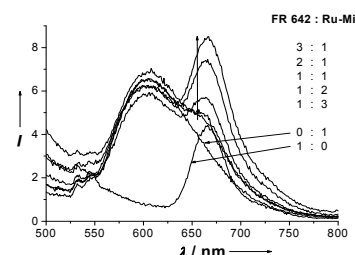
This books series is now being edited by Prof. Gerald Urban (Freiburg).



**446. Resonance Energy Transfer Immunoassay Based on a Thiol-Reactive Ruthenium Donor and a Longwave Emitting Acceptor.** J. Weh, A. Duerkop, O. S. Wolfbeis; *ChemBioChem* (2007), 8, 122-128. DOI: 10.1002/cbic.200600316.

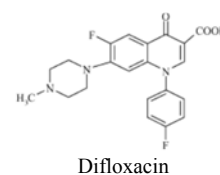
Journal IF: 4.1.

**Abstract:** We describe an immunoassay that applies a (new) thiol-reactive ruthenium metal ligand complex as the donor dye in a luminescence energy transfer (LET) detection scheme. Unlike amine reactive labels, the LET using a thiol label allows improved specificity and better reproducibility of labeling positions on proteins, because the number of reactive thiol groups of proteins is distinctly smaller. The absorption and emission maxima of the ruthenium donor dye are at 460 nm and 600 nm, respectively, and a Stokes' shift of 140 nm warrants distinct separation of excitation and emission wavelengths even in turbid samples. A cyanine dye (FR 642) with an absorption peak at 642 nm was chosen as the acceptor label in the LET system. Anti-HSA can be determined at concentrations down to 220 pmol/L.



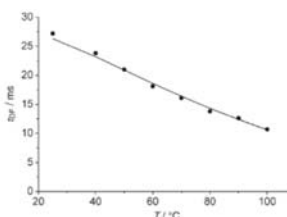
**445. Sensitive Luminescent Determination of DNA Using the Terbium(III)-Difloxacin Complex.** A. V. Yegorova, Y. V. Scripinets, A. Duerkop, A. A. Karasyov, V. P. Antonovich, O. S. Wolfbeis; *Anal. Chim Acta* (2007), 584, 260-267. DOI: 10.1016/j.aca.2006.11.065. journal IF: 2.9.

**Abstract:** The interaction of the terbium-difloxacin complex (Tb-DFX) with DNA has been examined by using UV-vis absorption and luminescence spectroscopy. The Tb-DFX complex shows an up to 85-fold enhancement of luminescence intensity upon titration with DNA. The long decay times allow additional detection schemes like time-resolved measurements in microplate readers to enhance sensitivity by off-gating short-lived background luminescence. Optimal conditions are found at equimolar concentrations of Tb<sup>3+</sup> and DFX (0.1 or 1 μM) at pH 7.4. Under these conditions, the luminescence intensity is linearly dependent on the concentration of ds-DNAs and ss-DNA between 1–1500 ngmL<sup>-1</sup> and 4.5–270 ngmL<sup>-1</sup>, respectively. The detection limit is 0.5 ngmL<sup>-1</sup> for ds-DNAs and 2 ngmL<sup>-1</sup> for ss-DNA. The mechanism for the luminescence enhancement was also studied.



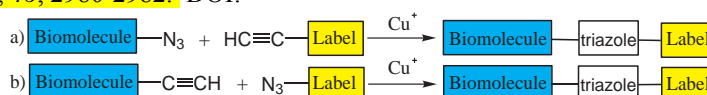
**444. An Optical Thermometer Based on the Delayed Fluorescence of C<sub>70</sub>.** C. Baleizao, S. Nagl, S. M. Borisov, M. Schaefer-ling, O. S. Wolfbeis, M. N. Berberan-Santos; *Chem. Eur. J.* (2007), 13, 3643-3651. DOI: 10.1002/chem.200601580. Journal IF: 5.0.

**Abstract:** The thermometer is based on the thermally activated delayed fluorescence of fullerene C<sub>70</sub>. It consists of C<sub>70</sub> molecularly dispersed in various polymer films. In the absence of oxygen and for temp. above 20 °C, the red fluorescence of C<sub>70</sub> in the films is so intense that it is easily perceived by the bare eye. The fluorescence intensity of C<sub>70</sub> increases with temp. by a factor of up to 90, depending on the polymer. This results in a working range from –80 °C to at least 140 °C. Perylene was incorporated as an internal reference in order to enable ratiometric measurements. The sensitivity of the lifetime of the delayed fluorescence to temp. is also high, and results in an even wider working range. The graph shows the temp. dependence of the experimental (circles) and calculated (solid line) lifetimes the delayed fluorescence of C<sub>70</sub> at 700 nm.



**443. Highlight Article: The Click Reaction in the Luminescent Probing of Metal Ions, and Its Implications on Biolabeling Techniques.** O. S. Wolfbeis; *Angew. Chem. Intl. Ed.* (2007), 46, 2980-2982. DOI: 10.1002/anie.200604897. Journal IF: 10.3.

**Abstract:** The copper(I)-catalyzed cycloaddition ("click reaction") enables micromolar concentrations of intra-cellular Cu<sup>+</sup> ion to be sensed via photonic energy transfer. It also has a large potential in terms of labelling chemistries.



**442b. Novel Europium-Tetracycline Probe for Phosphate Determination in Microtiter Plate.** M. Turel, A. Lobnik, A. Duerkop, O. S. Wolfbeis; *Proc. SPIE (Soc. Photoinstrum. Eng.)* (2006) vol. 6284, DOI: 10.1117/12.714179

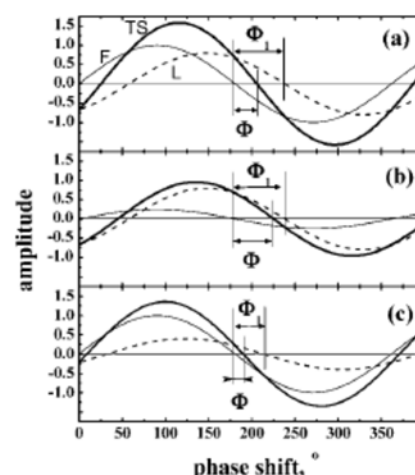
**Abstract:** A new luminescent europium probe is presented for the determination of phosphate (P) in microtiter plate format. The assay is based on the quenching of the luminescence of the europium-tetracycline 1:1 complex by phosphate using a reagent concentration of 20.8 μmol/L. The probe is excited at 400 nm and displays large Stokes' shift of 210 nm. The emission maximum is located at 616 nm. The system works best at neutral pH 7. The linear range of the calibration plot is from 5 μM to 0.75 mM of P, and the limit of detection is 5 μmol/L.

**442. Modified Dual Lifetime Referencing Method for Simultaneous Optical Determination and Sensing of Two Analytes.**

S. M. Borisov, G. Neurauder, C. Schroeder, I. Klimant, O. S. Wolfbeis; *Appl. Spectrosc.* (2006), 60, 1167-1173. DOI: 10.1366/000370206778664590. journal IF: 1.9.

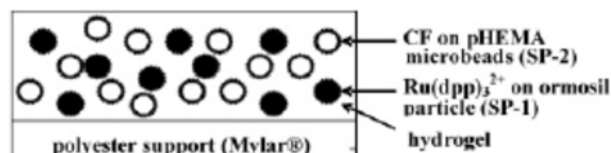
**Abstract:** Simultaneous fluorometric sensing of two analytes becomes possible using a modified dual lifetime referencing (m-DLR) method. In this scheme, two luminescent indicators are needed that have overlapping absorption and emission spectra but largely different decay times. They are excited by a single light source, and both emissions are measured simultaneously. In the frequency domain m-DLR method, the phase of the short-lived fluorescence of a first indicator is referenced against that of the long-lived luminescence of the second indicator. The analytical information is obtained by measurement of the phase shifts at two modulation frequencies. The method is demonstrated to work for the case of dually sensing oxygen and carbon dioxide. It benefits from simple instrumentation and optical setup. The approach is perceived to be of wide applicability. Examples include (1) analysis of two luminescent analytes, (2) analytical determinations that make use of two probes, and (3) sensing of two species such as carbon dioxide and oxygen (as demonstrated here), or oxygen and chlorophyll, provided the luminophores meet the condition of having largely different decay times and overlapping absorption and emission spectra.

The figure shows a schematic representation of the frequency-domain m-DLR method for three situations. Phases are shown for a fluorescent indicator (F; thin line; virtually identical to those of the light source); for a long-lived luminescent luminophore (L; dashed line); and for the total signal resulting from a mixture of the two (TS; thick line). In panel (a), both indicators are in the absence of any analytes. In (b), the fluorescence intensity of the short-lived indicator is reduced by an analyte. In (c), the emission of the long-lived indicator is partially quenched.

**441. Indicator-Loaded Permeation-Selective Microbeads for Use in Fiber Optic Simultaneous Sensing of pH and Dissolved Oxygen.**

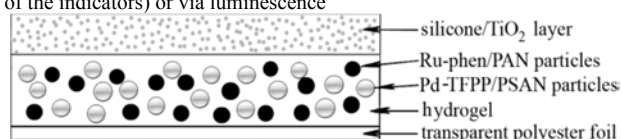
G. S. Vasylevska, S. M. Borisov, C. Krause, O. S. Wolfbeis; *Chem. Mat.* (2006), 18, 4609-4616. DOI: 10.1021/cm060967n. Journal IF: 5.1.

**Abstract:** New materials are described that lead to sensors capable of simultaneously sensing of pH and oxygen via a single fiber optic sensor. They make use of pH probe based on carboxyfluorescein, and of a ruthenium(II) complex acting as a probe for dissolved oxygen. The selectivity of the probes was considerably improved by incorporating them into two kinds of microparticles, each of specific permeation selectivity. The pH probe was immobilized on particles made from proton permeable amino-modified poly(hydroxy-ethyl methacrylate), while the oxygen probe was physically immobilized in beads made from an organically modified sol-gel. Both kinds of beads were dispersed into a hydrogel matrix and placed at the distal end of an optical fiber waveguide for optical interrogation. A phase-modulated blue-green LED serves as the light source for exciting luminescence whose average decay times or phase shifts serve as the analytical information.

**439. Composite Luminescent Material for Dual Sensing of Oxygen and Temperature.**

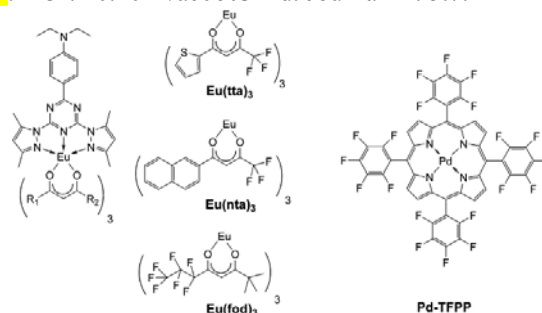
S. Borisov, A. Vasilevska, C. Krause, O. S. Wolfbeis; *Adv. Funct. Mater.* (2006), 16, 1536-1542. DOI: 10.1002/adfm.200500778. journal IF: 6.8.

**Abstract:** A novel kind of composite material is presented that contains two indicators incorporated into a single polymer matrix, thus allowing simultaneous determination of oxygen partial pressure and temperature (*T*). The *T*-sensitive ruthenium complex was chosen for its highly *T*-dependent luminescence. A fluorinated palladium(II) tetraphenylporphyrin served as the oxygen probe. The indicators were incorporated into either poly(styrene-co-acrylonitrile) microparticles (to sense oxygen) or into poly(acrylonitrile) (for sensing *T* since this polymer is virtually impermeable to oxygen). The luminescence of both dyes can be separated either spectrally (due to different absorption and emission spectra of the indicators) or via luminescence decay time. The material is suitable for *T*-compensated oxygen sensing, for example in high-resolution oxygen profiling, and for imaging *T* in the range between 0 and 60 °C. This enables *T* to be "seen" in this important range. Simultaneous imaging of barometric pressure and *T* also has been achieved. It enables contactless imaging of the two parameters, for example in wind tunnels. Due to the use of a biocompatible hydrogel matrix, the material conceivably is suited for biomedical applications.

**438. Temperature-Sensitive Europium(III) Probes and Their Use for Simultaneous Optical Sensing of Temperature and Oxygen.**

S. M. Borisov, O. S. Wolfbeis; *Anal. Chem.* (2006), 78, 5094-5101. DOI: 10.1021/ac060311d. Journal IF: 5.7.

**Abstract:** Certain luminescent europium(III) complexes (see the Fig.) can act as new probes for optical sensing of temperature (*T*). They can be excited with a 405-nm LED and possess strong brightnesses. The decay times of the probes contained in a poly(vinyl methyl ketone) film and in poly(tert.-butyl styrene) microparticles are highly *T*-dependent between 0 and 70 °C. The *T*-sensitive microparticles were dispersed, along with oxygen-sensitive microbeads consisting of a Pd(II)porphyrin oxygen probe in a styrene co-polymer, in a thin layer of a hydrogel to give a dually-sensing material that can be photoexcited by a single light source. The two emissions can be separated by appropriate optical filters. The response to oxygen and *T* is described by 3D plots, and unbiased values can be obtained for *T* and oxygen, respectively, from the two luminescence signals if refined in an iteration step. The sensing scheme is intended for use in *T*-compensated sensing of oxygen, in contactless sensing of oxygen and *T* in (micro)biological and medical applications, in high resolution oxygen profiling, and for simultaneous imaging of air pressure and *T* in wind tunnels.



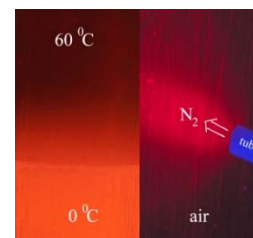


**437. Book Chapter: Fiber Optic Chemical Sensors and Biosensors: a View Back.** O. S. Wolfbeis, B. Weidgans, in: F. Baldini A. N. Chester, J. Homola, S. Martelucci (eds.), *Optical Chemical Sensors*, NATO Sci. Ser. II, vol. 224, Springer, Dordrecht (NL), 2006; chapter 2, pp. 17-44; DOI: 10.1007/1-4020-4611-1\_2. ISBN 1-4020-4609-X.

**Abstract:** The past 30 years have seen enormous progress in opto-electronics, information technology and biotechnology, and fiber optic chemical sensors (FOCS) as well as fiber optic biosensors (FOBS) are one of the outcomes. Chemical sensors have been defined as follows: *Chemical sensors are miniaturized analytical devices that can deliver real-time and on-line information on the presence of specific compounds or ions in complex samples.* In the easiest and simplest case, a sensor probe is inserted into the sample of interest to obtain an analytical signal that can be converted into a concentration unit. Chemical sensors ideally act fully reversibly, as do physical sensors for temperature, pressure, and the like. This has been achieved in few cases of FOCS only, and hardly in FOBS (except for some enzyme-based systems). However, despite the fact that most biosensors respond irreversibly or need to be regenerated, clinicians often refer to such single-shot detection elements as biosensors, provided a “reagent” or a “biology” is immobilized on a solid support. True sensors are expected to be small and to work even in complex samples, ideally without sample treatment.

**436. Composite Material for Simultaneous and Contactless Sensing and Imaging of Oxygen and Carbon Dioxide.** S. M. Borisov, C. Krause, S. Arain, O. S. Wolfbeis; *Adv. Mat.* (2006), 18, 1511-1516. DOI: 10.1002/adma.200600120. Journal IF: 7.9.

**Abstract:** A sensor is described that enables simultaneous imaging and monitoring of carbon dioxide and oxygen. It relies on the measurement of the phase shift of the luminescence decay time of a material that is composed of spectrally carefully selected indicators (with well-separated wavelengths of excitation and emission) that are contained in microbeads and polymers with excellent permeation selectivities along with optical and adhesive properties. The sensor material is used to monitor the growth of *Pseudomonas putida*. The Picture shows the orange-colored luminescence of the ruthenium probe contained in poly-acrylonitrile microparticles is highly temperature (*T*) dependent (luminescence drops with *T*). Right: After correction for *T* effects, the dark red luminescence of the Pd porphyrin contained in microbeads of an oxygen-permeable copolymer reflects areas of low oxygen (where nitrogen is blown on; this resulting in high luminescence) and areas of higher oxygen tension (where luminescence is weaker). The two signals (orange and red), though spectrally overlapping, can be resolved via luminescence lifetime measurements.

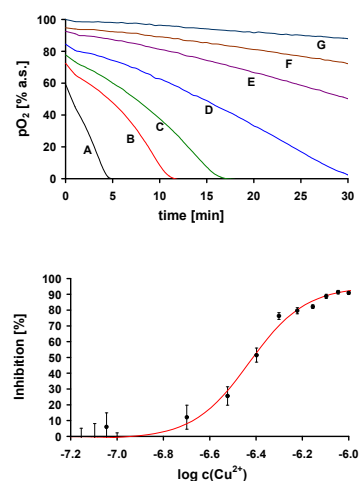


**435. Biannual Review: Fiber Optic Chemical Sensors and Biosensors (2004-2005).** O. S. Wolfbeis; *Anal. Chem. (Wash.)* (2006), 78, 3859-3873. DOI: 10.1021/ac060490z. journal IF: 5.7.

**Abstract:** This biannual review covers the time period from January 2004 to December 2005 and is written in continuation of previous reviews. An electronic search in SciFinder and MedLine resulted in >600 hits. Since the number of citations in this review is limited, a stringent selection had to be made. Priority was given (a) to fiber-optic chemical sensors (FOCS) for defined chemical, environmental, and biochemical parameters, and (b) to new sensing schemes and materials. The review does not include the following: (a) Sensors for nonchemical species such as temperature, current and voltage, stress, strain, displacement, structural integrity (e.g. of constructions), liquid level, and radiation; (b) sensors for monitoring purely technical processes such as injection molding, extrusion, or oil drilling, even though these are important applications of optical fiber technology; and (c) FOCS that obviously have been rediscovered or describe marginal modifications only of prior work.

**432. Characterization of Microtiterplates with Integrated Optical Sensors for Oxygen and pH, and Their Applications to Enzyme Activity Screening, Respirometry, and Toxicological Assays,** S. Arain, G. T. John, C. Krause, J. Gerlach, O. S. Wolfbeis, I. Klimant; *Sensors Actuat., part B* (2006), 113, 639-648. DOI: 10.1016/j.snb.2005.07.056. Journal IF: 2.3.

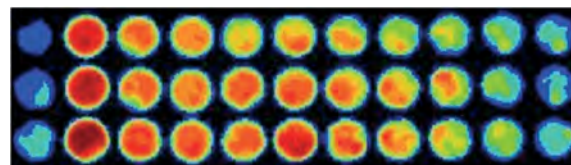
**Abstract:** We describe microplates (MTPs) with integrated, fluorescence-based sensors for pH and oxygen, and their application for enzyme screening and monitoring of bacterial respiratory activity. Thin, hydrophilic sensing films consisting of an analyte-sensitive indicator and a reference fluorophore, are deposited on the bottom of the MTP. This allows for calibration-free quantification of pH and pO<sub>2</sub> with an acceptable accuracy and resolution for enzyme activity screening, respirometry, or toxicological assays. Specifically, enzyme activity screening is demonstrated for glucose oxidase using oxygen-sensitive plates, and for bacterial growth monitoring of *Escherichia coli* and *Pseudomonas putida*. Furthermore, a toxicological assay monitoring the respiration activity of *P. putida* was converted into a microplate format. The Figure (top) shows the decrease in oxygen tension due to the respiratory activity of different concentrations of *P. putida*. The concentration of bacteria (in cfu/mL) are: (A) 7.0 × 10<sup>8</sup>, (B) 3.5 × 10<sup>8</sup>, (C) 2.6 × 10<sup>8</sup>, (D) 1.7 × 10<sup>8</sup>, (E) 8.6 × 10<sup>7</sup>, (F) 4.2 × 10<sup>7</sup>, (G) 2.0 × 10<sup>7</sup>. Lower panel: Inhibition of the growth of 1.6 × 10<sup>8</sup> cfu/mL of *P. putida* at different concentrations of Cu(II).



**431. Novel Method for Time-Resolved Fluorometric Determination and Imaging of the Activity of Peroxidase, and its Application to Enzyme-Linked Immunosorbent Assays,** Z. Lin, M. Wu, O. S. Wolfbeis, M. Schaeferling; *Chem. – Eur. J.* (2006), 12, 2730-2738. DOI: 10.1002/chem.200500884. Journal IF: 5.0.

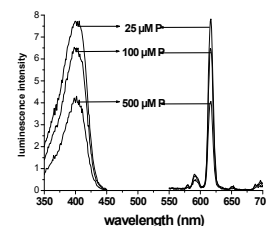
**Abstract:** A new format for enzyme-linked immunosorbent assays (ELISA) is described, using the europium(III) tetracycline complex [Eu(Tc)] as a fluorescent probe for hydrogen peroxide (HP). [Eu(Tc)] forms a strongly fluorescent complex with HP, and the peroxidase-catalyzed decomposition of the system [Eu(Tc)-HP] can be monitored via the decrease in fluorescence due to the formation of the weakly fluorescent [Eu(Tc)]. Due to this effect, the europium probe can be used to detect the presence of peroxidases linked to antibodies. Furthermore, the fluorescence decay time of [Eu(Tc)-HP] is in the

range of 60 μs, which enables the application of time-resolved detection methods. These show superior properties compared to intensity-based techniques due to better elimination of background signals. The time-resolved (“gated”) fluorescence assays cover a dynamic range from 0.1 – 8 ng/mL for the quantitation of bovine IgG by peroxidase-labeled anti-bovine IgG in a sandwich-type ELISA. Multiplexed samples can alternatively be visualized directly and evaluated quantitatively by means of fluorescent imaging with the help of an array of light-emitting diodes (LEDs) and a CCD camera. The figure shows a typical array of images as obtained by time-resolved imaging of microwell spots (sandwich assay format).



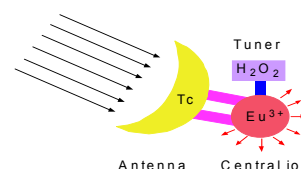
**428. Microtiter Plate Assay for Phosphate Using a Europium-Tetracycline Complex as a Sensitive Luminescent Probe, A. Duerkop, M. Turel, A. Lobnik, O. S. Wolfbeis; *Anal. Chim. Acta* (2006), 555, 292-298. DOI: 10.1016/j.aca.2005.09.007. Journal IF: 2.9.**

**Abstract:** A new luminescent Eu(III) probe is presented for the determination of phosphate (P) in microtiter plate format. The assay is based on the quenching of the luminescence of the Eu(III)-tetracycline 1:1 complex by phosphate using a reagent concentration of 20.8  $\mu\text{mol/L}$ . The probe is excited at 400 nm and displays a Stokes' shift of 210 nm. The emission maximum is located at 616 nm. The system works best at neutral pH 7. The linear range of the calibration plot is from 5  $\mu\text{mol/L}$  to 0.75 mmol/L of phosphate, and the limit of detection is 5  $\mu\text{mol/L}$ . The Figure shows the excitation and emission spectra of  $\text{Eu}_3\text{Tc}$  in presence of various concentrations of phosphate in MOPS buffer of pH 7.



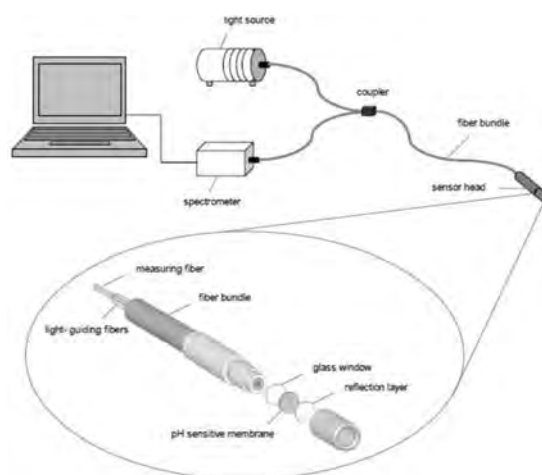
**427. Nonenzymatic Direct Assay of Hydrogen Peroxide at Neutral pH Using the  $\text{Eu}_3\text{Tc}$  Fluorescent Probe. A. Duerkop, O. S. Wolfbeis; *J. Fluoresc.* 2005, 15, 755-761. DOI: 10.1007/s10895-005-2984-6. Journal IF: 2.6.**

**Abstract:** A detailed study is presented on the use of an easily accessible probe (the europium-tetracycline 3:1 complex; referred to as  $\text{Eu}_3\text{Tc}$ ) for determination of hydrogen peroxide (HP).  $\text{Eu}_3\text{Tc}$  undergoes a 15-fold increase in luminescence intensity on exposure to an excess of HP. Data are given on the time dependence of the reaction, on the pH dependence of the absorption and emission spectra. HP can be quantified in aqueous solution of pH 6.9 over a 2 – 400  $\mu\text{M}$  concentration range with a limit of detection of 960 nM. The assay is validated using standard additions, and mean recoveries are found to be between 97.0 and 101.8 %. Species that interfere in concentrations below 1 mM include phosphate, copper(II), fluoride and citrate. The method is critically assessed with respect to other optical methods for determination of HP.



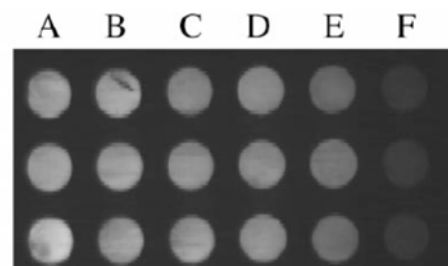
**426b. Fiber Optic pH Sensor for Early Detection of Danger of Corrosion in Steel-Reinforced Concrete Structures. N. Dantan, W. R. Habel, O. S. Wolfbeis. *Proc. SPIE (Soc. Photoinstrum. Eng.)* 2005, vol. 5758 (Smart Structures and Materials), 274–285. DOI: 10.1117/12.600703**

**Abstract:** Corrosion in steel-reinforced concrete structures is a critical issue. Corrosion appears if the pH value of the concrete matrix decreases to below 10 due to deterioration of the calcium hydroxide layer on the steel surface. At present, several reliable systems for determination of chemical parameters in aggressive environments are available on the market, but can not be used for long-term monitoring of pH in concrete structures. This paper describes a fiber optic pH sensor for this purpose. Particular attention is paid to the requirements on such a sensing system. The pH indicator N9 (from Merck) was chosen as the pH-sensitive fluorescence energy acceptor because the absorption spectrum of its (blue) basic form overlaps quite well with the wide red emission band of the diphenylbipyridyl ruthenium(III) complex whose lifetime consequently varies with pH values. The pH-sensitive layer was prepared by first covalently immobilizing the pH indicator dye N9 on carboxycellulose (CM52; from Servagel) via a vinyl sulfonyl group according to the Remazol method. The ruthenium complex was then immobilized on the cellulose via electrostatic interaction. The colored cellulose was added to a solution of polyurethane in water/ethanol, and the resulting cocktail was spread onto a polyester film in a wet thickness of typically 250  $\mu\text{m}$ . The pH sensor shows good response (via measurement of the pH-dependent phase shift of the emission) and works under strongly alkaline conditions for one year. Therefore, it represents a promising approach for in-situ long-term monitoring in concrete structures.



**426. Fluorescence Quenching of the Europium Tetracycline Hydrogen Peroxide Complex by Copper(II) and other Metal Ions, C. Cano-Raya, M. D. Fernández Ramos, L. F. Capitán Vallvey, O. S. Wolfbeis, M. Schaeferling; *Appl. Spectrosc.* (2005), 59, 1209. DOI: 10.1366/000370205774430945. Journal IF: 1.9.**

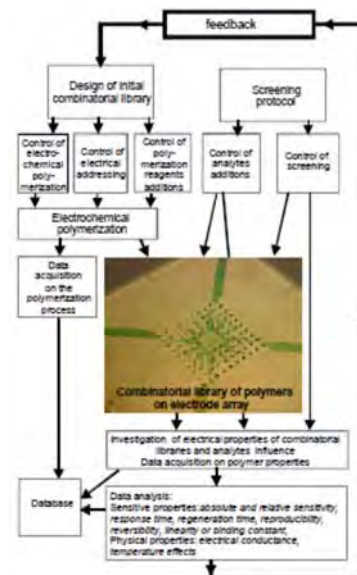
**Abstract:** The europium-tetracycline complex [ $\text{Eu}(\text{Tc})$ ] on addition of hydrogen peroxide (HP) undergoes a 15-fold increase in luminescence intensity. Luminescence is quenched by  $\text{Cu}^{2+}$ ,  $\text{Fe}^{3+}$ ,  $\text{Ag}^+$ ,  $\text{Al}^{3+}$ ,  $\text{Zn}^{2+}$ ,  $\text{Co}^{2+}$ ,  $\text{Ni}^{2+}$ ,  $\text{Mn}^{2+}$ ,  $\text{Ca}^{2+}$  and  $\text{Mg}^{2+}$ . The strongest quenching (both static and dynamic) is induced by  $\text{Cu}^{2+}$ , and these processes were quantified by means of their quenching constants. Stern-Volmer plots were also derived from lifetime imaging measurements accomplished by the Rapid Lifetime Determination (RLD) technique based on microwell plate assays, and also by the Time-Correlated Single Photon Counting technique (TCSPC). A time-resolved fluorescent method for determination of copper is presented. The response to copper is linear up to 1.6  $\mu\text{M}$ , providing a detection limit of 0.2  $\mu\text{M}$ . The figure shows grey-scale images of solutions of the [ $\text{Eu}(\text{Tc})(\text{HP})$ ] complex in a microwell plate exposed to different concentrations of  $\text{Cu}(\text{II})$ . Data were acquired by the rapid lifetime determination (RLD) method.



**425. Complete System for Combinatorial Synthesis and Functional Investigation of Conductive Polymers.** V. M. Mirsky, V. Kulikov, O. S. Wolfbeis; *Polym. Mater. Sci. Eng. Preprints (Am. Chem. Soc.)* (2005), 93, 1053. Web: <https://opus4.kobv.de/opus4-UBICO/frontdoor/index/index/docId/18148>; <https://epub.uni-regensburg.de/20301/>

**Abstract:** We describe here an automated high-throughput system to perform automated electropolymerization as used in various fields of science and technology. It allows polymer layers of controlled thickness to be prepared, and to form multilayer systems. The method is compatible with inorganic electroplating. Applications of electropolymerization include fabrication of chemical sensors and biosensors, deposition of corrosion protective coatings, development of organic electronic devices and electrochromic windows.

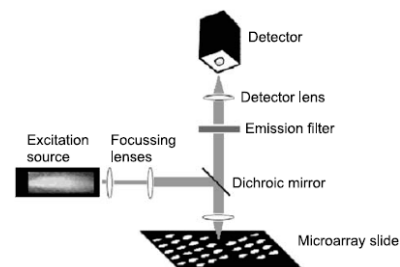
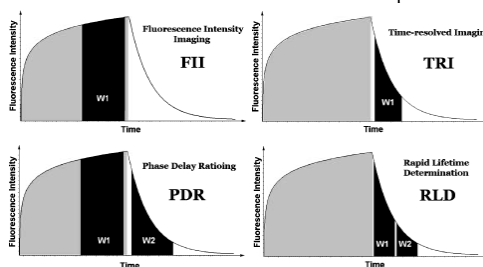
The graph shows the complete system for combinatorial electropolymerization and high-throughput characterization. Also shown is the protocol (work-flow) for functional characterization of the resulting materials.



**424. Review. Fluorescence Analysis in Microarray Technology,** S. Nagl, M. Schaeferling, O. S. Wolfbeis; *Microchim. Acta* 2005, 151, 1-21. DOI: 10.1007/s00604-005-0393-9. journal IF: 1.6.

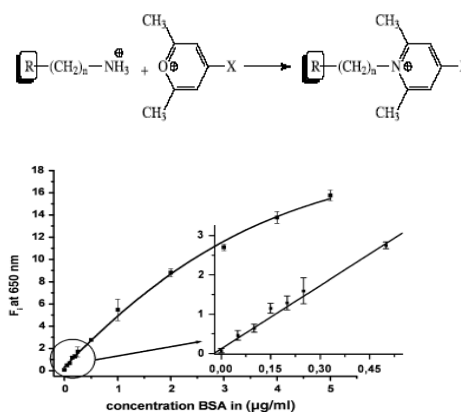
**Abstract:** We review the most common methods and the state-of-the-art of all areas in microarray fluorescence analysis. Starting with an overview on microarray formats with a focus on (a) their demands on the readout, (b) common organic fluorescent stains, (c) the use of semiconductor nanocrystals (quantum dots), polymer and silica nanoparticles and (d) of fluorescent proteins as labels. Ways to enhance the intrinsically low signal on biochips have become increasingly important as they offer a sound approach towards the detection of low concentration sample content.

The three main categories are presented, viz. amplification using DNA, enzymes, and dendrimers. As much diversity as on the microarrays themselves can be found at the detection device. Standard optical microarray detectors, and non-standard methods using fluorescence anisotropy, fluorescence lifetime imaging (FLIM) and fluorescence resonance energy transfer (FRET), and their advantages and disadvantages are discussed. The figures show common methods for intensity or lifetime based imaging (left), and a typical optical arrangement (right).



**423. Novel Type of General Protein Assay Using a Chromogenic and Fluorogenic Amine-Reactive Probe,** B. K. Hoefelschweiger, A. Duerkop, O. S. Wolfbeis; *Anal. Biochem* 2005, 344, 122-129. DOI: 10.1016/j.ab.2005.06.030. Journal IF: 3.0.

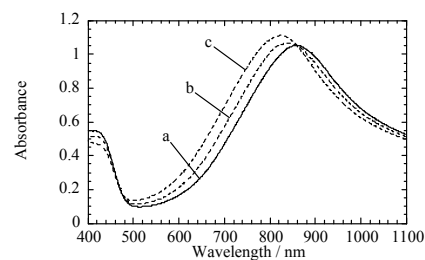
**Abstract:** A new and simple 1-reagent method is presented for general protein assay. It makes use of one of two new reactive labeling reagents (referred to as Py labels) that can be applied for both photometric and fluorimetric assays at neutral pHs at room temperature. The Py labels undergo a large spectral change on conjugation to the amino group of proteins and typically change their color from blue to red. Therefore, and unlike in other assays, there is no need to separate the unconjugated (blue) label from the red conjugate which can be determined by direct photometry with a limit of detection of 1.2 µg/mL for HSA. The assay can be extended to fluorometry since the fluorescence of the free Py label is weak (with a quantum yield of <1 %) but increases strongly (to > 40%) on conjugation. The strong fluorescence of the red conjugates can be determined directly and without interference by the blue free dye. The fluorometric assay resulted in a limit of detection of 60 ng/mL for BSA. Validation of the fluorescence assay of blood plasma samples spiked with BSA gave recoveries in the range from 91 to 103%. The Figure on the right shows the calibration plot (and standard deviations for n = 5) for a fluorometric BSA assay. The inset shows the plot for the low concentration range.





**422. Optical Ozone Sensing Properties of Poly(2-chloroaniline), Poly(N-methylaniline) and Polyaniline Films,** M. Ando, C. Swart, E. Pringsheim, V. M. Mirsky, O. S. Wolfbeis; *Sensors Actuat., B:* (2005), 108, 528-534. DOI: 10.1016/j.snb.2004.12.083. Journal IF: 2.3.

**Abstract:** The ozone-sensitive visible/near-IR absorbance changes of poly(2-chloroaniline), poly(N-methylaniline) and polyaniline (PANI) films were investigated. These films, which were assumed to be present partially in a protonated form and partially in a reduced form, were prepared by chemical oxidation of the monomers followed by treatment with the reducing agent disodium disulfite. The p(2ClANI) film was sensitive to ozone down to 2.5 ppm, but saturation of sensitivity started to appear above 50 ppm. By contrast, the PANI and p(NMeANI) films were sensitive to ozone in a range of 50-100 ppm without showing saturation of sensitivity. The figure shows the ozone-induced changes in the absorption of a PANI film. (A) Visible/near-IR absorption spectra of the film in air with and without ozone. (a) in atmospheric air. (b, c) In air containing 50 and 100 ppm of ozone, respectively.



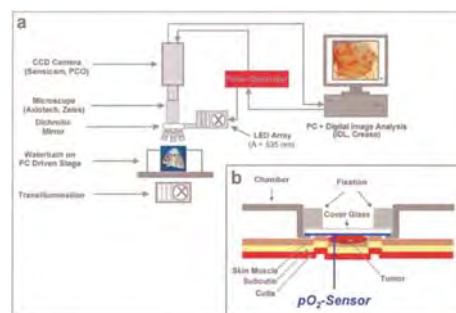
**421. In Vivo Phosphorescence Imaging of pO<sub>2</sub> Using Planar Oxygen Sensors.** P. Babilas, G. Liebsch, V. Schacht, I. Klimant, O. S. Wolfbeis, R.-M. Szeimies, C. Abels, *Microcirculation (Philadelphia)* (2005), 12, 477-487. DOI: 10.1080/10739680591003314. Journal IF: 2.4.

**Objective:** Oxygen-dependent quenching of luminescence of metal porphyrin complexes has been used to image the pO<sub>2</sub> distribution over tumor and normal tissue.

**Methods:** An exptl. setup is described using a platinum(II)-octaethyl-porphyrin immobilized in a polystyrene matrix as transparent planar sensor.

**Results:** Sensitivity over a broad range is high at low pO<sub>2</sub> values ( $\pm 0.2$  mm Hg at 0 mm Hg;  $\pm 1.5$  mm Hg at 160 mm Hg pO<sub>2</sub>). Due to intrinsically referencing via lifetime encoding there was no modification of the sensor response in vivo in the dorsal skinfold chamber model with amelanotic melanoma (AMEL-3) in awake hamsters when compared to the in vitro calibration. pO<sub>2</sub> measurements over normal tissue ( $25.8 \pm 5.1$  mm Hg) and tumor tissue ( $9.2 \pm 5.1$  mm Hg) were in excellent agreement with previous results obtained in this model using a surface multiwire electrode.

**Conclusions:** Using the presented method the surface pO<sub>2</sub> distribution can be mapped with a high temporal resolution of approximately 100 ms and a spatial resolution of at least 25  $\mu$ m. Moreover, the transparent sensor allows the simultaneous visualization of the underlying microvasculature.

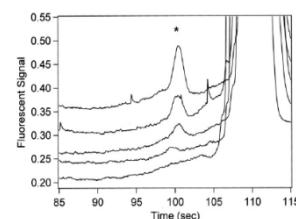


**420. Time-Resolved Fluorescent Chirality Sensing and Imaging of Malate in Aqueous Solution.** Z. Lin, M. Wu, O. S. Wolfbeis; *Chirality* (2005), 17, 464-469. DOI: 10.1002/chir.20185. Journal IF: 2.2.

**Abstract:** Chiral discrimination of malates in aqueous solutions at near-neutral pH is achieved through fluorescence measurement and imaging using the europium(III)-tetracycline complex (EuTc) as a fluorescent probe. The method is based on the significantly different fluorescence properties of the ternary complexes (Eu-Tc-malate) formed between EuTc and the enantiomeric malates. The enantiomeric excess (ee) of chiral malates can be quantified by both steady-state and time-resolved fluorescence, using either a conventional fluorescence microplate reader or fluorescence imaging. It offers a facile and sensitive method for high-throughput chiral discrimination.

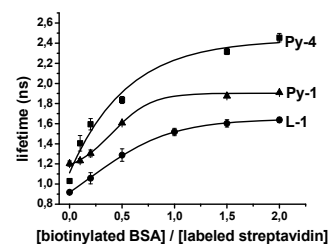
**419. Determination of Picomolar Concentrations of Proteins Using Novel Amino Reactive Chameleon Labels and Capillary Electrophoresis Laser-Induced Fluorescence Detection,** D. B. Craig, B. K. Wetzl, A. Duerkop, O. S. Wolfbeis; *Electrophoresis*, 2005, 26, 2208-2213. DOI: 10.1002/elps.200410332. Journal IF: 4.1.

**Abstract:** Py-1 and Py-6 are novel amino-reactive fluorescent reagents. The names given to them reflect that they consist of a pyrylium group attached to small aromatic moieties. Upon reaction with a primary amine there is a large spectral shift in the reagent, rendering them effectively fluorogenic. The reagents were used to label a test protein (HSA), and the sample was analyzed by capillary electrophoresis and laser-induced fluorescence detection. The detection limits after a 60-min labeling reaction is 6.5 ng/mL (98 pM). Separation of immunoglobulin G (IgG), HSA, lipase, and myoglobin after labeling with Py-6 were performed. Unlike many other amino reactive reagents used to label protein amino groups, reaction with Py-1 and Py-6 do not alter the charge of the protein and the advantage of this with respect to electrophoretic separations is discussed. The graph shows the electropherogram of HSA (peaks marked with an \*) in concentrations of 15, 7.5, 3.8 and 1.9 ng/mL. The bottom line is the blank.



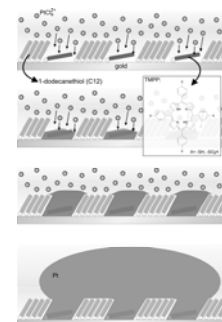
**418. Screening Scheme Based on Measurement of Fluorescence Lifetime in the Nanosecond Domain.** B. K. Hoefelschweiger, L. Pfeifer, O. S. Wolfbeis; *J. Biomol. Screen.* (2005), 10, 687-694. DOI: 10.1177/1087057105277493. Journal IF: 2.8.

**Abstract:** We demonstrate that the fluorescence lifetime of certain fluorescent labels is a useful parameter to detect affinity binding between biotin and streptavidin, and between biotinylated bovine serum albumin and streptavidin. The assay is performed in a microplate format and lifetimes are determined using dye laser-induced fluorescence. Four fluorescent labels are presented that undergo a significant change in their lifetime upon affinity binding. This fluorescence lifetime affinity assay has several attractive features in that it (a) requires single labeling only; (b) represents a homogeneous assay; (c) allows each of the two binding partners to be labeled; and (d), is compatible with the standard microwell formats used in high-throughput screening.



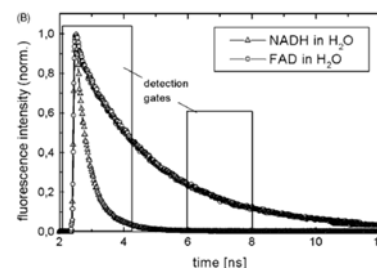
**416. Size-Controlled Electrochemical Synthesis of Metal Nanoparticles on Monomolecular Templates**, T. Hirsch, M. Zharnikov, A. Shaporenko, J. Stahl, D. Weiss, O. S. Wolfbeis, V. M. Mirsky; *Angew. Chem.* (2005), 44, 6775-6778. DOI: 10.1002/anie.200500912. Journal IF: 10.3.

*Abstract:* A new technique is described for preparation of metallic nanoparticles on electrode surfaces which does not require the use of STM. The method is based on the reduction of metals on nanoelectrodes formed by the recently developed spreader-bar technique. A variation of the reduction current provides a simple way to control the size of nanoparticles. This novel nanoelectrochemical approach was tested with deposition of platinum and copper but we do not see any principal limitation for its extension to other conductive and semiconductive materials such as different metals, electrochemically synthesized polymers, nanocomposites and others. Also the size of formed nanoparticles which is in our work between 20 and 1000 nm can probably be reduced.

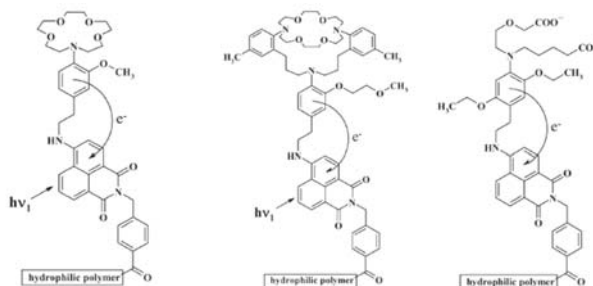


**415. Improved Routine Bio-Medical and Bio-Analytical Online Fluorescence Measurements Using Fluorescence Lifetime Resolution**. L. Pfeifer, K. Stein, U. Fink, A. Welker, B. Wetzl, P. Bastian, O. S. Wolfbeis; *J. Fluoresc.* (2005), 15, 423-432. DOI: 10.1007/s10895-005-2634-z.

*Abstract:* This article describes the technical set up of a time-resolving instrument with either a fixed time-gated detection principle for improved evaluation of tissue metabolite by an online monitoring of the tissue autofluorescence or a direct fluorescence lifetime detection principle for lifetime-based fluorescent assays.

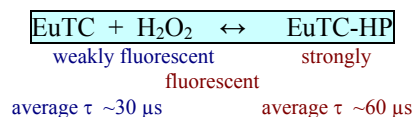


**414. Review: Materials for Fluorescence-Based Chemical Sensors**, O. S. Wolfbeis; *J. Mater. Sci.* 2005, 15, 2657-2669. DOI: 10.1039/b501536g. Journal IF: 4.3. *Abstract:* Optical chemical sensors are capable of continuously recording a chemical species and thus have found (and will find) numerous applications in areas such as the chemical industry, in biotechnology and medicine. Among the many optical methods are employed for sensing purposes, fluorescence has attracted particular attention because it is sensitive, has numerous parameters that can serve as an analytical information and knows effects unknown to other spectroscopies. The implementation of spectroscopic schemes into a useful sensing scheme has been hampered by the lack of appropriate materials including polymers and particles, indicator probes, molecular receptors, carriers, catalysts and fluorescent semiconductor materials. This article addresses the progress made in the past years and addresses some of the futures challenges. The graphs below shows fluorescent probes for Na, K and Ca immobilized on a hydrophilic polymer and used, in the form of sensor layers, in a commercially available blood electrolyte sensor (Terumo).



**412. Fluorescence Imaging of the Activity of Glucose Oxidase Using a Hydrogen Peroxide Sensitive Europium Probe**, M. Wu, Z. Lin, M. Schaeferling, A. Duerkop, O. S. Wolfbeis; *Anal. Biochem.* 2005, 340, 66-73. DOI: 10.1016/j.ab.2005.01.050. Journal IF: 3.0.

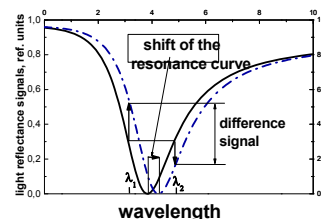
*Abstract:* A method for optical imaging of the activity of glucose oxidase (GOx) using a fluorescent europium(III) tetracycline probe (EuTC) for hydrogen peroxide is presented. A decay time in the microsecond range and the large Stokes shift of 210 nm of the probe facilitate intensity-based, time-resolved, and decay-time-based imaging of glucose oxidase. Four methods for imaging the activity of GOx were compared, and rapid lifetime determination imaging was found to be the best in giving a linear range from 0.32 to 2.7 mUnit/mL. The detection limit is 1.7 ng/mL. Fluorescent imaging of the activity of GOx is considered to be a useful tool for GOx-based immunoassays with potential for high-throughput screening, immobilization studies, and biosensor array technologies.



**411. Double Wavelength Technique for SPR Detection: Basic Concept and Applications for Single Sensors and Arrays**, A. Zybin, C. Grunwald, V. M. Mirsky, J. Kuhlmann, O. S. Wolfbeis, K. Niemax; *Anal. Chem. (Wash.)* 2005, 77, 2393-2399.

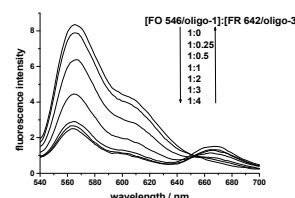
DOI: 10.1021/ac048156v. Journal IF: 5.7.

**Abstract:** The double-wavelength measurement scheme is based on surface irradiation by a parallel beam composed of two laser beams with different wavelengths. After rough tuning the incidence angle to resonance, the laser wavelengths are tuned to the opposite sides of the resonance curve and fixed to positions where the slopes are steepest and the reflectivity for both wavelengths is the same, i.e., the photodetector currents are equal. The lasers are alternatively switched on and off with a frequency of a few kHz, so that always only one of the lasers is operating at a time. If the reflectivity signals for both wavelengths are equal, the photodetector produces a direct current signal. Any shift of the SPR curve results in a difference in reflectivity and in an alternative current (AC) signal at the photodiode.



**410. New Longwave Absorbing Fluorochromes and Their Application to Oligonucleotide Labeling and Fluorescence Resonance Energy Transfer Hybridization Studies,** M. Gruber, B. Oswald, B. Wetzl, J. Enderlein, O. S. Wolfbeis; *J. Fluoresc.* **2005**, *15*(3), 207-214. DOI: 10.1007/s10895-005-2619-y. Journal IF: 2.6.

**Abstract:** We describe two new fluorescence resonance energy transfer (FRET) labels along with their covalent linkage to oligonucleotides, and their use as donor and acceptor, respectively, in FRET hybridization studies. The dyes belong to the cyanine dyes, and water solubility is imparted by a phosphonate which represents a new solubilizing group in DNA labels. They were linked to amino-modified synthetic oligonucleotides via oxysuccinimide (OSI) esters. The studies include the determinations of molecular distances and of limits of detection, which are in the order of 5 pmol/L for a 15-mer. The graph gives a plot of FRET efficiency in the titration of a labeled 15-mer with its complementary strand (A) and with 2 mismatched strands (B, C).



**409. Nanometer-Thick SPR Sensor for Gaseous HCl.** A. V. Samoylov, V. M. Mirsky, Q. Hao, C. Swart, Y. M. Shirshov, O. S. Wolfbeis; *Sensors Actuators, part B (Chemical)* **(2005)**, *106B*, 369-372. DOI: 10.1016/j.snb.2004.08.029. Journal IF: 2.3.

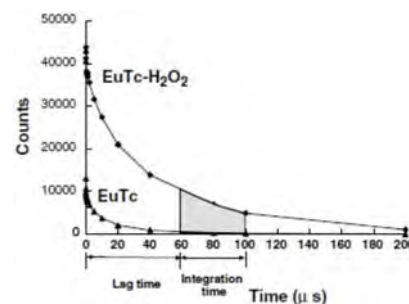
**Abstract:** The optical properties of electrochemically polymerized N-methylaniline are changed in the presence of gaseous hydrogen chloride. This effect was used for preparation of chemical sensors with transduction based on surface plasmon resonance. The interaction of hydrogen chloride with a two nm layer of poly-(N-methylaniline) on gold leads to the shift of the surface plasmon resonance. The analysis of the resonance spectra demonstrates that the effect is caused by an increase of the imaginary component of the refractive index; a minor contribution is also provided by film condensation leading to an increase of the real component of the refractive index and a decrease in the thickness. The sensor is selective and quasi-reversible. The concentration dependence of the gas effect obeys Langmuir's adsorption isotherm with a reciprocal value of the binding constant of  $850 \pm 160$  ppm.

**408. High-Throughput Analysis of Bulk and Contact Conductance of Polymer Layers on Electrodes.** V. Kulikov, V. M. Mirsky, T. Delaney, D. Donoval, A. W. Koch, O. S. Wolfbeis; *Measurement Sci. Technol.* **(2005)**, *16*, 95-99. DOI: 10.1088/0957-0233/16/1/013. Journal IF: 1.2.

**Abstract:** An approach for high-throughput analysis of bulk and contact conductance of polymer layers is described and evaluated. The approach, based on simultaneous two- and four-point conductance measurements, was realized as a high-throughput method and applied for investigation of conductive polymers on an array of interdigital platinum electrodes. Several examples demonstrate distinctive influence of combinatorially varied conditions of polymer synthesis (polymerization charge, content of copolymers) as well as chemical treatment of the synthesized polymers in bulk and contact resistance of metal/polymer/metal systems. The technique can be widely applied to material research for investigation of bulk and contact electrical properties.

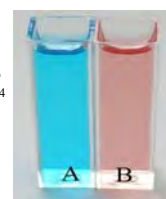
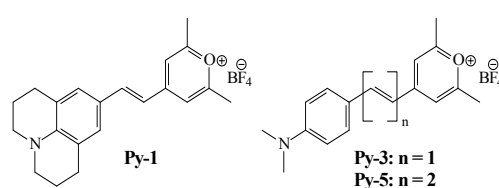
**405. Time-Resolved Enzymatic Determination of Glucose Using a Fluorescent Europium Probe for Hydrogen Peroxide.** M. Wu, Z. Lin, A. Duerkop, O. S. Wolfbeis; *Anal. Bioanal. Chem.* **(2004)**, *380*, 619-626. DOI: 10.1007/s00216-004-2785-9. Journal IF: 2.9.

**Abstract:** An enzymatic assay for glucose based on the use of the fluorescent probe for hydrogen peroxide, europium(III) tetracycline (EuTc), is described. The weakly fluorescent EuTc and enzymatically generated  $H_2O_2$  form a strongly fluorescent complex (EuTc- $H_2O_2$ ) whose fluorescence decay profile is significantly different. Since the decay time of EuTc- $H_2O_2$  is in the microseconds time domain, fluorescence can be detected in the time-resolved mode, thus enabling substantial reduction of background fluorescence. The scheme represents the first  $H_2O_2$ -based time-resolved fluorescence assay for glucose not requiring the presence of a peroxidase. The time-resolved assay (with a delay time of 60  $\mu$ s and using endpoint detection) enables glucose to be determined at levels as low as 2.2  $\mu$ M, with a dynamic range of 2.2-100  $\mu$ M. The method also was adapted to a kinetic assay in order to cover higher glucose levels (mM range). The latter was validated by analyzing spiked serum samples and gave a good linear relationship for glucose levels from 2.5 to 55 mM. Noteworthy features of the assay include easy accessibility of the probe, large Stokes' shift, a line-like fluorescence peaking at 616 nm, stability towards oxygen, a working pH of approximately 7, and its suitability for both kinetic and endpoint determination.



**404. Chameleon Labels for Staining and Quantifying of Proteins,** B. K. Wetzl, S. M. Yarmoluk, D. Craig, O. S. Wolfbeis; *Angew. Chem. Intl. Ed.* **2004**, *43*, 5400-5402. DOI: 10.1002/anie.200460508. Journal IF: 10.3.

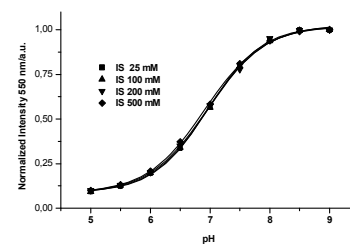
**Abstract:** A new class of protein stains and label (the Py dyes) is presented for use in proteomics and in protein assay. They undergo a color change, typically from blue (see A) to red (see B) on binding to proteins. The unreacted stains are almost non-fluorescent (with a quantum yield of <1 %), but the protein-conjugated forms are highly fluorescent. Unlike many other types of labels, the Py dyes do not alter the charge of a protein, and thus does not change its electrophoretic properties. The figure on the far right shows the color of label Py-1 before (A) and after (B) conjugation to HSA.





**403. Fluorescent pH Sensors with Negligible Sensitivity to Ionic Strength, B. Weidgans, C. Krause, I. Klimant, O. S. Wolfbeis; *Analyst* 2004, 129, 645-650. DOI: 10.1039/b404098h. Journal IF: 3.2.**

**Abstract:** Optical determination of pH has the fundamental disadvantage of measuring a signal that depends on the ionic strength of the sample. The effect of ionic strength on the signal depends on the charge of the indicator and its environment, e.g. the matrix. We present novel lipophilic fluorescein esters carrying one negative charge. They are embedded into an uncharged, highly proton-permeable hydrogel to give optical pH sensors that show a negligible cross-sensitivity towards ionic strength. The dyes differ in their substituents. This variation of substituents results in dissociation constants between 5.5 and 8.5. Two indicators may be used in one sensor, and this results in an optical pH sensor with a range that extends from pH 4.5 to 8.



**402. Book Chapter: Application of Combinatorial Electropolymerization to the Development of Chemical Sensors. V. M. Mirsky, V. Kulikov, Q. Hao, O. S. Wolfbeis; *Materials Res. Soc. Symp. Proc.* (2004), 804(Combinatorial and Artificial Intelligence Methods in Materials Science II), 111-116. DOI: 10.1557/PROC-804-JJ4.1**

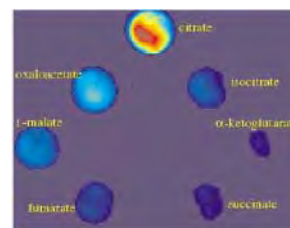
**Abstract:** Combinatorial electropolymerization with electrical addressing was realized on the array of 96 electrode groups, each from four electrodes. The polymer synthesis was combined with subsequent high-throughput investigation of analytical properties of synthesized polymers. Two- and four-point techniques were applied simultaneously to measure electrical properties of synthesized polymers and contact resistances between electrodes and polymers and modifications of these parameters on addition of analyte. The system was used for development of sensitive materials for detection of gaseous hydrogen chloride.

**401. Review: Fiber Optic Chemical Sensors and Biosensors (2002-2003). O. S. Wolfbeis; *Anal. Chem. (Wash.)* (2004), 76, 3269-3283. DOI: 10.1021/ac040049d. journal IF: 5.7.**

**Abstract:** This biannual review covers the time period from January 2002 to January 2004 and is written in continuation of previous reviews. Since the number of citations in this review is limited, a stringent selection had to be made. Priority was given to fiber-optic sensors (FOS) for defined chemical, environmental, and biochemical significance and to new schemes and materials. The review does not include (a) FOS that obviously have been rediscovered; (b) FOS for nonchemical species such as temperature, current and voltage, stress, strain, and displacement, for structural integrity (e.g., of constructions), liquid level, and radiation; and (c) FOS for monitoring purely technical processes such as injection molding, extrusion, or oil drilling, even though these are important applications of optical fiber technology.

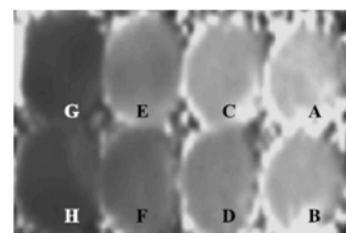
**400. Fluorescent Imaging of Citrate and Other Intermediates in the Citric Acid Cycle, Z. Lin, M. Wu, M. Schaeferling, O. S. Wolfbeis; *Angew. Chem. Intl. Ed.* 2004, 43, 1735-1738. DOI: 10.1002/anie.200353169. journal IF: 10.3.**

**Abstract:** Citrate and other intermediates of the Krebs cycle (isocitrate, ketoglutarate, succinate, fumarate, malate, oxaloacetate) can be sensed and imaged by time-resolved fluorescence spectroscopy using the  $\text{Eu}^{3+}$ -tetracycline complex as a fluorescent probe. Time-resolutions enables discrimination between different intermediates, and enzymatic conversions are not needed for making the species susceptible to imaging. The complexes with different intermediates can be discriminated via their different "fluorescence" decay times.



**399. Time-Resolved Fluorescent Imaging of Glucose, M. Schaeferling, M. Wu, O. S. Wolfbeis; *J. Fluoresc.* 2004, 14, 561-568. DOI: 10.1023/B:JOFL.0000039343.02843.12. Journal IF: 2.6.**

**Abstract:** A method for the fluorescent imaging of glucose is described that is based on the detection of enzymatically produced hydrogen peroxide, using the europium(III) tetracycline complex as the fluorescent probe incorporated into a hydrophilic polymer layer. Co-adsorption of glucose oxidase (GOx) makes these sensor layers respond to the hydrogen peroxide produced by the GOx-assisted oxidation of glucose. These hydrogels are integrated into a 96-microwell for a parallel and simultaneous detection. Glucose is visualized by means of time-resolved luminescence lifetime imaging. Unlike in previous methods, the determination of  $\text{H}_2\text{O}_2$  does not require the addition of peroxidase or a catalyst to form a fluorescent product. The lifetime-based images obtained are compared to conventional fluorescence intensity-based methods with respect to sensitivity and the dynamic range of the sensor layer. The Figure shows grey-scale ratiometric fluorescence images of sensor membrane spots placed in a microwell plate following exposure to various concentrations of glucose (from 0 to 1 M).



**397. Optical Sensors in Intelligent Food Packaging Technology. A. McEnvoy, C. von Bueltzingsloewen, C. McDonagh, B. D. MacCraith, I. Klimant, O. S. Wolfbeis; *Proc. Soc. Photoinstrum. Eng. (Proc. SPIE)* (2003), 4876, 806-815 (publ. 2004). DOI: 10.1117/12.464210**

**Abstract:** Modified Atmosphere Packaged (MAP) food employs a protective gas mixture, which normally contains selected amounts of carbon dioxide ( $\text{CO}_2$ ) and oxygen ( $\text{O}_2$ ), in order to extend the shelf life of food. Conventional MAP analysis of package integrity involves destructive sampling of packages followed by carbon dioxide and oxygen detection. For quality control reasons, as well as to enhance food safety, the concept of optical on-pack sensors for monitoring the gas composition of the MAP package at different stages of the distribution process is very attractive. The objective of this work was to develop printable formulations of oxygen and carbon dioxide sensors for use in food packaging. Oxygen sensing is achieved by detecting the degree of quenching of a fluorescent ruthenium complex entrapped in a sol-gel matrix. In particular, a measurement technique based on the quenching of the fluorescence decay time, phase fluorometric detection, is employed. A scheme for detecting  $\text{CO}_2$  has been developed which is compatible with the oxygen detection scheme. It is fluorescence-based and uses the pH-sensitive 8-hydroxypyrene-1,3,6-trisulfonic acid (HPTS) indicator dye encapsulated in an organically modified silica (ORMOSIL) glass matrix. Dual Luminophore Referencing (DLR) has been employed as an internal referencing scheme, which provides many of the advantages of lifetime-based fluorometric methods. Oxygen cross-sensitivity was minimized by encapsulating the reference luminophore in dense sol-gel microspheres. The sensor performance compared well with standard methods for both  $\text{O}_2$  and  $\text{CO}_2$ . The results of preliminary on-pack print trials are presented and a preliminary design of an integrated dual gas optical read-out device is discussed.

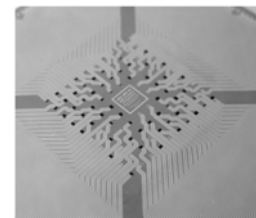
**396. A Combinatorial Approach for Development of Materials for Optical Sensing of Gases**, A. Apostolidis, I. Klimant, D. Andrzejewski, O. S. Wolfbeis; *J. Combinat. Chem.* **2004**, *6*, 325-331. DOI: 10.1021/cc034040l. Journal IF: 3.2.

**Abstract:** A combinatorial approach is used for development of materials for use in optical oxygen sensors. Combinatorial chemistry is shown to speed up the search for new materials by a factor of up to 1000. Various polymers, solvents, indicators, plasticizers, and other additives are varied, and a robotic station is programmed to mix the components. Spots of the sensing materials are deposited in the wells of glass substrates resembling microtiterplates (MTPs) and analyzed in a test stand, where they are exposed to gaseous oxygen of varying partial pressure.



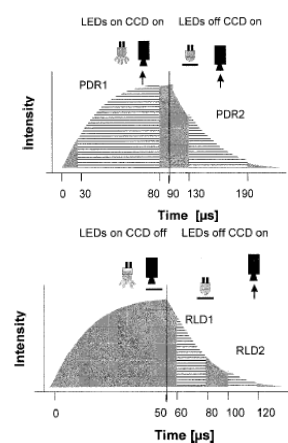
**394. Multiparameter High Throughput Characterization of Combinatorial Chemical Microarrays of Chemosensitive Polymers**, V. M. Mirsky, V. Kulikov, Q. Hao, O. S. Wolfbeis; *Macromol. Rapid Comm.* **25** (2004) 253-258. DOI: 10.1002/marc.200300210. Journal IF: 3.2.

**Abstract:** High-throughput characterization (HTC) of combinatorial libraries demands a compromise between completeness of the study and reasonable investigation time. This compromise can be found by the development of test protocols consisting of the minimal number of the most informative measurements. We describe a method for multiparametric HTC of HCl-sensitive materials for use in fire alarm systems. The approach was specifically applied to the characterization of conductometric sensor materials (electrochemically generated copolymers of aniline and 2-aminobenzoic acid) for detection and quantitation of HCl which is a gas developed by overheated PVC.



**392. Time-Resolved Luminescence Imaging of Hydrogen Peroxide Using Europium-Tetracycline Sensor Membranes in a Microwell Format**, M. Schaeferling, M. Wu, J. Enderlein, H. Bauer, O. S. Wolfbeis; *Appl. Spectrosc.* **57** (2003) 1386-1392. DOI: 10.1366/00037020322554554. Journal IF: 1.9.

**Abstract:** We demonstrate an optical imaging scheme for hydrogen peroxide in a microwell-based format using the europium(III) tetracycline complex as the fluorescent probe, which is incorporated into a poly(acrylonitrile)-co-poly(acrylamide) polymer matrix. The resulting sensor membranes are integrated into a 96-microwell plate. Hydrogen peroxide can be visualized by means of time-resolved imaging. The imaging system consists of a fast, gated CCD camera and a pulsed array of 96 LEDs. Fluorescence lifetime images were acquired by both rapid lifetime detection and phase delay rationing, and compared with intensity-based methods with respect to sensitivity and dynamic range. The response time of the sensor is comparatively high, typically in the range of 10 to 20 min, but the response is reversible. The largest signal changes are observed at pH 6.5 – 7.5. Below is a schematic representation of the time gates in the PDR imaging method (left), and in the RLD imaging method (right). In the PDR scheme, the luminescence is measured first in the excitation period (PDR1), and then in the emission period (PDR2). In the RLD scheme, both time gates (RLD1 and RLD2) are detected during the emission period.

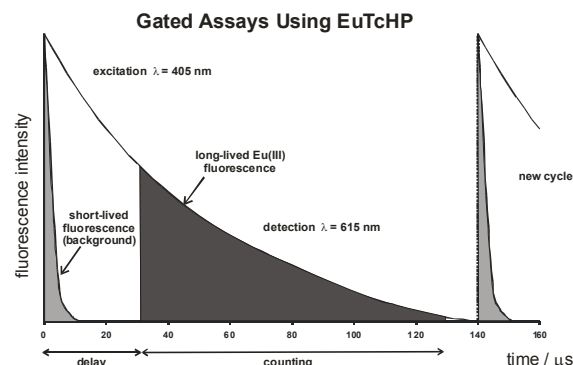


**391. Enantioselective Artificial Receptors Formed by the Spreader-Bar Technique**. M. I. Prodromidis, Th. Hirsch, V. M. Mirsky, O. S. Wolfbeis; *Electroanalysis* **15** (2003) 1795-1798. DOI: 10.1002/elan.200302756. journal IF: 2.4.

**Abstract:** Chiroselective binding sites have been created on thin gold films by application of the spreader-bar approach. Impedometric techniques and surface plasmon resonance were applied to detect binding. (R)-(+)-1,1'-Binaphthyl-2,2'-diol (R-BNOH) and (S)-(-)-1,1'-binaphthyl-2,2'-diol (S-BNOH) were used as model analytes. The artificial receptors were prepared by co-adsorption of 16-mercaptohexadecane (matrix) with a thiol-modified chiral selector (template). The conjugates of D,L-thioctic acid and (R)-(+)- or (S)-(-)-1,1'-binaphthyl-2,2'-diamine were used as templates. Different concentration ratios of the matrix and template were tested. No chiral selectivity of surfaces formed by either the matrix or the template alone was observed. The use of alkylthiols shorter than 16-mercaptohexadecane led to the formation of surfaces with no chiral selectivity. The gold electrodes coated by the spreader-bar technique displayed an enantioselectivity of up to 4.7 or up to 2.5 as measured by the capacitive and SPR methods, respectively.

**390. Detection of Hydrogen Peroxide in River Water Using a Europium Tetracycline Microplate Luminescence Assay with Time-Resolved ("Gated") Detection**. W. Lei, A. Duerkop, M. Wu, O. S. Wolfbeis; *Microchim Acta* **143** (2003) 269-274. DOI: 10.1007/s00604-003-0087-0. journal IF: 1.6.

**Abstract:** Hydrogen peroxide (HP) in river water was determined using the highly luminescent Eu(III)-tetracycline hydrogen peroxide (EuTc-HP) complex. A 15-fold increase in luminescence intensity of EuTc is observed at 616 nm after formation of EuTc-HP. In order to eliminate interferences by other fluorescent substances that exist in river water, a time-resolved scheme is employed: EuTc-HP has a main decay time of 61 ms, while background fluorescence decays within a few ns. Thus, by performing measurements after a delay time of typically 30 ms, the signal becomes highly specific for EuTc-HP. Under optimized conditions (pH 7 in MOPS buffer), the calibration plot for the determination of HP was linear over the range of 2 to 160 mM. The limit of detection is 1.1 mM concentrations of HP. An average recovery of 99.5% was obtained for measurements of river water samples spiked with HP. The relative standard deviation of less than 2% indicates the high accuracy and precision of the method.



**389. Book: Optical Sensors: Industrial, Environmental and Diagnostic Applications**, R. Narayanaswamy, O. S. Wolfbeis (eds.); Springer Verlag, 2004, 441 pp. ISSN 1612-7617; ISBN 3-540-40888-X. Web: <https://www.springer.com/de/book/9783540408864>

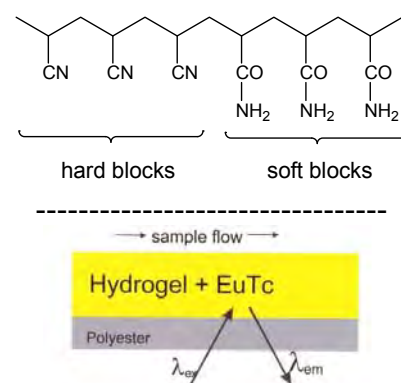
**Contents:** (1) Optical Technology until the Year 2000: A Historical Overview (by O. S. Wolfbeis); (2) Molecularly Imprinted Polymers for Optical Sensing Devices (by M. E. Diaz-Garcia & R. Badia); (3) Chromogenic and Fluorogenic Reactants: New Indicator Dyes for Monitoring Amines, Alcohols and Aldehydes (by G. J. Mohr); (4) Design, Quality Control and Normalization of Biosensor Chips (by C. Preininger & U. Sauer); (5) Rapid, Multiplex Optical Biodetection for Point-of-Care Applications (by F. Y.S. Chuang & B. W. Colston); (6) Multi-functional Biochip for Medical Diagnostics and Pathogen Detection (by T. Vo-Dinh, G. Griffin, D. L. Stokes, D. N. Stratis-Cullu, M. Askari & A. Wintenberg); (7) Surface Plasmon Resonance Biosensors for Food Safety (by J. Homola); (8) NIR Dyes for Ammonia and HCl Sensors (by P. Simon & F. Kvasnik); (9) Piezo-Optical Dosimeters for Occupational and Environmental Monitoring (by K. R. Bearman, D. C. Blackmore, T. J. N. Carter, F. Colin, S. A. Ross & J. D. Wright); (10) Interferometric Biosensors for Environmental Pollution Detection by L. M. Lechuga, F. Prieto & B. Sepulveda); (11) Fiber Optic Sensors for Humidity Monitoring (by M. C. Moreno-Bondi, G. Orellana & M. Bedoya); (12) Optical Sensing of pH in Low Ionic Strength Waters (by B. R. Swindlehurst & R. Narayanaswamy); (13) Environmental and Industrial Optosensing with Tailored Luminescent Ru(II)Polypyridyl Complexes (by G. Orellana & D. Garcia-Fresnadillo); (14) TIFR Array Biosensor for Environmental Monitoring (by K. E. Sapsford & F. S. Ligler); (15) Optical Techniques for Determination and Sensing of Hydrogen Peroxide in Industrial and Environmental Samples (by K. Voraberger).



**388. Book Chapter: Optical Sensor Technology until the Year 2000: a Historical Overview.** O. S. Wolfbeis; in: *Optical Sensors: Industrial, Environmental and Diagnostic Applications*, R. Narayanaswamy, O. S. Wolfbeis (eds.), Springer, 2004, pp. 1-34; ISBN 3-540-40888-X.

**387. Reversible Optical Sensor Membrane for Hydrogen Peroxide Using an Immobilized Fluorescent Probe, and its Application to a Glucose Biosensor.** O. S. Wolfbeis, M. Schaeferling, A. Duerkop; *Microchim. Acta* **143** (2003) 221-227. DOI: 10.1007/s00604-003-0090-5. Journal IF: 1.6.

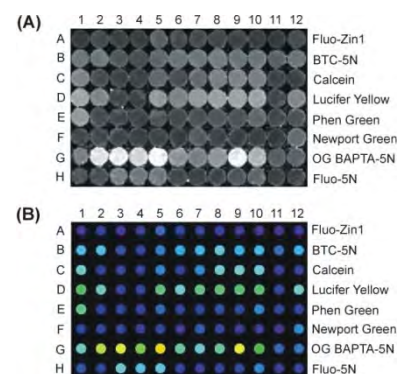
**Abstract:** An optical sensor for hydrogen peroxide (HP) based on the probe europium tetracycline (EuTc) incorporated into a poly(acrylonitrile)-co-poly(acrylamide) polymer (Hypan<sup>tm</sup>); see the figure) is described. Upon optical excitation with 400-nm light, the EuTc in the membrane (see the figure) displays fairly strong fluorescence peaking at 616 nm. Its intensity increases up to 3-fold if the sensor is exposed to solutions containing HP (see Fig. 3). The effect is reversible and can thus be used for continuous sensing. The largest signal changes with HP are observed at pH levels between 6.5 and 7.5, the dynamic range is from 10 to 300 ppm. In order to image the spatial distribution of HP concentrations, sensor membranes were placed on the bottom of the wells of a micro titer plate, and their fluorescence was imaged via measurement of the luminescence decay time of EuTc. If glucose oxidase is immobilized on the layer, a glucose sensor is obtained in which the HP sensor acts as the transducer. It can quantify glucose in concentrations between 0.1 and 5 mM.



**386. Cross-Reactive Metal Ion Sensor Array in a Microtiterplate Format.** T. Mayr, C. Igel, G. Liebsch, I. Klimant, O.S. Wolfbeis; *Anal. Chem.* **75** (2003) 4389-4396.

DOI: 10.1021/ac020774t. Journal IF: 5.7.

**Abstract:** A cross-reactive array in a micro titer plate (MTP) format is described that is based on a versatile and highly flexible scheme. It makes use of rather unspecific metal ions probes having almost identical fluorescence spectra, thus enabling (a) interrogation at identical analytical wavelengths, and (b) imaging of the probes contained in the wells of the MTP using a CCD camera and an array of blue-light-emitting diodes as a light source. The response of the indicators in the presence of 5 divalent cations generated a characteristic pattern that was analyzed by chemometry. The fluorescence intensity of the indicators was transferred into a time-dependent parameter applying a scheme called *dual lifetime referencing*. In this method, the fluorescence decay profile of the indicator is referenced against the phosphorescence of an inert reference dye. The intrinsically referenced measurements were performed using blue LEDs as light sources and a CCD camera without intensifiers as the detector (see the graphs below). The pictures obtained form the basis for evaluation by pattern recognition algorithms. Support vector machines are capable of predicting the presence of significant concns. of metal ions with high accuracy.

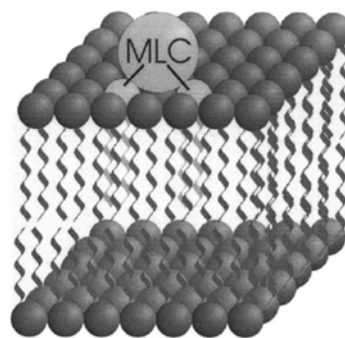
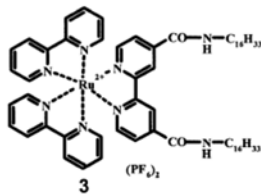
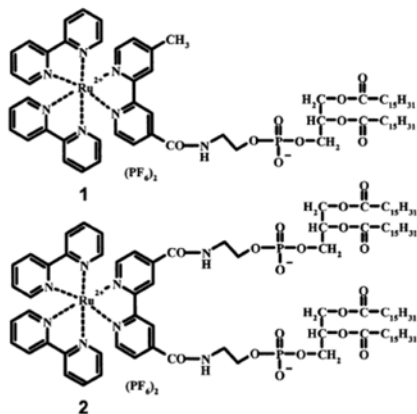


**385. Fluorescence Studies on Fluid Ordered Membranes Using Lipophilic Ruthenium-Ligand Complexes with Long Luminescence Decay Times.** C. M. Augustin, O. S. Wolfbeis; *J. Mol. Liquids*, **107** (2003) 141-154. DOI: 10.1016/S0167-7322(03)00146-6.

**Abstract:** The fluidity of lipid membranes contained in aqueous medium was studied using new fluorescent lipophilic ruthenium-ligand complexes containing dipalmitoyl-glycerophospho-ethanolamine (PE) or hexadecyl side groups, respectively. The new probes display long luminescence decay times and polarized emission, thus making them viable molecular sensors for studying the dynamics and molecular orientation of ordered liquids. Experiments are reported in which the probes were incorporated into lipid bilayers of vesicles, and their luminescence was studied with respect to temperature-dependent emission intensity, decay time and steady-state luminescence polarization.

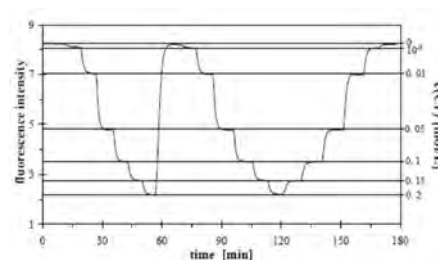
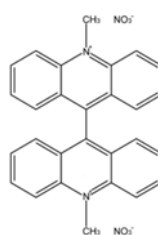
The figures show the chemical structures of the three probes and how the metal-ligand complexes are supposed to become integrated into lipid membranes.





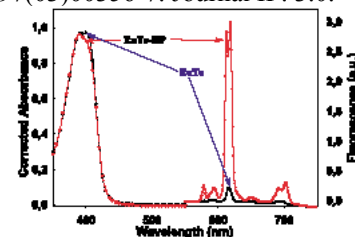
**384. Serum Chloride Optical Sensors Based on Dynamic Quenching of the Fluorescence of Photo-immobilized Lucigenin, C. Huber, T. Werner, C. Krause, O. S. Wolfbeis; *Microchim. Acta* 142 (2003) 245-253. DOI: 10.1007/s00604-003-0034-0. Journal IF: 1.4.**

**Abstract:** We describe an optical sensor for continuous measurement of chloride at extracellular (serum) levels (20 – 200 mM). The sensor is based on dynamic quenching of the fluorescence of lucigenin in a hydrogel. The decrease in fluorescence intensity on exposure to 100 mM chloride typically is -60%. It allows the determination of chloride in the 1 to 200 mM range, with a precision of  $\pm 3$  mM at 120 mM. Bromide, iodide and salicylate interfere, while the effect of pH and oxygen is negligibly small. Response times are in the order of 2 – 5 min. It is used in Roche's blood chloride analyzer.



**383. Determination of the Activity of Catalase Using a Europium(III)-Tetracycline-Derived Fluorescent Substrate, M. Wu, Z. Lin, O. S. Wolfbeis; *Anal. Biochem.* 320 (2003) 129-135. DOI: 10.1016/S0003-2697(03)00356-7. Journal IF: 3.0.**

**Abstract:** A one-step method is described for the fluorometric determination of the activity of the enzyme catalase (EC 1.11.1.6), based on the finding that H<sub>2</sub>O<sub>2</sub> in the Eu<sup>3+</sup>-tetracycline-hydrogen peroxide system is consumed by catalase. This is accompanied by a large decrease in both fluorescence intensity (see the figure) and decay time. The limit of detection (LOD) for catalase at 30 °C for a 10-min kinetic assay is 1.0 unit/mL. At an It is a one-step, simple, and sensitive method suitable for both continuous kinetic and one-point detections, does not require the addition of other substrates, and works best at neutral pH (with an optimum at pH 6.9). The reagent has the typical spectral features of a europium-ligand complex including a 219-nm Stokes shift, a line-like emission (centered at 616 nm), and a decay time in the microsecond domain. The EuTc-HP complex also is the first europium-based probe that is compatible with the 405-nm diode laser.



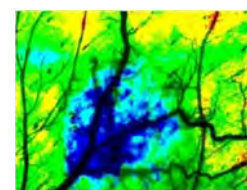
**382. Set of Fluorochromophores in the Wavelength Range from 450 to 750 nm and Suitable for Labeling Proteins and Amino-Modified DNA, B. Wetzl, M. Gruber, B. Oswald, A. Duerkop, B. Weidgans, M. Probst, O. S. Wolfbeis; *J. Chromatogr. B*, 793 (2003) 83-92. DOI: 10.1016/S15170-0232(03)00366-0. Journal IF: 2.7.**

**Abstract:** We describe the synthesis and spectral properties of new dyes and reactive labels. They absorb in the visible range between 450 and 700 nm and display analytically useful fluorescence. They were made amino-reactive by esterification with *N*-hydroxysuccinimide. The resulting oxysuccinimide esters were covalently linked to the amino groups of human serum albumin (HSA) or certain DNA oligomers. Most dyes contain one reactive group only in order to avoid cross linking of biomolecules. Labeling of amino-modified biomolecules was performed by standard protocols, and the labeled proteins and oligonucleotides were separated from the unreacted dye by gel chromatography using Sephadex G25 as the stationary phase in the case of proteins, and reversed-phase HPLC in the case of DNA oligomers. The dyes also have been used as donor-acceptor pairs in fluorescence energy transfer systems and in energy transfer cascades.



**381. Effects of Light Fractionation and Different Fluence Rates on Photodynamic Therapy with 5-Aminolaevulinic Acid in-vivo, P. Babilas, V. Schacht, G. Liebsch, O. S. Wolfbeis, M. Landthaler, R. M. Szeimies; *Brit. J. Cancer* 88 (2003) 1462-1469. DOI: 10.1038/sj.bjc.6600910. DOI: 10.1038/sj.bjc.6600910. journal IF: 4.5.**

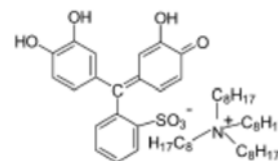
**Abstract:** Photodynamic therapy (PDT) was performed on hamsters with amelanotic melanoma. Prior to, and up to 24 h after PDT tissue, the *p*O<sub>2</sub> was measured using luminescence lifetime imaging. The efficacy of PDT was evaluated by measuring the tumor volume of amelanotic melanoma cells grown subcutaneously in the back of the hamsters. Only high-dose PDT resulted in a significant decrease of *p*O<sub>2</sub>, while low-dose PDT failed to induce a significant decrease. The image shows the distribution of oxygen in tumorous skin, with a larger underoxygenation in the blue (= tumorous) areas before PDT. This area disappears following successful PDT.



**380. Characterization of an Optical Sensor Membrane Based on the Metal Ion Indicator Pyrocatechol Violet. I.**

Steinberg, A. Lobnik, O. S. Wolfbeis; *Sensors Actuat.* **90B** (2003) 230-235. DOI: 10.1016/S0925-4005(03)00033-9. journal

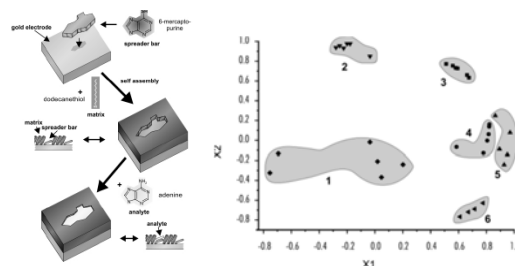
IF: 2.3. **Abstract:** A non-specific photometric metal ion indicator Pyrocatechol Violet (PV) was tested potential use in for its a metal-sensitive optrode membrane. The water-soluble indicator was lipophilised in the form of an ion pair with tetraoctylammonium cation (TOA; see the formula), and subsequently immobilised in a plasticised PVC membrane. The spectral response of the membrane in the presence of various transition metal ions was studied. It was found that the ability of PV to form complexes with metal ions significantly reduced following immobilisation, with the exception of Cu(II). A number of factors responsible for the improved selectivity and high sensitivity of immobilised PV towards Cu(II) were identified. Amongst those, the most important is the presence of quaternary ammonium salt in the membrane which induced a significant bathochromic shift of the PV–Cu(II) chelate absorption maximum, as well as the intensification of the chelate absorption band. The membrane responds to Cu(II) irreversibly by changing colour from yellow to green (absorption maximum at 740 nm), and typically, an exposure time of 10 min enables the determination of Cu(II) in the 1–100 mM range. A comparison of selectivity and sensitivity characteristics between the water soluble form of the indicator and the immobilised form was performed, and the effects of pH and lipophilic surfactant additives on the response mechanism are discussed.



**379. A Strategy for Preparation of Sensor Arrays: Molecularly Structured Monolayers as Recognition Elements.** Th. Hirsch, H. Kettenberger, O. S. Wolfbeis, V. M. Mirsky; *Chem. Comm.* (2003) 432-433. DOI: 10.1039/B210554C. journal IF: 4.5.

**Abstract:** The spreader-bar approach is a simple method for producing a large variety of receptors with different selectivities. A sensor array consisting of 5 such receptors is presented. A pattern recognition provides selective detection of different purines and pyrimidines.

The figures at the right show patterns of different concentrations of caffeine (1), uracil (2), adenine (3), cytosine (4), thymine (5) and uric acid (6) on an array of artificial receptors formed by thiolated derivatives of purines (ASH, GSH) and pyrimidines (CSH, TSH, USH) presented in the plot of principal components. X1 and X2 signify the first and the second principal components. Capacitive transduction was used.

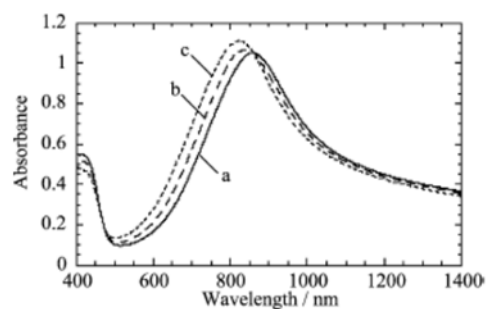


**378. Characterization of a Reservoir-Type Capillary Optical Microsensor for pCO<sub>2</sub> Measurements.** K. Ertekin, I. Klimant, G. Neurauter, O. S. Wolfbeis; *Talanta* **59** (2003), 261-267. DOI: 10.1016/S0039-9140(02)00495-2. journal IF: 2.8.

**Abstract:** A reservoir type of capillary microsensor for pCO<sub>2</sub> measurements is presented. The sensor is based on the measurement of the fluorescence intensity of the anionic form of the pH indicator 1-hydroxy-3,6,8-pyrenetrilsulfonate in the form of its ion pair with a quaternary ammonium base in an ethyl cellulose matrix. The glass capillary containing the reservoir sensor was prepared by immersing the tip of the optical fiber into the sensing agent very close to the sensor tip thus providing a very small volume for the sensing reaction. The purpose of the sensing approach is to regenerate the dye/buffer system by diffusion, which may be poisoned by interfering acids, or bleach by photolysis. The fresh cocktail from the reservoir takes the place of protonated form of the dye. The internal buffer system also makes the protonation/deprotonation equilibria reversible. The distal tip of the internal buffer containing reservoir is coated with a gas-permeable but ion-impermeable teflon membrane. The dynamic range for the detection of pCO<sub>2</sub> is between 1 and 20 hPa, which corresponds to the range of dissolved CO<sub>2</sub> in water. The response time is 15 s and the detection limit is 1 hPa of pCO<sub>2</sub>. The recovery performance of this sensor can be improved by means of mechanical adjustment of the sensor tip in a micrometric scale.

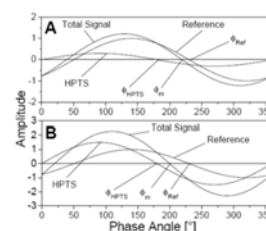
**377. Optical Ozone Detection by Use of Polyaniline Film.** M. Ando, C. Swart, E. Pringsheim, V. M. Mirsky, O. S. Wolfbeis; *Solid State Ionics* **152/153** (2002) 819-822. DOI: 10.1016/S0167-2738(02)00338-7. journal IF: 2.2.

**Abstract:** We report on the optical ozone sensitivity of a polyaniline (PANI) film prepared on the inner wall of a polystyrene cuvette by chemical oxidation of aniline from aqueous solution. The PANI film showed changes of optical absorbance in the presence of 50–100 ppm ozone in air at room temperature. The absorbance change was largest at wavelengths in the range of 500–800 nm. The absorbance changes brought about by ozone was partially reversible after removal of ozone from the atmosphere. These results suggest that PANI is a potential material for optical ozone detection. The figure shows visible/near-IR absorption spectra of the PANI film in air with and without ozone. (a) In fresh air. (b) In air containing 50 ppm ozone. (c) In air containing 100 ppm ozone. Temperature: 25 °C. Relative humidity: 50%.



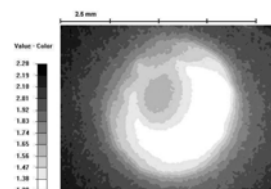
**376. Sol-Gel Based Optical Carbon Dioxide Sensor Employing Dual Luminophore Referencing for Application in Food Packaging Technology.** C. von Bueltingsloewen, A. K. McEnvoy, C. McDonagh, B. D. MacCraith, I. Klimant, C. Krause, O. S. Wolfbeis; *Analyst* **127** (2002) 1478-1483. DOI: 10.1039/b207438a. Journal IF: 3.2.

**Abstract:** An optical sensor for the measurement of carbon dioxide in *Modified Atmospheric Packaging* applications has been developed. It is based on the fluorescent pH indicator 1-hydroxypyrene-3,6,8-trisulfonate immobilized in a hydrophobic organically modified silica (ormosil) matrix. A lipophilic alkyl ammonium hydroxide was used as an internal buffer system. Fluorescence is measured in the phase domain by means of the *Dual Luminophore Referencing* (DLR) sensing scheme which provides many of the advantages of lifetime-based fluorometric sensors and makes it compatible with established optical oxygen sensor technology. The sensor displays a resolution of better than 1% CO<sub>2</sub> and a limit of detection of 0.08%. Cross-sensitivity to chloride and pH was found to be negligible. Temperature effects were studied, and a linear Arrhenius correlation between ln k and 1/T was found. The sensor is stable over a period of at least seven months.



**375. Determination of Oxygen Gradients in Engineered Tissue Using a Fluorescent Sensor**, K. Kellner, G. Liebsch, I. Klimant, O. S. Wolfbeis, T. Blunk, M. B. Schulz, A. Goepferich; *Biotechnol. Bioeng.* **80** (2002) 73-83. DOI: 10.1002/bit.10352. Journal IF: 3.0.

*Abstract:* A fluorescent sensor for oxygen is placed at the bottom of a Petri dish in which cultures of chondrocyte cells are grown. The sensor layer is used to image the oxygen distribution on the bottom of the dish and – in particular – to recognize irregularities during growth due to inadequate oxygen supply.



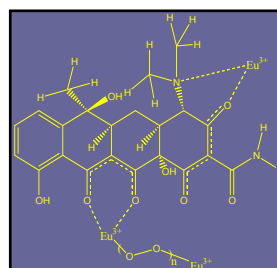
**374. Book Chapter. Advanced Luminescent Labels, Probes and Beads, and Their Application to Luminescence Bioassay and Imaging**, O. S. Wolfbeis, M. Boehmer, A. Duerkop, J. Enderlein, M. Gruber, I. Klimant, Ch. Krause, J. Kuerner, G. Liebsch, Zh. Lin, B. Oswald, M. Wu; *Springer Series in Fluorescence Spectroscopy*, vol. 2 (R. Kraayenhof, A. J. W. G. Visser, H. C. Gerritsen, eds.); Springer Verlag, Berlin-Heidelberg, 2002; pp. 3-42. DOI: 10.1007/978-3-642-56067-5\_1.

*Abstract:* An overview is given on our recent activities in the following areas: (1) general logics for designing fluorescent probes and labels; (2) new diode laser-excitable probes for non-covalent protein detection; (3) diode laser-compatible amine-reactive covalent labels; (4) diode laser-assisted fluorescent single molecule detection of dyes and labeled proteins; (5) new labels for flow cytometric determination of HSA; (6) new DNA labels; (7) fluorescence resonance energy transfer gene assays; (8) reactive ruthenium ligand complexes as markers for bioassays; (9) diode laser-excitable fluorescent polymer beads; (10) polyaniline-coated nanobeads as fluorescent pH probes; (11) phosphorescent poly(acrylonitrile) nanospheres as markers for optical assays; (12) competitive binding of streptavidin to biotinylated nanobeads as studied by resonance energy transfer; (13) nanobeads as reference dyes in luminescent lifetime imaging using DLR; (14) phosphorescent nanospheres for use in advanced time-resolved multiplexed bioassays; (15) beads dyed with a europium-based label and excitable with the 405-nm diode laser; and (16) a europium(III)-based probe for use in oxidase-associated reactions.



**373. Europium Ion-Based Luminescent Sensing Probe for Hydrogen Peroxide**, O. S. Wolfbeis, A. Duerkop, M. Wu and Z. Lin; *Angew. Chem.* **114** (2002); 4681-4684; *Intl. Ed. Engl.* **41** (2002) 4495-4498. DOI: 10.1002/1521-3773(20021202)41:23<4495::AID-ANIE4495>3.0.CO;2-I. Journal IF: 10.3.

*Abstract:* The fluorescence of the Eu(III) complex with tetracycline (EuTc) undergoes a 15-fold increase in intensity and a change in its decay time if exposed to hydrogen peroxide. Thus, EuTc can act as a molecular probe for H<sub>2</sub>O<sub>2</sub> (HP). This is exploited (a), to detect HP in trace quantities (< 1ppm); (b) to detect glucose (via formation of HP by glucose oxidase); (c) the determination of the activity of oxidases; and (d) the detection of enzyme inhibitors. The probe is best excited at 400-405 nm (and thus compatible with the 405-nm diode laser), displays a narrow emission band peaking at 616 nm, and has a QY of 4%. The decay profile of EuTc is composed of 3 main components, with decay times of ca. 9, 30, and 170 microseconds, respectively. The first picture shows the assumed chemical structure of EuTc, and the second the pink (616-nm) line-like "fluorescence" that can be observed on addition of hydrogen peroxide to a virtually non-fluorescent solution of the EuTc complex.



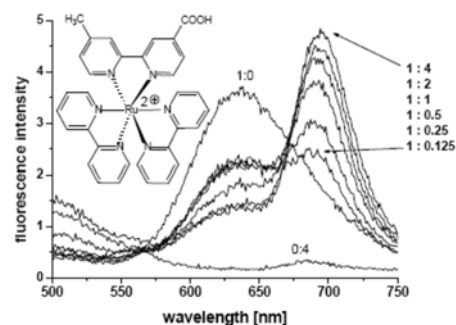
**372. Fiber Optic Multi-Channel Protein Detector for Use in Preparative Continuous Annular Chromatography**, A. Apostolidis, H. Lehmann, G. Schwotzer, R. Willsch, A. Prior, J. Wolfgang, I. Klimant, O. S. Wolfbeis; *J. Chromatogr. A* **967** (2002) 183-189. DOI: 10.1016/S0021-9673(02)00755-0. journal IF: 3.6.

Continuous annular chromatography is an effective method in the separation of preparative scale quantities of biological compounds including proteins where established batch chromatography borders on it. The need for identification or quantification of proteins triggered the development of respective detection units. Here, we describe two types of optical multi-channel detectors. The first is a fiber optic multi-channel detector suitable for the separation of aqueous protein solutions. The second is a technically improved (circular optic) device suitable for application in multi-channel detection. Specifically, UV-absorption measurements of proteins at 280 nm were carried out using newly designed fiber optic detectors having eight and 16 channels. Calibration plots were established for a series of stock solutions of known concentrations of proteins. Mathematical functions were derived from these calibration data to simulate the response of the detector. Limits of detection and the ranges of validity of the fit functions were determined. The 16-channel detector has a theoretical limit of detection that is equivalent to absorbance changes of 10<sup>-4</sup> units.

**371. Time-Resolved Luminescence Energy Transfer Immunobinding Study Using a Ruthenium-Ligand Complex as a Donor Label**, C. M. Augustin, B. Oswald, O. S. Wolfbeis; *Anal. Biochem.* **305** (2002) 166-172. DOI: 10.1006/abio.2002.5633. Journal IF: 3.0.



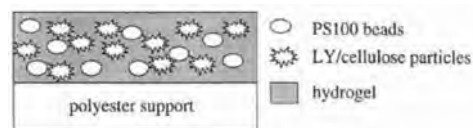
**Abstract:** A novel immunosystem is described that exploits the effect of luminescence energy transfer from a luminescently labeled antigen to a fluorescent antibody. A ruthenium-ligand complex (D-455) with absorption/emission maxima at 456/639 nm, respectively, was employed as the donor label, and a squaraine-type label (636/655 nm) as the fluorescent acceptor label. Specifically, the system HSA/anti-HSA was studied. HSA was labeled with the donor dye D-455, and anti-HSA was labeled with the acceptor dye A-631. On formation of the antigen-antibody complex, energy transfer occurs. The radiationless energy transfer affects both the decay time of D-455 and the intensities of the emissions of both D-455 and A-631. The decay time of around 500 ns of D-455 allows frequency-domain measurements in the low kHz range and therefore can be based on the use of conventional optoelectronics. This also suggests gated measurements to be performed. The major difference to existing HSA immunoassays is the use of a slow decaying ruthenium-ligand complex as the donor, and of a longwave emitting cyanine acceptor dye having a high quantum yield and a decay kinetics that is governed by the rate of energy transfer from the slow decaying donor.



**370. Dual Lifetime Referenced Optical Sensor Membrane for the Determination of Copper(II) Ions.** T. Mayr, I. Klimant, O. S. Wolfbeis, T. Werner. *Anal. Chim. Acta* **462** (2002) 1-10. DOI: 10.1016/S0003-2670(02)00234-9. journal IF: 2.9.

**Abstract:** A sensor membrane has been developed for the determination of copper(II) ions that displays excellent performance due to internal referencing of luminescence intensities. The applied sensing scheme (dual lifetime referencing) makes use of the indicator Lucifer Yellow (LY) and an inert reference luminophore (a ruthenium complex entrapped in polyacrylonitrile beads). Both are contained in a hydrogel matrix. The copper-dependent fluorescence intensity change of LY can be converted in either a phase shift or time dependent parameter.

The sensing membrane is capable of determining copper(II) with an outstanding high selectivity over a dynamic range between 1 and 1000 pM in neutral or weakly acidic conditions. The advantages of the referencing method over intensity based measurements was demonstrated by the measurement of turbid solutions. The scheme was also applied to two-dimensional measurements in the time domain. Sensor integrated microtiterplates were imaged with a CCD camera gated with square pulses in the microsecond range.



**369. Review: Fiber Optic Chemical Sensors and Biosensors (2000-2001).** O. S. Wolfbeis; *Anal. Chem. (Wash.)* **74** (2002) 2663-2678. DOI: 10.1021/ac020176e.

journal IF: 5.7.

**Abstract:** This biannual review covers the time period from January 2000 to December 2001. Priority is given to fiber-optic sensors (FOS) for defined chemical, environmental, and biochemical significance and to new schemes and materials.

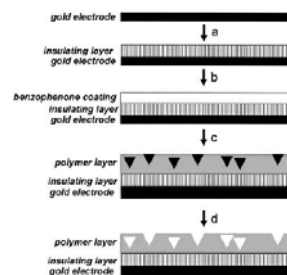


**368. Capacitive Creatinine Sensor Based on a Photografted Molecularly Imprinted Polymer.** T. Panasyuk-Delaney, V. M. Mirsky, O. S. Wolfbeis;

*Electroanalysis* **14** (2002) 221-224. DOI: 10.1002/1521-

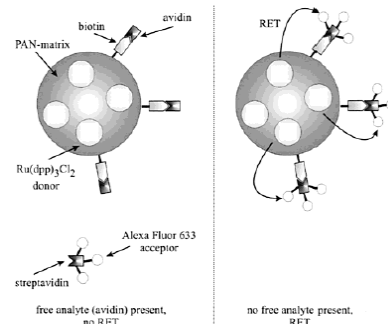
4109(200202)14:3<221::AID-ELAN221>3.0.CO;2-y. Journal IF: 2.4.

**Abstract:** The first reversible chemosensor for creatinine based on artificial chemoreceptors is described. The receptor layer was prepared by molecularly imprinted photo-polymerization of acrylamidomethyl-propanesulfonic acid and methylene-diacrylamide. The polymer layer was grafted onto the surface of gold electrodes coated with an alkanethiol monolayer. Creatinine binding was detected by a decrease in the electrode capacitance. The sensor response is reversible and highly selective: no response to addition of sodium chloride, creatine, urea or glucose were observed. The detection limit for creatinine is 10 μM which is suited for medical applications.



**367. Homogeneous Luminescence Decay Time-Based Bioassay Using Energy Transfer from Nanospheres.** J. M. Kuerner, O. S. Wolfbeis, I. Klimant; *Anal. Chem.* **74** (2002) 2151-2156. DOI: 10.1021/ac0111098. Journal IF: 5.7.

**Abstract:** A novel scheme is presented for homogeneous assays based on resonance energy transfer (RET) from phosphorescent biotinylated nanospheres to fluorescently-labeled streptavidin (SA). The nanospheres, with a diameter of well below 50 nm, are made from carboxylated polyacrylonitrile (PAN) and dyed with the ruthenium complex Ru(dpp). RET occurs from Ru(dpp) to the label if labeled SA binds to the surface of the nanospheres. Luminescence quenching by oxygen or other species can be neglected due to the shielding effect of the polymer matrix. A competitive binding assay was established, where avidin and labeled SA compete for the biotin binding sites on the nanosphere. The process of binding to the surface can be detected by measurement of the luminescence intensity or the apparent decay time which is in the order of 2.5 to 4.5 μs.



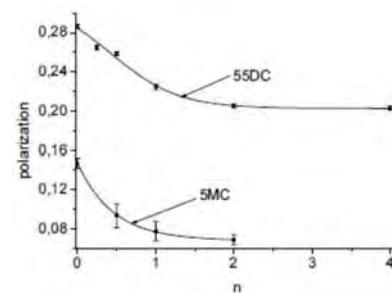
**366. Polarization Immunoassays Using Reactive Ruthenium Metal-Ligand Complexes as Luminescent Labels.** A. Duerkop, F. Lehmann, O. S. Wolfbeis; *Anal. Bioanal. Chem.* **372** (2002) 688-694. DOI: 10.1007/s00216-002-1232-z. Journal IF: 2.6.

**Abstract:** The first competitive fluorescence polarization immunoassay using ruthenium metal-ligand complexes (termed 5-MC and 55-DC) as labels is described. These were newly synthesized and characterized in terms of their spectra, their covalent linkage to proteins, and their use in both homogeneous and competitive immunoassays. Linkage to proteins was achieved by the N-hydroxysuccinimide ester method,

which was demonstrated for the systems HSA–anti-HSA and myoglobin–anti-myoglobin.

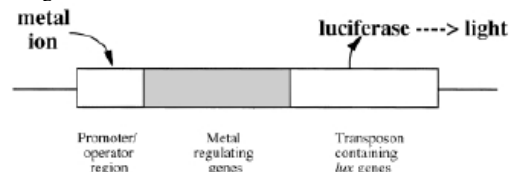
The values of the fundamental polarization are 0.18 for 5-MC and 0.33 for 55-DC. Polarization immunoassays with labeled HSA and myoglobin were performed in the homogeneous format and resulted in an increase of the fluorescence polarization of up to 100%. In the competitive assay, a decrease in polarization of >90% was detectable. When the competitive HSA immunoassay was validated against an independent test both methods gave almost the same results.

The figure shows the changes in polarization in a competitive polarization immunoassay of HSA (labeled with 5-MC or 55-DC) on addition of increasing concentrations of unlabeled HSA competing for polyclonal anti-HSA, where  $n$  is the molar ratio of unlabeled HSA added to labeled HSA initially present in solution



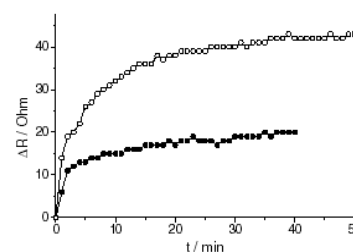
**365. Engineered Bacteria-Based Biosensors for Monitoring of Bioavailable Heavy Metals, S. Leth, S. Maltoni, R. Simkus, B. Mattiasson, P. Corbisier, I. Klimant, O. S. Wolfbeis, E. Csoeregi; *Electroanalysis* 14 (2002) 35-42. DOI: 10.1002/1521-4109(200201)14:1<35::AID-ELAN35>3.0.CO;2W. Journal IF: 2.4.**

**Abstract:** An integrated analytical system is presented that is based on immobilized engineered micro-organisms and measurement of bioluminescence and capable of monitoring bioavailable heavy metal ions (Cu being chosen as a model ion). A strain of micro-organisms from *Alcaligenes eutrophus* was genetically engineered by inserting a luxCDABE operon from *Vibrio fischeri* under the control of a copper-induced promoter. As a result, copper ions induce bioluminescence whose intensity is proportional to the concentration of the triggering ions, representing the basis of the design of the novel biosensor. Micro-organisms were immobilized in polymer matrices compatible with fiber optics and characterized. The lowest detection limit was achieved with microorganisms cultivated from glycerol stock solutions in the RM media and immobilized in a calcium alginate matrix.



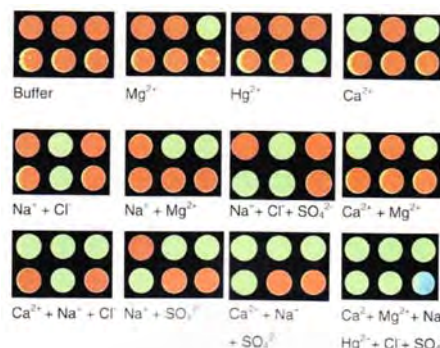
**364. Self-Assembled Monolayers as Selective Filters for Chemical Sensors, V. M. Mirsky, M. Vasjari, I. Novotny, V. Rehacek, V. Tvarozek, O.S. Wolfbeis; *Nanotechnology* 13 (2002) 1-4. DOI: 10.1088/0957-4484/13/2/309. Journal IF: 3.0.**

**Abstract:** A self-assembled monolayer of hexadecanethiol deposited on a gold surface can block the effects of water and volatile sulfuric compounds on the lateral conductivity of the gold layers, but does not block the effects of iodine and mercury. The results indicate a selective permeability of hexadecanethiol monolayers for mercury vapor, thus providing a method for development of ultrathin filters for chemical sensors. The figure shows the kinetics of the changes of lateral resistance of thin gold layers due to exposure to 10 ng L<sup>-1</sup> of mercury vapor: bare gold layers (open symbols), gold layers each coated by a self-assembled monolayer of 1-hexadecanethiol (filled symbols).



**363. Multi-Ion Imaging Using Fluorescent Sensors in a Microtiterplate Array Format. T. Mayr, G. Liebsch, I. Klimant, O. S. Wolfbeis; *Analyst* 127 (2002) 201-203. DOI: 10.1039/b1110776. journal IF: 3.2.**

**Abstract:** A novel type of sensor array destined for water analyses is described. The sensor delivers simple on/off patterns of complex ion mixtures. Fluorescent indicators for Ca<sup>2+</sup>, Na<sup>+</sup>, Mg<sup>2+</sup>, SO<sub>4</sub><sup>2-</sup>, Cl<sup>-</sup> and Hg<sup>2+</sup> were arranged in microtiterplates and the analytical information was imaged with a CCD camera within microseconds using an intrinsically referencing method.



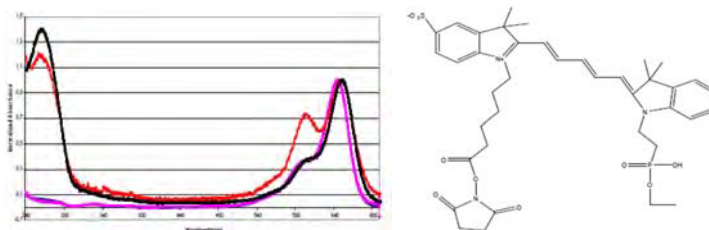
**361. Inert Phosphorescent Nanospheres as Markers in Optical Assays, J. M. Kuerner, I. Klimant, Ch. Krause, H. Preu, W. Kunz, O. S. Wolfbeis; *Bioconjug. Chem.* 12 (2001) 883-889. DOI: 10.1021/bc000130x. Journal IF: 3.8.**

**Abstract:** An encapsulation technique is presented to produce highly phosphorescent, inert nanospheres which are suitable luminescent markers. It is based on the co-precipitation of phosphorescent ruthenium(II)-tris(polypyridyl) complexes and polyacrylonitrile derivatives from a solution in N,N-dimethylformamide. The typical particle diameter is less than 50 nm. The nanospheres were characterized with respect to their spectral properties, quantum yields of the luminophores, luminescence decay time, stability in aqueous buffered suspensions, and in terms of size, shape and surface charge of the particles, as well as storage stability, quenching by oxygen, and dye leaching.



**360. Single- and Dual-NIR Fluorescent Labeled Nucleic Acid Conjugate for Nucleic Acid Detection. Z. Lin, M. Wu, S. Ren, M. Arbter, M. Boehmer, V. M. Mirsky, O. S. Wolfbeis; *Proc. SPIE (Soc. Photoinstrum. Eng.)* vol. 4414 (2001) 111-114. DOI: 10.1117/12.440165**

**Abstract:** A near-infrared fluorescent labeled nucleic acid conjugate for the nucleic acid detection was synthesized, and characterized preliminarily for the detection of the nucleic acid. The solubility of the label was improved by introducing phospho groups into the molecule. The conjugate combines the molecular recognition properties of the oligonucleotides with the near-infrared fluorescent label PR646. Both single- and dual-labelled conjugates were studied for their hybridization with the complementary nucleic acid. The dual labelled conjugate has indicated that the self-quenching effect exists in ssDNA form while the fluorescence increases greatly after hybridization with the complementary nucleic acids. The time-resolved fluorescence was also studied.

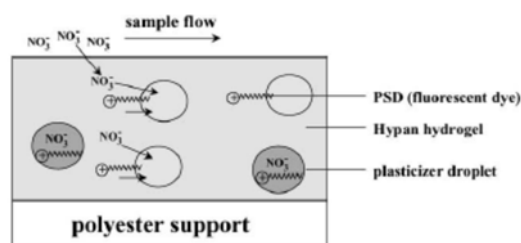


**359. Detection of DNA Hybridization via Surface Plasmon Resonance: Comparison of Immobilization of Oligonucleotides by ss- and ds-DNA.** M. Wu, Z. Lin, V. Mirsky, O. S. Wolfbeis; *Proc. SPIE (Soc. Photoinstrum. Eng.)* **4414** (2001) 23-26. DOI: 10.1117/12.440180

**Abstract:** A surface plasmon resonance biosensor for nucleic acid detection was constructed, optimized and characterized. The kinetic response to hybridization was also studied. The biosensor was used as a platform for the study of the surface coverage control by single-strand or double-strand oligonucleotide immobilization via gold-thiol chemistry. The dsDNA immobilization method shows higher surface coverage than the ssDNA immobilization and offers a new way of surface control for such SPR based DNA sensors.

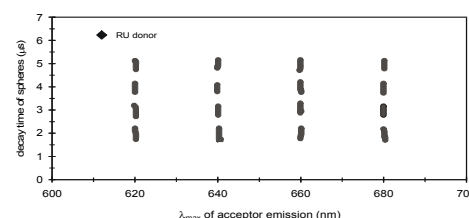
**358. Nitrate-Selective Optical Sensor Applying a Lipophilic Fluorescent Potential-Sensitive Dye.** Ch. Huber, I. Klimant, Ch. Krause, T. Werner, O. S. Wolfbeis; *Anal. Chim. Acta* **449** (2001) 81-93. DOI: 10.1016/S0003-2670(01)01363-0. journal IF: 2.9.

**Abstract:** An optical sensor has been developed for continuous determination of nitrate that is based on a polymer-stabilized emulsion system consisting of a hydrogel with entrapped plasticizer droplets. The droplets contain a cationic potential-sensitive fluorescent dye (PSD) located near its surface. The cationic PSD also acts as an anion-exchange catalyst that extracts nitrate out of the aqueous solution to form a complex (PSD<sup>+</sup>/NO<sub>3</sub><sup>-</sup>) that moves into the plasticizer droplet due to its lipophilicity. This process causes a decrease of micro-polarity near the dye, resulting in an increase in the fluorescence intensity of the PSD. In a second detection scheme, the fluorescence intensity information of the PSD is converted into a fluorescence phase shift by mixing into the membrane particles that contain an inert long-lifetime reference luminophore. The second sensing scheme is referred to as "dual lifetime referencing". Both schemes can be used for reversible sensing of nitrate in the 0.1–50 mM range, with response times in the order of 3 min.



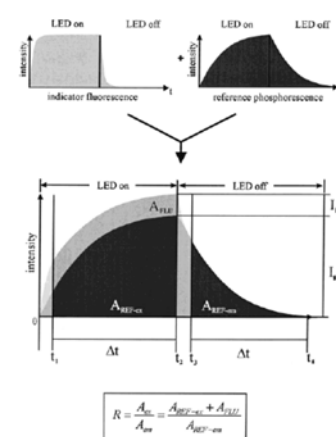
**357. A New Type of Phosphorescent Nanospheres for Use in Advanced Time-Resolved Multiplexed Bioassays.** J. M. Kuerner, I. Klimant, Ch. Krause, E. Pringsheim, O. S. Wolfbeis; *Anal. Biochem.* **297** (2001) 32-41. DOI: 10.1006/abio.2001.5295. Journal IF: 3.0.

**Abstract:** Optically encoded phosphorescent nanospheres are presented. They are distinguishable by their individual decay time and spectral distribution of their emission spectra. They are composed of a phosphorescent ruthenium metal ligand complex (MLC) dissolved, along with certain strongly fluorescent cyanine dyes, in modified polyacrylonitrile-based nanospheres. Since the MLC (the donor) and the cyanine (the acceptor) are in close spatial proximity, efficient resonance energy transfer (RET) does occur. Thus, the nanospheres emit dual luminescence, one from the acceptor dye, the other from the donor MLC. Variation of the concentrations of the acceptor dye results in a varying efficiency of RET, thus making the spheres distinguishable. Hence, a set of multiplexable sphere labels is obtained by using one MLC (acting as the phosphorescent donor and present in constant concentration) and one acceptor dye (which varies both in terms of spectral properties and concentration).



**355. Fluorescent Imaging of pH with Optical Sensors Using Time Domain Dual Lifetime Referencing.** G. Liebsch, I. Klimant, Ch. Krause, O. S. Wolfbeis; *Anal. Chem.* **73** (2001) 4354-4363. DOI: 10.1021/ac0100852. Journal IF: 5.7.

**Abstract:** We present a referenced scheme for fluorescence intensity measurements which is useful for imaging applications. It is based on the conversion of the fluorescence intensity information into a time dependent parameter. A phosphorescent dye is added, in the form of approx. 10 µm particles to the sample containing the pH-sensitive fluorescent indicator. Both the ref-dye and the pH probe are excited simultaneously by a blue LED, and an overall luminescence is measured. In the time-resolved imaging method presented here, two images taken at different time gates were recorded with a CCD-camera. The first image is recorded during excitation and reflects the luminescence signal of both the fluorophore (pH) and the phosphor (reference). The second image which is measured after a certain delay (after switching off the light source), is solely caused by the long-lived phosphorescent dye. Since the intensity of the fluorophore contains the information on pH, whereas phosphorescence is pH-independent, the ratio of the images displays a referenced intensity distribution that reflects the pH at each picture element (pixel). The scheme is useful for LED light sources and CCD cameras that can be gated with square pulses in the microsecond range. The fundamentals and potential of this new method - to which we refer to as *time domain dual lifetime referencing* - are demonstrated.

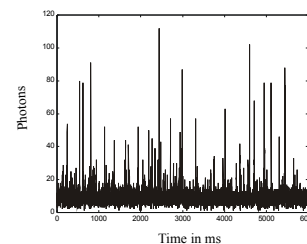


**354. Novel Diode Laser-Compatible Fluorophores and Their Application to Single Molecule Detection, Protein Labeling**



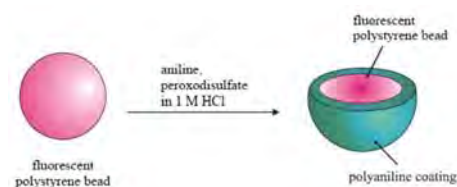
**and Fluorescence Resonance Energy Transfer Immunoassay**, B. Oswald, M. Gruber, F. Lehmann, M. Probst, O. S. Wolfbeis; *Photochem. Photobiol.* **74** (2001) 237-242. DOI: 10.1562/0031-8655(2001)074<237:NDLCFA>2.0.CO.2. Journal

IF: 2.1. **Abstract:** We describe a series of new long-wave absorbing and fluorescing cyanine dyes and labels (based on a general logic for the design of such dyes), their spectra, linkage to proteins, use in single mol. detection (SMD), and as donors and acceptors, resp., in fluorescence resonance energy transfer studies. The new labels represent water-sol. and reactive fluorophores whose quantum yields increase substantially if noncovalently or covalently bound to proteins. Due to their strong absorptions between 550 and 700 nm they are excitable by LEDs or diode lasers. Their high molar absorptances (around 100 000) and adequate fluorescence quantum yields (up to 0.68 if bound to proteins) along with their availability as reactive NHS esters make them viable labels for proteins and oligomers, e.g. in context with SMD or fluorescence energy transfer immunoassay which is demonstrated for the system HSA/anti-HSA. The figure shows photon bursts of single molecules of dye RB-634 in water diffusing through a Gaussian volume of approximately 8 fL.



**353. Fluorescent Beads Coated with Polyaniline: A Novel Nano-Material for Optical Sensing of pH**. E. Pringsheim, D. Zimin, O. S. Wolfbeis; *Adv. Mat.* **13** (2001) 819-822. DOI: 10.1002/1521-4095(200106)13:11<819::AID-ADMA819>3.0.CO;2-D. Journal IF: 7.9.

**Abstract:** Fluorescent nanobeads are presented that can be used for optical sensing of pH. The sensing scheme is based on the finding that aniline, if oxidized in presence of fluorescent polystyrene beads, is deposited on the particles as a thin film of polyaniline (PANI). The resulting coated beads, typically 360 nm in diameter, were characterized by fluorescence spectroscopy, atomic force microscopy and flow cytometry. It is found that the fluorescence intensity of the PANI-coated beads undergoes pH-dependent changes even though the fluorophore is inert to pH. This is due to an inner filter effect caused by the pH-sensitive PANI coating which modulates fluorescence intensity. The beads thus can act as fluorescent bead probes for physiological pHs.

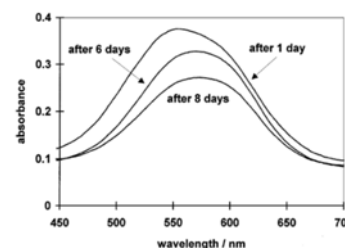


**352. Impedometric Herbicide Chemosensors Based on Molecularly Imprinted Polymers**. T. Panasyuk-Delaney, V. M. Mirsky, M. Ulbricht, O. S. Wolfbeis; *Anal. Chim. Acta* **435** (2001) 157-162. DOI: 10.1016/S0003-2670(00)01280-0. Journal IF: 2.9.

**Abstract:** The technique of grafting polymerization has been used for preparation of thin films of molecularly imprinting polymers on the surface of polypropylene membranes and on hydrophobized gold electrodes. The herbicide desmetryn was used as a template. The solid supports used were hydrophobic, while the polymer was hydrophilic. The adsorbed layer of benzophenone, irradiated by UV-light, initiated a radical polymerization near the surface. Polymer films were characterized by weighing, contact angle measurements and impedance spectroscopy. The electrodes coated with the molecularly imprinted polymers displayed fairly specific binding of desmetryn, as detected by the decrease in the capacitance of the electrode. Only small capacitive effects were observed on addition of terbuneton or atrazine, while metribuzin displayed a decrease in capacitance similar to that of desmetryn.

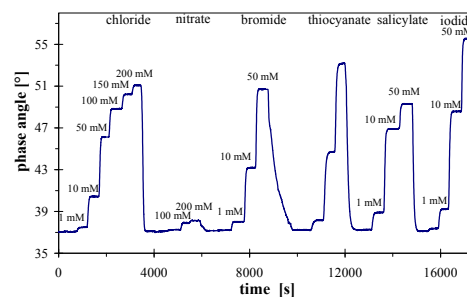
**351. Probing the Polarity of Sol-Gels and Ormosils via the Absorption of Nile Red**. A. Lobnik, O. S. Wolfbeis; *J. Sol-Gel Sci. Technol.* **20** (2001) 303-311. DOI: 10.1023/A:1008734320809. journal IF: 1.0.

**Abstract:** Conventional sol-gels are rather hydrophilic. A more hydrophobic material is obtained preparing organically modified siloxanes (ormosils). The polarity-sensitive probe Nile Red (NR) was doped in various sol-gels to probe their micro-polarity. The experiments show that the NR is an excellent probe and sensitive to the polarity of its microenvironment. Spectroscopic studies reveal remarkable changes in the absorption band positions and intensities as a function of the polarity of the sol-gel, which depends on the different precursors used. Furthermore, sol aging, gelation and temporal stability as a function of different ormosils have been investigated.



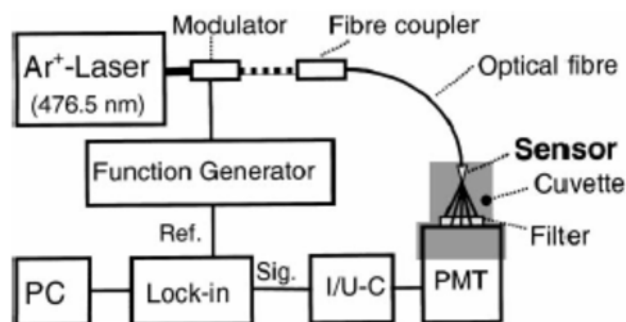
**350. Dual Lifetime Referencing as Applied to a Chloride Optical Sensor**, Ch. Huber, I. Klimant, Ch. Krause, O. S. Wolfbeis; *Anal. Chem. (Wash.)* **73** (2001) 2097-2103. DOI: 10.1021/ac9914364. journal IF: 5.7.

**Abstract:** A membrane with an optical response to chloride has been developed that contains two luminophores that display two largely different decay times. The first luminophore (the reference) is a chloride-insensitive ruthenium metal-ligand complex possessing a decay time in the microsecond range. The second luminophore is the short-lived chloride-quenchable fluorescent probe lucigenin. Both are contained in a hydrogel matrix and are photoexcited by a blue LED emitting sinusoidally modulated light. Under these conditions, the chloride-dependent fluorescence intensity of lucigenin can be converted in an analyte-dependent fluorescence phase shift that depends on the ratio of the two luminescence intensities and can be measured at modulation frequencies of typically 45 kHz. The dynamic range of this sensor can be adjusted by either varying the ratio of the two luminophores or selecting a particular optical filter combination. The figure shows the sensitivity of a typical sensor membrane toward chloride, nitrate, bromide, thiocyanate, salicylate, and iodide, and also demonstrates the complete reversibility of the sensor membrane.



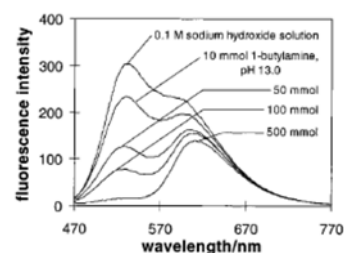
**349. Sub-Micron Sensors for Ion Detection Based on Measurement of Luminescence Decay Time**. I. Koroncz, J. Reichert, H.-J. Ache, Ch. Krause, T. Werner, O. S. Wolfbeis; *Sensors Actuators, part B (Chemical)* **74B** (2001) 47-53. DOI: 10.1016/S0925-4005(00)00710-3. journal IF: 2.3.

**Abstract:** Submicron optochemical sensors for pH and chloride were developed by coating silanised optical fibre tips of ~300 nm diameter and aluminium-coated SNOM fibres of ~50 nm aperture with polymeric membranes containing luminescent indicators. Luminescence decay time was measured using a phase-modulation technique. Changes in decay time are induced by resonance energy transfer from a ruthenium complex (the donor) to the pH indicator bromothymol blue (the acceptor). The donor/acceptor ion pair was immobilised in a hydrogel membrane and undergoes a change in decay time with pH. The chloride sensor was made by combining the ion pair for optical transduction with the chloride-carrier tridodecylmethylammonium chloride in a plasticised PVC membrane. Chloride ions present in the solution are carried into the membrane. In order to maintain electroneutrality, an equivalent molar quantity of protons is coextracted into the membrane where the dye is protonated. Both sensors are suitable for measurements in physiological fluids.



**348. Fluoro Reactands and Dual Luminophore Referencing: A Technique to Optically Measure Amines.** G. J. Mohr, I. Klimant, U. Spichiger, O. S. Wolfbeis; *Anal. Chem.* **73** (2001) 1053-1056. *Chem. Abstr.* 2001:64376. DOI: 10.1021/ac000945z. journal IF: 5.7.

**Abstract:** An optical sensor for aqueous 1-butylamine is presented which combines two novel techniques: A fluorescent indicator dye (fluoro reactand) embedded in a thin polymer layer performs a reversible chemical reaction with the analyte, causing changes in luminescence intensity. At the same time, inert phosphorescent beads dispersed within the polymer layer provide luminescence signals that act as an internal reference for the indicator dye. As a consequence, the optical sensor is independent of light source fluctuations, ambient light, drifts in optoelectronic setup, or optical fiber bending.



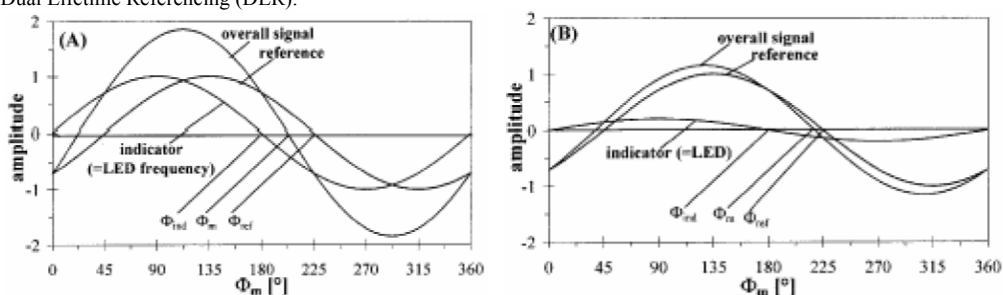
**347. Book Chapter. Dual Lifetime Referencing (DLR) – A New Scheme for Converting Fluorescence Intensity into a Frequency-Domain or Time-Domain Information,** I. Klimant, Ch. Huber, G. Liebsch, G. Neurauder, A. Stangelmayer, O. S. Wolfbeis; in: *New Trends in Fluorescence Spectroscopy*, B. Valeur, J. C. Brochon (eds.); Springer Verlag, Berlin (2001), chap. 13, pp. 257-274. DOI: 10.1007/978-3-642-56853-4\_13

**Abstract:** We present a new and universally applicable scheme for converting fluorescence intensity into a phase shift, a signal that is hardly affected by many potential interferences. It is based on the addition of a luminescent reference dye having a decay time much longer than that of the fluorescent indicator. This scheme is called *Dual Lifetime Referencing* (DLR). In the preferred case of using a phosphorescent luminophore as the reference dye, the time domain is in the microsecond range, so that modulation frequencies in the lower kHz range are adequate. This enables the use of inexpensive optoelectronic devices and thus also provides cost advantages. In this overview, the fundamentals of time-domain DLR and frequency-domain DLR are demonstrated and the potential of the new method is assessed with respect to alternative schemes. Phase angle ( $\phi_m$ ) and the intensity ratio of the indicator dye ( $A_{ind}$ ) and reference luminophore ( $A_{ref}$ ) are related as shown in the following equation:

$$\frac{A_m \cdot \cos \Phi_m}{A_m \cdot \sin \Phi_m} = \cot \Phi_m = \frac{A_{ref} \cdot \cos \Phi_{ref} + A_{ind}}{A_{ref} \cdot \sin \Phi_{ref}} = \cot \Phi_{ref} + \frac{1}{\sin \Phi_{ref}} \cdot \frac{A_{ind}}{A_{ref}}$$

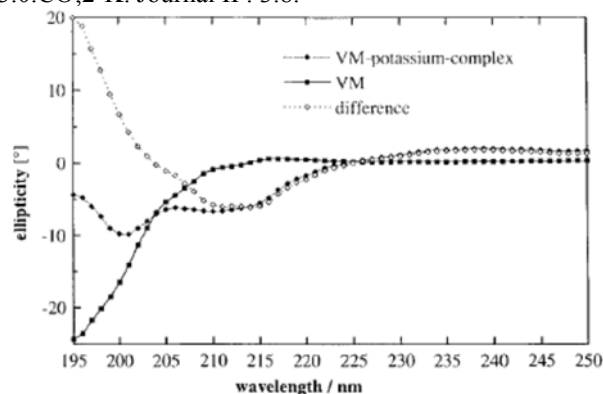
Thus, a linear relation exists between  $\cot(\phi_m)$  and the ratio of  $A_{ind}/A_{ref}$ , because the phase angle of  $\phi_{ref}$  of the reference luminophore can be assumed to be constant. This method is referred to as Dual Lifetime Referencing (DLR).

The graph shows the situations for the case where fluorescence intensity of the indicator is high (A) and where it is low (B). The overall signals are distinctly different.



**346. Chiroptic Recognition of Potassium Ion.** O. S. Wolfbeis, D. Opitz, T. Werner, A. Quart, *J. Mol. Recognition* **14** (2001) 13-17. DOI: 10.1002/1099-1352(200101/02)14:1<13::AID-JMR514>3.0.CO;2-K. Journal IF: 3.8.

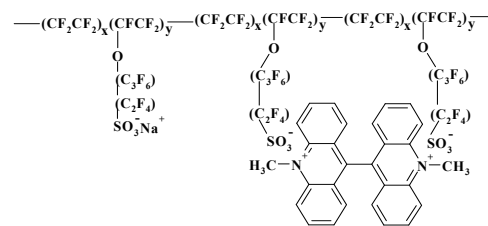
**Abstract:** The high specificity in the recognition and specific binding of potassium ion by the decapeptide valinomycin (VM) is exploited for its recognition and quantitation using both circular dichroism (CD) and optical rotation dispersion (ORD). The specific rotation of VM is comparably small ( $2.34^\circ \text{ ml} \cdot \text{g}^{-1} \cdot \text{cm}^{-1}$ ), so that an  $8 \mu\text{M}$  ( $= 8.89 \text{ mg} \cdot \text{ml}^{-1}$ ) solution of VM in 95% ethanol rotates polarized light of  $\lambda = 426 \text{ nm}$  passing a 2-cm cuvette by 0.076 degree only. It is shown, however, that VM undergoes large changes in both ORD and CD on binding to potassium ion. VM, potassium ion and the anionic dye merocyanine 540 form a ternary complex (VM/K/MC) which displays an induced CD with a positive maximum at 488 nm and a negative maximum at 470 nm. The ternary complex also displays fluorescence that is weaker by about 30% when compared to that of the dye alone. The induced CD of the ternary complex is interpreted in terms of the large conformational change which VM is known to undergo on binding potassium ion, thereby forming the pre-requisite for a van-der-Waals interaction between its outwardly directed lipophilic domains and the lipophilic domains of the anionic dye. The method is likely to be applicable to the fluorescent detection of all kinds of ions for which chiral receptors are known, e. g. in studies on the rôle of ions in biological systems including ion channels.



The figure shows the circular dichroism of valinomycin (VM), of the VM/K+ complex, and the difference spectrum

**345. Optical Sensor for Seawater Salinity**, Ch. Huber, I. Klimant, Ch. Krause, T. Werner, T. Mayr, O. S. Wolfbeis; *Fresenius' J. Anal. Chem.* **368** (2000) 196-202. DOI: 10.1007/s002160000493. journal IF: 5.7.

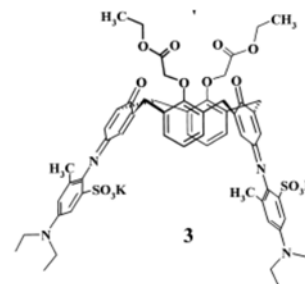
**Abstract:** Seawater salinity (SS) is measured via chloride which is responsible for most of SS. The sensing scheme is based on a fluorescent chloride probe immobilized on a Nafion film. In one approach, the probe undergoes a massive decrease in fluorescence intensity on exposure to chloride ion and this is related to SS. In the second approach, the intensity information is converted into a phase shift information by adding phosphorescent reference particles. The second scheme, referred to as dual luminophore referencing (DLR), is superior. See paper 347. The figure shows a schematic of the electrostatically immobilized chloride probe lucigenin. The graph shows a schematic of electrostatically immobilized lucigenine.



Fluorescent chloride probe immobilized on Nafion

**344. New Longwave Absorbing Chromogenic Calix[4]arene for Calcium Determination in Aqueous Environment**. T. Werner, J. M. Kuerner, Ch. Krause, O. S. Wolfbeis; *Anal. Chim. Acta* **421** (2000) 199-205. DOI: 10.1016/S0003-2670(00)01049-7. journal IF: 2.9.

**Abstract:** A new calcium ion selective and water-soluble calix[4]arene chromoionophore has been synthesized from the 25,27-bis[(ethoxycarbonyl)methoxy]-26,28-dihydroxy-calix[4]arene (1) and the N4,N4-diethyl-2-methyl-1,4-phenylenediamine-6-sulfonic acid (2). The 1,3-bis(indoaniline)-derived 2,4-bis-[(ethylcarbonyl)methoxy]-calix[4]arene (3) was obtained by introducing sulfonic groups into a phenylenediamine-derived chromophore followed by oxidative incorporation of two units of 2 into 1. The new chromophoric calix[4]arene (formula 3) possesses an absorbance maximum at 604 nm in buffered aqueous environment. Upon complexation of calcium a bathochromic shift of 84 nm occurs along with an increase in the absorption coefficient. The dissociation constants and the cross sensitivity to other alkali and alkaline earth ions were evaluated.



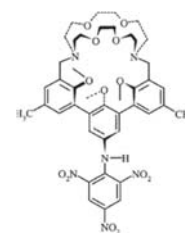
**343. Cell-Type Specific Protoporphyrin IX Metabolism in Human Bladder Cancer in Vitro**. R. Krieg, S. Fickweiler, O. S. Wolfbeis, R. Knuechel, *Photochem. Photobiol.* **72** (2000) 226-233.

DOI: 10.1562/0031-8655(2000)072<0226:CTSPIM>2.0.CO;2. journal IF: 2.1.

**Abstract:** 5-Aminolevulinic acid (ALA)-supported fluorescence endoscopy of the urinary bladder results in a detection rate of bladder cancer superior to that of white light endoscopy. The different accumulation of the metabolite protoporphyrin IX (PPIX) in tumor cells after ALA instillation is poorly understood; however, it is crucial to optimize diagnosis and potential phototherapy. For systematic analysis of cell-type specific PPIX accumulation and metabolism two human bladder carcinoma cell lines (RT4 and J82), a normal urothelial cell line (UROtsa), and a fibroblast cell line (N1) were chosen, and grown in two different growth states to model important tissue components of the urinary bladder, i.e. tumor, normal epithelium and stroma. To quantitate PPIX content, fluorescence intensities measured by flow cytometry were matched with cellular PPIX extraction values, and related to relative ferrochelatase activity, cellular iron content, number of transferrin receptors per cell and porphobilinogen deaminase (PBGD) activity. For in vitro experiments, the initial correlation of relative flow cytometric and spectrometric measurements of PPIX provides a calibration curve for consequent flow cytometric PPIX quantification. Lower fluorescence of normal cells could be explained by significant differences of ferrochelatase activity and iron content in comparison to tumor cells. However, the content of iron was not related to transferrin receptor content. PBGD activity seemed to play a minor role for the differential accumulation of PPIX in urothelial cells. In conclusion, the in vitro culture of urothelial cells and fibroblasts indicates that the most important metabolic step for PPIX accumulation in the urinary bladder is the transition from PPIX to heme. Further investigation of PPIX metabolism does support the validation of photodynamic diagnosis, and might also lead the way to a highly specific tumor related molecule.

**342. Hydrophilic Sensor Membrane Based on a Cation-Selective Protic Chromoionophore**. Ch. Krause, T. Werner, O. S. Wolfbeis; *Fresenius J. Anal. Chem.* **367** (2000) 426-428. DOI: 10.1007/s002160000390. journal IF: 5.7.

**Abstract:** The first potassium optode based on a protic chromoionophore immobilized in a hydrogel matrix is presented. The highly selective protic chromoionophore consists of a cryptohemispherand moiety and a trinitroanilino chromophore part. The acidifying power of potassium ions over sodium ions is 0.6 pH units. This correlates with the findings in solution. In contrast to several crown and aza-crown based chromophores the highly preorganized moiety allows ion detection even in aqueous environment. The detection limit for potassium ions at pH 7.7 is 5 mM.



**341. Review: Fiber Optic Chemical Sensors and Biosensors (1998-1999)**. O. S. Wolfbeis; *Anal. Chem. (Wash.)* **72** (2000) 81R-89R. DOI: 10.1021/a1000013k. journal IF: 5.7.

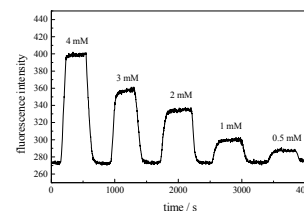
**Abstract:** This biannual review covers the time period from October 1997 to January 2000. Priority was given to fiber-optic sensors (FOS) for defined chemical, environmental, and biochemical significance and to new schemes and materials. The review does not include (a) FOS that obviously have been re-discovered; (b) FOS for nonchemical species such as temperature, current and voltage, stress, strain, and displacement, for structural integrity (e.g., of constructions), liquid level, and radiation; and (c) FOS for monitoring processes such as composite curing, injection molding and extrusion, or oil drilling, even though these are important applications of optical fiber technology.

**340. Sol-Gel Based Glucose Biosensors Employing Optical Oxygen Transducers, and a Method for Compensating for Variable Oxygen Background**. O. S. Wolfbeis, I. Oehme, N. Papkovskaya, I. Klimant; *Biosens. Bioelectron.* **15** (2000) 69-76. DOI: 10.1016/S0956-5663(99)00073-1. Journal IF: 4.1.

**Abstract:** Various types of thin-film glucose biosensors based on the use of the enzyme glucose oxidase (GOx) have been developed. The luminescent oxygen probe Ru(dpp) - whose emission is quenched by oxygen - is used to measure the consumption of oxygen. Three different combinations of oxygen transducer and sol-gel

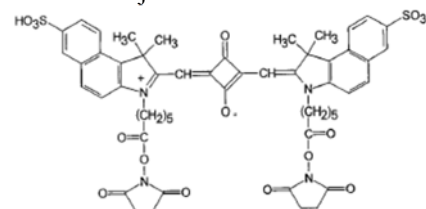


immobilized GOx were tested. In all cases, it was found to be essential to add sorbitol which results in a more porous sol-gel in which diffusion is not impaired. In an Appendix, equations are derived which describe the response of such sensors, how the effect of varying oxygen supply can be compensated for by making use of two sensors, one sensitive to oxygen only, the other to both oxygen and glucose, and how such sensors can be calibrated using 2 calibrators only. The response to glucose is fully reversible.



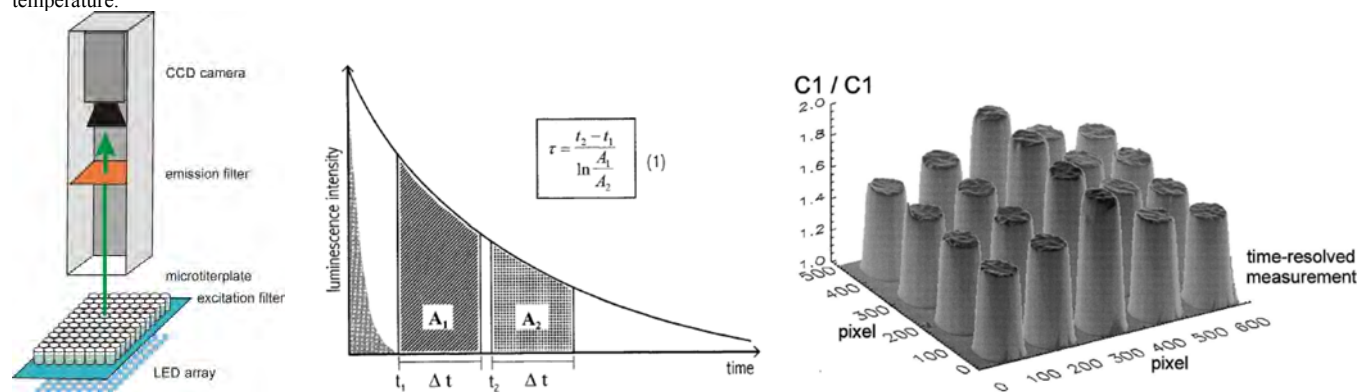
**339. Red Laser Induced Fluorescence Energy Transfer in an Immunosystem.** B. Oswald, F. Lehmann, L. Simon, E. Terpetschnig, O. S. Wolfbeis; *Anal. Biochem.* **280** (2000) 272-277. DOI: 10.1006/abio.2000.4553. journal IF: 3.0.

**Abstract:** We describe two near-infrared fluorescent squaraine dyes (Sq-635 and Sq-660), their spectra, their covalent linkage to proteins, and their use as donor and acceptor, respectively, in a fluorescence resonance energy transfer (FRET) immunoassay based on the use of red lasers. The dyes show quantum yields of around 10% in the free form and up to 68% when bound to proteins. If converted into their N-hydroxysuccinimide esters, they can be linked to free amino groups of proteins. To improve water solubility, two sulfo groups were introduced. The emission spectrum of Sq-635 overlaps the absorption spectrum of Sq-660 (a benzo-squarylium dye; formula shown), a fact that makes them a useful pair of dyes for use in FRET immunoassay which is demonstrated for human serum albumin/anti-human serum albumin.



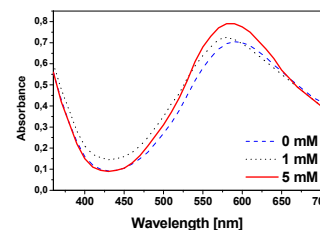
**338. Luminescence Lifetime Imaging of Oxygen, pH, and Carbon Dioxide Distribution Using Optical Sensors.** G. Liebsch, I. Klimant, B. Frank, G. Holst, O. S. Wolfbeis; *Appl. Spectrosc.* **54** (2000) 548-559. DOI: 10.1366/0003702001949726. Journal IF: 1.9.

**Abstract:** We present a modular system for time-resolved two-dimensional luminescence lifetime imaging of planar optical chemical sensors. It is based on a fast gateable CCD camera without image intensifier and a pulsable LED array as a light source. A software was developed for data acquisition with a maximum of parameter variability and for background suppression (see the figure below). This allows the operation of the system even under daylight. Optical sensors showing analyte specific changes of their luminescence decay time were tested and used for sensing  $pO_2$ ,  $pCO_2$ , pH values, and temperature. The luminophores employed are either  $Pt^{2+}$ -porphyrins or  $Ru^{2+}$ -polypyridyl complexes, contained in polymer films, and can be efficiently excited by blue LEDs. The decay times of the sensor films vary from 70  $\mu s$  for the  $Pt^{2+}$ -porphyrins to several 100 ns for the  $Ru^{2+}$ -complexes. In a typical application, 7-mm diameter spots of the respective optical sensor films were placed at the bottom of the wells of microtiterplates. Thus, every well represents a separate calibration chamber with an integrated sensor element. Both luminescence intensity-based and time-resolved images of the sensor spots were evaluated and compared. The combination of optical sensor technology with time-resolved imaging allows for the determination of the distribution of chemical or physical parameters in heterogeneous systems and is therefore a powerful tool for screening and mapping applications. The Figures show the experimental setup, the principle of rapid lifetime determination (RLD), and a typical image obtained with ratiometric data (that suppress background light) for microplate wells filled with solutions of different temperature.



**337. Polyaniline-Coated Microtiter Plates for Use in Longwave Optical Bioassays.** S. A. Piletsky, T. L. Panasyuk, E. V. Piletskaya, T. A. Sergeeva, A. V. Elskaya, E. Pringsheim, O. S. Wolfbeis; *Fresenius' J. Anal. Chem.* **366** (2000) 807-810. DOI: 10.1007/s002160051575. Journal IF: 2.6.

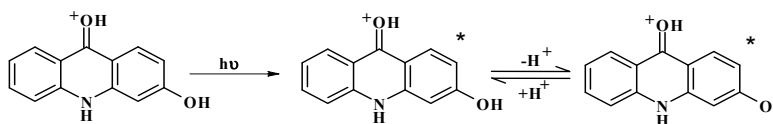
**Abstract:** A technique for coating the wells of microtiterplates with polyaniline layers and with polyaniline/enzyme layers is presented. The resulting wells are shown to be useful for assaying enzyme substrates (as exemplified for glucose via pH) and hydrogen peroxide (via the redox properties of the film). Analyte detection is based on monitoring the absorption spectra of the polyaniline, which turn purple as a result of redox processes, or green on formation of acids by enzymatic reactions. Hydrogen peroxide (a species produced by all oxidases) and glucose (which yields protons on enzymatic oxidation) have been determined in the millimolar to micromolar concentration range. High sensitivity, film stability and good reproducibility of the measurements make the system an attractive alternative to existing biosensing schemes. The graph shows the effect of  $H_2O_2$  on the spectra of polyaniline with adsorbed peroxidase.



**336. Phototautomeric Equilibrium in the Lowest Excited Singlet State of 3-Hydroxyacridone,** O. S. Wolfbeis, Ch. Huber, S. G. Schulman; *J. Phys. Chem. A* **104** (2000) 3900-3904. DOI: 10.1021/jp9927449. Journal IF: 3.1.

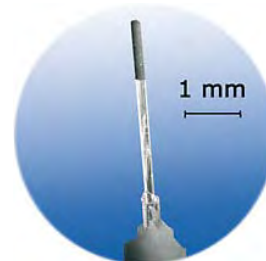
**Abstract:** The pH dependences of the absorption and fluorescence emission of 3-hydroxyacridone (3-HA) were studied. Three species (the cation, the neutral molecule and the anion) were identified in absorption. The same species, albeit at different pH ranges, were identified in fluorescence. Their

decay times are highly different. In addition, a new species having an unusually long-wavelength emission that has no equivalent in the ground state was identified in the pH 4 to  $H_0 - 4$  range. This species is assigned to an excited state tautomer formed predominately by adiabatic double proton transfer during the lifetime of the excited state.



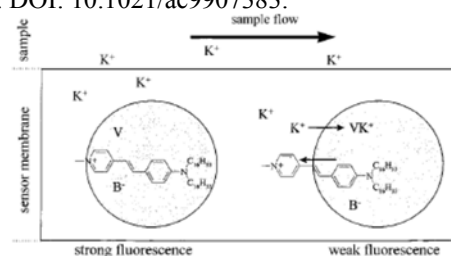
**335. Fiber Optic Microsensor for High-Resolution  $p\text{CO}_2$  Sensing in Marine Environment.** G. Neurauter, I. Klimant, O. S. Wolfbeis; *Fresenius' J. Anal. Chem.* **366** (2000) 481-487. DOI: 10.1007/s002160050097. journal IF: 2.6.

**Abstract:** A fast responding fiber-optic microsensor for sensing  $p\text{CO}_2$  in marine sediments with high spatial resolution is presented. The tip diameter varies typically between 20 and 50  $\mu\text{m}$ . In order to make the pH indicator 8-Hydroxypyrene-1,3,6-trisulfonate soluble in the ethyl cellulose matrix, it was lipophilised with tetraoctylammonium as the counterion [HPTS (TOA)<sub>4</sub>]. The microsensor was tuned to sense very low levels of dissolved carbon dioxide which are typically present in marine systems. The detection limit is 0.04 hPa  $p\text{CO}_2$  which corresponds to 60 ppb  $\text{CO}_2$  of dissolved carbon dioxide. A soluble teflon derivative with an extraordinarily high gas permeability was chosen as a protective coating to eliminate interferences by ionic species like chloride or pH. Response times of less than 1 min were observed. The performance of the new microsensor is described with respect to reproducibility of the calibration curves, dynamic range, temperature behavior, long term stability and storage stability. The effect of hydrogen sulfide as an interferent which is frequently present in anaerobic sediment layers was studied in detail.



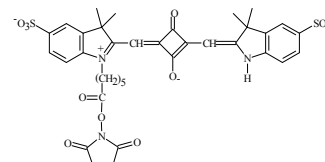
**334. Emulsion-Based Fluorosensors for Potassium(I) Featuring Improved Stability and Signal Change.** Ch. Krause, T. Werner, Ch. Huber, O. S. Wolfbeis; *Anal. Chem. (Wash.)* **71** (1999) 5304-5308. DOI: 10.1021/ac9907383.

**Abstract:** A novel kind of optical sensor for potassium(I) is presented which is based on the use of lipophilic droplets containing valinomycin and entrapped in a structured hydrogel. A positively charged solvatochromic dye located near the surface of the droplets responds to the valinomycin-assisted extraction of potassium(I) from the sample by dramatic decrease of fluorescence intensity. The dynamic range is from 5 to 100 mM potassium, with negligible cross sensitivity to ionic strength. Cross sensitivity to pH is negligible too in the pH range from 6.5 to 7.3. The effect of interfering lipophilic anions is discussed. Response times within the dynamic range are less than 3 min on going from low to high potassium ion concentrations but about 10 min in the reverse direction. Response is fully reversible with only small drifts in baseline. The measurement uncertainty of determining 5 mM potassium(I) is better than 0.2 mM.



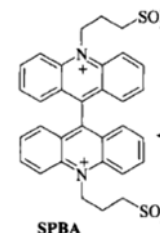
**333. Synthesis, Spectral Properties and Detection Limits of Reactive Squaraine Dyes, a New Class of Diode Laser Compatible Fluorescent Protein Labels,** B. Oswald, L. Patsenker, J. Duschl, H. Szmackinski, O. S. Wolfbeis, E. Terpetschnig; *Bioconj. Chem.* **10** (1999) 925-931. DOI: 10.1021/bc9801023.

**Abstract:** We describe the synthesis and spectral characterization of two reactive long-wavelength fluorescence labels one or two N-hydroxysuccinimidyl esters. Both are squaraine derivatives and consist of a cyanine-type chromophore and a central squaraine bridge. To improve water solubility, we introduced two sulfonic acid groups into the heterocyclic ring systems and for covalent attachment to proteins a reactive N-hydroxy-succinimide ester (NHS ester) was synthesized.



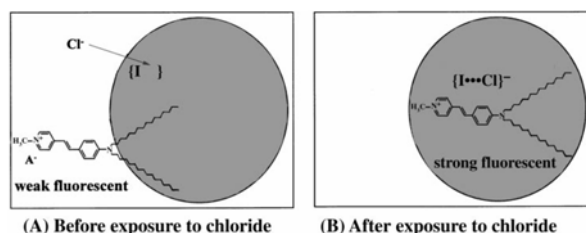
**332. Anion Induced Fluorescence Quenching of a New Zwitterionic Biacridine Derivative.** T. Werner, K. Faehrich, Ch. Huber, O. S. Wolfbeis; *Photochem. Photobiol.* **70** (1999) 585-589. DOI: 10.1111/j.1751-1097.1999.tb08255.x

**Abstract:** The effect of halides and different buffer anions on the quenching of the fluorescence of the new probe 10,10'-bis(3-sulfopropyl)-9,9'-biacridine (SPBA) has been studied using fluorescence and decay time measurements. The linearity of the Stern-Volmer plot indicates that fluorescence quenching by halides can be described reasonably well by a single-exponential decay with a K of 4.1 times  $10^6 \text{ M}^{-1}\text{s}^{-1}$  for chloride, 7.83 times  $10^6 \text{ M}^{-1}\text{s}^{-1}$  for bromide and 1.12 times  $10^7 \text{ M}^{-1}\text{s}^{-1}$  for iodide. We have found that SPBA is collisionally quenched also by the buffers 3-(N-mor-pholino)propanesulfonic acid (MOPS) and N-2-hydroxy-ethylpiperazine-N'-ethansulfonic acid (HEPES). The bimolecular rate constants are  $1.67 \times 10^6 \text{ M}^{-1}\text{s}^{-1}$  for HEPES and 1.44 times  $10^6 \text{ M}^{-1}\text{s}^{-1}$  for MOPS.



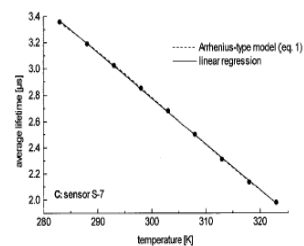
**331. Novel Chloride-Selective Optode Based on Polymer-Stabilized Emulsions Doped with a Lipophilic Fluorescent Polarity-Sensitive Dye.** Ch. Huber, T. Werner, Ch. Krause, O. S. Wolfbeis; *Analyst* **124** (1999) 1617-1622. DOI: 10.1039/a905260g.

**Abstract:** A chloride-selective optical sensor layer is presented which is based on a polymer-stabilised emulsion system consisting of a hydrogel with entrapped plasticizer droplets. The droplets contain a neutral chloride-selective ionophore and a polarity-sensitive cationic fluorescent dye (PSD) located near the droplet surface. The ionophore extracts chloride out of the aqueous solution through the hydrogel into the plasticizer droplets, followed by a displacement of the positively charged PSD into the plasticizer droplet. This concerted process causes a decrease of micro-polarity near the dye, resulting in a dramatic increase in its fluorescence intensity. The sensing scheme can be used for reversible sensing of chloride in the 1–80 mM concentration range with response times on the order of less than 3 min. The sensor membrane has been investigated in terms of signal change, stability, limits of detection and selectivity for the analyte over interferents.



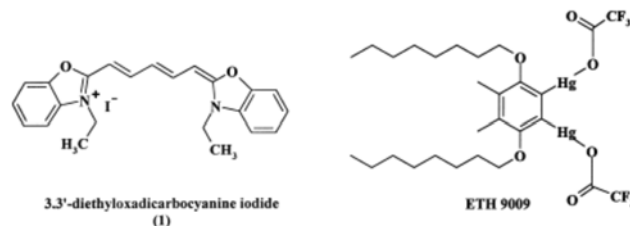
**330. Luminescence Lifetime Temperature Sensing Based on Sol-Gels and Poly(acrylonitrile)s Dyed with Ruthenium Metal Ligand Complexes.** G. Liebsch, I. Klimant, O. S. Wolfbeis; *Adv. Mater.* **11** (1999) 1296-1299. DOI: 10.1002/(SICI)1521-4095(199910)11:15<1296::AID-ADMA1296>3.0.CO;2-B

**Abstract:** Temperature ( $T$ )-sensitive luminescent materials are obtained by embedding the Ru(II)-tris-1,10-phenanthroline complex into a poly(acrylonitrile) (PAN) or a densified sol-gel matrix. Both the luminescence intensity and the luminescence decay time are strongly affected by  $T$ , while the gas-impermeable matrices prevent dynamic quenching by oxygen or other quenchers.  $T$  sensors can be prepared in the form of transparent planar films and coatings, or as a powder. The  $T$  dependence was established in the 10 to 40 °C range and the films are demonstrated to be useful for  $T$ 's up to 100 °C. The materials respond completely reversibly, are highly luminescent, have fast response and possess lifetimes in the microsecond time regime. They can be used as a  $T$ -sensitive paint for single-point measurements, for imaging or for internal  $T$  compensation in optical chemical sensors.



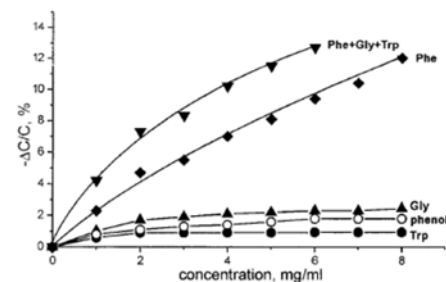
**329. Overcoming the pH-Dependency of Optical Sensors: A pH-Independent Chloride Sensor Based on Co-Extraction.** Ch. Huber, T. Werner, Ch. Krause, O. S. Wolfbeis, M. J. P. Leiner, *Anal. Chim. Acta* **398** (1999) 137-143. DOI: 10.1016/S0003-2670(99)00414-6.

**Abstract:** A chloride-selective optode is presented which is based on a polymer-stabilized emulsion system which consists of a hydrogel into which plasticizer droplets are incorporated containing a neutral chloride-selective ionophore. A solvatochromic cationic fluorescent dye is located in the hydrogel. When the ionophore extracts chloride out of the aqueous solution into the plasticizer droplets, the positively charged dye is co-extracted for reasons of electro-neutrality. This concerted reaction causes a decrease of micro-polarity near the dye, resulting in an increase of its fluorescence intensity along with a bathochromic shift of the emission maximum. This system can be used for pH-independent reversible sensing of chloride in the 10–100 mM concentration range with response times in the order of 3 min.



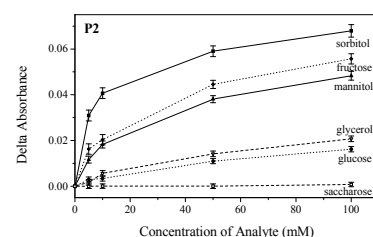
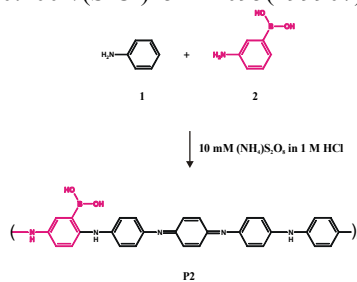
**328. Electro-Polymerized Molecularly Imprinted Polymers as Receptor Layers in Capacitive Chemical Sensors.** T. L. Panasyuk, V. M. Mirsky, S. A. Piletsky, O. S. Wolfbeis; *Anal. Chem.* **71** (1999) 4609-4613. DOI: 10.1021/ac9903196

**Abstract:** The first application of molecularly imprinted polymers to chemical sensors with capacitive detection is described. The sensitive layer was prepared by electropolymerization of phenol on gold electrodes in the presence of the template (phenylalanine). The insulating properties of the polymer layer were studied by electrochemical impedance spectroscopy. Electrical leakages through the polymer layer were suppressed by deposition of a self-assembled monolayer of mercaptophenol before polymerization and of alkanethiol after polymerization. At the final stage of the sensor preparation, the template was removed. The multi-layer system obtained displayed a decrease in electrical capacitance on addition of phenylalanine.



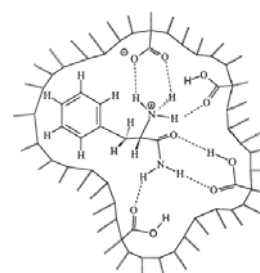
**326. A Polyaniline with Near-Infrared Optical Response to Saccharides.** E. Pringsheim, E. Terpetschnig, S. A. Piletsky, O. S. Wolfbeis; *Adv. Mater.* **11** (1999) 865-868. DOI: 10.1002/(SICI)1521-4095(199907)11:10<865::AID-ADMA865>3.0.CO;2-B

**Abstract:** Copolymerization of aniline and 3-aminophenylboronic acid yields a sugar-binding polymer film whose absorption spectra between 500 and 800 nm undergo large changes on addition of saccharides including saccharose, fructose, glucose, sorbitol, mannitol, and glycerol at neutral pH. The spectral shifts depend on the concentration of the saccharides and are fully reversible, thus allowing continuous sensing. Such films represent an alternative to enzyme-based glucose sensors because of their ease of preparation, compatibility with LED and diode laser light sources, and their thermal and temporal stability. The figure on the left shows the chemistry of the polymerization, and the other the response of the material to saccharides.



**325. Application of Non-specific Fluorescent Dyes for Monitoring Enantio-Selective Ligand Binding to Molecularly Imprinted Polymers.** S. A. Piletsky, E. Terpetschnig, H. S. Anderson, I. A. Nichols, O. S. Wolfbeis; *Fresenius' J. Anal. Chem.* **364** (1999) 512-516. DOI: 10.1007/s002160051377

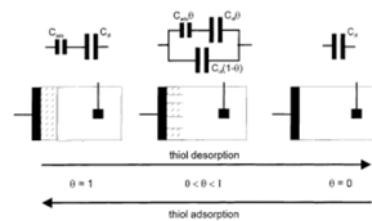
**Abstract:** The displacement of non-specific dyes from molecularly imprinted polymer (MIP) chromatographic stationary phases has been used for the detection and quantification of ligand-polymer binding events. A blank polymer and an L-Phe-amide-imprinted polymer were prepared using methacrylic acid as the functional monomer and ethylene glycol dimethacrylate as a crosslinker. The MIP is first loaded with dye, and a solution of the dye in the eluent is passed through the MIP. If analyte is injected into the dye solution in the eluent, part of the dye is competitively replaced by the analyte from the MIP. Specifically, the competitive displacement of rhodamine B by amino acids and phenylalaninamide (Phe-NH<sub>2</sub>), respectively, has been studied under polar and hydrophobic elution conditions. Enantioselective binding of Phe and Phe-NH<sub>2</sub> to the imprinted polymer was shown to occur in the micromolar concentration range.





**323. Electrical Control of Alkanethiols Self-Assembly on a Gold Surface as an Approach for Preparation of Micro-Electrode Arrays.** M. Riepl, V. M. Mirsky, O. S. Wolfbeis; *Microchim. Acta* **131** (1999) 29-34. DOI: 10.1007/s006040050006

**Abstract:** It is shown by capacitive monitoring that the self-assembly of alkanethiols on gold electrodes and desorption of these self-assembled monolayers from the electrodes are controlled by the electrode potential. At neutral pH, chemical adsorption of alkanethiols was observed at an electrode potential of +300mV vs SCE, but only physical adsorption was detected when the electrode potential was -1400 mV vs SCE. At electrode potentials between these values (-300mV, -600 mV), chemical adsorption of alkanethiols occurred, but the alkanethiol monolayers were not stable in the absence of the alkanethiol in the bulk solution and were desorbed from the gold electrode. The desorption rate was higher at more negative electrode potentials. These results can be used in designing methods for electrically addressable immobilization of different receptors on (micro)electrode arrays. This has been demonstrated by deposition of two different types of alkanethiols onto a two-electrode array.



**322. Fast Response Oxygen Micro-Optodes Based on Novel Soluble Ormosil Glasses**, I. Klimant, F. Ruckruh, G. Liebsch, A. Stangelmayer, O. S. Wolfbeis; *Microchim. Acta* **131** (1999) 35-46. DOI: 10.1007/s006040050007

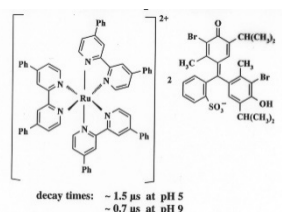
**Abstract:** Phenyl-substituted ormosils are used as a matrix for oxygen microsensors. The new ormosils combine features of classical polymers such as solubility in organic solvents and those of sol-gel glasses such as mechanical stability and a porous structure. They make possible a simple and fast fabrication of microsensors with reproducible properties. The effect precursor composition and thermal treatment on the sensing properties have been studied. Oxygen-sensitive films with ruthenium(II)-tris-(4,7-diphenyl-1,10-phenanthroline) and platinum(II)-octaethyl porphyrine as indicators were characterised with respect to their mechanical and photophysical properties. Photostability, oxygen sensitivity, response behavior and signal intensities of the sensing films and the micro-optodes were examined. The microsensors are fast responding, photostable and can be produced with a sufficient batch to batch reproducibility. The new sensors can be autoclaved and show fast response. The figure shows the tip of the 20-µm fiber sensor coated with the ruthenium probe displaying red fluorescence.



**321. Fiber Optic Ion Microsensors Based on Luminescence Lifetime.** T. Werner, I. Klimant, Ch. Huber, Ch. Krause, O. S. Wolfbeis; *Microchim. Acta* **131** (1999) 25-28. DOI: 10.1007/s006040050005

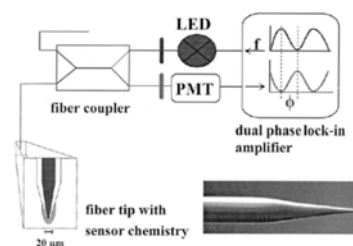
**Abstract:** Fiber optic ion-microsensors based on luminescence decay time have been developed for chloride and potassium. The fiber tip coatings consist of the respective ion-selective lipophilic ion carrier, plasticized PVC, and the ruthenium(II) tris-diphenyl-bipyridyl ion pair with bromothymol blue (see the formula) which acts as a proton donor.

The efficacy of radiationless fluorescence energy transfer from the donor (the ruthenium complex) to the acceptor (BTB) is mediated by the ion concentration within the samples. The response to chloride is based on the co-extraction of chloride along with protons from the aqueous sample into a plasticized PVC membrane, whereas in the presence of potassium ions in the sample, the neutral BTB becomes deprotonated on extraction of potassium ions, which is accompanied by the release of protons. Both processes result in a change in the absorbance of BTB. The absorption band of deprotonated BTB overlaps the emission band of the ruthenium complex, thus allowing radiationless energy transfer to take place.



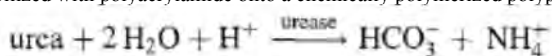
**319. Long-Lifetime Based pH Micro-Optodes without Oxygen Interference,** U. Kosch, I. Klimant, O. S. Wolfbeis; *Fresenius J. Anal. Chem.* **364** (1999) 48-53. DOI: 10.1007/s002160051299

**Abstract:** The first decay time-based fiber optic pH microsensors are presented which are without cross-sensitivity to molecular oxygen. They are based on radiationless energy transfer from the donor ruthenium(II)-tris(1,10-phenanthroline) to a pH-sensitive sulfonephthalein acceptor dye. The microsensors have decay times in the microsecond range, a fact that makes them compatible with existing devices designed for optical oxygen microsensing. The sensor tips have diameters of 20 to 30 µm. Outstanding features are the excellent mechanical stability and the inertness to quenching by oxygen. The dynamic range depends on the pK<sub>a</sub> of the selected pH indicator. The sensors were characterized with respect to the dynamic range, response, storage stability and photostability. A high resolution pH measurement in a marine sediment core serves as an example for its utility.

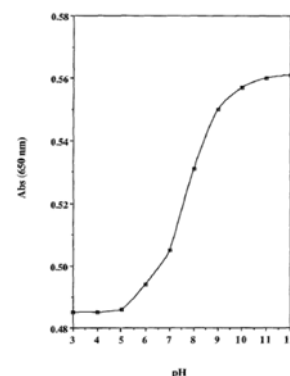


**318. Characterization of a Urea Optical Biosensor Based on Polypyrrole,** S. de Marcos, R. Hortigüela, J. Galban, J. R. Castillo, O. S. Wolfbeis; *Microchim. Acta* **130** (1999) 267-272. DOI: 10.1007/BF01242915.

**Abstract:** A new optical sensor for urea determination is presented. It is based on the enzymatic reaction with urease, which is first photoimmobilized with polyacrylamide onto a chemically polymerized polypyrrole (PPy) film.

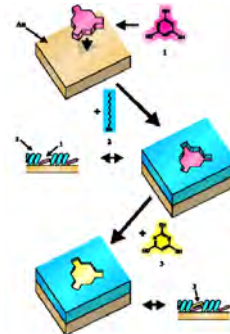


This causes a consumption of protons and an increase in the pH value. PPy acts as both the support and also as the indicator because PPy films display an absorbance spectrum in the near IR range that is pH dependent. The variation of absorbance is thus directly related to the change of pH caused during the enzymatic reaction, which is also dependent on the urea concentration. The linear range of the sensor is from 0.06 to 1 M of urea, which is the common level of urea concentration found in blood and urine samples. The main advantage of this sensor is that no indicator dye or pH indicator is needed. The graph shows a plot of the absorbance of PPy at 650 nm as a function of the pH value.



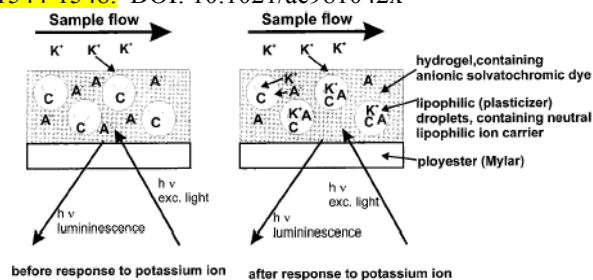
**316. A Spreader-Bar Approach to Molecular Architecture: Formation of Stable Artificial Chemoreceptors.** V. M. Mirsky, Th. Hirsch, S. A. Piletsky, O. S. Wolfbeis; *Angew. Chem. Intl. Ed. Engl.* **38** (1999) 1108-1110. DOI: 10.1002/(SICI)1521-3773(19990419)38:8<1108::AID-ANIE1108>3.0.CO;2-C

**Abstract:** We describe a spreader-bar approach that allows for the first time noncross-linked monolayers to be obtained, whose structure can not be distorted by lateral diffusion. An artificial interface with a high affinity for barbituric acid (a starting material for many pharmaceuticals) was created by co-adsorption of thiobarbituric acid (the template) and dodecanethiol (the matrix) onto a gold substrate. This process leads to the formation of binding sites with a structure complementary to that of thiobarbituric acid. Binding of barbituric acid and of other species to the resp. surface was detected by capacitance measurements. A high selectivity of this artificial chemo-receptor for barbituric acid was observed.



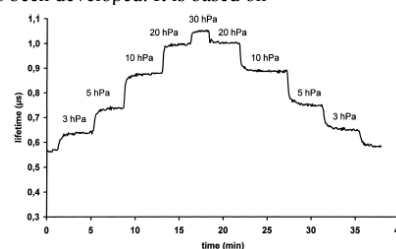
**315. pH-Insensitive Ion Selective Optode: A Coextraction-Based Sensor for Potassium Ions.** Ch. Krause, T. Werner, Ch. Huber, O. S. Wolfbeis, M. J. P. Leiner; *Anal. Chem. (Wash.)* **71** (1999) 1544-1548. DOI: 10.1021/ac981042x

**Abstract:** A novel type of optical potassium sensor is presented whose response mechanism is virtually insensitive to pH and ionic strength. It is based on a co-extraction mechanism using a lipophilic ion carrier and a fluorescent anion, the two contained in an oil-in-water emulsion. The latter is composed of lipophilic plasticizer droplets containing valinomycin, and of a hydrogel containing the highly solvatochromic anionic dye merocyanine 540. On exposure to potassium ions, these are extracted, along with the anionic fluorophore, into the plasticizer phase wherein the dye is much more fluorescent than in hydrogel. The dynamic range typically is from 0.1 to 50 mmol/L potassium. Response times are < 3 min within this concentration range. The figure shows a schematic of the sensor layer and its composition before and after exposure to potassium ions.



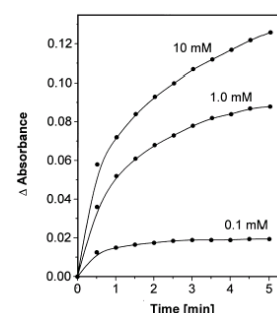
**314. Microsecond Lifetime-Based Optical Carbon Dioxide Sensor Using Luminescence Resonance Energy Transfer.** G. Neurauter, I. Klimant, O. S. Wolfbeis; *Anal. Chim. Acta* **382** (1999) 67-75. DOI: 10.1016/S0003-2670(98)00748-X

**Abstract:** A lifetime-based optical sensor for measurement of dissolved and gaseous carbon dioxide has been developed. It is based on radiationless energy transfer from a ruthenium metal ligand complex (the donor), to thymol blue (a common pH indicator and acting as an acceptor). Both were placed in a hydrophobic matrix. In presence of carbon dioxide, thymol blue is protonated and changes its color from blue to yellow resulting in a decrease in the rate of energy transfer and consequently an increase in decay time. The decay time as pCO<sub>2</sub> dependent parameter was measured in the frequency domain with a blue LED as a light source modulated at a frequency of 75 kHz. The sensor displays a phase shift up to 16 degree in the range from 0 hPa to 30 hPa of pCO<sub>2</sub>, corresponding to a change in decay time from 0.38 μs to 1.05 μs. The detection limit was found to be 0.5 μM (22 ppb) of dissolved carbon dioxide and the response times are in the order of 15 s.



**313. Composite Films of Prussian Blue and N-Substituted Polypyrroles: Covalent Immobilization of Enzymes and Application to Near-Infrared Optical Biosensing.** R. Koncki, O. S. Wolfbeis; *Biosensors Bioelectron.* **14** (1999) 87-92. DOI: 10.1016/S0956-5663(98)00095-5

**Abstract:** We demonstrate the feasibility of optical biosensing using a material which - in essence - is a modified inorganic film to which various enzymes were covalently attached. Thin and transparent blue films composed of Prussian Blue and incorporated into a network of N-substituted polypyrroles are sensitive to pH in the pH 5 - 9 range at 720 nm wavelength and can be modified with enzymes to result in the respective biosensors. Several methods of enzyme immobilization, using bifunctional crosslinking reagents, and various enzymes were tested. Best results were obtained using the one-step carbodiimide method which resulted in highly active, stable and transparent biosensor films for optical determination of urea and acetylcholine. The operational stability exceeded one month and even after two months of dry storage at room temperature the activity did not drop. The biosensors allow optical determination of the respective substrates in the millimolar concentration range. The figure shows the response of the sensor layer BFA-1 to various concentrations of acetylcholine (in mM).



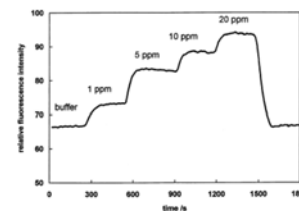
**312. A Minimal Binding Domain of the Low Density Lipoprotein Receptor Family.** T. M. Bajari, K. A. Lindstedt, M. Riepl, V. M. Mirsky, J. Nimpf, O. S. Wolfbeis, H. A. Dresel, E. K. F. Bautz, W. J. Schneider, *Biol. Chem.* **379** (1998) 1053-1062. DOI: 10.1515/bchm.1998.379.8-9.1053

**Abstract:** As more relatives of the low density lipoprotein receptor (LDLR) are discovered, defining their minimal binding domain(s) becomes a challenge. Here we have chosen the multifunctional chicken oocyte receptor for yolk deposition (termed LR8), and the pan-receptor ligand, receptor associated protein (RAP), as model systems to characterize a minireceptor using the phage display approach. Displayed fragments derived from the entire 819 residue LR8 molecule, followed by selection via panning on RAP, led to the definition of an 80 residue stretch LR8 minireceptor. It contains 12 cysteines, and represents parts of the second, the entire third, and parts of the fourth, of the eight clustered 'ligand binding repeats' in LR8; only two of the eight stretches of negatively charged residues of LR8, i.e., EDGSDE and DSGEDEE, are present. The latter sequence is reminiscent of that in the fifth repeat of the human LDLR, thought to be most critical for interaction with positive charge clusters in ligands. Baculovirus-mediated expression of the soluble minireceptor in insect cells showed it to fold as a monomer, and sulfhydryl-reduction-sensitive interaction with RAP was demonstrated for immobilized as well as soluble minireceptor. Furthermore, the LR8-derived minireceptor provided a RAP-responsive surface when covalently coupled to the surface of a gold electrode. In addition to its use in defining minimal binding domains, the phage display approach provides powerful tools for dissection, and consequently, manipulation, of the function of receptors so as

to direct their binding activity toward' ligands of diagnostic and/or therapeutic interest.

**311. Sol-Gel Based Optical Sensor for Dissolved Ammonia.** A. Lobnik, O. S. Wolfbeis; *Sensors Actuators B51* (1998) 203-207. DOI: 10.1016/S0925-4005(98)00189-0

**Abstract:** Ormosils were prepared in different ratios of tetramethoxysilane and organically modified sol-gel precursors of type R-Si(OR)<sub>3</sub> and R<sub>2</sub>Si(OR)<sub>2</sub>. Aminofluorescein was incorporated into various ormosils and the resulting materials were tested for their response to pH and dissolved ammonia. R<sub>2</sub>Si(OR)<sub>2</sub>-based layers were recognized as the most promising materials because of their high permeability to ammonia, impermeability to ions, long operational lifetime and good photostability.



**310. Polarity Studies on Ormosils Using Solvatochromic Fluorescent Probes,** A. Lobnik, O. S. Wolfbeis; *Analyst* **123** (1998) 2247-2250. DOI: 10.1039/A804583F

**Abstract:** Ormosils (organically modified siloxanes) are a relatively new family of materials, prepared by the sol-gel method, with properties that are intermediate between those of glasses and polymers. To probe the micropolarity of various solvents and ormosils, a ketocyanine dye (KC) with unique solvatochromic properties in fluorescence was used. KC is an excellent probe and is sensitive to the polarity of its microenvironment. Fluorescence studies revealed remarkable changes in the fluorescence band positions or intensities as a function of the polarity of the ormosil, which depend on the different ormosil precursors used. Storage stability was also investigated.

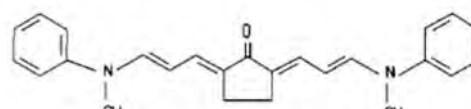


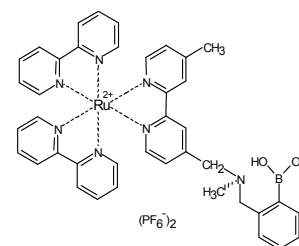
Fig. 1 Structure of ketocyanine dye (KC).

**309. Book Chapter. Fluorescence Techniques for Probing Molecular Imprinted Polymers,** O. S. Wolfbeis, E. Terpetschnig, S. Piletsky, E. Pringsheim, O. S. Wolfbeis; in: *Applied Fluorescence in Chemistry, Biology and Medicine*, W. Rettig, B. Strehmel, S. Schrader, H. Seifert (eds.), Springer, Berlin, 1998, pp. 277-295. DOI: 10.1007/978-3-642-59903-3\_12

**Abstract:** There is a growing interest in the design of artificial receptors and enzymes because the modeling of enzymes and receptors is helpful for understanding natural molecular recognition processes. In addition, artificial receptors and catalytic systems can be used to control processes such as the preparation and purification of chemicals, but in particular to design diagnostic tools. There is a growing interest in the design of artificial receptors and enzymes because the modeling of enzymes and receptors is helpful for understanding natural molecular recognition processes. In addition, artificial receptors and catalytic systems can be used to control processes such as the preparation and purification of chemicals, but in particular to design diagnostic tools. Imprinted polymers form a rather recent class of materials with recognition capabilities. The term refers to matrices of organic polymers possessing cavities of specific size, shape and charge and therefore are capable of recognizing molecules fitting into such cavities. Such materials are obtained by polymerizing monomers and cross-linkers in the presence of the molecule to be recognized ("template"). During polymerization, the geometry of the template-monomer complex is maintained in the growing polymer matrix. Removal of the templates leaves cavities displaying a shape and arrangement of functional groups corresponding to those of the template. Table 1 (not exhaustive) gives an overview on materials that are frequently used, on typical analytes („templates“) that have been investigated, and on potential fields of applications.

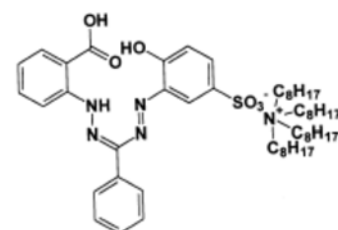
**306. Set of Luminescence Decay Time Based Chemical Sensors for Clinical Applications.** O. S. Wolfbeis, I. Klimant, T. Werner, Ch. Huber, U. Kosch, Ch. Krause, G. Neurauder, A. Duerkop; *Sensors Actuators B51* (1998) 17-24. DOI: 10.1016/S0925-4005(98)00181-6

**Abstract:** We present a sensing scheme capable of measuring the 10 parameters most important in analysis of blood gases, electrolytes and enzyme substrates. Detection is based on the variation in the decay time of the luminescence of a single class of luminophores, namely the ruthenium diimine complexes. The resulting family of sensors is operated within a limited range of modulation frequencies and consistent in terms of spectroscopy, analytical wavelengths and opto-electronic components. Except for oxygen which directly modulates decay time, a specific receptor for each single analyte was placed in close spatial proximity to the luminophore which itself is inert to the analyte. The receptor affects both the decay time and intensity of luminescence. Sensors are presented for pH, oxygen, carbon dioxide, potassium, sodium, calcium, chloride, ammonia, urea and glucose, and the sensing schemes and respective figures of merit are discussed. The glucose sensing scheme makes use of a boronic acid derived from a ruthenium ligand complex that is capable of reversibly binding monosaccharides. Specifically, sensors are described for the following clinical analytes: pH-value, oxygen, CO<sub>2</sub>, CO<sub>2</sub>, K<sup>+</sup>, Na<sup>+</sup>, Ca<sup>++</sup>, chloride, ammonia, urea, glucose.



**305. The Effect of Polymeric Supports and Methods of Immobilization on the Performance of an Optical Copper(II)-Sensitive Membrane Based on the Colorimetric Reagent Zincon,** I. Oehme, S. Prattes, O. S. Wolfbeis, G. J. Mohr, *Talanta* **47** (1998) 595-606. DOI: 10.1016/S0039-9140(98)00084-8

**Abstract:** A comparative study on the effect of different immobilization methods and matrix materials on the performance of copper(II)-sensitive membrane layers is presented. The indicator dye Zincon was immobilized in hydrophilic and hydrophobic polymers by various methods including: (a) physical entrapment of the Zincon-tetraoctylammonium ion pair in plasticized PVC, hydrogel, polystyrene, ethyl cellulose, poly-HEMA, AQ-polymer and in sol-gel glass; (b) electrostatic immobilization on an anion exchanger cellulose; and (c) covalent immobilization on cellulose via a sulfatoethylsulfonfyl reactive group. The response to copper(II) ion was evaluated kinetically via the initial slope of the change in absorbance within 1 min. Layers made of hydrogel and PVC provide the highest sensitivity, while covalent immobilization is the most reproducible one, and sol-gel layers display the best mechanical stability.



**304. Capacitive Study of Self-Assembled Monolayers: Surface Charge Effects and Kinetics of Surfactant Adsorption,** R. Schweiss, V. M. Mirsky, O. S. Wolfbeis; *Mat. Sci. Forum* **287/288** (1998) 427-430 (TransTech Publ., Winterthur, CH). ISSN

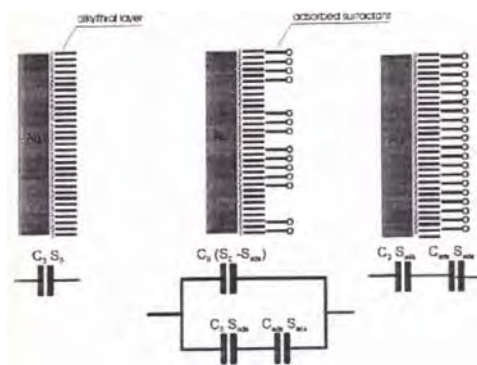


0255-5476. DOI: 10.4028/www.scientific.net/MSF.287-288.427

**Abstract:** Adsorption and desorption kinetics of different surfactants onto/from the surface of gold electrodes covered by self-assembled monolayers of 1-octadecanethiol were monitored in aqueous solutions by means of capacitive measurements. The formation of an adsorbed layer with a specific capacitance  $C_{ads}$  and an area of  $S_{ads}$  leads to a decrease in the electrode capacitance  $C_0$  for the value  $\Delta C$  according to

$$\frac{\Delta C}{C} = \frac{S_{ads}}{S_0} \frac{C_0}{C_0 + C_{ads}}$$

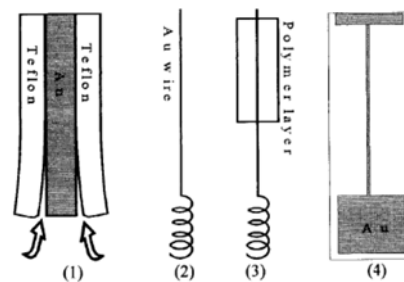
The effects of temperature, surfactant concentration and of the surfactants hydrophobic chain length were studied. A linear dependence between the initial slope of the adsorption kinetics and surfactant concentration was observed. This effect can be used for analytical determination of surfactants. The adsorption kinetics suggests a fractal geometry of the surfactants adsorption. The influence of pH value and ionic strength on the capacitance of gold electrodes covered by end-terminated alkythiols was studied. The curves obtained depend on the ionic strength and have minima near the  $pK_a$  of the terminal group.



### 303. Thin Film Electrodes for Capacitive Chemo-, Biosensors:

**Optimization of the Electrode Geometry,** V. M. Mirsky, M. Riepl, Ch. Krause, I. Novotny, M. Splonskowski, V. Rehacek, V. Tvarozek, H. Hummel, O. S. Wolfbeis; *Mat. Sci. Forum* **287/288** (1998) 423-426 (TransTech Publ., Winterthur, CH). ISSN 0255-5476. DOI: 10.4028/www.scientific.net/MSF.287-288.423

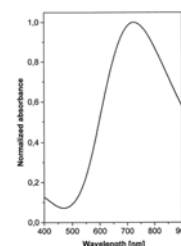
**Abstract:** Different types of electrodes for capacitive chemical sensors and biosensors were investigated. It is found that precise measurements are impossible if the electrodes have a traditional geometry because of a meniscus artifact. The figure shows the different electrode geometries: (1) Thick gold wire coated with a Teflon tube. (2) Thin gold wire. (3) Thin gold wire partially coated with a polymer layer. (4) Thin film gold electrode.



### 302. Optical Chemical Sensing Based on Thin Films of Prussian Blue, R. Koncki, O. S. Wolfbeis; *Sensors Actuat. B51* (1998) 355-358. DOI: 10.1016/S0925-4005(98)00287-1

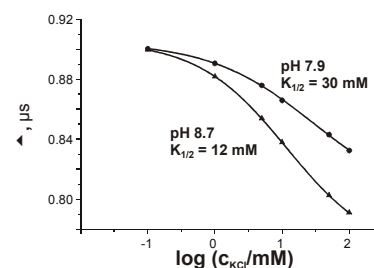
**Abstract:** The potential applications of films of Prussian Blue for optical chemical sensors are investigated. The films are chemically deposited on a non-conductive support, mechanically stable, thin, homogenous and optically transparent. The maximum of the absorption is observed at 720 nm and is fully compatible with semiconductor light sources. Strong reductants cause decoloration of the film. This effect can be used for optical determination of reductants such as ascorbic acid. The film is also suitable for optical determination of pH because the absorption spectra undergo reversible changes in the pH 5-9 range.

The figure on the right shows the absorption spectrum of Prussian Blue that extends far into the near infrared.



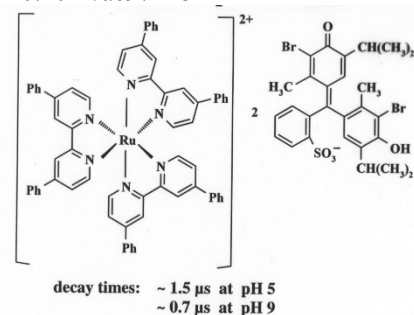
### 301. Luminescence Decay Time Based Determination of Potassium Ion. Ch. Krause, T. Werner, Ch. Huber, I. Klimant, O. S. Wolfbeis; *Anal. Chem.* **70** (1998) 3983-3985. DOI: 10.1021/ac9802224

**Abstract:** A luminescence decay time based potassium ion sensor is presented which applies the ion-exchange principle. The bulk membrane consists of valinomycin, plasticized PVC, and the ruthenium(II)tris-4,4'-diphenyl-2,2'-bipyridyl bromothymol blue ion pair as a proton donor. The efficacy of radiationless fluorescence energy transfer from the donor (the ruthenium complex) to the acceptor (BTB) is mediated by the potassium ion concentration. The concentration of potassium ions can be calculated from either luminescence intensity or decay time. At pH 8.7 the working function ranges from 1 to 100 mM KCl. The graph shows the effect of pH on the response to the concentration of potassium ion.



### 300. Strategies to Design pH Optodes with Luminescence Decay Times in the Microsecond Time Regime, U. Kosch, I. Klimant, T. Werner, O. S. Wolfbeis; *Anal. Chem. (Wash.)* **70** (1998) 3892-3897. DOI: 10.1021/ac971282x

**Abstract:** We present the first optical pH sensor with luminescence decay times longer than 1 μs. It is based on radiationless energy transfer from a luminescent ruthenium(II) complex as the donor to a colored pH indicator as the acceptor. The metal-ligand complex ruthenium(II) tris-4,4'-diphenyl-2,2'-bipyridyl was selected as the donor, and bromothymol blue and a reactive azo dye were selected as pH-sensitive acceptors. Strategies for co-immobilization of transition metal complexes and pH indicators into a hydrogel matrix were evaluated and discussed. pH transition intervals between 7 and 9 allow the measurement in the physiological range and also under marine conditions. Signal changes of up to 50% over 2.5 pH units are observed, depending on the respective acceptor content in the sensing film. Luminescence lifetime measurements of the sensing films were performed in the frequency domain with a blue LED as the light source. The effect of molecular oxygen (acting both as a quenching and a bleaching agent, thereby limiting the accuracy and the long-term stability of such sensors) was found to be crucial for practical applications. Since leaching of the acceptor also limits the stability of the sensing films, several strategies to reduce this effect were evaluated.

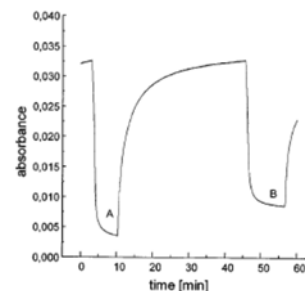


**299. Optical Sensors for Dissolved Sulfur Dioxide, A. Stanglmayer, I.**

**Klimant, O. S. Wolfbeis; *Fresenius J. Anal. Chem.* **362** (1998) 73-76.**

DOI: 10.1007/s002160051037

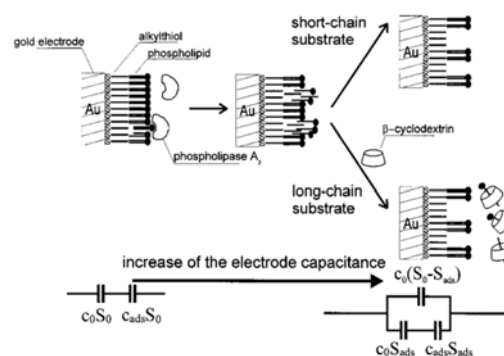
**Abstract:** Plastic thin film colorimetric sensor membranes for sulfur dioxide have been developed and characterized. The membranes can be used for sensing trace amounts of sulfur dioxide both in the gas phase and in aqueous solution. Lipophilic pH indicator ion pairs were immobilized in a gas-permeable, but ion-impermeable silicone membrane. On exposure to SO<sub>2</sub> the films undergo a visually detectable color change from blue to yellow. No cross-sensitivity to pH and CO<sub>2</sub> was observed. The response time depends on the thickness of the sensing membranes and dye loading within the membrane, as well as on the respective SO<sub>2</sub> concentration. Test strips with response times of <1 min were developed. The sensitivity to SO<sub>2</sub> depends on the pK<sub>a</sub> of the indicator. An increase in the pK<sub>a</sub> results in a lower limit of detection. The new optical sensors offer good chemical and mechanical stability, and are cheap and easy to manufacture. The figure shows the reversible response to 250 ppm (A) and 125 ppm (B) of SO<sub>2</sub>.



**298. Capacitive Approach to Determine Phospholipase A2 Activity towards Natural Substrates, V. M. Mirsky, M. Mass,**

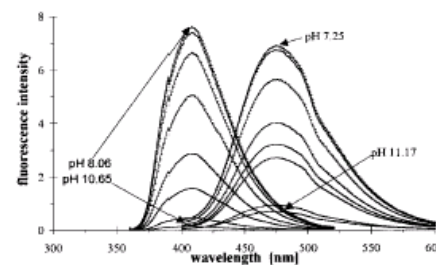
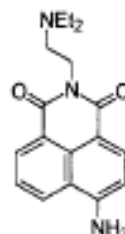
**Ch. Krause, O. S. Wolfbeis; *Anal. Chem. (Wash.)* **70** (1998) 3674-3678.** DOI: 10.1021/ac980102w

**Abstract:** A capacitive approach has been employed to develop a novel method to determine phospholipase activity. The sensing electrodes have a structure of the type Au/(CH<sub>2</sub>)<sub>17</sub>CH<sub>3</sub>/substrate/electrolyte. Hydrolysis of the substrate, mediated by phospholipase A<sub>2</sub>, leads to the formation of water-soluble products from the insoluble substrate. This results in desorption of these products into aqueous phase and corresponding increase of the electrode capacitance. The requirement of high water solubility of the reaction products can be achieved in two ways. In the first, short-chain phospholipids are used as the substrate, in which case, water-soluble products are formed and no additional reagents are required to promote desorption of these products. The sensors prepared by this strategy provide sensitive qualitative detection of phospholipases. The second way is based on the use of a water-soluble acceptor (for example cyclodextrin) to solubilize the products of hydrolysis. It allows semiquantitative detection of phospholipase activity toward long-chain natural substrates. The reaction kinetics for this case was found to be monoexponential and linearly dependent on the phospholipase concentration. The detection limit of this method, as tested with phospholipase A<sub>2</sub> from bee venom and soy bean lecithin as the substrate, is 0.5 ng/mL (500 i-units/mL).



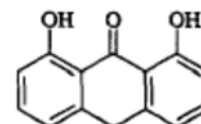
**297. Arenedicarboximide Building Blocks for Fluorescent Photoinduced Electron Transfer pH Sensors Applicable with Different Media and Communication Wavelengths, L. M. Daffy, A. Prasanna de Silva, H.Q. N. Gunaratne, Ch. Huber, P.L. M. Lynch, T. Werner, O. S. Wolfbeis; *Chem. Eur. J.* **4** (1998) 1810-1815.** DOI: 10.1002/(SICI)1521-3765(19980904)4:9<1810::AID-CHEM1810>3.0.CO;2-Y

**Abstract:** N-(aminoalkyl)-4-aminonaphthalene-1,8-dicarboximides (see formula), N-(aminoalkyl)-4-acetamido naphthalene-1,8-dicarboximides and N,N'-bis(aminoalkyl)-perylene-3,4,9,10-tetracarboxy-diimides show good fluorescent 'off-on' switching in aqueous alcohol solution with protons according to the fluorescent PET sensor design. The excitation maxima are compatible with the blue LED. The probe undergoes substantial fluorescence enhancement with protons when immobilized in a poly(vinyl chloride) (PVC) containing a plasticizer and a borate additive. The fluorophore can be used to sense protons, but also to sense cations such as sodium and potassium if combined with the respective crown ether receptors. All fluorophores may be covalently immobilized on cellulose. The second graph shows the pH dependence of the fluorescence of the N-acetylated probe.



**296. UV/Vis and Fluorescence Study on Anthralin and its Alkylated Derivatives, A. Sellner, E. Terpetschnig, W. Wiegrober, O. S. Wolfbeis; *J. Photochem. Photobiol. A: Chemistry*, **116** (1998) 39-45.** DOI: 10.1016/S1010-6030(98)00277-9

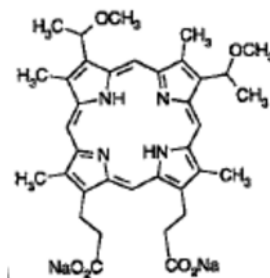
**Abstract:** Anthralin and some of its C- or O-alkylated derivatives were investigated by UV/VIS- and fluorescence spectroscopy in different solvents and buffer systems, respectively. The effects of substituents on the formation of anthralin anion as well as the constitution of the resulting anions confirm that C-H acidity at position 10 is necessary for the formation of a fully aromatic anionic form. It is concluded that the resulting anion is the pharmacologically active species of the antipsoriatic anthralin. Tautomerism of the neutral molecule is not observed.



**295. Photosensitization of Skin-Derived Cell Lines by Dimegin in Vitro, S. Fickweiler, R. M. Szeimies, C. Abels, G. V. Ponomarev, F. Hofstaedter, O. S. Wolfbeis, M. Landthaler; *Photodermatol. Photoimmunol. Photomed.* **14** (1998) 125-131.** DOI: 10.1111/j.1600-0781.1998.tb00026.x

**Abstract:** The deuteroporphyin-IX derivative Dimegin [2,4-di-( $\alpha$ -methoxyethyl)-deuteroporphyin IX] was investigated with respect to cellular uptake, intracellular localization and cell survival following photodynamic treatment in human cell lines derived from the skin (SCL1 and SCL2, squamous cell carcinoma; HaCaT keratinocytes; N1 fibroblasts). Using flow cytometry, we determined the cellular fluorescence as a marker of the uptake of Dimegin after incubation for 24 h. The intracellular localization of Dimegin was analysed using fluorescence microscopy and co-staining with fluorescent dyes specific for cell organelles. Following irradiation with an incoherent light source (580–740 nm) using a light dose of 24 J/cm<sup>2</sup>, phototoxicity was determined by means of trypan blue dye exclusion, MTT assays and growth curves. The relative Dimegin fluorescence of the different cell lines declined as follows: SCL1>HaCaT>N1>SCL2. Intracellular localization of Dimegin was found

in the mitochondria. For all cell lines Dimegin concentrations above 15 mM yielded a significant phototoxic effect. The EC50 for SCL1 cells was  $8.9 \pm 2.0 \mu\text{M}$  Dimegin. The EC50 for the cell lines increased as follows: SCL1 < HaCaT < N1 < SCL2, thus correlating with the cellular fluorescence of Dimegin. The results of the MTT assay were confirmed by trypan blue dye exclusion assay and growth curves. In conclusion, the study shows that Dimegin is an effective photosensitizer with a rapid mechanism of action in vitro, resulting in an immediate loss of plasma membrane integrity following irradiation.



Chemical structure of Dimegin

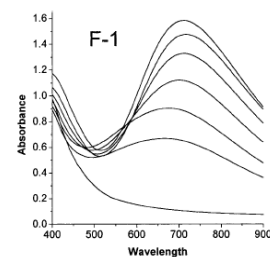
294. Journal Volume Edited: **Biomedical Sensors, Fibers, and Optical Delivery Systems**, F. Baldini, N. I. Croitoru, M. Frenz, I. Lundstroem, M. Miyagi, R. Pratesi, O. S. Wolfbeis (eds.), *Proc. SPIE (Soc. Photo-Instrum. Eng.)*, vol. **3570** (BIOS EUROPE '98; 8-12 September 1998, Stockholm, Sweden). Web: <https://www.spiedigitallibrary.org/conference-proceedings-of-SPIE/3570.toc>

293. Book Chapter: **Luminescent Probes for NIR Sensing Applications**, E. Terpetschnig, O. S. Wolfbeis; in: S. Daehne, U. Resch-Genger, O. S. Wolfbeis (eds.), *Near-Infrared Dyes for High Technology Applications*, NATO ASI Ser. 3 (High Technology), vol. **52**, Kluwer Acad. Publ., Dordrecht (NL), 1998; pp. 161-182. DOI: 10.1007/978-94-011-5102-3\_8

We give reasons for the current research activity in the area of red and near-infrared emitting fluorophores, discuss the main dye classes along with their advantages and disadvantages, and give examples for typical applications in the areas of chemical and biochemical sensing. Sections include 1. Introduction; 2. Representative Classes of Red and NIR Luminescent Dyes (longwave rhodamines, phenoxazines, porphyrins and phthalocyanines, Cyanine Dyes); 3. NIR-Probes for Use in Chemical Sensing; 4. Probes and Labels for Protein Analysis (Labels for Protein Derivatization, Protein-Binding Probes); 5. Labels for Immunoassay (Phycobiliproteins, Cyanines, metal-ligand complexes; multi-color labeling); 6. Probes and Labels for DNA Analysis (Intercalating Probes, Labels, Specific Hybridization Assays).

292. **Composite Films of Prussian Blue and N-Substituted Polypyrroles: Fabrication and Application to Optical Determination of pH**, R. Koncki, O. S. Wolfbeis; *Anal. Chem.* **70** (1998) 2544-2550. DOI: 10.1016/S0956-5663(98)00095-5

**Abstract:** A new and simple chemical method for deposition of thin blue films composed of Prussian Blue and N-substituted polypyrroles on non-conductive supports is presented. It is found that only pyrroles which are difficult to polymerize can be used for the preparation of such films. The resulting films were examined by SEM - EDAX, VIS-NIR and IR spectroscopy. The films are stable, thin, and optically transparent. The absorption maxima are at 720 nm and spectral changes can be monitored using LED light sources. The composite films are suitable for optical determination of pH over the pH 5 - 9 range because their abs. depends on pH in the physiological pH range. The films represent an alternative to indicator-based pH sensor materials because they do not require a dye to be immobilized. The pH measurements are highly reproducible, reversible in the physiol. range, and not interfered by ionic strength, alkaline cations, and typical oxidants and reductants. The figure shows the change in the absorption spectra of material F-10n going from pH 3 (top) to pH 10 (bottom).

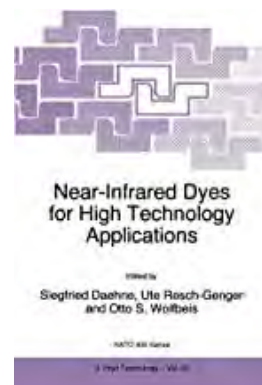


pH-dependence of the absorption spectra of the new materials

291. Book edited: **Near-Infrared Dyes for High Technology Applications**, S. Daehne, U. Resch-Genger, O. S. Wolfbeis (eds.), NATO ASI Ser. 3 (High Technology), vol. **53**, Kluwer Acad. Publ., Dordrecht (NL), 1998; 458 pages. ISBN 0792351010.

Contents:

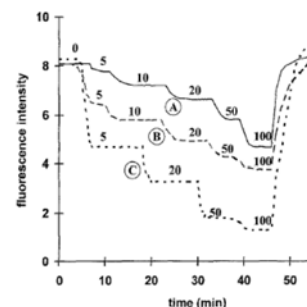
- (1) Advances in Methodology: Recent Developments in Fluorescence Spectroscopy: Three-Photon Excitation, Two-Color Two-Photon Excitation, Light Quenching and Development of Long-Lifetime Probes for Biophysics and Clinical Chemistry (by J.R. Lakowicz et al.)
- (2) Near-Infrared Fluorescence Instrumentation for DNA Analysis L. Middendorf, et al.
- (3) Highlights in Biochemistry and Biophysics. Ultrasensitive Detection and Identification of Biomolecules with Diode Lasers - from DYES to DNA; (by M. Sauer, et al.)
- (4) Incorporation of Dyes in Resting and Stimulated Leukocytes (D. Frackowiak, et al. Application of Red Fluorescent Probes for the Measurement of Individual Cell Cytoplasmic pH Values, (by J. Slavik)
- (5) Molecular Probes Based on Cyanine Dyes for Nucleic Acid Research (by T.G. Deligeorgiev).
- (6) New NIR Dyes: Synthesis, Spectral Properties and Applications in DNA Analyses (by N. Narayanan, et al.)
- (7) Frontiers in Analytical Chemistry and Sensor Technology. Luminescent Probes for NIR Sensing Applications (by E. Terpetschnig, O.S. Wolfbeis).
- (8) NIR Fluorophores in Practical Analytical Chemistry (by A.R. Swamy, et al.)
- (9) Long Wavelength Emitting Fluorescence Probes for Metal Ions (by K. Rurack, et al.)
- (10) Advances in High Technology Applications. NIR Dyes for Information Recording, from Origin to Update (by M. Matsuoka).
- (11) Tuning of Color by Different Alignment of Dye Molecules (by L. Daehne, E. Biller).
- (12) Spectral Sensitization of Silver Halides in NIR Region (by B.I. Shapiro).
- (13) Optical Properties and Applications of Near Infrared Dyes in Polymeric Media (by O.V. Przhonska).
- (14) Insolubilisation and Fluorescence Induced by Laser Diode Irradiation of IR-Dyes Embedded in Polymer Films. Thermally Induced Latex Coalescence and Acid Generation (by C.D. Catry, et al.)
- (15) NIRPhotosensitizers in Photodynamic Therapy (by E.A. Lukyanets).
- (16) New Chromophores. Molecular Engineering of NIR Dyes (by S. Daehne, M.L. Dekhtyar).
- (17) New NIR Dyes Based on the Cyclopentadienylm Chromophore and Related Compounds (by R. Gompper, et al.)
- (18) New Cyanine Dyes Absorbing in the NIR Region (by A.I. Tolmachev, et al.)
- (19) Near-Infrared Cyanine Dyes: A New Approach to an Old Problem (by Yu.L. Bricks, N.N. Romanov).
- (20) Adventures in Search of New Dyes Absorbing in the Red or Near Infrared Region (by H. Hartmann).





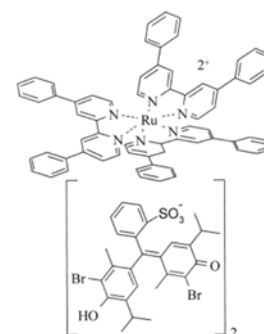
**290. Fiber Optic Fluorescence Carbon Dioxide Sensor for Environmental Monitoring.** O. S. Wolfbeis, B. Kovacs, K. Goswami, S. M. Klainer, *Microchim. Acta* **129** (1998) 181-188. DOI: 10.1007/BF01244739

**Abstract:** Fiber-optic sensors were developed for monitoring dissolved carbon dioxide in water samples in the 0 to 900 ppm concentration range. A pH-sensitive fluorescent dye (HPTS) was reacted with a cationic quaternary ammonium salt to form an ion pair which was electrostatically bound to the surface of particles of aminocellulose which then were dispersed into a into a gas-permeable silicone polymer. The green fluorescence of the base form was monitored using a fiber optic fluorometer. The use of the aminocellulose enhanced the stability and lifetime of the sensor and also increased the fluorescence of the sensor membrane because the particles act as scattering centers. The characteristics of the sensors are described with respect to dynamic range, reproducibility, long-term stability and temperature dependence.



**289. Energy Transfer-Based Lifetime Sensing of Chloride Using a Luminescent Transition Metal Complex.** Ch. Huber, T. Werner, Ch. Krause, I. Klimant, O. S. Wolfbeis; *Anal. Chim. Acta* **364** (1998) 143-151. DOI: 10.1016/S0003-2670(98)00151-2

**Abstract:** A bulk membrane responsive to chloride has been developed containing a luminescent ruthenium complex placed in close proximity to the pH-sensitive absorber bromothymol blue (BTB), both contained in a plasticized poly(vinyl chloride) (PVC) membrane along with an anion-selective carrier. The response is based on the co-extraction of chloride along with protons from the aqueous sample into the PVC membrane and results in a large change in the absorbance of BTB. The absorption band of deprotonated BTB overlaps significantly with the emission band of the ruthenium complex so that radiationless energy transfer can take place and decay times are rather short (ca. 0.60 ms). If, however, chloride is co-extracted into the bulk along with a proton, the dye is converted into the yellow phenolic form. Hence, no energy transfer occurs and decay times are in the order of 1 ms. The signal changes can also be detected by measuring fluorescence intensity. The dynamic range can be adjusted via the sample pH and is from 30 to 180 mM chloride at pH 7.0 and thus covers the physiological range.



Chemical structure of the ion pair employed as an optical probe

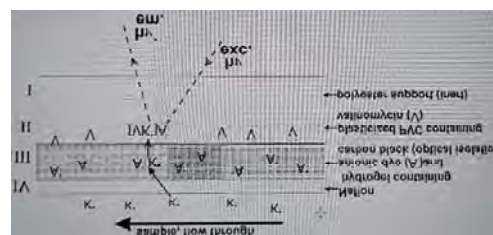
**288. pH Optical Sensors Based on Sol-Gels: Chemical Doping versus Covalent Immobilization.** A. Lobnik, I. Oehme, O. S. Wolfbeis; *Anal. Chim. Acta* **367** (1998) 159-165. DOI: 10.1016/S0003-2670(97)00708-3

**Abstract:** pH sensitive fluorescent sol-gels were obtained by both covalent immobilization of amino fluorescein (AF) via isocyanate or epoxy groups, and by co-condensation of tetramethoxysilane (TMOS) and phenyltrimethoxysilane (Ph-TriMOS) in the presence of AF. The gel precursors were deposited on glass supports, cured, and characterized in terms of response to pH, pK<sub>a</sub> values, effects of ionic strength, response time, leaching, long-term stability, and photostability. The addition of Ph-TriMOS is found to exhibit a pronounced effect on the performance of the materials. Sensor layers based on TMOS doped with AF were found to be most appropriate for purposes of sensing pH in giving large relative signal changes and displaying rapid response times over the pH range 4 – 9. Typical reagents include the following:



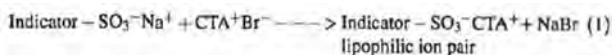
**286. Multilayer Potassium Sensor Based on Solid-State Co-Extraction.** Ch. Krause, T. Werner, O. S. Wolfbeis; *Anal. Sci.* **14** (1998) 163-167. DOI: 10.2116/analsci.14.163

**Abstract:** A highly selective solid state multilayer sensor (see the picture) is presented which enables fluorescence optical determination of potassium ions. It is based on co-extraction using valinomyacin along with a fluorescent anion, both contained in different layers. The sensor membrane is composed of two layers of highly different lipophilicity. The lipophilic phase contains the carrier valinomyacin whilst the hydrophilic phase contains the anionic fluorophore sulforhodamine B. On exposure to potassium ions, the lipophilic phase becomes fluorescent after coextraction of both potassium ions and the anionic fluorophore. To prevent leaching of the dye, an additional blocking layer (nafion) was spread on the sensor. The dynamic range is from 0.1 to 50 mM K<sup>+</sup> with very low cross-sensitivity to pH and ionic strength. The response times vary from 1 to 2 h.

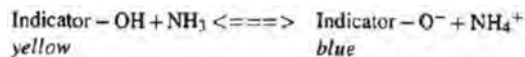


**285. Optochemical Sensor for Ammonia Based on a Lipophilic pH Indicator in a Hydrophobic Matrix.** M. Trinkel, W. Trettnak, F. Reininger, R. Benes, P. O'Leary, O. S. Wolfbeis; *Intl. J. Environ. Anal. Chem.* **67** (1997) 237-251. DOI: 10.1080/03067319708031407

**Abstract:** An optical sensor for the determination of ammonia in water based on ion pairing has been investigated. A pH-sensitive dye is immobilized as an ion pair in a silicone matrix. The colour of the dye changes from yellow to blue depending on the concentration of ammonia in the sample solution. This change is reversible. The concentration of ammonia can be determined by measuring the transmittance at a given wavelength. All measurements were performed with a dual-beam optical meter. The measurement range was from  $5.9 \times 10^{-5}$  to  $1 \times 10^{-4}$  M (0.01 to 17 mg/l) in 0.1 M phosphate buffer of pH 8. The detection limit was 10 µg/l. The response times at a flow rate of 2.5 ml/min were 4 min for t<sub>90</sub> and 10 min for t<sub>100</sub> at a change from 41.9 to 82.5 µM ammonia and 12 min for t<sub>90</sub> and 48 min for t<sub>100</sub> at a change from 160 to 0 µM ammonia. The operational lifetime of the ammonia sensor was limited to a period of a few days only. A continuous decrease in baseline signal and relative signal change was observed over the whole measurement. The storage stability was more than 10 months (dry). With respect to possible application of the ammonia sensor to environmental analysis, the influence of pH, typical interferences, such as amines and various detergents on the sensor response was investigated. No interference due to pH was observed in the range from pH 5 to pH 9. With methyl- and ethylamine the response was not completely reversible. The sensor was affected by cationic detergents, but not by anionic or neutral detergents.



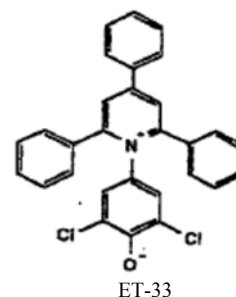
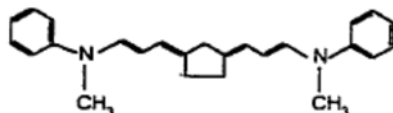
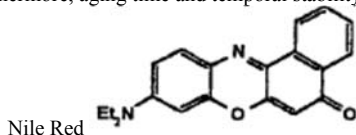
Preparation of the silicone-soluble indicator/CTA ion pair



Color change cause by ammonia

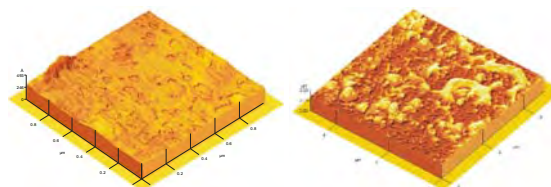
**284. Characterization of Sol-Gel and Ormosils via Polarity-Sensitive Probes, A. Lobnik, O. S. Wolfbeis; *Proc. SPIE, vol. 3136 (Sol-Gel Optics, IV) (1997) 284-293*. DOI: 10.1117/12.284126**

**Abstract:** Conventional sol-gels are rather hydrophilic. A more hydrophobic material is obtained by preparing organically modified siloxanes (ormosils). We have used three different solvatochromic dyes, (1) ET-33, the best solvatochromic probe known so far, (2) Nile red (NR), and (3) a ketocyanine (KC) dye, all with unique solvatochromic properties in both absorption and fluorescence, to probe the micro-polarity of sol-gels. Because ET-33 has a very low molar absorbance and is not fluorescent at all, and KC was hardly soluble in the sol-gel solution, NR was preferably used. NR is an excellent probe and sensitive to the polarity of its microenvironment. Spectroscopic studies reveal remarkable changes in the absorption band positions as a function of the polarity of the sol-gel which depends on the different precursors used. Furthermore, aging time and temporal stability as a function of different ormosils have been investigated.



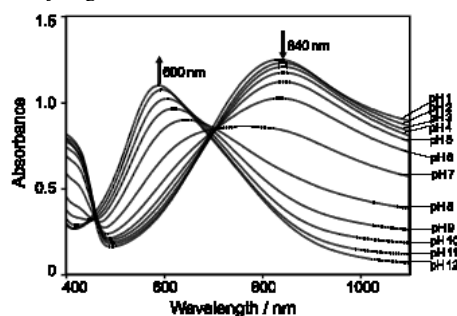
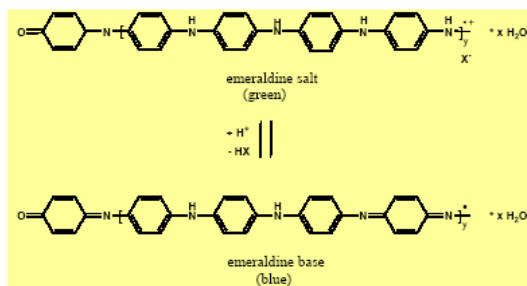
**283. Capacitive Monitoring of Protein Immobilization and Antigen-Antibody Reactions on Mono-molecular Alkylthiol Films on Gold Electrodes, V. M. Mirsky, M. Riepl & O. S. Wolfbeis; *Biosensors & Bioelectron. 12 (1997) 977-989*. DOI: 10.1016/S0956-5663(97)00053-5**

**Abstract:** Self-assembled monolayers of omega-mercaptohexadecanoic acid on gold electrodes are stable at neutral pH and display purely capacitive behavior at frequencies of around 20 Hz. Covalent immobilization of anti-HSA on the activated surface was monitored by capacitive analysis. Subsequent binding of the antigen (HSA) led to a decrease of the capacitance, thus providing a means for sensitive quantitation of HSA. The limit of detection was as low as 15 nM (1mg/L). The figure shows AFM images of a HS-C16-carboxy acid covered gold electrode (1.0 μm x 1.0 μm) before (left) and after immobilization of HSA (right; size 5.0 μm x 5.0 μm).



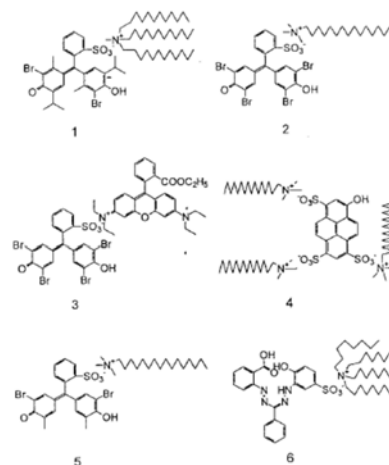
**282. Optical Sensing of pH Using Thin Films of Substituted Polyanilines. E. Pringsheim, E. Terpetschnig, O. S. Wolfbeis; *Anal. Chim. Acta 357 (1997) 247-252*. DOI: 10.1016/S0003-2670(97)00563-1**

**Abstract:** Polyanilines (PANI) are viable materials for use in optical sensing of pH. Thin films of substituted PANI readily deposit on the inner walls of polystyrene cuvettes when substituted anilines are chemically polymerized in hydrochloric acid solution. The films have been characterized by absorption spectra which have maxima between 600 and 810 nm, except for halogenated or p-substituted anilines. They undergo pH-dependent changes in their absorption spectra in the physiological pH range, and substituents exhibit a strong effect on pKa values. PANI films are advantageous over indicator-based pH sensor films in that they are not based on the use of indicator dyes, are compatible with LED and diode laser light sources, and can be easily prepared. Copolymers of aniline and anthranilic acid are shown to be useful supports for immobilization of the enzyme urease, and the resulting films can be used to detect urea. Films of substituted PANIs are redox-active and also respond to reductants such as ascorbic acid and hydrogen sulfide.



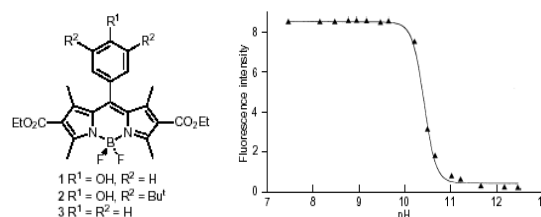
**281. Novel Optical Sensor Materials Based on Solubilization of Polar Dyes in Apolar Polymers**, G. J. Mohr, T. Werner, I. Oehme, C. Preininger, I. Klimant, B. Kovacs, O. S. Wolfbeis; *Adv. Mater.* **9** (1997) 1108-1113. DOI: 10.1002/adma.19970091410

**Abstract:** Materials for use in optical sensors for various analytes are presented which are prepared by ion pairing of anionic indicator dyes and incorporating the resulting materials into appropriate polymers. Procedures are described for immobilization of indicator dyes carrying a sulpho group which are water soluble and, hence, are insoluble in the polymers frequently used in optical sensors. In order to make the dyes polymer-soluble, the alkali counterion is replaced by positively-charged hydrophobic long-chain aliphatic ammonium ions or even positively-charged dyes, thereby forming highly lipophilic ion pairs. These are soluble in polymers such as silicone, poly(vinyl) or hydrogel. The resulting sensor membranes show high optical density and, hence, give strong optical signals. This technique obviously overcomes the problem of poor dye loading and indicator leaching. The immobilization technique is generic in that it can be applied to almost all indicators possessing a sulpho group or a related anionic function. It allows many classical colorimetric and fluorescent indicators to be made lipophilic, so to develop sensor materials for numerous applications, and represents a general logic to make ionic species soluble in organic polymers.



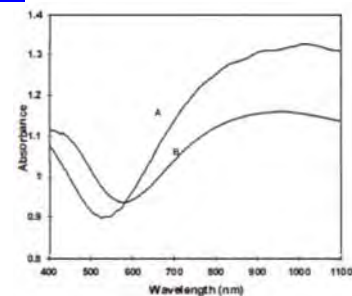
**280. Phenol/phenolate-Dependent on/off Switching of the Luminescence of 4,4-Difluoro-4-bora-diaza-indacenes**, T. Gareis, C. Huber, O.S. Wolfbeis and J. Daub, *Chem. Comm.* **1997**, 1717-1718. DOI: 10.1039/a703536e

**Abstract:** We describe the protonation-dependent switching of the fluorescence of phenol type derivatives of the bodipy's (a widely used group of fluorescent labels). The lack of emission of the phenolate forms in alkaline solutions is attributed to photo-induced electron transfer (PET) between the phenolate and the bodipy chromophores, resulting in quenching of fluorescence.



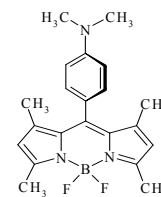
**279. Characterization of Polypyrrole Films for Use in Optical Sensing**, S. de Marcos, O. S. Wolfbeis; *Sensors & Materials* **9** (1997) 253-265. No DOI known. Web: [https://www.myukk.org/SM2017/sm\\_pdf/SM290.pdf](https://www.myukk.org/SM2017/sm_pdf/SM290.pdf)

**Abstract:** A study has been performed on the properties of polypyrrole (PPy) as a new material for use in optical sensing. PPy was synthesized by chemical oxidation of pyrrole (Py) using various oxidizing agents including aqueous ferric chloride, and very homogeneous thin films were obtained on plastic supports such as polyester membranes and polystyrene slides after a reaction time of 25- 30 min. Elemental analyses of PPy films are inconsistent with the chemical structure of a pure polypyrrole in that, in addition to the expected presence of C, H, N and Cl (for the chloride-doped forms), we find oxygen in typical fractions of 9.5%. We suggest a chemical structure of a hydroxylated PPy, which is consistent with these findings. PPy films were also analyzed by FTIR and SEM methods. The absorption spectra of PPy are characterized by a long-wavelength absorption band that extends far into the near infrared (NIR). The NIR spectra of PPy change with pH and on exposure to ammonia vapors, a fact that can be exploited for sensing purposes. The figure shows the absorption spectra of polypyrrol films obtained by oxidative polymerization employing (A) ferric chloride solution, and (B) peroxodisulfate solution.



**278. Novel Optical pH Sensor Based on a Boradiaza-indacene Derivative**, T. Werner, Ch. Huber, S. Heintl, M. Kollmannsberger, J. Daub, O. S. Wolfbeis; *Fresenius J. Anal. Chem.* **359** (1997) 150-154. DOI: 10.1007/s002160050552

**Abstract:** A pH optical sensor is described that is based on a Bodipy dye (see the figure) which undergoes pH-dependent quenching of its luminescence through photo-induced electron transfer (PET) from a dimethylamino group to the Bodipy fluorophore. The effect can be used to measure pH in the 1 - 3 range using hydrogel membranes with incorporated dye.



**277. Solid State Supramolecular Optical Sensors**, O. S. Wolfbeis, Ch. Huber, T. Werner, *Proc. NATO Adv. Res. Workshop on Chemosensors of Ion and Molecule Recognition*, NATO ASI Series; vol. 492; A. T. Czarnik, J. P. Desvergne (eds.), Kluwer Acad. Publ., Dordrecht-Boston-London, 1997; p. 61-75. DOI: 10.1007/978-94-011-3973-1\_5

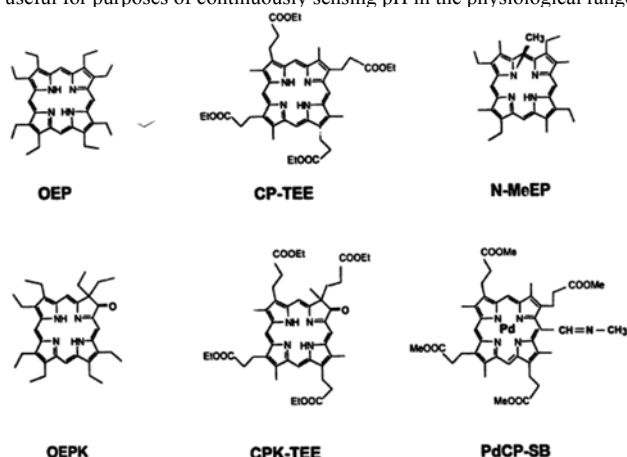
**Abstract:** We describe examples for an optical gas sensor (oxygen) and an optical ion sensor (pH), and discuss how the existing need for complete mass transfer in solid-state optical sensors determines the choice of the appropriate polymer. Examples are given for biomedical instrumentation based on mass-fabricated optical sensors for oxygen, carbon dioxide and pH. We also show that specific recognition of ions, particularly of the clinically important alkali ions, is much more difficult in solid-state sensors. We discuss existing schemes for ions and demonstrate that none of them satisfies the need for rapid, pH-independent determination of ions in whole blood at room temperature and without addition of any reagent. The photo-induced electron transfer (PET) effect represents an attractive alternative to the use of fluoro-ionophores, but it is shown that PET — while being extremely useful when studied in solution — not necessarily does not occur in solid-state sensor matrices to the extent it does in fluid solution, a fact that is explained mainly in terms of rotational restriction.

**276. Protonation of Porphyrins in Liquid PVC Membranes: Effects of Anionic Additives and Application to pH-Sensing**, D. B. Papkovsky, G. V. Ponomarev, O. S. Wolfbeis; *J. Photochem. Photobiol., Part A: Chemistry* **104** (1997) 151-158. DOI: 10.1016/S1010-6030(97)04592-9

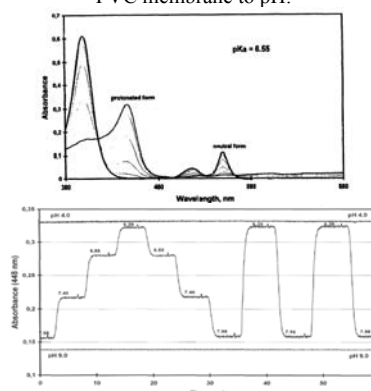
**Abstract:** We report on a study on the protonation of representative porphyrins, metalloporphyrins, porphyrin-ketones and a Pd-porphyrin Schiff base in aqueous solution and when dissolved in plasticized PVC membranes. The respective protolytic forms were characterized by absorption and emission spectra as well as apparent pK<sub>a</sub> values. It is shown that the protonation of porphyrins dissolved in PVC membranes is much more difficult than in solution, resulting in an



extraordinarily large decrease in the apparent  $pK_a$  values which can be as large as 5  $pK$  units when compared to the corresponding data for the porphyrins in solution. In certain cases, no protonation at all occurred within the pH 2-12 range. At the same time, N-MeEP which is much more basic (its intrinsic  $pK$  being 11.2) can be protonated in such membranes into the monocation at weakly acidic pH, but the apparent  $pK_a$  also is lowered by about 6 units. On addition of a tetraphenylborate anion to the PVC membranes, protonation was found to proceed much easier. Both the monocation and dication was identified in case for the porphyrins, while for the porphyrin-ketones direct protonation into dication took place, and N-methyl-etioporphyrin was present as the monocation over the whole pH 2-12 range. Membranes composed of solutions of porphyrin-ketones or the Pd-porphyrin Schiff base in plasticized PVC were identified as being useful for purposes of continuously sensing pH in the physiological range.



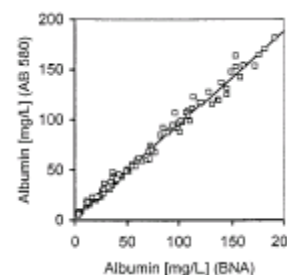
The figures below show typical spectra and the response of a dye-doped plasticized PVC membrane to pH.



**275. Microalbuminuria and Borderline-Increase Albumin Excretion Determined with a Centrifugal Analyzer and by the Albumin 580 Fluorescence Assay, M. K. Kessler, A. Meinitzer, W. Petek, O.S. Wolfbeis; *Clin. Chem.* 43, 996-1002 (1997).**

DOI: 10.1093/clinchem/43.6.996

**Abstract:** We report on a new automated fluorescence assay for determination of albumin in urine. The dye AlbuminBlue 580 specifically binds to albumin to exhibit strong red fluorescence. The albumin concentration is calculated from emission intensity at 616 nm (excitation at 590 nm) and a calibration curve. Two Cobas Fara programs cover working ranges of 2–200 and 1–50 mg/L with detection limits of 1.4 and 0.4 mg/L, respectively. A test of 100 urine samples submitted to routine analysis gave results that agreed well with those by a nephelometric assay. No interference was detected from other urine components, including several proteins and 46 drugs. The high specificity and sensitivity make the method ideal for determination of microalbuminuria. In addition, the method is fast, inexpensive, and well-suited for clinical laboratory application and thus may be used instead of immuno assays. The figure shows a the correlation between the AB 580 fluorescence assay (y axis) and the Behring immunonephelometric assay (BNA; x axis) for urinary albumin.

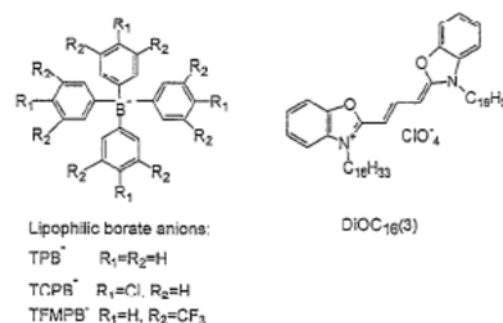


**274. Review: Optical Sensors for Determination of Heavy Metal Ions, I. Oehme, O. S. Wolfbeis; *Microchim. Acta* 126 (1997) 177-192. DOI: 10.1007/BF01242319**

**Abstract:** A review is given on optical means for single shot testing (probing) as well as continuous monitoring (sensing) of heavy metal ions (HMs). Following an introduction into indicator based approaches, we discuss the types of indicator dyes and polymeric supports used, as well as existing sensing schemes for HMs. The wealth of information is compiled in the form of tables and critically reviewed. Notwithstanding the tremendous work performed so far, it is obvious that still severe limitations do exist in terms of selectivity, limits of detection, dynamic ranges, applicability to specific problems, and reversibility. On the other side, such sensors have found - and will find - their application whenever rapid and cost-effective testing is required, where personnel is scarce or unskilled, and in field tests. Despite their limitations, the number of such sensors (and of irreversible probes) for HMs is likely to increase in future.

**273. Fluorescence-Based Sensor Membrane for Mercury(II) Detection, I. Murkovic, O. S. Wolfbeis; *Sensors Actuators* 39B (1997) 246-251. DOI: 10.1016/S0925-4005(97)80212-2**

**Abstract:** A novel optical sensor membrane for the detection of mercury(II) (Hg(II)) is presented. The sensing layer is composed of plasticized poly(vinyl chloride) (PVC) containing a lipophilic borate salt as a reagent for Hg(II), and the amphiphilic oxacarboxyanine dye DiOC<sub>16</sub>(3) as the optical transducer. The sensing scheme is based on the decomposition of the borate anion in the presence of Hg(II). Since this decomposition cannot be monitored optically, the borate anion is coupled to a fluorescent oxacarboxyanine cation to form a lipophilic ion pair. The decomposition of the borate anion leads to the formation of non-fluorescent dye aggregates which can be followed fluorometrically. The extraction of Hg(II) from the water phase into the membrane leads to a continuous and irreversible decrease in fluorescence intensity, so that a kinetic approach is used for calibration. An exposure time of 30 min allows for the determination of Hg(II) at 100 nM concentration levels. The membranes respond to Hg(II) with very high selectivity over other metal ions, and the pH effects are found to be negligible. The membrane can be regenerated by exposing it to a solution containing the same borate. Effects of substituted tetraphenylborates on the response of the membranes are reported.



**272. Application of Potential-Sensitive Fluorescent Dyes in Anion-Sensitive and Cation-Sensitive Polymer Membranes, G. J. Mohr, I. Murkovic, F. Lehmann, Ch. Haider, O. S. Wolfbeis; *Sensors Actuat.* 39B (1997) 239-245.**

DOI: 10.1016/S0925-4005(97)80211-0

**Abstract:** The applicability of two potential-sensitive dyes (PSDs) for optical sensing of ions is reported. In particular, nitrate- and nitrite-responsive as well as potassium- and mercury-sensitive polymer membranes have been developed. In general, membranes are composed of a plasticized polymer, an ion carrier and a fluorescent dye which optically transduces the extraction of the analyte ion in the polymer matrix. The nitrate sensor membrane is composed of rhodamine B octadecylester and the anion-exchange catalyst is tridodecyl-methylammonium chloride. Both are dissolved in plasticized PVC. The nitrite sensor is based on the same dye and the same polymer matrix but with benzylbis(triphenylphosphine) palladium(II) chloride acting as the nitrite-selective carrier. The potassium sensor membrane consists of the carbocyanine dye DiOC16(3), valinomycin and a lipophilic borate salt. The mercury 'sensor' is based on the irreversible decomposition of borate by mercury ions and is composed of DiOC16(3) and borate only. All sensor membranes have been investigated in terms of signal change, sensitivity, stability, limits of detection and the selectivity for the analyte over interferent ions. The mechanism of the sensor membranes is discussed on the basis of changes of the microenvironment of solvatochromic dyes, which result in analyte-dependent signal changes.

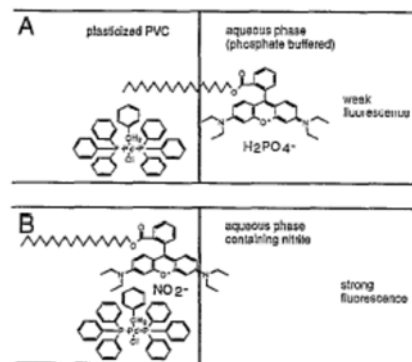
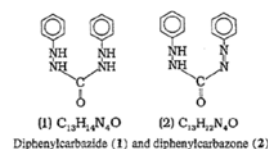


Fig. 2. Schematic representation of the microenvironment of a PSD in a nitrite sensor before (A) and after (B) extraction of nitrite from the aqueous into the lipophilic membrane phase.

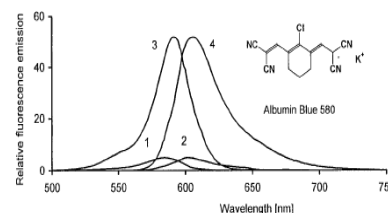
**271. Sol-Gel-Derived Optical Coatings for Determination of Chromate, M. Zevin, R. Reisfeld, I. Oehme, O. S. Wolfbeis; *Sensors Actuators B39* (1997) 235-238. DOI: 10.1016/S0925-4005(97)80210-9**

**Abstract:** An optical probe for chromate ion has been obtained by the sol-gel technique by depositing a porous film containing the reagent diphenylcarbazide on a glass support. Changes in the absorption of light as a result of the irreversible formation of a purple product between chromate and the reagent inside the sol-gel are monitored. The detection limit for chromate anion is as low as 1 ppb, but only after rather long exposure to samples. The morphology of the surface of the film has been studied using atomic force microscopy and is related to the technique of preparing the film.



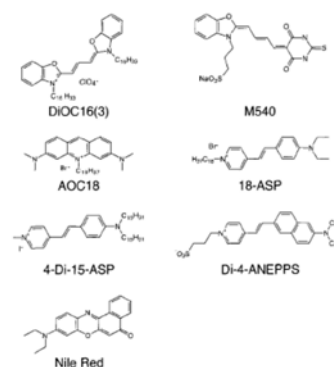
**270. Albumin Blue 580 Fluorescence Assay for Albumin, M. A. Kessler, A. Meinitzer & O.S. Wolfbeis; *Anal. Biochem.* 248, 180-182 (1997). DOI: 10.1006/abio.1997.2113**

**Abstract:** A new fluorogenic probe for albumin named AB 580 has become available. Its application to the determination of albumin in human serum and urine using an automated analyzer is reported. We also give an assay protocol for a more general application using a conventional spectrofluorometer. The figure shows the fluorescence excitation (curves 1, 3) and emission spectra (curves 2 and 4) of AB 580 in pH 7.4 buffer before (1, 2) and after addition (3, 4) of human serum albumin (final conc. 11 mg/L).



**269. Investigation of Potential-Sensitive Fluorescent Dyes for Application in Nitrate Sensitive Polymer Membranes, G. J. Mohr, F. Lehmann, R. Oestereich, I. Murkovic, O. S. Wolfbeis; *Fresenius J. Anal. Chem.* 357 (1997) 284-291. DOI: 10.1007/s002160050154**

**Abstract:** The applicability of various potential-sensitive dyes (PSDs; see the figure) for optical sensing of anions is reported. Specifically, nitrate-responsive polymer membranes have been developed which are composed of a plasticized polymer, an anion exchange catalyst, and a fluorescent dye. On exposure to nitrate, the fluorescence intensity of such membranes increases, while the wavelengths of the excitation and emission maxima remain virtually unchanged. The membranes typically are 2-4.µm thick and exhibit highest sensitivity to nitrate in the 2 to 200 mg l<sup>-1</sup> range. Signal changes on exposure to 100 mM nitrate can be as high as +300%. The detection limit is 0.2 mg L<sup>-1</sup>. The cationic PSD octadecyl acridine organe was tested in combination with a tin-organic and an indium-organic anion carrier rather than with tridodecylmethylammonium chloride, but both carriers were found to display no improved selectivity.



**268. Book Chapter: Chemical Sensing Using Indicator Dyes, O. S. Wolfbeis; in: *Optical Fiber Sensors, Volume 4: Applications, Analysis, and Future Trends*, J. Dakin, B. Culshaw (eds.), Artech House, Boston-London (1997), chap. 8, pp. 53-107. ISBN: 9780890069400.**

**Sections:** 1 Indicators; 2. Polymeric Supports and Coatings; 3. Immobilization Techniques; 4. Examppls for optical pH Sensors; 5. Oxygen Sensors; 6. Carbon Dioxide Sensors; 7. Ion Sensors; 8. References.



**267. Effects of the Polymer Matrix on an Optical Nitrate Sensor Based on a Polarity-Sensitive Dye. G. J. Mohr, O. S. Wolfbeis; *Sensors Actuators* 37 (1997) 103-109. DOI: 10.1016/S0925-4005(96)01994-6**

**Abstract:** A membrane responsive to nitrate has been developed; it is composed of a polymer matrix, an anion exchanger (tridodecylmethylammonium chloride), and a polarity-sensitive dye (rhodamine B octadecyl ester perchlorate). On exposure to nitrate, its fluorescence intensity increases, while the wavelength of the excitation and emission maxima remain unchanged. The effect of the polymer matrix (made from plasticized PVCs or certain hydrogels) on the relative signal change, sensitivity and selectivity has been investigated. It is shown that the sensitivity and selectivity for nitrate over other anions strongly

depends on the lipophilicity and polarity of the polymer: increasing lipophilicity results in both higher sensitivity and selectivity. The limit of detection (LOD) in the case of lipophilic matrices is of the order of 0.1 ppm nitrate, and highest signal changes are observed between 1 and 100 ppm. Hydrophilic matrices have an LOD of 1 ppm and are most sensitive to nitrate at levels between 10 and 1000 ppm. The selectivity factor of lipophilic matrices for nitrate over chloride is 200, whereas it is around 10 only in hydrophilic matrices. The optical signal of the sensor material is pH dependent and this dependence again is affected by the lipophilicity of the matrix. In general, lower lipophilicity increases the cross-sensitivity of the nitrate sensor to pH. As a result, the response of the sensor may be fine-tuned by the appropriate choice of the polymer material.

**266. New Polar Plasticizers for Luminescence-Based Sensors, D. B. Papkovsky, G. J.**

**Mohr, O. S. Wolfbeis; *Anal. Chim. Acta* 337 (1997) 201-205.** DOI: 10.1016/S0003-

2670(96)00409-6

**Abstract:** The widely used polar plasticizer 2-nitrophenyl octyl ether (NPOE) is found to act as a dynamic quencher of the luminescence of certain indicators, and quenching studies have been performed both in solution and in sensor membranes plasticized with NPOE. A series of 2-cyanophenyl-alkyl ethers (with C8, C10 and C12 alkyl chains) has been prepared and are found not to act as quenchers and hence represent an improved class of plasticizers for use in luminescence-based sensors.



CPDE, R = C<sub>8</sub>H<sub>17</sub>

CPDE, R = C<sub>10</sub>H<sub>21</sub>

CPDE, R = C<sub>12</sub>H<sub>25</sub>

**265. Journal Volume Edited: Biomedical Systems and Technologies. N. Croitoru, M. Frenz, T. A. King, R. Pratesi, A. M.**

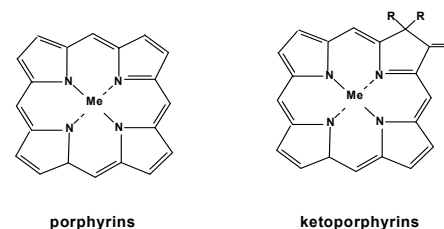
**Scheggi, S. Seeger, O. S. Wolfbeis (vol. eds.), *Proc. SPIE*, vol. 2928 (1996).** ISBN 0-8194-2330-0.

<https://www.spiedigitallibrary.org/conference-proceedings-of-SPIE/2928.toc>

**264. Longwave Luminescent Porphyrin Probes, D. B. Papkovsky, G. V. Ponomarev, O. S. Wolfbeis; *Spectrochim. Acta Part***

**A, 52, 1629-1638 (1996).** DOI: 10.1016/0584-8539(96)01731-X

**Abstract:** A set of luminescent dyes, namely the keto-porphyrin and their zinc(II), platinum(II) and palladium(II) complexes have been studied by absorption and luminescence spectroscopy including time-resolution. The metal-free porphyrin-ketones display strong and pH-dependent fluorescence due to a protolytic equilibrium that exists between the free base and the dication. The zinc(II) complexes also give strong fluorescence along with a weak long-decay emission at room temperature which is attributed to delayed fluorescence and phosphorescence, respectively. Pt(II) and Pd(II) complexes exhibit room-temperature phosphorescence without any detectable fluorescence. The new dyes display a considerably longwave-shifted luminescence along with substantially improved (photo)chemical stability. They are considered to be promising probes for very near-infrared luminescence studies.



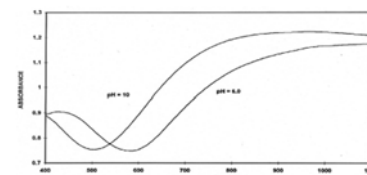
porphyrins

ketoporphyrins

**263. Optical Sensing of pH Based on Polypyrrole Films, S. de Marcos, O. S. Wolfbeis; *Anal. Chim. Acta* 334, 149-153**

**(1996).** DOI: 10.1016/S0003-2670(96)00290-5

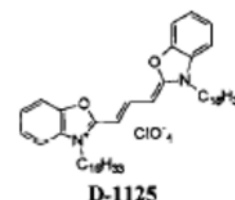
**Abstract:** An optical sensor for pH is presented which is based on the use of a thin polypyrrole (PPy) film obtained by chemical oxidation of pyrrole and deposited as a <1- $\mu$ m film on the walls of a polystyrene cuvette. The spectra of PPy display strong absorption in the near infrared (NIR) at around 900 nm, and a characteristic minimum at around 550 nm. The shape and intensity of the spectra are pH-dependent between pH 6 and 12, the minimum being shifted to shorter wavelengths at higher pH, and the absorbance of the longwave band increasing in the 600 to 900 nm range. The apparent pK<sub>a</sub> is around 8.6, but once exposed to pHs >6, the films need to be reconditioned with 0.1 N HCl in order to give the same response to pH. The films are an interesting alternative to indicator-based pH sensor films in that they do not require a dye to be immobilized, are fully compatible with LED and diode lasers light sources, and can be easily prepared. The figure shows the pH-dependence of the absorption spectra of a PPy film at pH 6.0 and pH 10.0.



**262. Fluorescent Potential-Sensitive Dyes for Use in Solid-State Sensors for Potassium Ion, I. Murkovic, A. Lobnik, G. J.**

**Mohr, O. S. Wolfbeis; *Anal. Chim. Acta* 334 (1996) 125-132.** DOI: 10.1016/S0003-2670(96)00294-2

**Abstract:** Fluorescent potential-sensitive dyes (PSDs) were screened for use in potassium-sensitive optical sensor membranes. A potassium-sensitive plasticized PVC layer containing valinomycin as an ion carrier, lipophilic borate salt as an anionic additive, and a PSD was chosen as a model for evaluating the applicability of PSDs. A commercial carbocyanine dye (3,3'-dihexadecyloxycarbocyanine perchlorate) was found to exhibit the best properties in terms of signal changes, photostability and operational life-time. The sensor membrane responds reversibly to potassium ion, with fluorescence intensity changes exceeding 50% and response times being of the order of 1 min. The response to potassium is slightly pH dependent. Typically, an 8% change in intensity is observed over the range pH 5-8. The new sensor membrane exhibits significantly improved signal changes compared to previous optodes based on related sensing schemes. We also report on the effects of different plasticizers and lipophilic additives on the response of the layers. The response mechanism is discussed with respect to the morphology of the membrane.



Formula of a typical dye

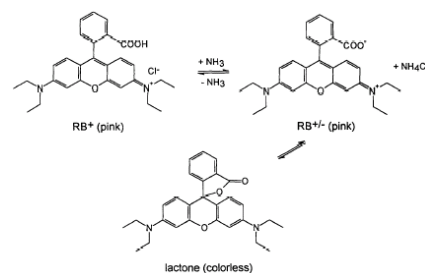
**261. Ammonia Fluorosensors Based on Reversible Lactonization of Polymer-Entrapped Rhodamine Dyes, and the**

**Effects of Plasticizers, C. Preininger, G. J. Mohr, I. Klimant, O. S. Wolfbeis; *Anal. Chim. Acta* 334, 113-123 (1996).** DOI:

10.1016/S0003-2670(96)00269-3

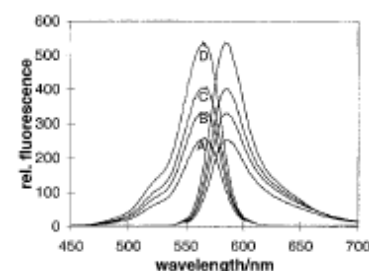


**Abstract:** A new kind of optical sensor for monitoring dissolved ammonia uses rhodamines immobilized in thin membranes made from ethyl cellulose, poly(vinyl chloride), or poly(vinyl acetate). The response to ammonia is the result of a change in the molecular structure of the rhodamine. On exposure to ammonia, the rhodamine is converted to a colorless and non-fluorescent lactone. As a result, fluorescence intensity is reduced. The polymer not only has a strong effect on the limits of detection, but also on the response time. Typical LODs are 0.1 ppm for ethyl cellulose and poly(vinyl chloride), but as low as 10 ppb for poly(vinyl acetate). The latter membranes provide highest sensitivity and lowest detection limits, but are not suitable for on-line monitoring of ammonia because they respond irreversibly. They may be applied, however, for single shot tests. Response times of the membranes are in the order of 2 to 5 min. The figure shows the chemical structures of (a) the cationic (RB<sup>+</sup>), (b) the zwitterionic (RB<sup>\*</sup>) and (c) the lactone forms of rhodamine B whose fraction varies with the concentration of ammonia.



**259. Optical Nitrite Sensor Based on a Polarity-Sensitive Dye and a Nitrite-Selective Carrier, G. J. Mohr, O. S. Wolfbeis; *Analyst* 121 (1996) 1489-1494. DOI: 10.1039/an9962101489**

**Abstract:** A membrane responsive to nitrite has been developed which is composed of plasticized PVC, the anion carrier benzylbis(triphenylphosphine) palladium(II)chloride, and the potential-sensitive dye (PSD) rhodamine B octadecyl ester perchlorate. On exposure to nitrite, fluorescence intensity increases, while the wavelengths of both the excitation and emission maxima remain unchanged. The sensor membrane exhibits its highest sensitivity to nitrite in the 5 to 5000 mg L<sup>-1</sup> range, and the detection limit is 0.5 mg L<sup>-1</sup>. The signal change on exposure to 100 mmol L<sup>-1</sup> nitrite is as high as +95% (see the figure). The effect of pH is significant: from pH 5.0 to pH 9.0 and in the absence of nitrite, the fluorescence intensity changes almost linearly by around -9% per pH unit. The selectivity coefficients relative to nitrite were determined by the separate solution method and were found to be 8 x 10<sup>-3</sup> for nitrate, 1.6 x 10<sup>-3</sup> for chloride, 8 x 10<sup>-4</sup> for hydrogen carbonate, and 3 x 10<sup>-4</sup> for sulfate.



**257b. Book edited: Optical and Electronic Phenomena in Sol-Gel Glasses and Modern**

**Application.** M. A. Aegerter, R. C. Mehrotra, I. Oehme, R. Reisfeld, S. Sakka, O. S. Wolfbeis, C. K. Jørgensen (eds.), *Structure and Bonding*, vol. 85 (1996). DOI: 10.1007/BFb0111486. Springer, Heidelberg - Berlin, 1996. Print ISBN: 978-3-540-60982-7; Online ISBN: 978-3-540-49750-9

CONTENTS:

- Sol-gel coating films for optical and electronic application (Sumio Sakka; Pages 1-49)
- Sol-gels and chemical sensors (Otto S. Wolfbeis, Renata Reisfeld, Ines Oehme; Pages 51-98)
- New materials for nonlinear optics (Renata Reisfeld; Pages 99-147)
- Sol-gel chromogenic materials and devices (Michel A. Aegerter; Pages 149-194)
- Luminescence of cerium(III) inter-shell transitions and scintillator action (Christian K. Jørgensen; Pages 195-214)
- Lasers based on sol-gel technology (Renata Reisfeld; Pages 215-233)

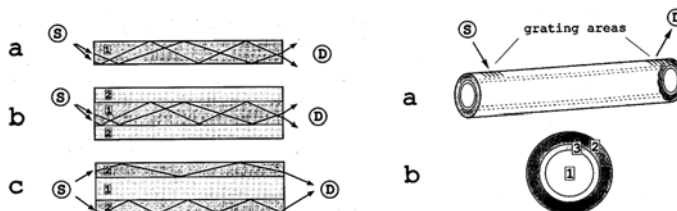


**257a. Review: Sol-Gels and Chemical Sensors, O. S. Wolfbeis, R. Reisfeld and I. Oehme, *Structure and Bonding*, vol. 85 (Optical and Electronic Phenomena in Sol-Gel Glasses), Springer, Berlin, pp. 51-98 (1996). DOI: 10.1007/BFb0111488**

**Contents:** 1. Introduction; 2. Techniques: Preparation of Sol-Gels for Sensors, Entrapment of Foreign Molecules, Entrapment of Organic and Inorganic Dopants, Entrapment of Biomaterials, Probing the Structure of Sol-Gels, Optical Sensing Techniques, 3. Sensor Applications: Studies of General Interest, Gas and Vapor Sensors, pH Sensors, Ion Sensors, Enzyme Based Biosensors, Immunosensors and Affinity Sensors, 4. References.

**256. Capillary Waveguide Sensors, O. S. Wolfbeis; *Trends Anal. Chem.* 15, 225-232 (1996). DOI: 10.1016/0165-9936(96)85131-4**

**Abstract:** Capillary waveguide sensors (CWSs) consist of a capillary with a chemically sensitive inner coating. They are multifunctional devices in being optical waveguides, sample cavities, sampling devices, flow-through cells, mechanical support for sensor coatings, and wavelength discriminators. The optical properties of the inner coating vary with the analyte to be measured, and can be detected by methods including measurement of refractive index, absorption, reflection, luminescence, and luminescence lifetime. Numerous optical configurations are discussed. Specifically, sensors are described which measure carbon dioxide, oxygen, and pH in clinical samples, but also environmental contaminants such as gasoline.

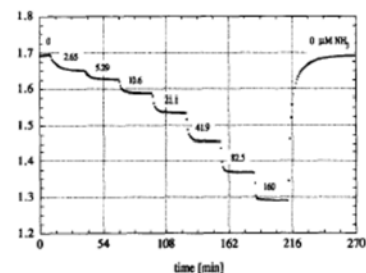


**255. Microplate Fluorescence Assay for Determination of Microalbuminuria, M. A. Kessler, A. Meinitzer, W. Petek, O. S. Wolfbeis; *Eur. Clin. Lab.* Feb. 1996, 20.**

**254. Study of the Performance of an Optochemical Sensor for Ammonia, M. Trinkel, W. Trettnak, F. Reininger, R. Benes, P. O'Leary, O. S. Wolfbeis; *Anal. Chim. Acta* 320 (1996) 235-243. DOI: 10.1016/0003-2670(95)00540-4**

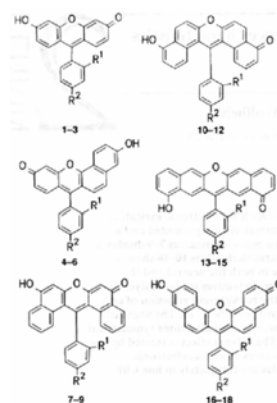
**Abstract:** The sensor is based on the pH indicator probe Bromophenol Blue that was immobilized as an ion

pair with cetyltrimethylammonium in a silicone matrix. The colour of the dye changes reversibly from yellow to blue with increasing concentration of ammonia in the sample. The concentration of ammonia can be determined by measuring the transmittance at a given wavelength. All measurements were performed with a dual-beam, solid state photometer. The analytical range is from 0.6  $\mu\text{M}$  to 1 mM (= 0.01 to 17  $\mu\text{g/mL}$ ) at pH 8. The 90% and 100% response times are 4 min and 10 min, respectively, for a change from 42 to 82  $\mu\text{M}$  solutions of ammonia. A continuous drift in signal baseline and ammonia sensitivity limit stability. Sensor performance is seriously affected by amines and cationic detergents.



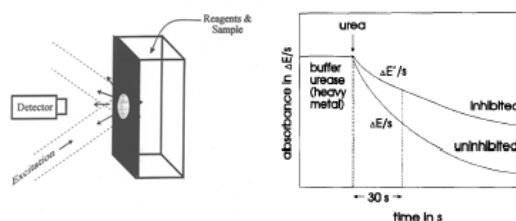
**253. Effects of Annulation on Absorption and Fluorescence Characteristics of Fluorescein Derivatives: A Computational Study, W. M.F. Fabian, S. Schuppler & O.S. Wolfbeis; *J. Chem. Soc. Perkin Trans. 2*, 1996, 853-856. DOI: 10.1039/P29960000853**

**Abstract:** Semiempirical molecular orbital calculations (AM1 for structures, INDO/S for electronic excitation energies) for fluorescein and various annulated (linear and angular) derivatives are presented and a strong dependence on the mode of condensation is obtained. While the benzo derivatives 7–9 display a small bathochromic shift only, both the linearly and angularly annulated derivatives 10–18 show a rather pronounced bathochromic shift of absorption and fluorescence in both the neutral and the dissociated forms. The longwave absorptions and emissions make these derivatives useful as dyes for measuring intracellular pH because the spectra are distinctly outside the background emission of cells. The longest wavelength absorptions and emissions are predicted for compounds 10–15. The angularly annulated derivatives 7–12 are found to deviate substantially from planarity. For all anions symmetrical structures are calculated to be more stable than unsymmetrical ones. The solvent effect is treated by the SCRF and also by the supermolecule approximation. Calculated structures as well as electronic transition energies (absorption and emission) for the solvated molecules are completely in line with results obtained for the gas phase.



**252. Disposable Cuvette Test with Integrated Sensor Layer for Enzymatic Determination of Heavy Metals, C. Preininger, O. S. Wolfbeis; *Biosensors Bioelectron.* 11, 981-990 (1996). DOI: 10.1016/0956-5663(96)87657-3**

**Abstract:** We report on a quick test for detection of heavy metals based on the inhibition of free urease contained in a disposable cuvette. The wall of the cuvette has been covered with sensors for either ammonia or ammonium ion, and the kinetics of the enzymatic reaction has been monitored by monitoring the color of the sensing layer rather than that of the whole solution. In this test, buffer, enzyme and sample are being placed in the cell. On addition of urea, enzymatic hydrolysis results in the formation of ammonia (and ammonium ion), and this is detected by one of the sensors. This sensing scheme is new in that it enables even strongly colored and highly turbid samples to be analyzed, because it is the absorption and fluorescence of the 4- $\mu\text{m}$  sensing layer on the wall that is monitored rather than the sample itself. The lowest limits of detection are found for Ag(I) (20 ppb), Hg(II) (70 ppb) and Cu(II) (250 ppb). A comparison of the ammonia gas-sensitive optode and the ammonium ion-sensitive optode showed the former to be more appropriate. The first figure shows the kinetics of the uninhibited and the inhibited enzymatic hydrolysis of urease as measured with a cuvette containing an ammonium-sensitive layer.



**251. Fiber Optic Glucose Biosensor Using Enzyme Membranes with 2-D Crystalline Structure, A. Neubauer, D. Pum, U. B. Sleytr, I. Klimant, O. S. Wolfbeis; *Biosensors Bioelectronics* 11 (1996) 317-325. DOI: 10.1016/0956-5663(96)88418-1.**

**Abstract:** Two-dimensional crystalline bacterial surface layers (S-layers) composed of identical (glyco)protein subunits turned out to be ideal matrices for immobilizing monolayers of functional macromolecules. Due to their crystalline character, S-layers exhibit a characteristic topography with a defined arrangement and orientation of functionalities, which is a prerequisite for a reproducible and geometrically defined binding of biomolecules. The proteinic nature of S-layers provides an adequate microenvironment for immobilized biomolecules, frequently along with the effect of a high retention of biological activity and enhanced stability towards drying. For the development of a fibre-optic glucose biosensor, monomolecular layers of glucose oxidase were covalently immobilized on the surface of S-layer ultrafiltration membranes (SUMs). During glucose measurements, the enzyme monolayer was attached to the transducer, an oxygen optode containing a ruthenium(II) complex whose fluorescence is dynamically quenched by molecular oxygen. The performance of the sensor, in terms of response time, linear range and stability, is comparable to existing optodes. Given its minute size, the system presented is considered to hold great promise for the development of micro-integrated optical biosensors.

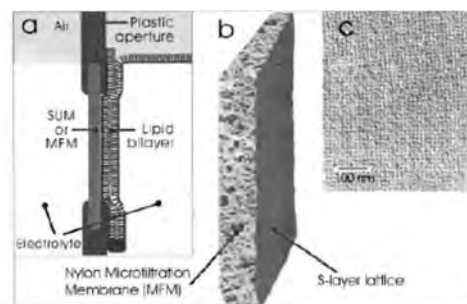
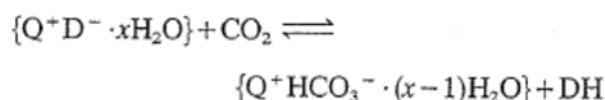


**Figure 1.** S-layer ultrafiltration membrane. (a) Schematic drawing of an SUM-supported lipid bilayer (not drawn to scale). The lipid membrane was generated on the S-layer face of the SUM. (b) S-layer fragments were deposited with pressure on a commercially available Nylon microfiltration membrane. (See text for further explanation.) (c) Electron microscopical image of a platinum/carbon replica of a freeze-dried SUM composed of the S-layer protein *B. shaeerius*CCM 2120 showing the square S-layer lattice. Bar, 100 nm.

**248. Sensitivity Studies on Optical Carbon Dioxide Sensors Based on Ion Pairing, B. H. Weigl, O. S. Wolfbeis; *Sensors Actuators 28B* (1995) 151-156. DOI: 10.1016/0925-4005(95)80041-7**

**Abstract:** A recent approach to optical carbon dioxide sensing makes use of ion pairs consisting of a pH indicator dye anion ( $\text{D}^-$ ) and an organic quaternary cation ( $\text{Q}^+$ ). The resulting 'dry' (as opposed to the better-known buffer-based 'wet' sensor chemistry) or 'plastic' sensor membranes comprise a pH indicator dye immobilized along with a quaternary cation, and an additional amount of quaternary hydroxide ( $\text{Q}^+\text{OH}^-$ ) within a polymer layer on a polyester support. Such sensors are applicable to optical sensing of carbon dioxide both in dry gases, where they have an extremely short response time, and in liquid samples. The sensitivity, or degree of response of a sensor to a given analyte concentration, is a vital parameter for describing its performance. In this work, it is shown that the sensitivity of carbon dioxide sensors, based on the ion-pairing method, is largely governed by the molar concentration ratio between the ion pair and the free quaternary hydroxide. We have found that the sensitivity of such optodes, as well as their degree of linearity, can be adjusted by varying the  $(\text{Q}^+\text{D}^-)/(\text{Q}^+\text{OH}^-)$

ratio. Certain environmental conditions, such as high temperature and the presence of acidic vapours, and also changes due to membrane aging, can shift the dynamic range to lower  $p\text{CO}_2$ , too. We discuss probable causes for the sensitivity shift. The mechanism of the optical response is outlined on the right. The protonated dye Cresol Red (DH) and the quaternary ammonium ions ( $\text{Q}^+\text{OH}^-$ ) form hydrated ion pairs ( $\text{Q}^+\text{D}^-$ ) of blue-green color. The hydrated ion pair was dissolved in ethyl cellulose where it reacts with  $\text{CO}_2$  and water to give the  $\text{Q}^+\text{HCO}_3^-$  ion pair and the protonated yellow dye with a different absorption maximum.

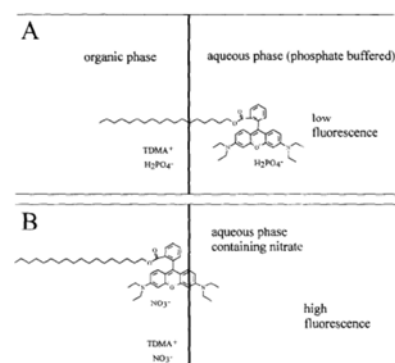


**246b. Series Volume edited: Medical Sensors II and Fiber Optic Sensors.** A. V. Scheggi, F. Baldini, P. R. Coulet, O. S. Wolfbeis, *Proceedings of SPIE - The International Society for Optical Engineering*, (1995), vol. 2331, pages 1 – 203. Web: <https://www.spiedigitallibrary.org/conference-proceedings-of-SPIE/2331.toc>

Contents: *Instrument for measuring human biting force*; by Kopola, Harri K.; Mantyla, Olavi; Makiniemi, Matti and 2 more *Time variable photoplethysmographic signal: its dependence on light wavelength and sample volume*; by Ugnell, Haekan; Oberg, P. Ake *Optical fiber sensor for the detection of laser-generated ultrasound in arterial tissues*; by Beard, Paul C.; Mills, Timothy N. *Evaluation of a new fiber-optic sensor for respiratory rate measurements*; by Oberg, P. Ake; Pettersson, Hans; Lindberg, Lars-Goeran *Novel fiber optic dental pulp vitalometer*; by Makiniemi, Matti; Kopola, Harri K.; Oikarinen, Kyosti *Multicomponent analysis of human blood using fiber optic evanescent wave spectroscopy*; by Simhi, Ronit; Bunimovich, David; Sela, Ben-Ami *Detection of small trace molecules in human and animal exhalation by tunable diode lasers for applications in biochemistry and medical diagnostics*; by Stepanov, Eugene V.; Kouznetsov, Andrian I.; Zyrianov, Pavel V. and 3 more *PulCar: an application-specific integrated circuit (ASIC) for an optoelectronic sensor* Covas, Marie; Contensou; by Jean-Noel; Bosch, Thierry M. *Single fiber, laser Doppler flowmetry (LDF) for detecting muscle microcirculation in the low leg and its technique improvement*; by Cai, Hongming; Oberg, P. Ake; Rohman, Hakan and 1 more *Zirconium fluoride glass fiber radiometer for low-temperature measurement*; by El Khoniss, A.; Mordon, Serge R.; Dhelin, Guy and 2 more *Rapid one-step assay for prostate specific antigen in whole blood using an optical immunoassay technology*; by Robinson, Grenville; Bacarese-Hamilton, Timothy; O'Neill, Paul M. and 3 more *Surface plasmon resonance response of a polymer-coated biochemical sensor*; by Millot, Marie-Claude; Vals, Thierry; Martin, Francoise *Fiber optic based multisensor to brain neurons in awake animals*; by Shen, Zheng; Lin, Shuzhi *Three wavelength optical oxymetry including the measurement of carboxyhemoglobin concentration*; by Pieralli, Christian; Devillers, Robert; Tribillon, Gilbert M. and 2 more *Sensing pads for hybrid and monolithic integrated optical immunosensors*; by Kunz, Rino E.; Duveneck, Gert L.; Ehrat, Markus *Sensing a heart infarction marker with surface plasmon resonance spectroscopy* by Kunz, Ulrich; Katerkamp, Andreas; Renneberg, Reinhard, and 2 more *Low-level luminescence as a method of detecting the UV influence on biological systems*; by Mei, Wei-Ping; Popp, Fritz A. *Solid State optical potassium sensor using a potential-sensitive dye*; by Wolfbeis, Otto S.; Kovacs, Barna; He, Huarui *Fiber optic biosensors for hydrogen peroxide and L-lactate*; by Schubert, Florian; Rinneberg, Herbert H.; *Ultrathin antibody networks for detection of antigens*; by Hartmann, Andreas; Bock, Daniel; Martin, Michael and 1 more *Investigation of occult choroidal neovascularization at low-light level: clinical results*; by Longobardi, Giuseppe; Ciamberlini, Claudio; Guarnieri, Vittorio and 4 more *Optical fiber sensors in foregut functional diseases*; by Baldini, Francesco; Bechi, Paolo; Bracci, Susanna

**246. Optical Sensing of Anions via Polarity Sensitive Fluorescent Dyes: A Bulk Sensor Membrane for Nitrate.** G. J. Mohr, O. S. Wolfbeis; *Anal. Chim. Acta* **316**, 239-246 (1995). DOI: 10.1016/0003-2670(95)00370-F

**Abstract:** We report on the first application of a lipophilic polarity-sensitive dye (PSD) to optically sense an anion. A membrane responsive to nitrate has been developed which is composed of poly(vinyl chloride), a plasticizer [bis-(2-ethylhexyl)-sebacate], an anion carrier (tridodecyl-methylammonium chloride), and a lipophilic cationic PSD (rhodamine B octadecyl ester perchlorate). On exposure to nitrate, fluorescence intensity increases, while the wavelength of the excitation and emission maxima remain unchanged. The sensor membrane exhibits its highest sensitivity to nitrate in the 0.6 to 60 ppm range, and the detection limit is 0.1 ppm. The signal change on exposure to 100 mM nitrate is as high as +95%. The effect of pH is significant. The results show that the PSD-based ion sensing scheme - which so far has been applied to cations only - is applicable to anions as well and in this case results in much larger signal changes.



**244. Oxygen-Sensitive Luminescent Materials Based on Silicone-Soluble Ruthenium Complexes,** I. Klimant & O.S. Wolfbeis; *Anal. Chem.* **67**, 3160-3166 (1995). DOI: 10.1021/ac00114a010

**Abstract:** New oxygen-sensitive luminescent materials were obtained by physically immobilizing luminescent ruthenium(II) diimine metal-ligand complexes in silicone rubber. The dyes were made silicone-soluble by converting them into the respective ion pairs with organic anions (see Table). Acetic acid releasing one-component RTV-silicones were found to provide the best matrix for sensor membranes. The dyed silicone prepolymeres were spread onto planar solid supports (see the figure), cured, and characterized in terms of quenching by oxygen, response time, interferences, storage stability, and photostability. Strong evidence is presented from quenching experiments that the luminescent ion pairs are present in both a monomolecular and an aggregated form, the respective quenching constants being highly different. This results in non-linear Stern-Volmer graphs. The new materials are considered to present a major improvement over existing ones in terms of response time, luminescence intensity, and long-term stability. They not only may be applied as planar films, but also as very thin coatings on various kinds of waveguides. We also describe several novel materials for use as light-tight optical isolations. They are spread onto the oxygen-sensitive films in order to minimize interferences by (a) ambient light and (b) potentially interfering sample properties such as color, turbidity, fluorescence, and varying refractive index.

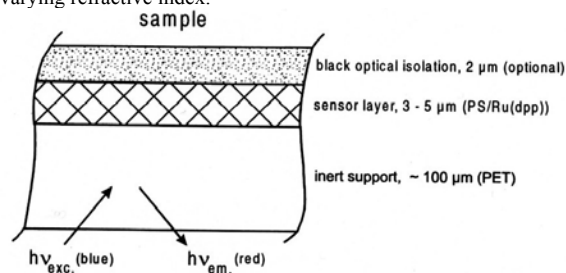


**Table 2. Chemical Structures of the New Silicone-Soluble Ion Pairs  $\text{Ru}(\text{dpp})_2\text{X}_2^+$  and  $\text{Ru}(\text{phen})_2\text{X}_2^+$**

ion pair	Ru (diimine)	anion (X)
1a	$\text{Ru}(\text{dpp})_2$	$\text{H-C}_{12}\text{H}_{25}\text{SO}_3^-$ (DS)
1b	$\text{Ru}(\text{dpp})_2$	$(\text{CH}_3)_3\text{SiCH}_2\text{CH}_2\text{CH}_2\text{SO}_3^-$ (TSPS)
2a	$\text{Ru}(\text{phen})_2$	$\text{H-C}_{12}\text{H}_{25}\text{SO}_3^-$ (DS)
2b	$\text{Ru}(\text{phen})_2$	$(\text{CH}_3)_3\text{SiCH}_2\text{CH}_2\text{CH}_2\text{SO}_3^-$ (TSPS)

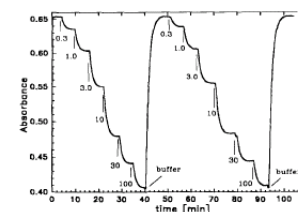
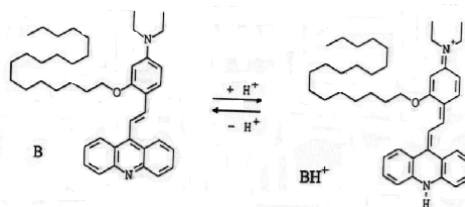
<sup>a</sup> dpp, 4,7-diphenyl-1,10-phenanthroline. <sup>b</sup> phen, 1,10-phenanthroline.

**243. Enzyme Biosensor for Urea Based on a Novel pH Bulk Optode Membrane,** R. Koncki, G. J. Mohr, O. S. Wolfbeis; *Biosensors Bioelectron.* **10**, 653-659 (1995). DOI: 10.1016/0956-5663(95)96955-X

**Abstract:** An absorbance-based enzymatic biosensor membrane for determination of urea was obtained by incorporating a lipophilic, fully LED- and diode

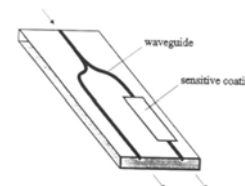


laser-compatible pH sensitive dye (see the formula) into a plasticized, carboxylated poly(vinyl chloride) membrane. It served as the optical transducer of the sensor. Urease was covalently linked to the surface of the pH bulk optode membrane to form a very thin cover. The resulting biosensor membrane allows rapid determination of urea over the 0.3 to 100 mM range. The reproducibility, stability, and effects of pH and buffer concentration on the response of sensor are reported. The second figure shows the reproducibility, signal change, and response time of the urea optical sensor (carrier: 5 mM phosphate buffer, pH 7.00). The numbers indicate urea concentrations in mM.



**242. Ammonia Detection via Integrated Optical Evanescent Wave Sensors, A. Brandenburg, R. Edelhaeuser, T. Werner, H. He, O. S. Wolfbeis; *Microchim. Acta* 121, 95-105 (1995). DOI: 10.1007/BF01248244**

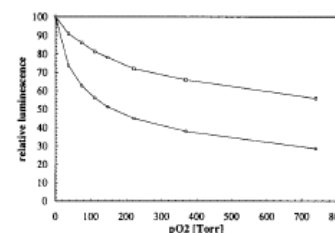
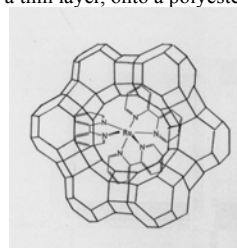
**Abstract:** Detection of ammonia in the gas phase is demonstrated by means of integrated optical components coated with sensitive films which reversibly change their spectral absorption with ammonia concentration. The evanescent wave of the guided light continuously probes the absorbance of the sensor membrane at 633 nm. The output intensity is compared to that of a reference channel not influenced by the sensitive film. Using indicator dyes Bromocresol Green and Bromophenol Blue in silicone, ammonia levels of <1 ppm are detectable, with a dynamic range from 1 to 200 ppm. The response depends on relative humidity, and acidic gases including sulfur dioxide, carbon dioxide, and nitric oxides are found to reduce the relative signal change caused by ammonia, whilst in the absence of ammonia they remain inert. The function of the film is lost within a few months after film preparation.



**241. Novel Oxygen Sensor Material Based on a Ruthenium Bipyridyl Complex Encapsulated in Zeolite Y: Dramatic Differences in the Efficiency of Luminescence Quenching by Oxygen on Going from Surface-Adsorbed to Zeolite-Encapsulated Fluorophors, B. Meier, T. Werner, I. Klimant, O. S. Wolfbeis; *Sensors Actuators* 29B, 240-245 (1995). DOI: 10.1016/0925-4005(95)01689-9**

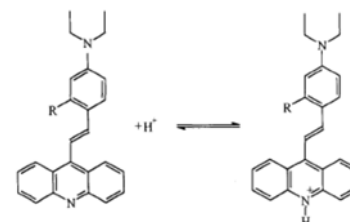
**Abstract:** Zeolite Y was ion-exchanged with ruthenium(III)-chloride, and the respective ruthenium(II) bipyridyl complex, which is an excellent fluorescent oxygen probe, was prepared *inside* the zeolite supercages. In addition, a Ru(bipy) dichloride solution was used for impregnation of the zeolite *surface*. In order to obtain sensor materials, they were incorporated into silicone polymers and spread, as a thin layer, onto a polyester support.

The resulting sensor membranes were tested with respect to luminescence intensity, quenching by molecular oxygen, response to oxygen, and long term stability under various conditions. Oxygen can be measured over the 0 to 760 Torr range, with the best resolution between 0 and 200 Torr. Both the quenching efficiency and the long-term stability of the Stern-Volmer quenching constant are significantly improved when compared to sensors where the probe is adsorbed onto silica gel. When spread on glass rather than polyester, the sensors lend themselves to operation at temperatures as high as 200 °C. The first figure shows a schematic of a zeolite with the Ru dye, and the second figure shows the quenching of the luminescence of membranes M-1 (circles, bottom) and M-2 (squares, top) by oxygen, demonstrating the differences in the quenchability of zeolite



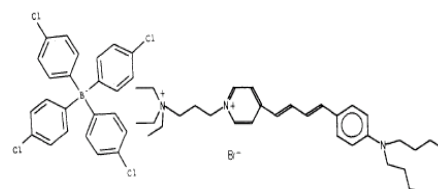
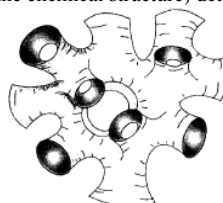
**240. Optode Membrane for Continuous Measurement of Silver Ions, I. Murkovic, I. Oehme, G. J. Mohr, T. Ferber, O. S. Wolfbeis; *Microchim. Acta (Vienna)* 121 (1995) 249-258. DOI: 10.1007/BF01248254**

**Abstract:** An optical sensor (optode) membrane for continuous monitoring of silver ion is presented. It is composed of plasticized poly(vinyl chloride) (PVC), a silver-sensitive chromo-ionophore, and a lipophilic borate salt acting as an anionic site. The membrane selectively responds to silver ion in the concentration range from 50 μM to 10 mM, giving a reversible colour change from blue to pink, with response times of the order of 2 min. The acridinium dye acts as both the recognition element and the chromo—ionophore. Its long-wave absorption band is at around 680 nm, which makes it compatible with existing LED light sources and diode lasers. A lipophilic octadecyl side chain renders it highly lipophilic and this prevents its leakage out of the PVC membrane. Hence, the operational lifetime exceeds 1 week, without any changes in the work function.



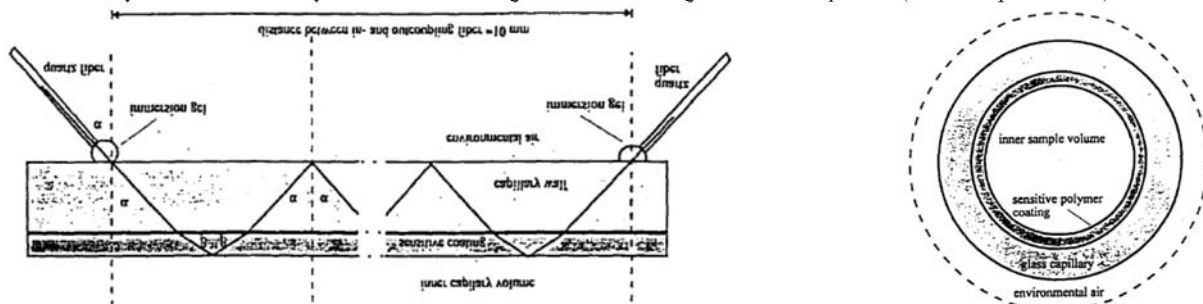
**239. Fluorescence-Based Ion Sensing Using Potential-Sensitive Dyes, O. S. Wolfbeis; *Sensors Actuators* 29B, 140-147 (1995). DOI: 10.1016/0925-4005(95)01675-9**

**Abstract:** A report is given on the use of potential-sensitive dyes (PSDs) for monitoring the potential created at the membrane-sample interface due to the transport of ions from the (aqueous) sample into the lipid membrane by a neutral ion carrier. Valinomycin acts as a carrier to transport potassium ion into the interior of a plasticized pvc membrane, and the PSD (a lipophilic dye; see the chemical structure) detects the potential by undergoing a change in fluorescence emission intensity. Depending on the dye used, the change in fluorescence is caused by either electronic rearrangement within the dye, spatial redistribution, or voltage-dependent partitioning. In parallel, a change in fluorescence polarization can be observed. Unlike many other kinds of ion optrodes, the work function is virtually independent of pH. Finally, we will discuss the micro-structure of the membrane, the function of the PSD, and the most likely sensing mechanisms.



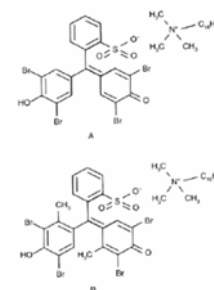
**237. Optical Sensor Instrumentation Using Absorption- and Fluorescence-Based Capillary Waveguide Optrodes, B. H. Weigl, S. Draxler, D. Kieslinger, H. Lehmann, W. Trettnak, O. S. Wolfbeis, M. E. Lippitsch, *Proc. SPIE* (Soc. Photo-Instrum. Eng.) **2508** (1995) 199-209. DOI: 10.1117/12.221733**

**Abstract:** An analytical instrument comprising absorption- and fluorescence-based capillary waveguide optrodes (CWOs) is described. Glass capillaries with a chemically sensitive coating on the inner surface are used for optical chemical sensing in gaseous and liquid samples. In case of absorption-based CWOs, light from a LED is coupled into and out of the capillary under a defined angle via a rigid waveguide and an immersion coupler. The coated glass capillary forms an inhomogeneous waveguide, in which the light is guided in both the glass and the coating. The portion of the light which is absorbed in the chemically sensitive coating is proportional to a chemical concentration or activity. This principle is demonstrated with a pCO<sub>2</sub>-sensitive inner coating. Typical relative light intensity signal changes with this type of optical interrogation are 98%, with an active capillary length of 10 mm. For fluorescence-based CWOs, the excitation light from an LED is coupled diffusely into the glass capillary and the optical sensor layer. A major portion of the excited fluorescence light is then collected within the coated capillary, and guided to the photodiode, which is located on the distal end of the capillary waveguide. Hereby, the excitation light is separated very efficiently from the fluorescent light. As an example, a CWO for pO<sub>2</sub> is described. By applying this optical geometry, it was possible to utilize fluorescence decay time of the sensor layer as the transducer signal even when using solid state components (LEDs and photodiodes).



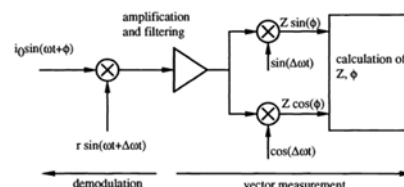
**236. Ammonia-Sensitive Polymer Matrix Employing Immobilized Indicator Ion Pairs, T. Werner, I. Klimant, O. S. Wolfbeis; *Analyst* **120**, 1627-1631 (1995). DOI: 10.1039/an9952001627**

**Abstract:** A new sensor material for monitoring ammonia in aqueous solutions is presented. It is based on lipophilic ion pairs consisting of an anionic pH indicator and a quaternary ammonium cation. The ion pairs are homogeneously distributed inside a layer of a silicone elastomer. Exposure to ammonia leads to de-protonation of the hydroxy group, and this causes the strong absorbance of the basic form of the indicator. The sensor can easily be manufactured from plastic materials and responds to ammonia over the concentration range from 0.015 to 20 mg/l, with a detection limit of 15 mg/l, and is not affected by pH because the silicone is proton-impermeable. The sensor is intended for use as a probe to monitor ammonia in surface waters.



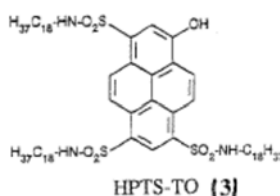
**235. Detection of Fluorescence Lifetime Based on Solid-State Technology, and Its Application to Optical Sensing, W. R. Gruber, P. O'Leary, O. S. Wolfbeis; *Proc. SPIE* **2388** (Adv. Fluoresc. Sensing Technol. II), 148-158 (1995). DOI: 10.1117/12.208474**

**Abstract:** An optical sensor instrument was developed that makes use of solid-state components and is capable of measuring oxygen in the 1 - 760 Torr range by measuring the effect of oxygen on the decay time of an immobilized ruthenium complex. The detection system is based on heterodyne demodulation (*heterodyning vector measurement*) techniques for reduction of the signal frequency range and was implemented into a custom CMOS integrated circuit.



**234. Application of a Novel Lipophilized Fluorescent Dye in an Optical Nitrate Sensor, G. J. Mohr, T. Werner, O. S. Wolfbeis; *J. Fluoresc.* **5**, 135-138 (1995). DOI: 10.1007/BF00727530**

**Abstract:** A new lipophilic pH-probe (1-hydroxypyrene-3,6,8-tris-octadecylsulfonamide; **HPTS-TO**; see left Figure) has been synthesized, and its spectral properties and applications in an optical nitrate sensor are shown. The sensor is highly pH-dependent and is characterized in terms of sensitivity, limits of detection, and selectivity over other anions found in drinking water. The figure on the right shows the mechanism of the co-extraction of an anion along with a proton from an aqueous sample phase into the sensor layer.



water phase	membrane phase
anion <sup>⊖</sup>	ionophore <sup>⊕</sup>
	anion - ionophore
H <sup>⊕</sup>	indicator (red)
	indicator - H <sup>⊕</sup> (blue)

**233. Effects of Polymer Matrices on the Time-Resolved Luminescence of a Ruthenium Complex Quenched by Oxygen, S. Draxler, M. E. Lippitsch, I. Klimant, H. Kraus, O. S. Wolfbeis; *J. Phys. Chem.* **99**, 3162-3167 (1995). DOI: 10.1021/j100010a029**

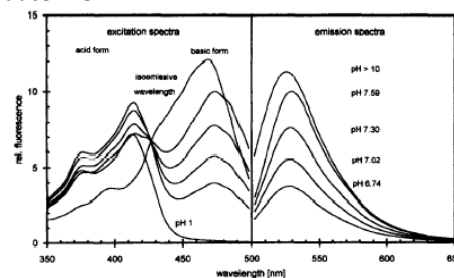
**Abstract:** Quenching of luminescence by oxygen of ruthenium diphenylphenanthroline in various polymers was studied by time-resolved spectroscopy. The luminescence decay was not single-exponential, and the Stern-Volmer plot was non-linear (downward-curved) in all cases. A new model for describing the non-exponential luminescence decay was developed, which considers the interaction of the fluorophore with the non-uniform environment provided by the polymer. This model has a better physical basis than the usual fits with multiple exponentials or lifetime distributions of arbitrary shape. Oxygen quenching is described by a single parameter, which, in favorable cases, depends linearly on oxygen pressure. This may be of advantage for the calibration of optical oxygen sensors based on luminescence quenching.

**Cross Section:**

**Cocktail:** polystyrene, Ru(dpp), toluene  
**Quantum yield:** 41%  
**Response to gaseous oxygen:** 3 s  
**Response to dissolved oxygen:** 100 s  
**Dye leaching:** not detectable after 1 week of storage in water  
**Interferents:** H<sub>2</sub>O<sub>2</sub>, SO<sub>2</sub>, chlorine  
**Not interfered by:** ionic species, CO<sub>2</sub>, organic vapors, surfactants

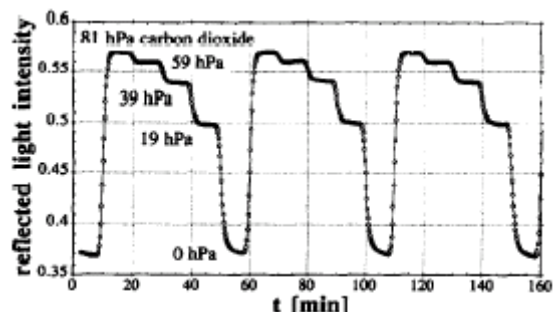
**232. Dependence of the Fluorescence of Immobilized 1-Hydroxypyrene-3,6,8-trisulfonate on Solution pH: Extension of the Range of Applicability of a pH Fluorosensor, S. G. Schulman, Sh.-X. Chen, F. Bai, M. J. P. Leiner, L. Weis, O. S. Wolfbeis; *Anal. Chim. Acta* **304**, 165-170 (1995). DOI: 10.1016/0003-2670(94)00631-U**

**Abstract:** The organic acid 1-hydroxy-3,6,8-pyrenetrisulfonate (HPTS), covalently immobilized on cellulose attached to a plastic strip, has been used as a fluorescent optical pH sensor for the neutral pH region. This is based upon the prototropic equilibrium in the ground electronic state between the conjugate acid and base forms of HPTS which can be observed fluorimetrically by exciting the conjugate base form exclusively. However, when both the conjugate acid and base forms (or the acid form alone) are excited, the fluorescence of immobilized HPTS also varies in the low pH region from about pH 3 to a little below pH 1. The proton transfer in the lowest excited singlet state which accounts for the variation of the fluorescence in the low pH region is here evaluated kinetically and its application to the use of immobilized HPTS as a fluorosensor in the low pH region is suggested.



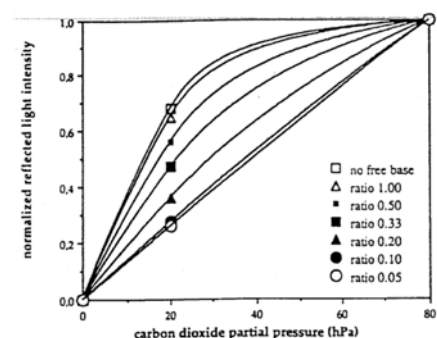
**230. New Hydrophobic Materials for Optical Carbon Dioxide Sensors Based on Ion Pairing, B. H. Weigl, O. S. Wolfbeis; *Anal. Chim. Acta* **302**, 249-254 (1995). DOI: 10.1016/0003-2670(94)00473-Y**

**Abstract:** A hydrophobic polymer material is presented which is optically sensitive to carbon dioxide. It is based on ion pairing between an indicator anion and a quaternary ammonium cation. The ion pair is dissolved in various kinds of silicone rubbers, and the resulting materials are shown to be useful for optically sensing carbon dioxide over the 0 to 100 hPa (0 to 76 Torr) partial pressure range. The detection limit is approximately 0.3 hPa. The material can be immobilized on glass or plastic supports, on optical fibers, or in capillaries. The silicone rubber based sensors are capable of measuring carbon dioxide both in gases (to which they respond within 1 sec) and in aqueous sample solutions (with response times ranging from 2 to 8 min). Due to the use of silicone rubber as the polymer support, there is no cross-sensitivity to pH within the pH 5 to 9 range. The figure shows the optical response of a carbon dioxide sensor with a silicone rubber matrix (membrane type M7) to 0.1 M phosphate buffer solutions of pH 7, tonometered with carbon dioxide of partial pressures ranging from 0 to 81 hPa (0 - 61.6 Torr; 0 - 81 mbar), corresponding to 0 - 122 ppm in water.



**228. Single Layer Capillary Optrode for Carbon Dioxide with Adjustable Sensitivity, B. H. Weigl, O. S. Wolfbeis; *Proc. SPIE* **2293** (*Adv. Fluoresc. Sensing*) (1994) 99-109. DOI: 10.1117/12.190960**

**Abstract:** A single layer hydrophobic polymer membrane is presented which is optically sensitive to carbon dioxide. It is immobilized on the inner surface of a glass capillary. The sensor material is based on ion pairing between an indicator anion ( $D^-$ ) and a quaternary ammonium cation ( $Q^+$ ). The ion pair ( $Q^+D^-$ ), together with a quaternary hydroxide ( $Q^+OH^-$ ), is dissolved in silicone rubber, and the resulting material is shown to be useful for optically sensing carbon dioxide over the 0 to 100 hPa (0 to 76 Torr) partial pressure range. The detection limit is approximately 0.3 hPa. The silicone rubber based sensors are capable of measuring carbon dioxide both in gases (to which they respond with a  $t_{90}$  of 1 sec) and in aqueous sample solutions (with response times ranging from 1 to 2 min); there is no need for an additional (proton-impermeable) coating. Due to the use of silicone rubber as the polymer support, there is no cross-sensitivity to pH within the pH 5 to 9 range. We found the inner surface of glass or plastic capillaries to be most suitable as a support for the sensor chemistry. Such capillaries can act as a mechanical support, they represent an optical waveguide structure and therefore enable various methods of optical interrogation, and they can serve as a sample cavity of well defined volume, which is suitable for direct sampling, or as a flow cell. Sensitivity, which determines the degree of response of the sensor to a given analyte concentration, is a vital parameter for the performance of a sensor. In this work, it is shown that the sensitivity of carbon dioxide sensors based on ion pairing largely depends on the molar (ion pair)/(free quaternary hydroxide) ratio. We have found that the sensitivity of such optrodes was well as their degree of linearity can be adjusted by varying the ( $Q^+D^-$ )/( $Q^+OH^-$ ) ratio.



**227. Solid State Optical Potassium Sensor Using a Potential-sensitive Dye, O. S. Wolfbeis, B. Kovacs, H. He, *Proc. SPIE* **2331** (1994) 63-70. DOI: 10.1117/12.629398**

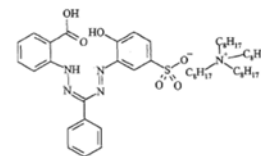
**Abstract:** In an extension of previous work on optical chemical sensors based on the use of potential-sensitive dyes incorporated in Langmuir-Blodgett films, we now describe solid-state potassium-sensitive membranes. The sensing scheme again is based on the use of valinomycin as the potassium carrier, but a plasticized PVC membrane is being used as a membrane material rather than a Langmuir-Blodgett film. A potential-sensitive dye detects the potential created at the sensor/sample interface. Unlike many other kinds of potassium optrodes, the response function is virtually independent of pH. Potassium can be continuously monitored over the concentration range from 10 - 50  $\mu$ M up to 10 mM, although relative signal changes do not exceed -20% at present. Membranes are designed in a way that they can be manufactured in large quantities, and the dye is compatible with LED light sources.

**226. LED-Compatible Copper(II)-Selective Optrode Membrane Based on Lipophilized Zincon, I. Oehme, B. Prokes, I. Murkovic, T. Werner, I. Klimant, O. S. Wolfbeis; *Fresenius' J. Anal. Chem.* **350** (1994) 563-567. DOI: 10.1007/BF00321805**

**Abstract:** An optical single shot test for copper(II) ion is presented. The membrane consists of a polyester support and an active layer composed of hydrogel, a hydroxylic plasticizer, and Zincon. The latter has been made lipophilic by ion-pairing with tetraoctyl-ammonium bromide. The membrane responds to copper ions in giving a color change from pink to blue. Because the layer irreversibly extracts copper from the solution, a kinetic approach has been used for



quantitation, in that the membrane has been exposed to the sample for 2 min and the initial slope of the response curve has been determined. A linear calibration graph has been obtained for the 1 to 100  $\mu\text{mol/l}$  (63.5  $\mu\text{g/kg}$  to 6.35  $\text{mg/kg}$ ) copper concentration range. The complexed form of the dye exhibits an absorption maximum of 620 nm which matches the emission band of the orange light-emitting diode (LED). Measurements have been performed at pH 6, because no complexation of zinc occurs in this range. The long term stability of the membrane exceeds 6 months when stored dry and in the dark. The strong binding of copper ions along with the fairly high selectivity of the membrane also suggests its use as a preconcentration phase.



Chemical structure of the lipophilic (= hydrogel-soluble) Zincon ion pair with tetraoctylammonium ion.

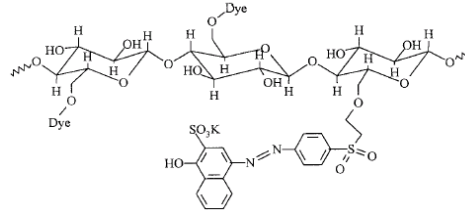
## 225. Novel Metal-Organic Ruthenium(II) Diimine Complexes for Use as Longwave Excitable Luminescent Oxygen Probes, I. Klimant, P. Belser, O. S. Wolfbeis; *Talanta* **41**, 985-991 (1994). DOI: 10.1016/0039-9140(94)E0051-R

**Abstract:** New ruthenium(II)diimine complexes are presented which are useful as luminescent oxygen probes. Because their luminescence excitation maxima are between 535 and 570 nm, they can be photo-excited by green LEDs which are much brighter than the blue LEDs used so far for existing ruthenium di-imines. The spectral, photophysical and solubility properties of the probes are investigated and discussed in terms of quenching, photostability, and lifetimes. The probes were incorporated into organic polymers so to obtain oxygen-sensitive materials for use in optical sensing. The membranes were characterized with respect to oxygen sensitivity, luminescence intensity, response times, and stability. Notwithstanding the poor luminescence of the new ruthenium(II) probes, their stability, LED compatibility, and efficient quenching by oxygen makes them an interesting alternative to existing probes. The table lists the spectral and photo-physical properties (in nm) of selected new oxygen probes. Decay times are given in ns (under nitrogen).

Oxygen Probe	abs. max.	em. max.	decay time
Ru(bpy)(DMCH) <sub>2</sub> (PF <sub>6</sub> ) <sub>2</sub>	559	742	540
Ru(bpy)(OMCH) <sub>2</sub> (PF <sub>6</sub> ) <sub>2</sub>	532	755	390
Ru(dpp) <sub>2</sub> (DMCH)(PF <sub>6</sub> ) <sub>2</sub>	532	732	640
Ru(dpp)(DMCH) <sub>2</sub> (PF <sub>6</sub> ) <sub>2</sub>	563	738	650

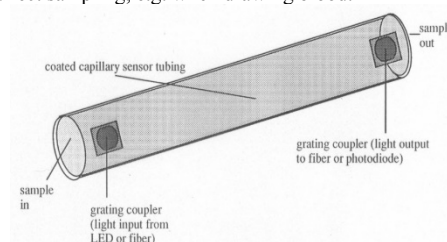
## 224. Optical Sensors for a Wide pH Range Based on Azo Dyes Immobilized on a Novel Support, G. J. Mohr, O. S. Wolfbeis; *Anal. Chim. Acta* **292**, 41-48 (1994). DOI: 10.1016/0003-2670(94)00096-4

**Abstract:** New reactive azo dyes are described which are useful for optical determination of pH. The dyes are covalently linked (via ethylsulfonyl groups) onto a novel type of transparent solid films consisting of a thin film of cellulose triacetate onto a polyester support. The triacetate was partially hydrolyzed and the dyes were then immobilized on the free hydroxy groups of the cellulose via vinylsulfonyl groups generated in situ. The resulting sensor membranes exhibit distinct color change when changing the pH and, in most cases, are compatible with LED light sources. Various membranes have been developed with pK<sub>a</sub> values ranging from 0.5 to + 11.28, thus practically covering the whole pH range. Because of the stability of (a) the dyes, (b) the covalent bond, and (c) the solid support, the new membranes exhibit excellent storage and operational lifetimes, good reproducibility, and a fast response to pH. The figure shows a schematic of the dye-to-cellulose conjugate.



## 223. Capillary Sensors: A Design Concept for Optrodes, B. H. Weigl, O. S. Wolfbeis; *Proc. SPIE* **2293** (1994) 54-63. DOI: 10.1117/12.190976

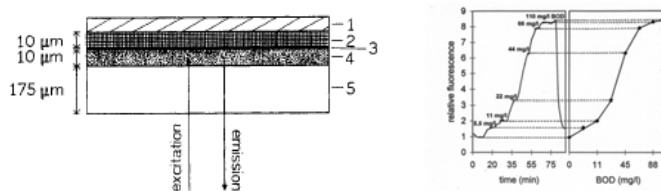
**Abstract:** We describe the use of glass or plastic capillaries in optical chemical sensing. They possess several attractive features in that (a) they can act as a mechanical support for optically sensitive materials (coatings); (b) they represent an optical waveguide structure and enable various methods of optical interrogation; and (c) they can serve as a sample cavity of well-defined volume and are suitable for direct sampling, e.g. when drawing blood. The method of immobilization and the performance of such 'capillary sensors' is exemplified by a fast-responding carbon dioxide sensor chemistry. Its response times vary from 100 to 300 ms. Such capillary sensors have, in general, extremely short response times for three reasons, namely (a), because the two sensing layers passed by the light beam when penetrating the capillary can be made very thin; (b), equilibration of two thin layers is faster than that of a single layer of the same total thickness; and (c), the sample flow is laminar, resulting in a fast and homogeneous exchange of sample volume. We also give arrangements for optical readout devices and show that capillary sensors can overcome some of the problems of optrode membranes mounted in flow cells or on fiber tips.



## 222. Optical Fiber Sensor for Biological Oxygen Demand (BOD), C. Preininger, I. Klimant, O. S. Wolfbeis; *Anal. Chem. (Wash.)* **66**, 1841-1846 (1994). DOI: 10.1021/ac00083a011

**Abstract:** We describe the first fiber optic microbial sensor for determination of biochemical oxygen demand (BOD). The sensing membrane at the tip of the fiber is shown in Fig. 1 and consists of layers of (a) an oxygen-sensitive fluorescent material, (b) *Trichosporon cutaneum* immobilized in poly(vinyl alcohol) and (c), a substrate-permeable polycarbonate membrane to retain the yeast cells. The layers are placed, in this order, on an optically transparent gas-impermeable polyester support. Tris-(4,7-diphenyl-1,10-phenanthroline)-ruthenium (II) perchlorate is used as the oxygen indicator. Typical response times are 5 to 10 min, and the dynamic range is from 0 to 110 mg/L BOD when using a glucose/glutamate BOD standard. Values estimated by this new biosensor correlate well with those determined by the conventional BOD(5) method. The main advantages of this optical sensor are (a), a more rapid estimation of BOD (in comparison to the BOD5 method which requires 5 days), (b), the fact that optical oxygen sensors do not consume oxygen, (c), the possibility of performing in situ monitoring using fiber optics, and (d), the option of designing inexpensive disposable sensor cells. The first figure shows a cross-section of a sensing membrane for detn. of BOD. Layer 1 is a polycarbonate cover; 2 is a layer of yeast immobilized in PVA; 3 is a ca. 1- $\mu\text{m}$  thick layer of charcoal acting as an optical isolator; 4 is an oxygen-sensitive fluorescent layer; 5 an inert and gas-impermeable polyester

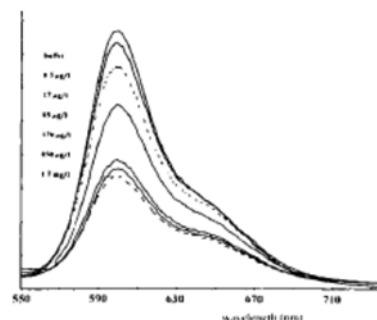
support. The second figure shows the response to various synthetic levels of BOD.



**221. Optical Sensor for Ammonia Based on the Inner Filter Effect of Fluorescence, T. Werner, I. Klimant, O. S. Wolfbeis; *J. Fluoresc.* 4 (1994) 41-44.**

DOI: 10.1007/BF01876651

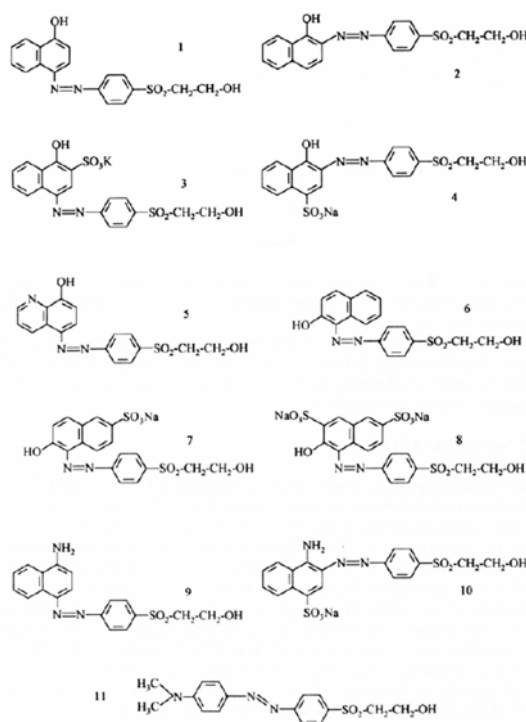
**Abstract:** A new indicator-immobilization technique for the development of a sensor material for monitoring ammonia gas in aqueous solutions is presented. It is based on the change in absorbance intensity of the lipophilized pH indicator Bromophenol Blue that was homogeneously dissolved in silicone rubber. Exposure to ammonia leads to a deprotonation of the indicator and this increases the absorbance of the base form of the indicator. The sensor responds over a 17 μg/L to 17 mg/L concentration range, with a detection limit of 12 μg/L. The figure shows the fluorescence emission spectra of the optode at various concentrations of ammonia (photo-excitation at 570 nm).



**220. Synthesis of Reactive Vinylsulphonyl Azo Dyes for Application in Optical pH Sensing, G. J. Mohr, T. Werner, O. S. Wolfbeis, R. Janoschek, *Dyes & Pigments* 24 (1994) 223-240.**

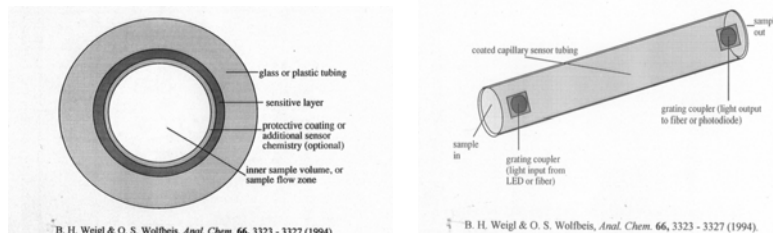
DOI: 10.1016/0143-7208(94)80011-1

**Abstract:** This work describes the application of a synthon (GM1) capable of forming a variety of reactive azo dyes useful as pH indicators. GM1 possesses two functional groups, namely (a) an amino group which allows diazo coupling to form an indicator chromophore, and (b) a 2-hydroxyethyl-sulphonyl group which, after activation, allows its immobilization on cellulose. GM1 has been diazo coupled with various aromatic phenols and amines to give a variety of pH probes. After the 2-hydroxyethylsulphonyl group has been converted into a reactive vinylsulphonyl group, the dye has been covalently linked to the hydroxy groups of cellulose. We use a novel type of a transparent solid film consisting of a polyester support covered with a thin layer of cellulose acetate which, during immobilization, is converted into cellulose. Cellulose membranes coloured with such pH indicating dyes can be applied for optical pH sensing. All dyes are characterized, both in dissolved and immobilized form, in terms of optical properties in the acid and conjugate base form, pKa values and indicator properties. Semiempirical AM1 calculations have been performed in order to compute deprotonation energies of three representative dyes, and data were compared with experimental pKa values. The figure shows the chemical structures of the reactive azo dyes 1 to 11.



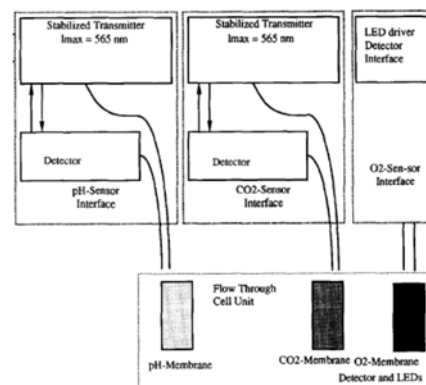
**219. Capillary Optical Sensors, B. H. Weigl, O. S. Wolfbeis; *Anal. Chem. (Wash.)* 66, 3323-3327 (1994).** DOI: 10.1021/ac00092a007.

**Abstract:** Glass or plastic tubings with a chemically sensitive coating on the inner surface are used for optical chemical sensing. Such devices possess several attractive features in that (a) they can act as a mechanical support for optically sensitive materials (coatings); (b), represent an optical waveguide structure and enable various methods of optical interrogation; (c), can serve as a sample cavity of well defined volume; and (d) are suitable for direct sampling. The performance of such capillary optrodes is exemplified by a fast-responding and fully reversible carbon dioxide sensor chemistry. Its response time to gases varies from 100 to 300 ms. We also give arrangements for optical readout devices and show that capillary sensors can overcome some of the problems of optrode membranes mounted in flow cells or on fiber tips.



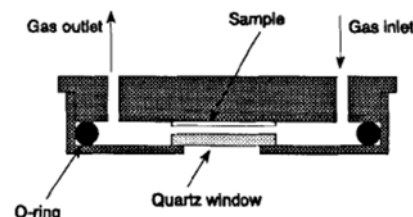
**218. Optical Triple Sensor for Measuring pH, Oxygen and Carbon Dioxide**, B. H. Weigl, A. Holobar, W. Trettnak, I. Klimant, H. Kraus, P. O'Leary, O. S. Wolfbeis; *J. Biotechnol.* **32**, 127-138 (1994). DOI: 10.1016/0168-1656(94)90175-9

**Abstract:** A triple sensor unit consisting of sensors for measurement of pH, oxygen and carbon dioxide is presented. The pH sensor and the carbon dioxide sensor are based on the color change of a pH-sensitive dye immobilized on a polymeric support. The resulting changes in absorption are monitored through optical fibers at one or two analytical wavelengths. The oxygen sensor is based on the quenching of the fluorescence of a metalorganic dye. The operation principle and the performance of all three sensors are described thoroughly with respect to their application in bioreactors. All three sensors are fully LED compatible. The chemical and mechanical stability, especially against common sterilization methods, are described in some detail. A calibration and measurement software comprising fit routines for the sensors and a mathematical treatment of the results are presented.



**216. Oxygen Detection via Optical Fibers Using Bis(histidinato)cobalt(II) as Indicator**, A. Del Bianco, F. Baldini, O. S. Wolfbeis, I. Klimant, *Mol. Cryst. Liq. Cryst.* **229** (1993) 241-245. DOI: 10.1080/10587259308032204

**Abstract:** A new kind of oxygen sensitive transducer was realized. It is based on the reflectance change of bis(histidinato)cobalt(II),  $\text{Co}(\text{His})_2$ , solution immobilized on a Thin Layer Chromatographic plate (TLC plate). The treated TLC plate was coated with a 2-component silicone layer in order to ensure a wet microenvironment and to guarantee a mechanical protection for the sensitive layer. Experimental characterization of such a probe has been carried out in order to determine the response time as a function of the pH of the solution.



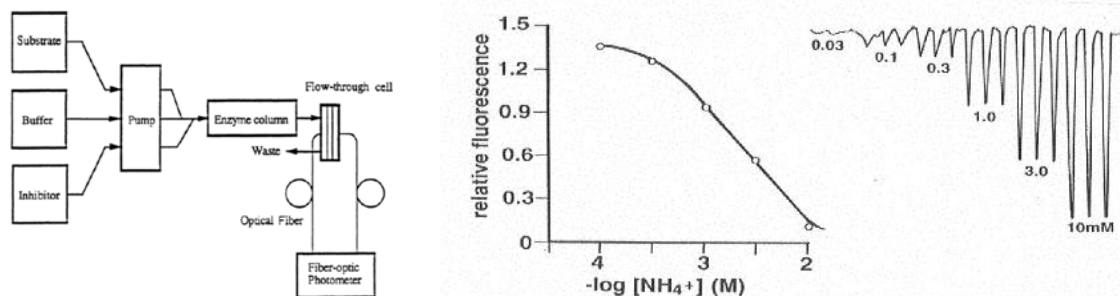
**214. Optrodes for Measuring Enzyme Activity and Inhibition**, O. S. Wolfbeis; *Proc. NATO Adv. Res. Workshop on Uses of Immobilized Biological Compounds*, G. G. Guilbault, M. Mascini (eds.), *NATO Adv. Sci. Ser., part E*, vol. **252** (1993) Kluwer Acad. Publ. (Springer), pp. 335-344. DOI: 10.1007/978-94-011-1932-0\_31

**Abstract:** In the first example, the activity of carboxylesterase is measured by using the acetate ester of HPTS which is colorless and virtually non-fluorescent but becomes yellow with a green fluorescence on hydrolysis by AChE. The HPTS ester was immobilized at the distal tip of an optical fiber. The rate of hydrolysis (i.e., of the formation of color and fluorescence) depends on the activity of AChE in the sample solution.

In a second example, the activity of the enzyme urease is determined by making use of an ammonium-selective sensor membrane. Urea is enzymatically hydrolyzed by urease under formation of ammonium ion whose concentration is quantified by using the optical ammonium sensor (carrying nonactin as the ammonium carrier and a lipophilic rhodamine as the proton carrier). The sensor was applied in a flow-injection scheme composed of an autosampler, a peristaltic pump, an injection valve with a 200- $\mu\text{L}$  sample loop, and a flow-through cell where the concentration of ammonium ion is optically interrogated by the optical fiber sensor. See the figure below.

In a third example, the activity of inhibitors of the enzyme acetylcholinesterase (AChE) is determined by a sensing scheme that is similar to the one described for carboxylesterase. The red chromogenic (but non-fluorescent) synthetic enzyme substrate 2-(2-acetoxy-5-methylphenylazo)-N-methyl-thiazolium methosulfate is hydrolyzed by AChE to give a blue product whose concentration can be measured by absorptiometry. However, in the presence of an inhibitor such as a pesticide or a nerve agent, the rate of the formation of the blue product is reduced. The resulting decrease in absorbance can be detected via fiber optics over distances as large as 10 km and may serve as an alarm, for example when destroying nerve agents in a desert.

In a fourth example, metal ions such as mercury(II) can be quantified via the inhibitory effect they exert on the activity of urease. This inhibition assay allows  $\text{Hg}(\text{II})$  ions to be determined by flow-injection analysis in concentrations as low as 200 nM.

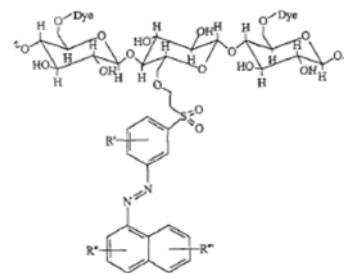


**212. Optical Sensor for the pH 10 – 13 Range Using a New Support Material**, T. Werner, O. S. Wolfbeis; *Fresenius J. Anal. Chem.* **346**, 564-568 (1993). DOI: 10.1007/BF00321245

**Abstract:** The pH-sensitive membrane for measuring high pH values consists of a polyester support covered with a thin layer of cellulose onto which a pH indicator is covalently immobilized. The sensor membrane is completely transparent and shows a pH-dependent color change that makes it capable of measuring pH in the 10 - 13 range. Its performance was studied with respect to relative signal change, reproducibility, and long-term use. The response time for 90% of the total signal change to occur was 1 min. The material has a response that is stable over hours of operation at high pHs. This is in contrast to conventional glass electrodes which tend to become unstable at high pH, but also suffer from interferences due to the so-called alkali error. This sensor presents an attractive alternative for measuring pH of highly alkaline solutions as they occur in chemical industry, scrubbers, and wastewater treatment plants. The immobilization scheme is of general interest in that it allows immobilization of vinylsulfonyle dyes with a broad variety of pKa values, thereby allowing the design of a variety of pH (and other)

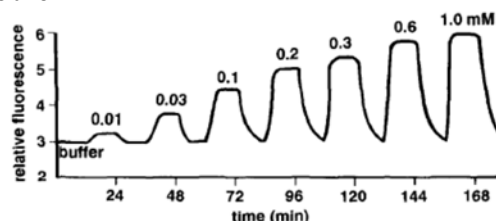


sensors possessing the same mechanical support.



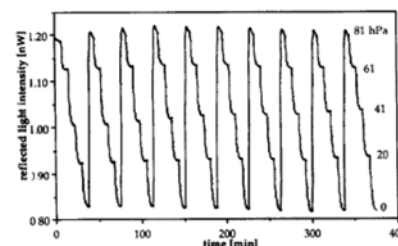
**211. Fluorescence Optical Urea Biosensor with an Ammonium Optrode as Transducer, O. S. Wolfbeis and Hong Li, *Biosensors Bioelectronics* 8, 161-166 (1993). DOI: 10.1016/0956-5663(93)85028-M**

**Abstract:** An optical sensor for determination of urea is presented that is based on the measurement of the amount of ammonium ion produced through the enzymatic action of urease at physiological pH. The ammonium optrode sensor acting as the transducer consists of a pvc material containing an ammonium ion carrier and a proton carrier (a protonated dye) whose color changes in accordance with the ammonium concentration. An urea biosensor was obtained by coupling this ammonium transducer to the enzymatic hydrolysis of urea. The sensor fully reversibly responds to urea, with detection limits varying from 0.03 to 0.6 mM at near neutral pH. The response is highly pH-dependent, and response times are about 4 min for enzyme membrane thicknesses of ca. 150  $\mu$ m.



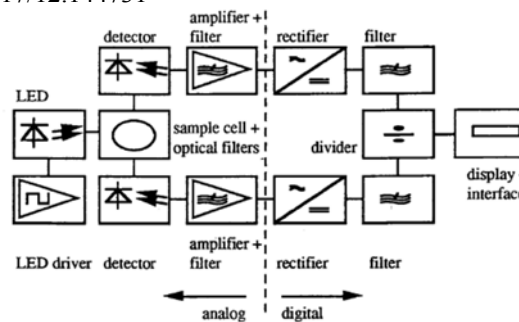
**209. Chemically and Mechanically Resistant Carbon Dioxide Optrode Based on a Covalently Immobilized pH Indicator, B. H. Weigl, A. Holobar, N. V. Rodriguez, O. S. Wolfbeis; *Anal. Chim. Acta* 282, 335-343 (1993). DOI: 10.1016/0003-2670(93)80219-B**

**Abstract:** An optical chemical sensor for dissolved carbon dioxide has been developed whose dynamic range was adjusted to CO<sub>2</sub> partial pressures ranging from 0 to 100 hPa. The change in the pH of a buffer layer, caused by diffusion of carbon dioxide through a hydrophobic membrane, is indicated by the colour change of a covalently immobilized dye, and monitored through optical fibers. The sensor is based on a commercial pH indicator (N9; from Merck) that was covalently immobilized on a new kind of transparent solid support (a plotter foil from Hewlett Packard; # 17703T). It also incorporates an optical isolation with a pigment to increase the reflectivity and to reduce adverse effects of straylight and ambient light. Two methods for layer manufacturing (spreading and spin coating) are described. The sensor membrane is fully LED compatible. The optrode shows a promising performance with respect to chemical and mechanical long-term stability, reproducibility, and sterilizability.



**210. Instrumentation for Optical Measurement of Dissolved Oxygen Based on Solid State Technology, W. R. Gruber, I. Klimant, O. S. Wolfbeis; *Proc. SPIE*, vol. 1885 (1993) 448-457. DOI: 10.1117/12.144731**

**Abstract:** A number of measurement schemes for the determination of dissolved or gaseous oxygen have been reported, most of them based on fluorescence quenching methods. They have the disadvantage of requiring large and heavy instrumentation and, therefore, are not suitable for micro-integrated technologies. As a result, the applicability is greatly limited. We introduce a system based on semiconductor devices (LEDs, photodiodes, low cost analogue and digital components) which is well suited for hybrid solutions, and represents a realistic alternative to existing micro integrated electrochemical probes. New LED-compatible sensor membranes were developed and characterized. The influence of straylight on the overall transfer function of the sensor system was investigated and possibilities for reduction or even elimination of this influence are presented. The overall performance of the instrument in terms of sensitivity, detection limits, long-term stability, and reproducibility is presented. The system was applied to the measurement of dissolved oxygen in drinking water and sea water.

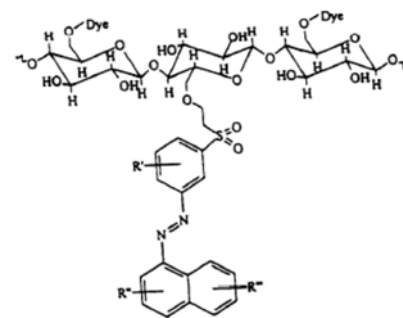


**209b. Robust Carbon Dioxide Optrode Based on a Covalently Immobilized pH Indicator. B. H. Weigl, A. Holobar, N. V. Rodriguez, O. S. Wolfbeis; *Proc. SPIE (Soc. Photo-Instrum. Eng.)* 2068 (1994) 2-10. DOI: 10.1117/12.170657**

**Abstract:** An optical chemical sensor for dissolved carbon dioxide has been developed whose dynamic range was adjusted to CO<sub>2</sub> partial pressures ranging from 0 to 100 hPa. The change in the pH of a buffer layer, caused by diffusion of carbon dioxide through a hydrophobic membrane, is indicated by the color change of a covalently immobilized dye and monitored through optical fibers. The sensor also incorporates an optical insulation with various resplendent pigments – such as titanium dioxide, Perlglanz (a mineralic glimmer pigment), aluminum bronze, gold microparticles, copper bronze – to increase the reflectivity and to reduce adverse effects of straylight and ambient light. Two methods for layer manufacturing (spreading and spin coating) are described. The sensor membrane is fully LED compatible. The optrode shows a promising performance with respect to chemical and mechanical long-term stability, reproducibility, and sterilizability.

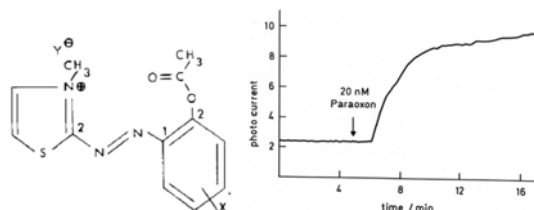
**209. Chemically and Mechanically Resistant Carbon Dioxide Optrode Based on a Covalently Immobilized pH Indicator, B. H. Weigl, A. Holobar, N. V. Rodriguez, O. S. Wolfbeis; *Anal. Chim. Acta* 282 (1993) 335-343. DOI: 10.1016/0003-**

2670(93)80219-B **Abstract:** An optical chemical sensor for dissolved carbon dioxide has been developed whose dynamic range was adjusted to CO<sub>2</sub> partial pressures ranging from 0 to 100 hPa. The change in the pH of a buffer layer, caused by diffusion of carbon dioxide through a hydrophobic membrane, is indicated by the color change of a covalently immobilized dye, and monitored through optical fibers. The sensor also incorporates an optical insulation with resplendent pigments – such as titanium dioxide, Perlglanz (a mineralic glimmer pigment), aluminum bronze, gold microparticles, copper bronze – to increase the reflectivity and to reduce adverse effects of straylight and ambient light. Two methods for layer manufacturing (spreading and spin coating) are described. The sensor membrane is fully LED compatible. The optrode shows a promising performance with respect to chemical and mechanical long term stability, reproducibility, and sterilizability.



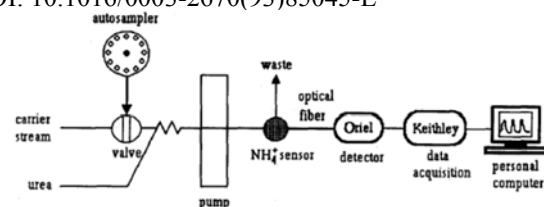
**208. Fiber Optic Remote Detection of Pesticides and Related Inhibitors of the Enzyme Acetylcholinesterase, W. Trettnak, F. Reininger, E. Zinterl, O. S. Wolfbeis; *Sensors Actuators B11*, 87-93 (1993). DOI: 10.1016/0925-4005(93)85242-3**

**Abstract:** A method for remote detection of inhibitors of the enzyme AChE is presented that makes use of a fiber optic photometer based exclusively on solid-state opto-electronic components including light-emitting diodes and photodiodes. The method employs a yellow synthetic enzyme substrate (see formula) which is hydrolyzed by the enzyme to give a blue product. In the presence of an inhibitor, the rate of the formation of this blue product is reduced. The resulting signal change is detected via fiber optics over time and may serve as an alarm.



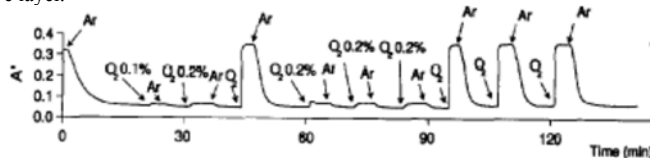
**207. Determination of Urease Activity by Flow Injection Analysis Using an Ammonium-Selective Optrode as the Detector, H. Li, O. S. Wolfbeis; *Anal. Chim. Acta* 276 (1993) 115-119. DOI: 10.1016/0003-2670(93)85045-L**

**Abstract:** Urease activity is determined by a combination of flow-injection analysis with optical sensor detection. Enzymatic hydrolysis of urea at pH 7.14 yields ammonium ions, which are determined using a fully reversible optical fibre ammonia sensor. Urea is contained in a buffered carrier stream into which urease samples of various activities are injected. The ammonium ions are measured fluorimetrically using a sensor membrane based on an ion-exchange sensing scheme using nonactin as the ion carrier. The amount of ammonium ion formed is a direct indication of the enzyme activity. The system linearly correlates with urease activity in the range 1-30 U/mL, the dynamic range being between 0.3 and 30 U/mL.



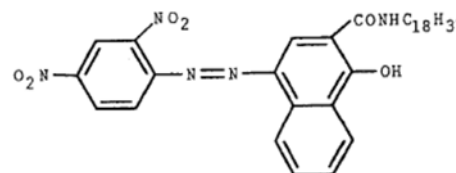
**206. A New Kind of Oxygen-sensitive Transducer Based on an Immobilized Metallo-organic Compound, A. Del Bianco, F. Baldini, M. Bacci, I. Klimant, O. S. Wolfbeis; *Sensors Actuat. B11* (1993) 347-352. DOI: 10.1016/0925-4005(93)85274-E**

**Abstract:** A new kind of oxygen-sensitive transducer has been realized based on the reflectance change of bis(histidinato)cobalt(II) [Co(His)<sub>2</sub>] immobilized on a thin-layer chromatographic plate (TLC plate). This plate is further coated with a two-component silicone rubber layer in order to maintain a wet environment for the cobalt complex and to provide mechanical protection of the oxygen-sensitive layer. An experimental characterization of the sensor material shows it to be capable of detecting oxygen at levels as low as 0.2% (v/v) in an argon stream with rate constants of 12 s and 65 s for the oxygenation and deoxygenation process, respectively. The figure shows a plot of a A' (= log I/R; where R is the reflectance) at 408 nm as a function of time of the TLC sensor plate following exposure to different oxygen concentrations. A 10 mM Co(His)<sub>2</sub> solution in phosphate buffer of pH 7.8 was deposited on the TLC plate and dried.



**205. Novel Type of Ion Selective Fluorosensor Based on the Inner Filter Effect: An Optrode for Potassium, H. He, H. Li, G. Mohr, B. Kovacs, T. Werner, O. S. Wolfbeis; *Anal. Chem. (Wash.)*, 65, 123-127 (1993). DOI: 10.1021/ac00050a006**

**Abstract:** An optrode for potassium ion has been designed that exploits the inner filter effect (IFE) of fluorescence. The sensing scheme makes use of neutral ion carriers as described by Simon et al., but transduction is based on the use of two different dyes, viz. an absorber and a fluoroscer. The absorber dye (see the figure) acts as the proton carrier, while the other is a stable and pH-independent fluorophore bound to minute particles contained in the sensor membrane. Fluorescence varies as a result of the varying absorption of the dye (yellow/blue; see Fig. 2) which in turn is modulated by potassium through the IFE. The sensor material is extremely sensitive to potassium to which it fully reversibly responds over the 1 μM to 10 mM concentration range with a useful dynamic range from 1 μM to 1 mM. The sensing approach presented here is generic in that it can be applied to almost any species for which respective carriers are known.



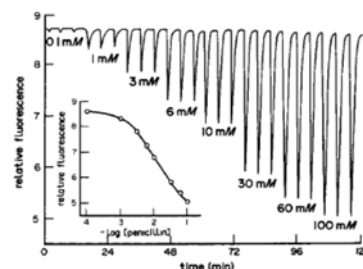
**204. Experimental Results on an Optical pH Measurement System for Bioreactors. A. Holobar, B. H. Weigl, W. Trettnak, R. Benes, H. Lehmann, N. V. Rodriguez, A. Wollschlager, P. O'Leary, P. Raspor, O. S. Wolfbeis; *Sensors Actuators B*, 11, 425-430 (1993). DOI: 10.1016/0925-4005(93)85283-G**

A pH-sensitive membrane is described for use in bioreactors. It consists of a two-layer polymeric support to which the pH indicator dye (the azo dye N9 as used in indicator paper strips from Merck and others) was covalently immobilized on a commercial plotter foil (Hewlett Packard, product # 1770311). It is composed of a 100 μm polyester layer covered, on both sides, with a 10 μm layer of cellulose acetate. In order to remove one of the two layers, the foil was

treated for a few minutes on one side with acetone until the cellulose triacetate layer had completely delaminated. The layer was removed with tweezers. The other side of the foil (still coated with cellulose triacetate) served as the substrate for the immobilization of the azo dye N9 via vinylsulfonyl chemistry (the Remazol method). The influences of ionic strength, buffer type, color and turbidity of the solution on the response to pH are studied. The membrane shows high reproducibility and long-term stability. An accuracy of  $\pm 0.1$  pH units was achieved at pH values between 6 and 10. The pH-sensing membrane can be sterilized chemically and by using heat.

**203. Non-enzymatic Optical Sensor for Penicillins, H. He, H. Li, G. Uray, O. S. Wolfbeis; *Talanta* 40, 453-457 (1993).** DOI: 10.1016/0039-9140(93)80258-S

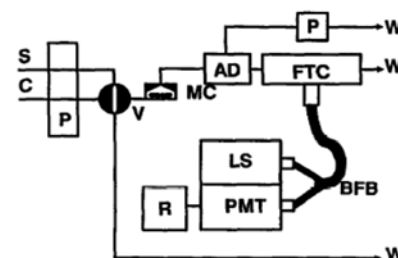
**Abstract:** We report on the first penicillin-sensitive fluorosensor not based on the use of an enzyme. Rather, the recognition process relies on the use of an anion carrier (which carries the penicillin anion from the aqueous sample into the membrane), a proton receptor (lipophilic Nile Blue which accepts the proton, thereby undergoing a change in fluorescence intensity), and a new lipophilic hydroxylic plasticizer material (which facilitates ion transport). All materials are contained in a dyed poly(vinyl chloride) membrane whose fluorescence is monitored. The sensor fully reversibly responds to penicillin V and penicillin G (range: 0.03 to 10 mM). Potential interferences by about 20 other anions have been investigated. Nitrate, salicylate, and ascorbate were found to interfere significantly. These species are, however, usually not present in penicillin bioreactors or drug formulations where penicillin sensing is most important. The method has been applied for determination of penicillin G in pharmaceutical formulations.



**202. Optical Sensors in Flow Injection Analysis, O. S. Wolfbeis; *J. Mol. Struct.* 292 (1993) 133-140.** DOI: 10.1016/0022-2860(93)80096-E

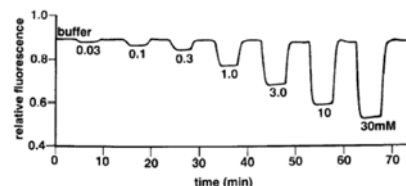
**Abstract.** Representative examples are given on how optical chemical sensors (optrodes) can be coupled to flow injection systems to result in flow injection analyzers. These have served two main purposes so far, namely testing the performance of optodes, and secondly as detectors in flow injection analysis (FIA). Specifically, the use of optrodes sensitive to pH, oxygen, ammonia and other chemical species as detectors in FIA will be described, all mainly in conjunction with enzymatic reaction schemes. Finally, optrodes are shown to be useful for determination of enzyme activity and enzyme inhibition by heavy metals.

The Fig. shows a schematic of the FIA manifold with fiber optic detection. Light from a source (LS) is guided through one bundle of the bifurcated fiber optic waveguide (BFB) to the optical sensor membrane placed in the flow-through cell (FTC). Reflected or fluorescent light is guided back to the detector (PMT) and the resulting electrical signal is recorded in R. The carrier stream (C) is propelled with a pump (P). The sample (S) is introduced by means of an injection valve (V). After passing a mixing chamber (MC), the flow passes an air damper (AD), and analyte concentrations eventually are detected in the FTC. In case of biosensors, an enzyme bed reactor is placed between V and MC, or between MC and AD.



**200. Optical Biosensor for Lysine Based on the Use of Lysine Decarboxylase and a Cadaverine-Sensitive Membrane, H. Li, H. He, O. S. Wolfbeis; *Biosensors Bioelectronics* 7, 725-732 (1992).** DOI: 10.1016/0956-5663(92)85055-F

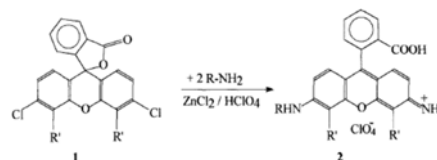
**Abstract:** We describe an optical biosensor for lysine based on the use of lysine decarboxylase and an optical transducer for detection of cadaverine which is formed as a result of enzymatic action. A plasticized pvc membrane containing a lipophilic tartrate as the amine carrier acts as the optical cadaverine sensor, and N,N'-dioctadecylrhodamine (described in paper 199 below) acts as the proton carrier/receptor. The dynamic range is from 0.1 to 100 mM for both cadaverine and lysine. The sensor is highly specific for lysine, nicotine being the only major interferent. Unlike in other enzyme-based detection schemes where the production of carbon dioxide (in case of decarboxylases) or consumption of oxygen (in case of oxidases) is measured, this scheme is based on the measurement of the organic ammonium ion (cadaverin cation) formed in the enzymatic reaction. The major advantage of this approach is due to the fact that in many real samples there is rather low and fairly constant background of organic amines.



The graph shows the fully reversible response of this sensor to various concentrations of cadaverine.

**199. New Lipophilic Rhodamines and Their Applications to Optical Potassium Sensing, T. Werner, H. He, M. A. Kessler, O. S. Wolfbeis; *J. Fluoresc.* 2 (1992) 93-98.** DOI: 10.1007/BF00867668

**Abstract:** New lipophilic fluorescent rhodamines were synthesized directly from 3,6-dichlorofluoresceins and the respective long-chain amines with excellent solubility in lipids and lipophilic membranes. Spectrophotometric and luminescent properties of the dyes are reported and discussed with respect to their application in new optical ion sensors. One rhodamine (2a) was applied in a poly(vinyl chloride)-based sensor membrane for continuous and sensitive optical determination of potassium ion, using valinomycin as the neutral ion carrier.



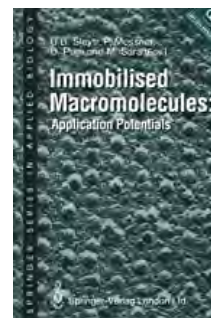


**198. Book Chapter: Immobilised Enzymes in Optical Biosensors**, O. S. Wolfbeis; in: *Immobilized Macromolecules: Application Potentials*, U. B. Sleytr, P. Messner, D. Pum, M. Sara (eds.), *Springer Series in Applied Biology* (Springer, London), chapter 11, pp. 161-174 (1992). ISBN: 978-1-4471-3481-7. DOI: 10.1007/978-1-4471-3479-4\_11

**Abstract:** Optical sensor technology has emerged in the past 15 years as an attractive alternative to existing sensory schemes such as electrochemistry. This is the result of a number of advantages of optical sensors over others which can include one or more of the following:

- (i) inertness to electromagnetic interference;
- (ii) the redundancy of reference cells;
- (iii) negligible cross talk.

This review covers all existing optical biosensors based on the use of immobilised enzymes and of chemical transducers (such as sensors for pH, oxygen, NH<sub>3</sub> or CO<sub>2</sub>).



**197. Review. Fiber Optic Biosensing Based on Molecular Recognition**, O.S. Wolfbeis; *Sensors Actuat. B5* (1992) 1-6. DOI: 10.1016/0925-4005(91)80212-3

**Abstract:** A review is given on the use of specific biorecognition elements (such as enzymes or optically active receptors) in optical sensing of chemical species. In enzyme-based sensors various options exist: depending on which species is immobilized, assays for substrates (such as glucose, lactate or cholesterol), enzymes (such as carboxylesterase) or inhibitors (such as organophosphates) can be designed. Respective examples are given. In the second part it is discussed how the intrinsic optical properties of certain enzymes or metabolites can be utilized for sensing purposes. In contrast to enzymes which 'digest' their substrates, the use of optically active receptors which do not metabolize their target molecules offers a scheme for specific recognition of substrates by a receptor. If the receptor is enantio-selective (i.e., preferentially binds one species out of a pair of optical isomers), a fairly specific recognition of enantiomers of biogenic amines (such as the β-blocker propranolol) becomes possible. In contrast to enzyme-based sensing where steady-state response is a result of kinetic equilibration, this type of substrate binding results in thermodynamic equilibria. Specific examples are given for each sensor type, and their respective limitations are discussed.

**TABLE 1.** Selection of biochemical analytes for which enzyme-based sensors have been described, and respective transducers<sup>a</sup>

Analyte	Enzyme	Transduction via
Glucose	glucose oxidases	pH, O <sub>2</sub>
	glucose dehydrogenase	<sup>b</sup>
Lactate	lactate mono-oxygenase	O <sub>2</sub> , CO <sub>2</sub>
	lactate oxygenase	O <sub>2</sub>
	cholesterol oxidase	O <sub>2</sub>
Cholesterol	cholesterol oxidase	O <sub>2</sub>
Ascorbate	ascorbate oxidase	O <sub>2</sub>
Bilirubin	bilirubin oxidase	O <sub>2</sub>
	ethanol oxidase	O <sub>2</sub>
Ethanol	alcohol dehydrogenase	O <sub>2</sub>
	urease	NH <sub>3</sub> , NH <sub>4</sub> <sup>+</sup>
Urea	urease	NH <sub>3</sub> , NH <sub>4</sub> <sup>+</sup>
Uric acid	uricase	O <sub>2</sub>
Penicillin	penicillinase	pH
Glutamate	glutamate decarboxylase	CO <sub>2</sub>
	glutamate oxidase	O <sub>2</sub>
Oxalate	oxalate decarboxylase	CO <sub>2</sub>

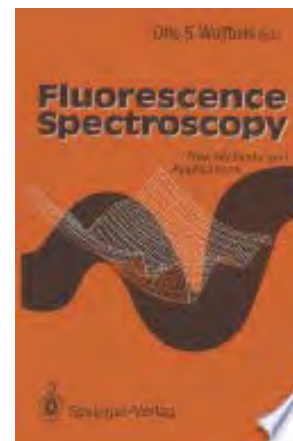
<sup>a</sup>Data from ref. 2 where the respective references may be found, with additional data from [7, 8] and unpublished results of the author's group.

<sup>b</sup>Through formation of fluorescent NADH.

**196. Book: Fluorescence Spectroscopy: New Methods and Applications**, O. S. Wolfbeis (ed.), Springer Verlag, Heidelberg, 1993; ISBN 3-540-55281-2. DOI: 10.1007/978-3-642-77372-3.

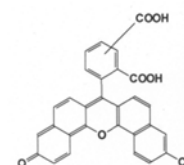
With chapters on

- \* Fluorescence Spectroscopy: Where We Are and Where We're Going (by S. G. Schulman)
- \* Interactions and Kinetics of Single Molecules as Observed by Fluorescence Correlation Spectroscopy
- \* Fast Optical Imaging Techniques (by C. D. MacKay)
- \* Kinetic Studies on Fluorescent Probes Using Synchrotron Radiation (by W. Rettig)
- \* Dynamics and Geometry in Dimeric Flavoproteins from Fluorescence Relaxation Spectroscopy (by A. Visser)
- \* Fluorescence Spectroscopy of Light Scattering Materials (by D. Oelkrug)
- \* Optical Sensors Based on Fluorescence Quenching (by W. Trettnak)
- \* Fluorescence in Forest Decline Studies (by H. Schneckenburger)
- \* Fluorescence Microscopy Studies of Structure Formation in Surfactant Monolayers (by H. Möhwald)
- \* Fluorescence Lifetime Imaging and Application to Calcium(II) Imaging (by J. R. Lakowicz)
- \* Ether Phospholipids in Membranes: Applications of Physe and Steady-State Fluorometry (by A. Hermetter)
- \* Pyrene-labelled Lipids as Fluorescent Probes in Studies on Biomembranes (by P. Kinnunen)
- \* Optical Detection of Intracellular Ion Concentrations (by J. Slavik)
- \* Analytical Applications of Very Near-IR Fluorimetry (by J. N. Miller)
- \* Fluorescence Detection in Flow Injection Analysis (by M. Valcarcel)
- \* Fluorescence Spectroscopy in Environmental and Hydrological Sciences (by M. C. Goldberg)
- \* Fluorescence Polarization Immunoassay (by C. Klein)
- \* Progress in Delayed Fluorescence Immunoassay (by I. Hemmilä)



**195. LED-Compatible Fluorosensor for Measurement of Near-Neutral pH Values**, O. S. Wolfbeis, T. Werner, N. V. Rodriguez and M. Kessler, *Microchim. Acta* **108**, 133-141 (1992). DOI: 10.1007/BF01242422

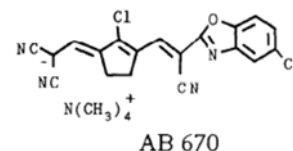
**Abstract:** We report on an optical sensor material suitable for fluorimetric measurement of pH in the 6 - 9 range using a new and LED-compatible fluorescent dye of the naphthofluorescein type. Its base form has a strong absorption band between 580 and 630 nm that matches the emission wavelengths of conventional yellow or orange LEDs. Two kinds of dye immobilization are reported. The first is based on covalent binding to a cellulosic matrix and the resulting material is intended for use in sensing membranes. The second involves physical entrapment of the dye in a sol-gel matrix which can be used for optical fiber tip coating and in evanescent wave type sensors. Both kinds of sensor materials are studied with respect to dynamic pH ranges, response times, sensitivity toward ion strength, and stability.



**194. Nonimmunological Assay for Urinary Albumin Based on Laser-induced Fluorescence**, M. A. Kessler, M. R. Hubmann, B. A. Dremel & O.S. Wolfbeis; *Clin. Chem.* **38**, 2089-2093 (1992). DOI: 10.1093/clinchem/38.10.2089

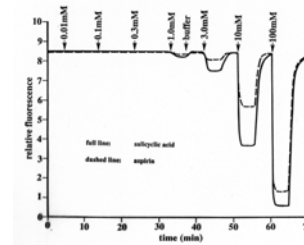
**Abstract:** We describe the first nonimmunological assay of albumin in urine with a detection limit of 1

mg/L. The method is simple, rapid, and accurate. It is based on the probe Albumin Blue 670, which becomes highly fluorescent on binding to albumin. An inexpensive diode laser was used as the light source for measurement of laser-induced fluorescence. The assay was coupled to a flow-injection anal. system capable of running 20 samples per h. The working range is from 1 to 100 mg/L, which covers albumin concs. found in non-pathological urine and pathological urine. This range made prediction of nephropathy possible at an early stage. Other serum proteins and Hb do not interfere. The coeffs. of variation were <4% and <7% within one day and from day to day, resp. A correlation coefficient of 0.990 (n = 100) was obtained for comparison with the Behring nephelometric assay.



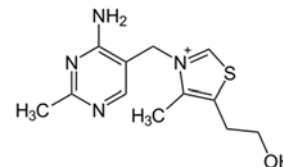
**192. Optical Sensor for Salicylic Acid and Aspirin Based on a New Lipophilic Carrier for Aromatic Carboxylic Acids, H. He, G. Uray, O. S. Wolfbeis; *Fresenius J. Anal. Chem.* **343**, 313-318 (1992). DOI: 10.1007/BF00322381**

**Abstract:** The sensor with high selectivity for salicylate and aspirin is based on a new lipophilic carrier for aromatic carboxylic acids, namely ( $\pm$ ) n-butyl O-(1-naphthylaminocarbonyl) lactate (BNAL). The sensing scheme involves co-extraction of both salicylate anion and a proton from the aqueous sample medium into a pvc layer using BNAL as a salicylate carrier, and a pH-sensitive dye as a lipid proton carrier, both contained in the PVC membrane. BNAL transports the salicylate anion into the pvc lipid membrane. The transport of the analyte is coupled to a proton transport. As a result, the dye undergoes a color change which is detected via measurement of fluorescence intensity. The sensor has a dynamic range from 0.1 to 30 mM salicylate at pH 5.00, but the response function is highly pH-dependent. The figure shows the reponse of the sensor to salicylate and aspirin.



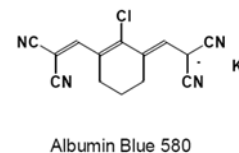
**191. A Thiamine-Selective Optical Sensor Based on Molecular Recognition, H. He, G. Uray, O. S. Wolfbeis; *Anal. Lett.* **25** (1992) 405-415. DOI: 10.1080/00032719208016104**

**Abstract:** A thiamine-selective optrode based on the use of new lipophilic esters of tartaric acid as thiamine carriers and a lipophilic fluorescent pH indicator dissolved in a PVC membrane is presented. The carrier transports thiamine dication into the PVC membrane, and one or two protons are released simultaneously from the dye which thereby undergoes a color change. The sensor is fully reversible, and responds to thiamine in the concentration range from 0.01 to 100 mM. Interferences by other nitrogen heterocycles out of the vitamin B group and of various purines and amines have been investigated, and the optical selectivity coefficients for vitamins B2, B3, B4, B6, and some purines and alkaloids were calculated. Cinchonidine, N,N-dimethylaniline, triethylamine and riboflavin interfere strongly, the latter due to its strong intrinsic fluorescence. The riboflavin interference can be overcome by shifting both the excitation and emission to longer wavelengths. All other substances tested can be tolerated up to an about hundred-fold excess. The method has been applied to determine thiamine in multivitamin formulations and the results were found to be satisfactory. In contrast to the majority of sensing schemes for bio-organic molecules, the one presented here does not involve an enzyme or any other biological component. Hence the sensor does not suffer from the typical disadvantages of protein-based sensors.



**188. Laser-induced Fluorometric Determination of Albumin Using Longwave Absorbing Molecular Probes, M. A. Kessler, O.S. Wolfbeis; *Anal. Biochem.* **200**, 254-259 (1992). DOI: 10.1016/0003-2697(92)90462-G**

**Abstract:** A novel fluorescence assay for HSA is described. It is based on longwave-absorbing probes that selectively bind to HSA to form fluorescent complexes. The two probes reported here (Albumin Blue 633 and Albumin Blue 670) are tailored to match the lines of the 633-nm HeNe laser and the 670-nm diode laser, respectively. In both cases, the strong laser-induced fluorescence (LIF) of the HSA/probe complexes makes the assay sensitive to HSA at trace levels. Detection limits of 0.2 mg/L were obtained. The assay is highly selective for HSA in that the response to other serum proteins is weaker by a factor of at least 100. Potential interferents are bovine serum albumin (BSA) and some detergents. Parameters of the probe - HSA interaction were obtained from a Scatchard evaluation. The assay presents a promising alternative to immunological determinations of HSA.



**186. Book Chapter: Applications of Optochemical Sensors for Measuring Environmental and Biochemical Quantities, W. Trettnak, M. Hofer, O. S. Wolfbeis; in: *Sensors: A Comprehensive Survey*, W. Goepel, J. Hesse, J. N. Zemel (eds.), VCH Publ., Weinheim, 1991, vol. 3/II, chapter 18, pages 931-967. DOI: 10.1002/9783527619269.ch5b**

**Summary:** This chapter contains sections entitled Environmental Sensors; In Vivo Sensors for Chemical Species; Biosensors; References.

**185. Book Chapter: Applications of Optochemical Sensors for Measuring Chemical Quantities, O. S. Wolfbeis, G. Boisdè, in: *Sensors: A Comprehensive Survey*, W. Goepel, J. Hesse, J. N. Zemel (eds.), VCH Publ., Weinheim, 1995, vol. 3/II, chapter 17, pages 867-930. ISBN: 9783527620135; DOI: 10.1002/9783527619269.ch4b**

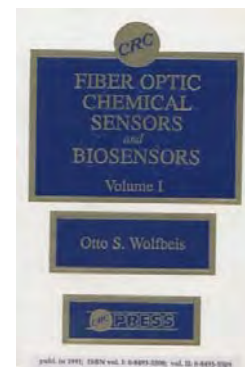
**Summary:** This chapter contains sections entitled - pH and Electrolyte Sensors; - Gas Sensors; - Optical Fibers in Process Control; - References.

**184. Book Chapter: Optochemical Sensors, O. S. Wolfbeis, G. Boisdè, G. Gauglitz, in: *Sensors: A Comprehensive Survey*, W. Goepel, J. Hesse, J. N. Zemel (eds.), VCH Publ., Weinheim, 1991, vol. 2/I, chapter 12, p. 573-645. DOI: 10.1002/9783527619269.ch12**

**Summary:** This chapter contains section entitled - Optical and Fiber Optic Sensors; - Light Guides; - Optical Sensing Principles; - References.

183. **Book Edited: Fiber Optic Chemical Sensors and Biosensors**, O. S. Wolfbeis (ed.), CRC Press, Boca Raton, Florida, volumes 1 (413 p.) and 2 (358 p.); 1991. ISBN 0-8493-5508-7 and 0-8493-5509-5.

*Contents:* 1. Introduction (O. S. Wolfbeis); 2. Spectroscopic Techniques (O. S. Wolfbeis); 3. Sensing Schemes (O. S. Wolfbeis); 4. Guided Wave Optics (O. Parriaux); 5. Intrinsic Fiberoptic Chemical Sensors (R. Lieberman); 6. Instrumentation for Fiber Optic Chemical Sensors (D. N. Modlin, F. P. Milanovich); 7. Sensor Chemistry (E. Koller, O. S. Wolfbeis); 8. pH Sensors (M. Leiner); 9. Electrolyte Sensors (W. R. Seitz); 10. Oxygen Sensors (O. S. Wolfbeis); 11. Gas Sensors (O. S. Wolfbeis); 12. Environmental Monitoring Applications of Fiber Optic Chemical Sensors (S. M. Klainer, K. Goswami, D. K. Dandge, S. J. Simon, N. R. Herron, D. Eastwood); 13. Fibers in Titrimetry (O. S. Wolfbeis); 14. Fiber Optic Chemical Sensors in Nuclear Plants (G. Boisdé, F. Blanc, P. Mauchien, and J. J. Perez); 15. Temperature Sensors (K. T. V. Grattan); 16. Transducer-Based and Intrinsic Biosensors (M. Arnold, J. Wangsa); 17. Immunosensors (T. Vo-Dinh, G. D. Griffin and M. J. Sepaniak); 18. Construction and Performance of an In-Vivo Oxygen Sensor (J. I. Peterson); 19. Biomedical and In-Vivo Applications of Fiber Sensors (O. S. Wolfbeis); 20. Chemiluminescence and Bioluminescence Based Fiber Optic Probes (L. J. Blum and P. R. Coulet); 21. Fiber Optic Chemoreception (U. J. Krull).



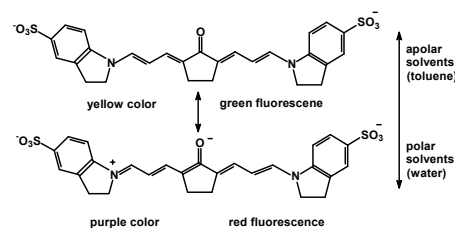
182. **Book Chapter: 2-Benzopyrylium-Salze**, M. A. Kessler, O. S. Wolfbeis; in: *Houben-Weyl: Methods of Organic Chemistry*, vol. E7a (Hetarene II), R. P. Kreher (Hrsg.), Georg Thieme Verlag, Stuttgart, 1991, 171-204. In German. Web: <https://www.thieme-connect.de/products/ebooks/lookinside/10.1055/b-0035-116492>

180. **LED-Compatible Fluoresensor for Ammonium Ion and Its Application to Biosensing**, O. S. Wolfbeis, H. Li, *Proc. SPIE (Soc. Photo-Instrum. Eng.)* **1587** (1991) 48-58. DOI: 10.1117/12.56532

*Abstract:* We present a fluorescence-based sensing scheme for ammonium ion using nonactin as the receptor/carrier. The ammonium-sensitive material consists of a PVC membrane containing the nonactin, a plasticizer, and a proton carrier (lipophilic Nile Blue). Sensing is based on the selective extraction of the ammonium ions into the PVC membrane, and a concomitant release of a proton from the dye, contained in the PVC membrane, into the sample solution. Upon deprotonation, the dye undergoes a color change from blue to red which is detected via fluorescence intensity measurements. The sensor fully reversibly responds to ammonium ion, with detection limits varying from 0.03 to 10 mM at near neutral pH. Response times are about 1 min for membrane thicknesses of ca. 2 micrometers. The sensor is fully compatible with solid-state electronics (i.e., LED light sources and photodiode detectors) but suffers from a strong pH dependence of the signal so that the pH of the sample must be kept constant. The sensor is of potential utility in monitoring ammonium ion in wastewater and surface water samples, but may also act as a transducer in all kinds of biochemical reactions during which ammonium ion is released or consumed. Examples of biosensors for urea and creatinine are given.

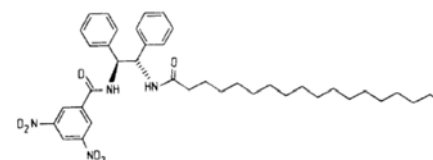
179. **Optical Sensor for On-line Determination of Solvent Mixtures Based on a Fluorescent Solvent Polarity Probe**, M. A. Kessler, J. G. Gailer, O. S. Wolfbeis; *Sensors Actuators B3*, 267-272 (1991). DOI: 10.1016/0925-4005(91)80016-D

*Abstract:* The new optical sensor for determination of solvent mixtures (such as water in organic solvent) is based on a fluorescent solvent polarity probe immobilized on an ion-exchange membrane. The probe responds to changes in polarity by both a shift in the fluorescence emission maximum and a change in the fluorescence quantum yield. The relative fluorescence intensity measured at 620 nm and 500 nm excitation serves as the analytical information. The sensor can be applied over a wide range of solvents. The response time is in the order of 15 s.



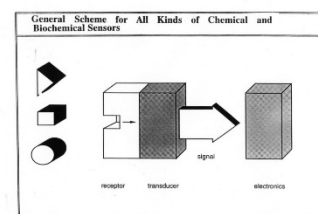
178. **Enantioselective Optrode for Optical Isomers of Biologically Active Amines Using a New Lipophilic Aromatic Carrier**, H. He, G. Uray, O. S. Wolfbeis; *Proc. SPIE*, **1510** (1991) 95-103. DOI: 10.1117/12.47128

*Abstract:* This paper presents a method for optically sensing enantiomers (optical isomers) of biological amines such as norephedrine, and drugs such as the  $\beta$ -blocker propranolol. It is based on the use of a new lipophilic chiral ammonium ion carrier (DODD; see the formula on the right) and a highly fluorescent lipophilic proton carrier (DZ 49) dissolved in a PVC membrane. Recognition of one of the enantiomers is accomplished by specific interaction of the amine with the optically active lipophilic substrate in a PVC membrane. The amine, which is present as an ammonium ion at physiological pH, is carried into the PVC membranes. Simultaneously, a proton is released from the proton carrier (a lipophilic xanthen dye) that thereby undergoes a change in both color and fluorescence intensity. The sensors respond to three analytes in the concentration range from 0.01 to 10 mM for propranolol, 0.3 to 100 mM for norephedrine, and 1 to 100 mM for 1-phenylethylamine. The selectivity coefficients ( $K_{opt}$ ) are 0.8, 0.7, and 0.8 for propranolol, norephedrine, and 1-phenylethylamine, respectively. It is of potential utility for specifically recognizing one out of several isomers, in particular bioactive amines, where one form usually is active only. The carrier showed stronger affinity for compounds which contain naphthyl rather than phenyl substituents.



177. **Review. Optical Sensing Based on Analyte Recognition by Enzymes, Carriers and Molecular Interactions**, O. S. Wolfbeis; *Anal. Chim. Acta* **250**, 181-201 (1991). DOI: 10.1016/0003-2670(91)85071-Y

*Abstract:* A review is given on how the use of enzymes, ion carriers, and natural or synthetic receptors or carriers that undergo specific interactions with the species to be recognized can result in specific recognition and, consequently, sensing.





**175. Book Chapter: Chemically Mediated Fiber Optic Biosensors**, B. P. H. Schaffar, O. S. Wolfbeis; in: *Biosensors Principles and Applications*, L. J. Blum, P. R. Coulet (eds.), M. Dekker, New York, chapter 8, pp. 163-194 (1991). DOI: 10.1201/9780367810849-8

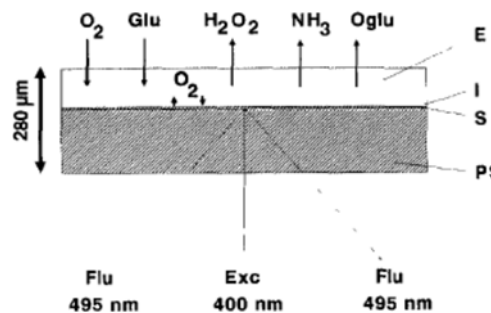
*Abstract:* Numerous types of fiberoptic chemical sensors are likely to be useful as transducers in fiberoptic biosensors (FOB). The field of FOB can be divided into two main classes, the intrinsic or non-mediated FOB and the chemically mediated FOB. Single-fiber-based FOB is imperative if measurements are to be performed in small sample volumes, as in many in vivo applications. FOB has been tested with nonreal samples, such as stock solutions in distilled water and/or defined buffers in well-thermostated sensor cells. Sensors are classified according to the type of transducer to point out that choice of an appropriate transducer is of great importance to the performance characteristics of the FOB. Also, the same transducer was used, namely a fiberoptic oxygen sensor based on the quenching of the fluorescence intensity of decacyclene dissolved in silicone rubber. A general drawback using pH optodes as transducers for FOB is the influence of both pH and buffer capacity of the analyte solution to the measured signal.

**174. Series Volume Edited: Chemical and Medical Sensors, Proc. of the 4. Eur. Congress on Optics**, 12/13 March 1991, The Hague, Netherlands, O. S. Wolfbeis (ed.), *Proc. SPIE (Soc. Photoinstrum. Eng.)*, vol. **1510**, 1-242 (1991). ISBN 0-8194-0619-8.

**173. Comparison of Two Fibre Optic L-Glutamate Biosensors Based on the Detection of Oxygen or Carbon Dioxide, and Their Application in Combination with Flow-Injection Analysis to the Determination of Glutamate**, B. A. A. Dremel, R. D. Schmid, O. S. Wolfbeis; *Anal. Chim. Acta* **248** (1991) 351-359. DOI: 10.1016/S0003-2670(00)84651-6

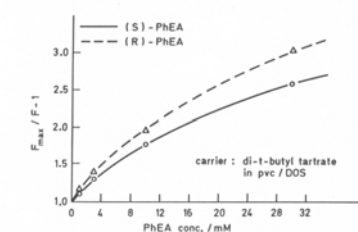
*Abstract:* A flow-injection system for the fibre-optical determination of l-glutamate in food and pharmaceutical preparations that makes use of two kinds of fibre-optic biosensors is presented. In the first type, an oxygen-sensitive optrode was covered with a membrane onto which was immobilized l-glutamate oxidase. The decrease in oxygen partial pressure in the presence of glutamate as a result of enzymatic reaction was determined via dynamic quenching of the fluorescence of an oxygen-sensitive indicator dye.

In the second type, a carbon dioxide-sensitive optrode was covered with a membrane of immobilized l-glutamate decarboxylase. The production of carbon dioxide in the presence of substrate was determined via the changes in the pH of a carbon dioxide sensor consisting of a membrane-covered pH-sensitive fluorescent pH indicator dye entrapped in a hydrogencarbonate buffer. The oxygen optrode-based glutamate biosensor shows a linear response from 0.02 to 1.0 mM glutamate with a relative standard deviation (r.s.d.) of 3% at the 2 mM level (5 measurements). The carbon dioxide optrode-based glutamate biosensor shows a linear response from 0.1 to 2.5 mM glutamate, with an r.s.d. of 3% at the 2.5 mM level (5 measurements). The application of both biosensor optrodes to determinations of l-glutamate in food and pharmaceutical samples is demonstrated. The advantages and disadvantages of both the oxygen and carbon dioxide optrodes are discussed in terms of sensitivity, selectivity and response time.



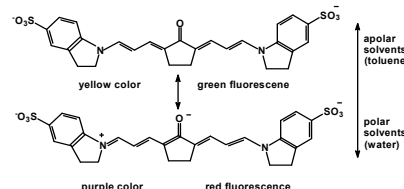
**172. Enantio-Selective Optodes**, H. He, G. Uray, O. S. Wolfbeis; *Anal. Chim. Acta* **246** (1991) 251-257. DOI: 10.1016/S0003-2670(00)80958-7

*Abstract:* Enantio-selective optical sensors (optodes) for ammonium ions of 1-phenylethylamine, propranolol and norephedrine based on the use of four different lipophilic (R, R)-tartrates as the carriers have been developed. The sensing scheme is based on the selective extraction of the organic ammonium ions into a poly(vinyl chloride) lipid membrane, and a concomitant release of a proton from a protonated dye, contained in the pvc membrane, into the sample solution. Upon deprotonation, the dye undergoes a color change that can be detected optically. The sensor is fully reversible, with detection limits varying from 0.007 to 0.7 mM for 1-phenylethylamine, 0.006 to 0.07 mM for propranolol, and 0.7 to 7.0 mM for norephedrine at near neutral pH. The differences in the free energies of the two enantiomeric complexes ( $\Delta\Delta G$ ) as well as the enantiomer selectivity coefficients were calculated from the calibration curves. Although the best selectivity coefficient was found for norephedrine (0.5) using (1R, 2S, 5R)-dimethyl (R, R)-tartrate as the receptor (carrier), (R,R)-di-tert.-butyl tartrate is found to be by far more effective in all other cases.



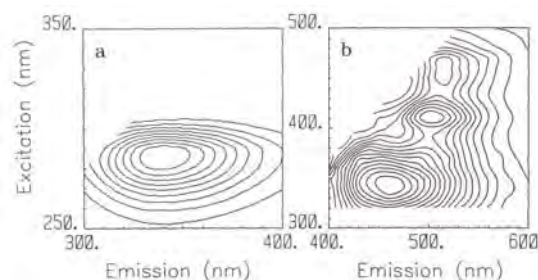
**171. New Highly Fluorescent Ketocyanine Polarity Probes**, M. A. Kessler, O. S. Wolfbeis; *Spectrochim. Acta, Part A* **47A** (1991) 187-192. DOI: 10.1016/0584-8539(91)80090-6

*Abstract:* The syntheses and spectral properties of three new and highly fluorescent solvent polarity probes are described. They are found to be extremely sensitive to solvent polarity in that spectral red shifts in both absorption and fluorescence spectra occur upon increasing solvent polarity. The emission data are compared with the standard  $E_T^N$  values of solvent polarity and a linear correlation is obtained over a wide range.



**169. Book Chapter: Total Luminescence Spectrometry and Its Application in the Biomedical Sciences**, M. J. P. Leiner, M. R. Hubmann, & O.S. Wolfbeis; in: *Luminescence Techniques in Chemical and Biochemical Analysis*, W. R. G. Baeyens, D. de Keukeleire and K. Korkidis (eds.), M. Dekker, New York, 1991, chapter 12, pp. 381 - 420. ISBN 9780824783693.

*Abstract:* A review on how 3-dimensional fluorescence spectra can be acquired in the form of a 2-dimensional matrix (left graph), and how the resulting data and patterns can be used in bioanalytical sciences. The graphs are the 3D emission spectra of human blood serum in the UV (a) and in the visible (b) part of the spectrum.



**168. Enantioselective Optode for the  $\beta$ -Blocker Propranolol, H. He, G. Uray, O. S. Wolfbeis; *Proc. SPIE*, vol. 1368 (1990) 175-181. DOI: 10.1117/12.24805**

**Abstract:** We present a scheme for sensing optical isomers (enantiomers) of biogenic amines such as the Bblocker propranolol. Recognition of one of the enantiomers of propranolol is accomplished by specific interaction of the amine (which is present in the protonated ammonium form at physiological pH) with an optically active substrate (dibutyl tartrate) in a PVC membrane. As the ammonium ion is carried into the PVC membrane a proton is simultaneously released from the proton carrier (a lipophilic phenolic xanthene dye which undergoes protolytic dissociation in the pvc membrane) which thereby suffers a color change. The sensor responds to propranolol but also to other biogenic amines such as 1-phenylethylamine and norephedrine in the 20  $\mu$ M to 10 mM range but has a pH-dependent response. The selectivity factors depend on the type of receptor and range from 0.0 to 0.30.

**167. Feasibility of Optically Sensing Two Parameters Simultaneously Using One Indicator, O. S. Wolfbeis; *Proc. SPIE (Soc. Photo-instrum. Eng.)* 1368 (1990) 218-222. DOI: 10.1117/12.24791**

**Abstract:** Two approaches are described for determination of two parameters simultaneously by using only one fluorescent indicator. The first is based on multi-wavelength analysis of the fluorescence excitation or emission spectrum of the pH indicator HPTS. The second is based on amplitude and lifetime analysis of the emission spectra. Both methods are suitable for determination of two species simultaneously but using only one indicator, provided one parameter (such as pH value) affects the ground state (absorption) properties, and the other affects the excited state properties (oxygen). Various other indicators are suggested for use in dual sensing, for example of pH/temperature,  $pCO_2/O_2$ , pH/chloride.

**Table 1. Potential dyes, optical parameters, and measurands in determination of two parameters using one optical indicator**

Indicator	Parameter # 1 (intensity)	Parameter # 2 (lifetime)
HPTS*)	pH	oxygen
7-hydroxycoumarins	pH	temperature (oxygen)
HPTS	$pCO_2$	oxygen
fluorescein	pH	oxygen
7-hydroxy-1-methyl-quinolinium ion	pH	chloride

\*) or other hydroxyxyrenes

**166. Fluorescence Based Optrodes for Alkali Ions Based on the Use of Ion Carriers and Lipophilic Acid/Base Indicators, H. He, O. S. Wolfbeis; *Proc. SPIE*, 1368 (1990) 165-174. DOI: 10.1117/12.24786**

**Abstract:** We present fluorosensors for potassium calcium and ammonium based on the use of ion carriers and a highly fluorescent lipophilic proton carrier. Fluorescent potassium-sensitive membranes have been prepared by dissolving chemically modified Nile Blue and valinomycin in a pvc/plasticizer mixture. Valinomycin being a highly selective potassium carrier binds potassium ion and carries it into the membrane. Simultaneously in order to maintain electro-neutrality of the membrane a proton dissociates from the proton carrier (Nile Blue) dissolved in the pvc membrane and diffuses into the aqueous phase. The dissociation of the protonated amino group of Nile Blue causes its color to change from blue to red. Depending on the choice of the excitation wavelength both the decrease in the fluorescence of the blue species and the increase in the fluorescence of the red species can be monitored. The sensor fully reversibly responds to potassium over the 100  $\mu$ M to 100 mM concentration range. By replacing valinomycin by carriers for ammonium and calcium ion the respective sensors are obtained. It also is found that the addition of hydroxylic plasticizers to the membrane material considerably accelerates the response time in both directions. While this kind of sensor suffers from cross sensitivity toward pH it has the advantage of full solid-state compatibility (LEDs or diode lasers may be used as light sources).

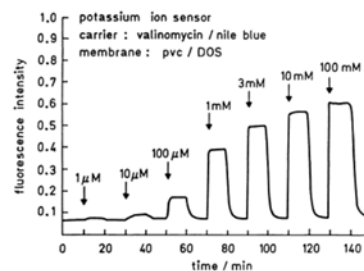
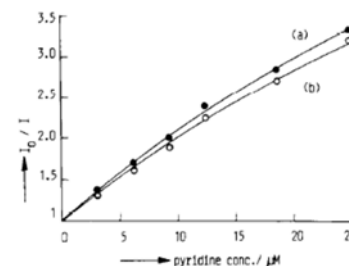


**Fig. 1. Relative signal changes, analytical range, and response time of the potassium fluorosensor using valinomycin as the ion carrier. Solvent: 0.1 M Tris buffer of pH 7.38**

**165. Extremely Efficient Quenching of the Fluorescence of Skatole by Pyridine, A. Sharma, O. S. Wolfbeis, M. K. Machwe, *Anal. Chim. Acta* 230 (1990) 213-215. DOI: 10.1016/S0003-2670(00)82785-3**

**Abstract:** The quenching of the fluorescence of skatole ( $\beta$ -methylindole) by pyridine has been studied in water and ethanol. Extremely efficient quenching is observed, which may be explained on the basis of the formation of a charge-transfer complex between skatole and pyridine. The findings are considered to be of potential utility for the development of methods for the determination of pyridine at sub- $\mu$ g ml<sup>-1</sup> levels.



**163. Oxygen Optrode for Use in a Fiber Optic Glucose Biosensor, M. C. Moreno-Bondi, O. S. Wolfbeis, M. J. P. Leiner and B. P. H. Schaffar, *Anal. Chem.* 62, 2377-2380 (1990). DOI: 10.1021/ac00220a021**

**Abstract:** Tris-(1,10-phenanthroline)-ruthenium(II) cation is adsorbed on silica gel, incorporated in a silicone matrix, and placed at the tip of the optical fiber. Oxygen has been monitored continuously in the 0 to 750 torr range, with the detection limit being as low as 0.7 torr. The device has been applied to the development of a fast responding and highly sensitive fiber optic glucose biosensor based on this highly sensitive oxygen transducer. The sensor relates oxygen consumption (as a result of enzymatic oxidation) to glucose concentration. The enzyme is immobilized on the surface of the oxygen optrode; carbon black is used as an optical isolation in order to prevent ambient light and sample fluorescence to interfere. Analytical ranges are from 0.06 to 1 mM glucose. The graph shows a cross section, with E being the enzyme, C a layer of carbon black, R the oxygen sensor layer, and P is the polyester support.



**162. Book Chapter: Fiberoptic Sensors in Bioprocess Control**, O. S. Wolfbeis; in: *Sensors in Bioprocess Control*, J. V. Twork, A. M. Yacynych (eds.), Taylor & Francis, New York, 1990; chapter 6, pp. 95-125. ISBN 9780367450823. DOI: 10.1201/9781003066408-6

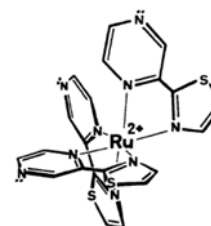
**Abstract:** This chapter gives an overview on the principles and applications of optical sensors, with particular emphasis given to problems associated with bioprocess control. Similar instrumentation may be used when absorbance, reflectance, or Raman scatter intensity are to be measured. A typical example is provided by the glucose detection principle: Glucose can be oxidized by the enzyme glucose oxidase to give gluconic acid (H) and hydrogen peroxide under consumption of oxygen. The following optical parameters have been used so far in spectroscopic sensors: absorbance, reflectance, interferometry light scattering, fluorescence intensity, fluorescence lifetime, chemiluminescence, phosphorescence, thermoluminescence, and refractive index. Absorbance-based measurements have been applied in optical sensing much less often than reflectance or fluorometry, because most real samples are too strongly colored to allow precise absorbance measurements, and because absorbance methods cannot be adapted to turbid solutions. The second (and more realistic type in case of FOCS) is diffuse reflection, where the light penetrates the medium and subsequently reappears at the surface after partial absorption and multiple scattering within the medium. Several models for diffuse reflectance have been proposed, all of which consider that incident light is scattered by particles within the medium.

**SENSORS  
IN BIOPROCESS  
CONTROL**

edited by  
John V. Twork · Alexander M. Yacynych

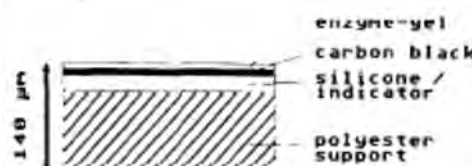
**161. New Luminescent Metal Complex for pH Transduction in Optical Fiber Sensing: Application to a CO<sub>2</sub>-Sensitive Device**, M. C. Moreno-Bondi, G. Orellana, C. Camara, O. S. Wolfbeis; *Proc. SPIE 1368* (1990) 157-164. DOI: 10.1117/12.24785

**Abstract:** The luminescence emission (652 nm) and lifetime (390 ns) of a novel Ru(II) tris-chelate complex tris(2-(2-pyrazinyl)thiazole)ruthenium(II) are quenched by acids (phosphoric acetic phthalic and dihydrogenphosphate) in aqueous solution. The quenching process is shown to occur via a proton transfer to the excited (triplet state) complex since the ground state complex undergoes no protonation in the 0-12 pH interval (pK<sub>a</sub> 1. 9). Quenching rate constants in the range  $1 \times 10^8$  to  $5 \times 10^9 \text{ M}^{-1}\text{s}^{-1}$  have been measured. The pH transducing system has been tested in solution using carbon dioxide and has been applied to the construction of a bifurcated fiber optic chemical sensor for this gas. Advantages of employing Ru(pzth)<sub>3</sub><sup>2+</sup> as a luminescent dye include among others: (1) a hydrogen carbonate buffer is not required in the reservoir chamber and (2) excitation in the visible region using inexpensive plastic optical fibers and collection of the emission through cut-off filters is feasible.



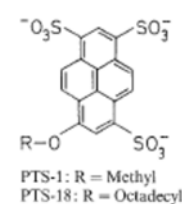
**159. A Fast Responding Fibre Optic Glucose Biosensor Based on an Oxygen Optrode**, B. P. H. Schaffar, O. S. Wolfbeis; *Biosens. Bioelectron.* 5 (1990) 137-148. DOI: 10.1016/0956-5663(90)80004-W

**Abstract:** A fast responding glucose biosensor for the continuous determination of glucose is presented. The biosensor is based on an oxygen optrode, which measures the consumption of oxygen via dynamic quenching of the fluorescence of an indicator by molecular oxygen. Glucose oxidase (GOx) is immobilised onto the surface of this oxygen optrode by adsorption to carbon black and by crosslinking with glutaraldehyde. Carbon black is used as an optical isolation to protect the optrode from the interference of ambient light and sample fluorescence. The measurements were performed in a flow through cell with air saturated glucose standard solutions (phosphate buffered saline of pH 6.9). The effect of four different qualities of GOx in relation to response times (the time required to reach 90% of the steady-state signal), was 8-60 s. The linear analytical range (0.01 to 2 mM glucose) and the long-term stability (t up to 20 weeks) were investigated. A simple device is presented capable of enlarging the analytical range up to 200 mM glucose concentration.



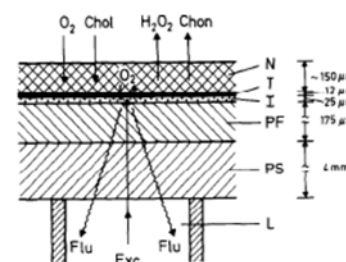
**158. A Sensitive Fluorometric Assay for Cationic Surfactants**, S. Marhold, E. Koller, I. Mayer, O. S. Wolfbeis; *Fresenius Z. Anal. Chem.* 336 (1990) 111-113. DOI: 10.1007/BF00322547

**Abstract:** The fluorimetric assay for cationic surfactants is based on their capability of quenching the fluorescence of 8-octadecyloxy-pyrene-1,3,6-trisulfonate (PTS-18). It is specific for cationic surfactants which can be determined in the 40 - 400 pg concentration range. The method is considered to be advantageous over former methods in that it only requires addition of the sample solution to the fluorophore solution, followed by measurement of fluorescence intensity of the probe. This is in contrast to existing methods where the detergent/dye ion pair has to be extracted before measurement.



**157. Fiber Optic Cholesterol Biosensor with an Oxygen Optrode as the Transducer**, W. Trettnak, O. S. Wolfbeis; *Anal. Biochem.* 184, 124-127 (1990). DOI: 10.1016/0003-2697(90)90023-3

**Abstract:** Cholesterol oxidase is immobilized on a nylon membrane and the consumption of oxygen is measured by following, via fiber optic bundles, the changes in the fluorescence of an oxygen-sensitive dye whose fluorescence is dynamically quenched by molecular oxygen. The dye is dissolved in a very thin silicone membrane placed beneath the enzyme layer. At pH 7.25, the analytical range of the sensor is from 0.2 to 3 mM and the time to reach a full steady state in a flowing solution ranges from 7 to 12 min. The schematic shows a cross section of the sensor layer and the directions of the diffusion of oxygen, H<sub>2</sub>O<sub>2</sub>, cholesterol (Chol) and cholestenone (Chon).



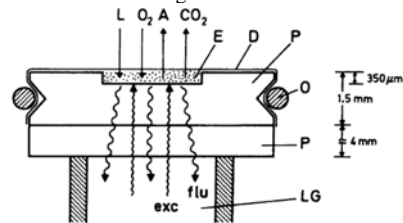
**156. A New Type of Fiber Optic Biosensor Based on the Intrinsic Fluorescence of Immobilized Flavoproteins**, O. S. Wolfbeis, W. Trettnak, *Proc. SPIE 1172* (1989) 287-292. DOI: 10.1117/12.963198

**Abstract:** We describe a new biosensor for monitoring the concentration of enzyme glucose, lactate, and other substrates that are metabolized by an oxidation



process. The method is based on the finding that enzymes having FAD as a prosthetic group change their fluorescence during interaction with a substrate.

Typical enzymes that have been studied include glucose oxidase (GOx), lactate mono-oxygenase (LMOx), and cholesterol oxidase (ChOx). Their fluorescence is monitored via fiber optic light guides at wavelengths above 500 nm, following fluorescence excitation at around 410 - 450 nm. The relative fluorescence intensities of the enzymes vary to a large extent, being highest for LMOx, and rather low for ChOx. Typical detection limits are in the 0.5 mM range for lactate and 1.5 mM for glucose at ambient oxygen pressure. A characteristic feature of this sensor is the narrow dynamic range which usually does not exceed 3 mM. This can be explained in terms of enzyme kinetics and diffusional processes. Unlike optical biosensors based on measurement of the intrinsic fluorescence of NADH, this sensor type has the advantages of full reversibility (because reduced FAD-based enzymes accept oxygen as a second substrate) and analytical wavelengths that are compatible with plastic or glass fiber optics. It is fairly simple in construction because the enzyme acts as both the recognition and transduction element. The method also has been applied successfully in a flow injection analysis-like type of arrangement.

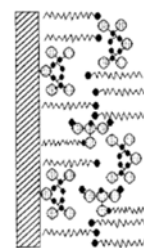


Schematic of the sensor tip. P: plexiglass support; D: dialysis membrane; E: enzyme; O: O-ring; LG: fiber optic light guide; L: lactate; A: acetate.

**154. A Sodium-selective Optrode, B. P. H. Schaffar, O. S. Wolfbeis; *Microchim. Acta* 99 (1989) 109-116. DOI: 10.1007/BF01242796**

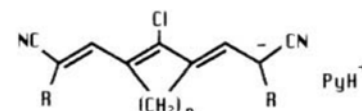
**Abstract.** An ion-selective optrode is presented for continuous determination of sodium ion. It is based on the measurement of the membrane potential between an aqueous sample solution and a lipid membrane phase with the help of a potential-sensitive fluorescent dye. The lipid membrane is composed of the rhodamine B C-18 ester together with the sodium selective ionophore ETH 157 and either arachidic acid or 1-octadecanol, and is prepared by using the Langmuir-Blodgett (LB) technique. The fluorescence intensity of the dye reversibly responds to the sodium ion concentration. Fluorescence decreases with increasing sodium concentration. Interferences by potassium or calcium can be compensated for by using a reference optrode. The sodium sensor works in the 1 to 100 mM sodium ion concentration range with a maximal signal change of - 4.2% of the full scale signal for 100 mM. The relationship between the relative signal change and the negative logarithm of the sodium concentration is linear over two orders of magnitude.

**sodium-selective optrode**



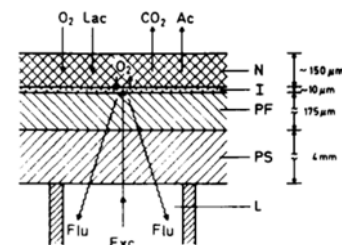
**151. A New He/Ne-Laser Excitable Fluorescent Surfactant Probe, M. A. Kessler, O. S. Wolfbeis; *Ber. Bunsenges. Phys. Chem.* 93 (1989) 927-931. DOI: 10.1002/bbpc.19890930821**

**Abstract.** The fluorescent probe shown at the right is used to probe surfactants and micelles. It can be photoexcited with the He-Ne laser and undergoes a strong increase in fluorescence emission and a longwave shift in the presence of non-ionic and cationic detergents.



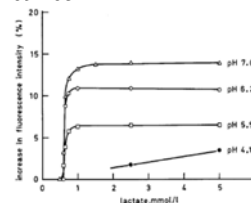
**150. Fiber Optic Lactate Biosensor with an Oxygen Optrode as the Transducer, W. Trettnak, O. S. Wolfbeis; *Anal. Lett.* 22, 2191-2197 (1989). DOI: 10.1080/00032718908051247**

**Abstract.** A biosensor for continuous determination of lactate is presented. Lactate monoxygenase was immobilized covalently on nylon membranes, and the consumption of oxygen was measured by following, via a fiber optic bundle, the changes in the fluorescence of an oxygen-sensitive dye dissolved in 10- and 25-μm silicone membranes placed beneath the enzyme layer. Oxygen is consumed as a result of the oxidation of lactate by the enzyme, and the decrease in its partial pressure is indicated by the fluorescent dye. For two types of sensors, the analytical ranges were from 2 - 50 mM and 0.3 - 6.0 mM, with response times of 2.3 - 3.0 and 4.0 - 6.0 min, respectively. The schematic shows a cross section of the sensor layer and the directions of the diffusion of oxygen, CO<sub>2</sub>, lactate and acetate.



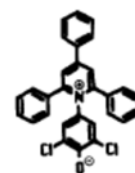
**149. A Fully Reversible Fiber Optic Lactate Biosensor Based on the Intrinsic Fluorescence of Lactate Mono-oxygenase, W. Trettnak, O. S. Wolfbeis; *Fresenius Z. Anal. Chem.* 334 (1989) 427-430. DOI: 10.1007/BF00469465**

**Abstract.** The intrinsic fluorescence intensity of the enzyme lactate monoxygenase is exploited in a new type of lactate biosensor. It is found that the fluorescence quantum yield of the coenzyme FAD changes during its interaction with lactate at the point of saturation. The changes in intensity are fully reversible in the presence of molecular oxygen and can be monitored via fiber optic light guides. Enzyme solutions were entrapped at the fiber end using a semipermeable membrane which retains the enzyme. The change in fluorescence occurs within a rather small range of lactate concentration (0.5 - 1 mM) with an lactate-invariable signal at higher levels. Response times are from 7.5 to 25 min, and regeneration times between 1 and 8 min. In order to achieve a more expanded analytical range and shorter response times, kinetic measurements are performed in a fashion similar to flow-injection analysis.



**146. ET(33), a Solvatochromic Polarity and Micellar Probe for Neutral Aqueous Solutions, M. A. Kessler & O.S. Wolfbeis; *Chem. Phys. Lipids* 50, 51-56 (1989). DOI: 10.1016/0009-3084(89)90025-X**

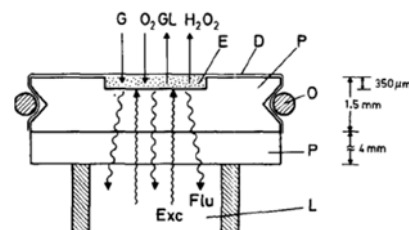
**Abstract.** The prepn. and spectra of ET(33), which is applicable to polarity studies at neutral pH, is described. The probe has a pK<sub>a</sub> value of 4.8 which makes it the first probe of the ET series that exists as a phenolate at near neutral pH. ET(33) shows an extremely large shift in absorption in going from water (λ<sub>max</sub> 409 nm) to THF (λ<sub>max</sub> 646 nm). Spectral properties of ET(33) are studied in various solvents and ethanol-water mixts., and an excellent correlation with standard ET(30) values is obtained. Since the dye is applicable in neutral aq. soln., it is used for detn. of the crit. micellar concn. (CMC) of CTAB at both pH 11 and at near neutral pH. The absorption of the probe is shifted from 409 nm in the sub-CMC range of CTAB to 462 nm at well above the CMC. The very good agreement of the data with literature data demonstrates that



ET(33) is a useful and long-wave-absorbing probe for micellar (and probably also lipid) studies at near neutral pH.

**145. Fully Reversible Fibre Optic Glucose Biosensor Based on the Intrinsic Fluorescence of Glucose Oxidase, W. Trettnak, O. S. Wolfbeis; *Anal. Chim. Acta* **221**, 195-203 (1989). DOI: 10.1016/S0003-2670(00)81956-X**

**Abstract.** In a new type of glucose biosensor, the intrinsic green fluorescence of the enzyme glucose oxidase (GOx) is used as the analytical information. It was found that the fluorescence of the coenzyme FAD contained in GOx changes during interaction with glucose. Fluorescence is excited at 450 nm and measured at >500 nm. The signal response is fully reversible because oxygen is accepted as a second substrate. A major feature of this sensor relies on the fact that the recognition element is identical with the transducer element. Enzyme solutions were entrapped at the end of a fibre using a semipermeable membrane which retains the enzyme. The change in fluorescence of FAD occurs within a rather small glucose concentration range (typically 1.5 - 2 mM glucose), with a glucose-invariable signal at lower and higher glucose levels. Response times of 2 - 30 min and regeneration times of 1 - 10 min are observed. To achieve an extended analytical range (e.g. 2.5 - 10 mM) and shorter response times, kinetic measurements are suggested. The schematic shows a cross section of the sensor layer and the directions of the diffusion of oxygen, glucose (G), hydrogen peroxide (H<sub>2</sub>O<sub>2</sub>) and gluconolactone (GL).

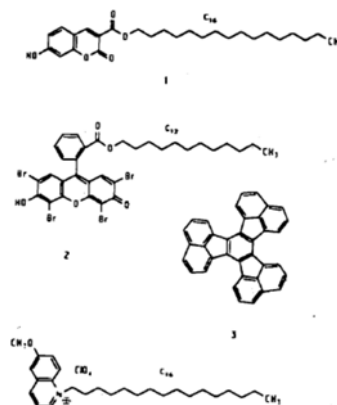


**144. Review. Novel Techniques and Materials for Fiber Optic Chemical Sensing, O. S. Wolfbeis; *Proc. 6<sup>th</sup> Intl. Conf. on Optical Fiber Sensors (OFS '89), Paris, 18 - 20 Sep. 1989*; Springer Proc. Phys. **44**, H. J. Arditty, J. P. Dakin, R. Th. Kersten (eds.), Springer Verlag, Heidelberg, 1989, p. 416-424. ISSN: 0930-8989. ISBN 978-3-642-75090-8**

**143. New Optical Chemical Sensors Based on the Langmuir-Blodgett Technique, B. P. H. Schaffar, O. S. Wolfbeis; *Proc. SPIE* **990**, 122-129 (1989). DOI:**

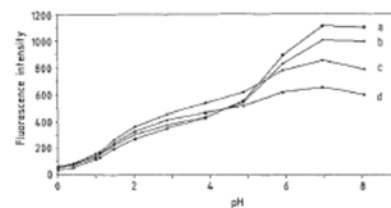
10.1117/12.959983

**Abstract.** This paper describes the application of Langmuir-Blodgett type layers in planar optical sensors for chemical parameters including alkali ions, oxygen, halides and pH. The major advantages of LB layer based sensors are the ease of reproducible fabrication, a well-defined layer thickness, and usually quite short response times. In addition, it offers analytical possibilities not provided by thick film techniques. As a result, potentiometric measurement of boundary potentials using electrochromic dyes have become possible. On the other hand, the type of bilayers used so far is prone to mechanical disruption, and poor signal-to-noise ratios are observed. Potential future techniques will include polymeric lipid membranes, the evanescent wave technique for gathering more intense signals, and the coupling of LB techniques to fiber optic waveguides. The chemical structures of the lipophilic indicator probes used in this work are shown on the right: (1): pH probe; (2) pH-probe (used along with ion carriers for alkali ions); (3) oxygen probe; (4) chloride probe. \*\*\*\*



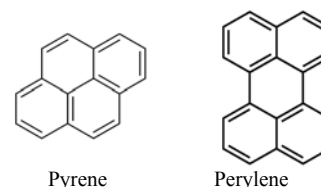
**142. Towards a Gastric pH Sensor: An Optrode for the pH 0 - 7 Range, H. E. Posch, M. J. P. Leiner, O. S. Wolfbeis; *Fresenius Z. Anal. Chem.* **334**, 162-165 (1989). DOI: 10.1007/BF00476679**

**Abstract.** This work describes the the first optical pH sensor capable of measurig pH values in the 0 - 7 range. The pH-sensitive material consists of fibrous amino-ethyl cellulose onto which fluorescein and eosin were covalently immobilized. Fluorescein was immobilized via its isothiocyanate, and immobilized eosin was obtained by bromination of the immobilised fluorescein. The material thus obtained was mechanically fixed at the end of a bifurcated optical fibre bundle. Fluorescence was excited at 490 nm and measured at >540 nm. The accuracy of the sensor is +/- 0.05 pH units, its response time ranges from 25 to 30 s.



**141. Fiber Optic Fluorosensor for Sulfur Dioxide Based on Energy Transfer and Exciplex Quenching, A. Sharma, O. S. Wolfbeis; *Proc. SPIE* **990** (1989) 116-120. DOI: 10.1117/12.959982**

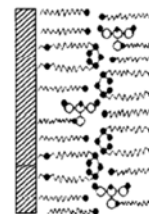
**Abstract:** A new type of fiber-optic sensor for sulfur dioxide is described that is based on the inhibition of the electronic energy transfer from pyrene (the donor) to perylene (the acceptor) both dissolved in thin layer of a silicone polymer that is attached to the end of a bifurcated fiber bundle. While the donor alone is efficiently quenched by sulfur dioxide, the acceptor is not. The donor-acceptor energy transfer systems, in contrast, is extremely efficiently quenched by SO<sub>2</sub> with an Stern-Volmer constant 3-fold larger than that for the quenching of pyrene alone. The excitation light wavelength was that for pyrene (333 nm), and the fluorescence was monitored at the fluorescence of perylene (470 nm) where pyrene itself is non-fluorescent. Stern-Volmer graphs describing the quenching by sulfur dioxide are given. The results are interpreted in terms of an extremely efficient quenching of the donor-acceptor exciplex.



**140. A Calcium-Selective Optrode Based on Fluorimetric Measurement of Membrane Potential. B. P. H. Schaffar, O. S. Wolfbeis; *Anal. Chim. Acta* **217**, 1-9 (1989). DOI: 10.1016/S0003-2670(00)80382-7**

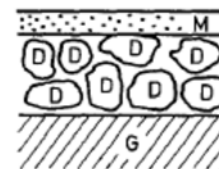
**Abstract.** The optrode is based on measurement of the fluorescence intensity of a potential-sensitive dye incorporated into a lipid membrane constructed by the Langmuir-Blodgett film technique. The membrane potential depends on the calcium ion concentration in the sample solution, when a calcium-selective ionophore

(ETH 1001) is incorporated into the lipid membrane. The fluorescence of the potential-sensitive dye is reduced with increasing calcium ion concentrations. The selectivity factors over magnesium, sodium and potassium are better than 10,000.



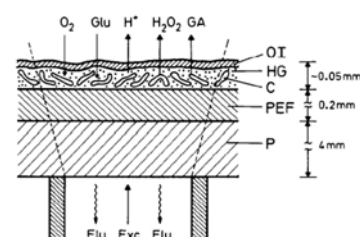
**139. Optical Sensor for Hydrogen Peroxide, H. E. Posch, O. S. Wolfbeis; *Microchim. Acta* 97 (1989), 41-50. DOI: 10.1007/BF01197282**

**Abstract.** Three types of sensors for continuous determination of hydrogen peroxide (HP) are described. The working principles are based on the decomposition of HP by a catalyst and on the measurement of the amount of oxygen thereby produced. The change in oxygen tension is quantitatively determined via the quenching of the fluorescence of a silica gel-adsorbed dye entrapped in silicone rubber. In the most suitable method, finely dispersed silver powder was embedded in a silicone rubber layer that is spread over an oxygen sensing membrane. The sensor is capable of continuously recording HP in the 0.1 to 10.0 mM concentration range, with a precision of  $\pm 0.1$  mM at 1 mM HP. Its response time varies from 2.5 to 5 min. The figure shows a cross section of the sensor layer, with *G* being the glass support, *D* the silica particles dyes with the fluorescent probe for oxygen, and *M* a top layer containing silver nanoparticles as the catalyst for decomposition of HP.



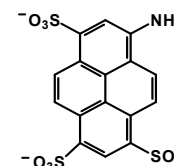
**138. Fibre-Optic Glucose Sensor with a pH Optrode as a Transducer, W. Trettnak, M. J. P. Leiner, O. S. Wolfbeis; *Biosensors* 4, 15-26 (1988). DOI: 10.1039/AN9881301519**

**Abstract.** Glucose oxidase was physically immobilised in a sensing layer at the end of a fibre optic light guide. The enzyme catalyses the oxidation of glucose to give gluconic acid, which, in turn, lowers the pH in the micro-environment of the sensor. The enzymatic reaction can therefore be monitored by following the changes in the fluorescence of a pH-sensitive dye incorporated into the sensing layer. 0.1 - 2 mM Glucose were detectable. Saturation was reached at glucose concentrations of 2 - 3 mM.



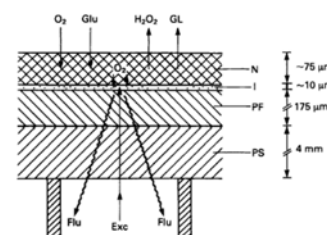
**136. 1-Aminopyrene-3,6,8-trisulfonate: A Fluorescent Probe for Thiamine and Pyridinium Ion, E. Koller, M. Kriechbaum & O.S. Wolfbeis; *Spectroscopy* 3, 37-39 (1988); *Spectroscopy Intl.* 1, 44-49 (1988). DOI: 10.1080/00032719208016104**

**Abstract.** The quenching of the fluorescence of 1-aminopyrene-3,6,8-trisulfonate (APTS) by the cationic quenchers thiamine, N-cetylpyridinium chloride (CPC), and  $\text{NAD}^+$  was investigated. It was found that CPC and thiamine cause strong static quenching. No changes were observed in the absorption and fluorescence of APTS in the presence of  $\text{NAD}^+$  within the spectroscopically useful concentration range even though  $\text{NAD}^+$  bears a positive charge. APTS is considered to be a useful long-wave absorbing and fluorescence reagent for the fluorometric determination of thiamine and CPC, both of which are virtually nonfluorescent.



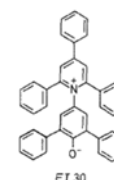
**135. A Fiberoptic Glucose Biosensor with an Oxygen Optrode as the Transducer, W. Trettnak, M. J. P. Leiner, O. S. Wolfbeis; *Analyst* 113, 1519-1523 (1988). DOI: 10.1039/AN9881301519**

**Abstract.** Glucose oxidase was covalently immobilized onto a nylon membrane and the consumption of oxygen was measured by following, via fibre optic bundles, the changes in the fluorescence of an oxygen-sensitive dye whose fluorescence is quenched by oxygen. The dye is dissolved in a very thin silicone membrane that is placed beneath the enzyme layer. As a result of the oxidation by the enzyme, some oxygen is consumed, which is indicated by the fluorescent dye. The analytical ranges are from 0.1 to 20 mM. The schematic shows a cross section of the sensor layer at the end of the optical fiber and the directions of the diffusion of oxygen, glucose (Glu), hydrogen peroxide ( $\text{H}_2\text{O}_2$ ) and gluconic acid (GA). The graph shows a cross-section of the sensor layers played at the tip of the optical fiber.



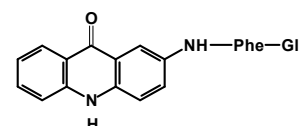
**134. An Improved Synthesis of the Solvatochromic Dye ET(30), M. A. Kessler, O. S. Wolfbeis; *Synthesis* 1988, 635-636. DOI: 10.1055/s-1988-27662**

**Abstract:** An improved synthesis of the well-known dye ET-30, which is used as a standard for the characterization of solvent polarity, using easily available starting materials is described. ET(30) undergoes one of the largest known solvent-induced shifts in absorbance, amounting to some 357 nm in going from 453 nm (water; yellow color) to 810 nm (green) in diphenyl ether. From the absorption data, the so-called ET-30 values have been calculated for >200 solvents.



**133. Fluorometric Continuous Kinetic Assay of  $\alpha$ -Chymotrypsin Using New Substrates Possessing Longwave Excitation and Emission Maxima, J. Baustert, O. S. Wolfbeis, R. Moser and E. Koller, *Anal. Biochem.* 171, 393-397 (1988). DOI: 10.1016/0003-2697(88)90503-9**

**Abstract.** A direct and continuous kinetic method for the fluorometric detn. of alpha-chymotrypsin and trypsin is described, and 2-aminoacridone (2-AA) is introduced as a new fluorophore in anal. biochem. N-Succinyl- and N-glutarylphenylalanine were coupled to 2-AA via a peptide bond and the resulting fluorogenic substrates were cleaved by the 2 enzymes. Since the substrate and product of hydrolysis have quite different spectral properties, the increase in the long-wave fluorescence of 2-AA (measured at 570 nm under 450-nm excitation) is a parameter for enzyme

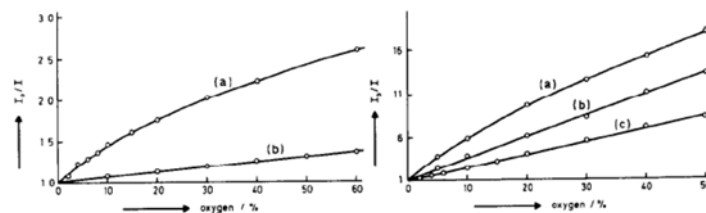




activity. Chymotrypsin (0.5 µg/mL) and trypsin (0.1 µg/mL) were detectable in a 3-min assay using the new substrates.

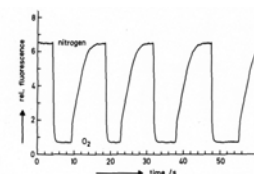
**131. Unusually Efficient Quenching of the Fluorescence of an Energy Transfer-Based Optical Sensor for Oxygen, A. Sharma, O. S. Wolfbeis; *Anal. Chim. Acta* **212**, 261-265 (1988). DOI: 10.1016/S0003-2670(00)84148-3**

**Abstract.** A two-fluorophore system consisting of pyrene as donor and perylene as energy acceptor undergoes efficient energy transfer when pyrene is electronically excited. The two-fluorophore system is strongly quenched, with a 4-fold increase in the Stern-Volmer quenching constant as compared to the quenching of pyrene. The findings have resulted in the design of a fluorescence-based optical oxygen sensor which offers a sensitivity greatly exceeding that of existing oxygen probes. The detection limit is 6 Pa oxygen. *Left figure:* Stern-Volmer plots for the quenching by oxygen of (a) pyrene, (b) perylene in silicone rubber at 740 Torr. *Right figure:* Stern-Volmer plots for the quenching by oxygen of the pyrene/peryene system in: (a) toluene; (b) ethanol; (c) silicone rubber.



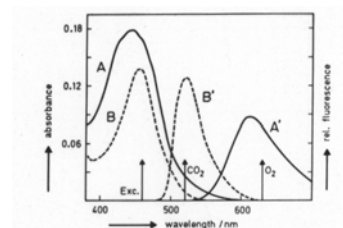
**130. Fiber Optic Oxygen Sensor Based on Fluorescence Quenching and Energy Transfer, A. Sharma, O. S. Wolfbeis; *Appl. Spectrosc.* **42**, 1009-1012 (1988). DOI: 10.1366/0003702884430470**

**Abstract.** A new type of oxygen sensor is described that is based on electronic energy transfer from a donor (whose fluorescence is efficiently quenched by molecular oxygen) to an acceptor (which is less affected by oxygen). We use pyrene as a donor and perylene as the acceptor. When excited at 320 nm, the two-fluorophore system shows strong fluorescence at 476 nm, where pyrene itself is non-fluorescent. Although perylene is not efficiently quenched by oxygen, the system strongly responds to oxygen because fluorescence is quenched with an efficiency that by far exceeds the quenching efficiency for pyrene or perylene alone. A fiber optic oxygen sensor was devised by incorporating the two dyes in a polymer matrix that has been attached to the end of an optical fiber. Oxygen can be detected in the 0-150 kPa range with ±0.3 kPa precision.



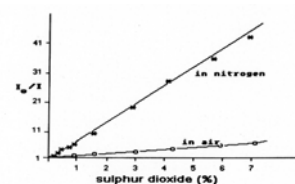
**129. Fiber Optic Fluorosensor for Oxygen and Carbon Dioxide, O. S. Wolfbeis, L. Weis, M. J. P. Leiner and W. Ziegler, *Anal. Chem.* **60**, 2028-2030 (1988). DOI: 10.1021/ac00170a009**

**Abstract.** The capability of fiber-optic light guides to transmit a variety of optical signals simultaneously has been exploited to construct an optical fiber sensor for measurement of both oxygen and carbon dioxide. The oxygen-sensitive material (a silicagel-absorbed fluorescent metal-organic complex) and the CO<sub>2</sub>-sensitive material (an immobilized pH indicator in a buffer solution) are entrapped in a gas-permeable polymer matrix that is attached to the distal end of the fiber. Both indicators have the same excitation wave length (in order to avoid energy transfer) but quite different emission maxima. The two emission bands can be separated with the help of interference filters and give independent signals. Oxygen can continuously be determined in the 0 to 200 Torr range with ±1 Torr accuracy, and CO<sub>2</sub> in the 0-150 Torr range with ± Torr. The figure shows the spectra and the analytical emission wavelengths (arrows) selective for either CO<sub>2</sub> or oxygen.



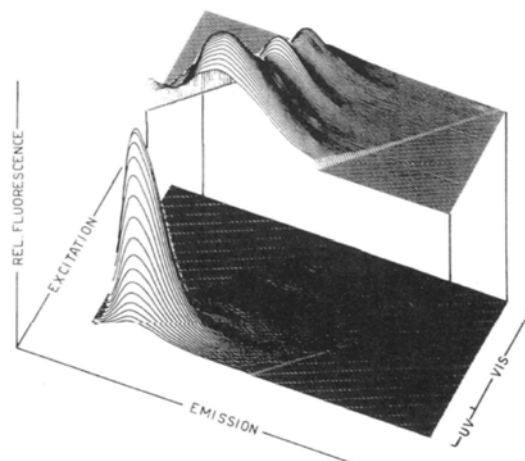
**128. Fibre-Optic Fluorosensor for Sulphur Dioxide, O. S. Wolfbeis and A. Sharma, *Anal. Chim. Acta* **208**, 53-58 (1988). DOI: 10.1016/S0003-2670(00)80735-7**

**Abstract.** The fluorescence of a polynuclear aromatic hydrocarbon [benzo(b)fluoranthene] immobilized in silicon polymer is efficiently quenched by sulphur dioxide. Stern-Volmer graphs are given which describe the relation between SO<sub>2</sub> concentration and relative fluorescence. Detection limits are about 0.01 % (v/v) SO<sub>2</sub> in air; the useful range is from 0.01 to 6% (v/v). Other gases likely to occur in air were found to be inert, except for oxygen which also acts as a dynamic quencher. Its interference is negligible for SO<sub>2</sub> levels below 6 % in air at constant oxygen pressure, because the quenching efficiency of SO<sub>2</sub> is about 26 times higher than that of oxygen.



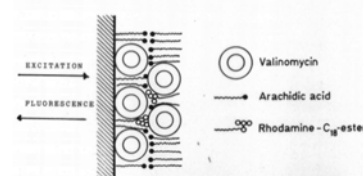
**126. Review: Biochemical Applications of 3-Dimensional Fluorescence Spectrometry, M. J. P. Leiner, O. S. Wolfbeis; *Proc. SPIE* **909** (1988) 134-138. DOI: 10.1117/12.945377**

**Abstract:** We investigated the 3-dimensional fluorescence of complex mixtures of biofluids such as human serum, serum ultrafiltrate, human urine, and human plasma low density lipoproteins. The total fluorescence of human serum can be divided into a few peaks. When comparing fluorescence topograms of sera, from normal and cancerous subjects, we found significant differences in tryptophan fluorescence. Although the total fluorescence of human urine can be resolved into 3-5 distinct peaks, some of them do not result from single fluorescent urinary metabolites, but rather from several species having similar spectral properties. Human plasma, low density lipoproteins possess a native fluorescence that changes when submitted to in-vitro auto-oxidation. The 3-dimensional fluorescence demonstrated the presence of 7 fluorophores in the lipid domain, and 6 fluorophores in the protein domain. The above results demonstrated that 3-dimensional fluorescence can resolve the spectral properties of complex mixtures much better than other methods. Moreover, other parameters than excitation and emission wavelength and intensity (for instance fluorescence lifetime, polarization, or quenchedability) may be exploited to give a multi-dimensional matrix, that is unique for each sample. Consequently, 3-dimensional fluorescence as such, or in combination with separation techniques is considered to have the potential of becoming a useful new method in clinical chemistry and analytical biochemistry.



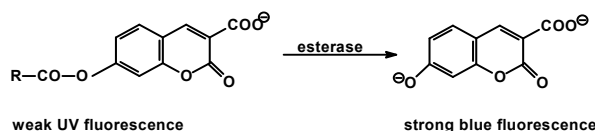
**125. Effect of Langmuir Blodgett Layer Composition on the Response of Optrodes for Potassium Based on the Fluorometric Measurement of Membrane Potential, B. P. H. Schaffar, O. S. Wolfbeis and A. Leitner, *Analyst* 113, 693-697 (1988). DOI: 10.1039/an9881300693**

**Abstract.** An ion-selective optrode (ISO) for the continuous determination of potassium is based on the optical measurement of the membrane potential between an aqueous sample solution and a lipid phase incorporating a potential-sensitive dye. The lipid phase is composed of a chemically modified rhodamine B dye together with either octadecan-1-ol or arachidic acid, with valinomycin as a neutral ion carrier. The fluorescence intensity of the potential-sensitive rhodamine dye depends on the potassium concentration in the sample solution and decreases with increasing potassium concentrations. The over-all response is the net result of at least two effects, the strongest of which is the K<sup>+</sup> concentration, but interferences were observed with other metal ions. It is shown that these interferences can be compensated for by using a reference optrode. The response of membranes made of octadecan-1-ol and valinomycin is characterised by a decrease in the fluorescence intensity of up to 17% towards 100 mM potassium ion solutions. The selectivity factor for potassium over sodium is 10<sup>4</sup> and this can be greatly increased by using a reference optrode.



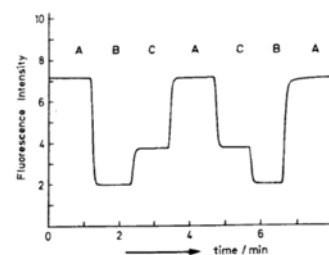
**124. A Sensitive Kinetic Assay of Serum Albumins Based on Their Enzyme-like Hydrolytic Activity Using a New Chromogenic and Fluorogenic Substrate, A. Gürakar & O.S. Wolfbeis; *Clin. Chim. Acta* 172, 35-46 (1988). DOI: 10.1016/0009-8981(88)90118-0**

**Abstract.** A new albumin assay, based on the unusual enzyme-like activity of the protein that promotes hydrolysis of ester bonds in fatty acid arylesters was designed for clin. routine use. The substrate introduced shows improved anal. wavelengths and is suitable for both photometric and fluorometric assays. Experiments have been performed with a conventional photometer, a fluorometer, and an automated analyzer. Detection limits are as low as 10 µg/mL photometrically and 20 ng/mL fluorometrically. The method provides a sensitive quantitative determination of even minute amounts. of albumin in liquid solution, and a simple semiquantitative test may be performed by fixing the dye on a test strip which then is immersed into a sample solution and observing the development of yellow color intensity.



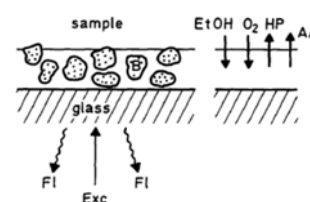
**123. Recent Progress in Optical Oxygen Sensing, O. S. Wolfbeis, M. J. P. Leiner, *Proc. SPIE* 906 (1988) 42-48. DOI: 10.1117/12.945253**

**Abstract:** Following a brief review on the history of optical oxygen sensing (which shows that a variety of ideas exists in the literature that awaits the extension to fiber optic sensing schemes), the present state of probing oxygen by optical methods is discussed in terms of new methods and materials for sensor construction. Promising sensing schemes include simultaneous measurement of parameters such as oxygen and carbon dioxide with one fiber, measurement of fluorescence lifetimes and radiative energy transfer efficiency as well as phosphorescence quenching. New longwave-excitable fluorophores have been introduced recently, two-band emitting indicators can help to eliminate drift problems, and new methods have been found by which both indicators and enzymes may be entrapped in silicone rubber, which opens the way for the design of new biosensors. In a final chapter, the application of fiber optic oxygen sensors for blood gas measurement and as transducers in biosensors are presented. The graph shows the response of the sensor on cycling between nitrogen (A), oxygen (B) and air (C).



**122. A Fibre Optic Ethanol Biosensor, O. S. Wolfbeis and H. E. Posch, *Fresenius Z. Anal. Chem.* 332, 255-257 (1988). DOI: 10.1007/BF00492971**

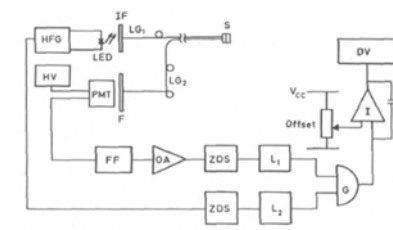
**Abstract.** The sensor layer contains an oxygen-sensitive fluorescing indicator which reports the decrease in the local oxygen partial pressure as the result of the enzymatic oxidation of ethanol by an oxidase. The sensor measures in the 50-500 mmol/l ethanol range, which an accuracy of ± 4 mmol/l at 100 mmol/l. The detection limit is 10 mmol/L of ethanol. The schematic shows a cross section of the planar sensor layer and the directions of the diffusion of oxygen, ethanol (EtOH), hydrogen peroxide (HP) and acetaldehyde (AA).



### 121. Fibre Optic Oxygen Sensor with the Fluorescence Decay Time as Information

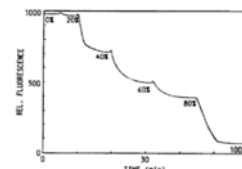
Carrier, M. E. Lippitsch, J. Pusterhofer, M. J. P. Leiner, O. S. Wolfbeis; *Anal. Chim. Acta* **205**, 1-6 (1988). DOI: 10.1016/S0003-2670(00)82310-7

**Abstract.** A sensor is described that measures the *decay time* of the indicator fluorescence rather than its *intensity*. A simple opto-electronic device is described for measuring lifetimes of a long-lived fluorophore with a frequency-modulated LED as light source. Measurement of lifetime provides a more linear Stern-Volmer plot and offers certain advantages with respect to the performance of the sensor, because it has an internal reference system that is an attractive alternative to the frequently-used two-wavelength referencing method. Long-term stability is distinctly better because the phase shift is independent of indicator bleaching and leaching as well as lamp intensity fluctuations. The detection limit is ca. 2 torr of oxygen.



### 120. Fibre-Optic Humidity Sensor Based on Fluorescence Quenching, H. E. Posch, O. S. Wolfbeis; *Sensors Actuators* **15**, 77-83 (1988). DOI: 10.1016/0250-6874(88)85019-4

**Abstract.** The sensor is based on the quenching of fluorescence of silica-gel-absorbed perylene dyes by water vapour. The perylene-based sensors show a total signal change of 95 % in going from 0 to 100 % relative humidity, but the response is not linear. The advantage of this type of sensor are a fairly simple optical system, the use of LED-excitabile dyes and a simple method for the preparation of sensor layers. Oxygen, however, interferes in showing some quenching as well.



### 119. Optic and Fibre-Optic Sensor for Vapours of Polar Solvents, H. E. Posch, J. Pusterhofer, O. S. Wolfbeis; *Talanta* **35**, 89-94 (1988). DOI: 10.1016/0039-9140(88)80044-4

**Abstract.** An optical sensor is described which continuously measures the concentration of vapours of polar organic solvents such as alcohols, ethers, esters and ketones, but does not respond to hydrocarbons and chlorinated hydrocarbons. The detection is based on reversible decolorization of the blue thermal printer paper (dyed with Crystal Violet or its lactone) as used in thermal printers and plotters. The sensing layer is placed in a flow-through cell. An LED acts as a source of yellow light and a phototransistor measures the transmitted light. Detection limits vary from 10 to 1000 ppm for some of the most common technical solvents. Blue printer papers include those from Hewlett-Packard (8388, 9210-0479; 5580-8735; 9270-0962) or Perkin-Elmer (119 849). Black papers include those from Perkin-Elmer (BO 126 708) or Kontron. When using the blue HP 8388 paper, the strongest decolorations are caused by vapors of n-butanol >dioxane >ethanol >ethyl acetate >tetrahydrofuran, while chloromethanes, cyclohexane or toluene have virtually no effect.

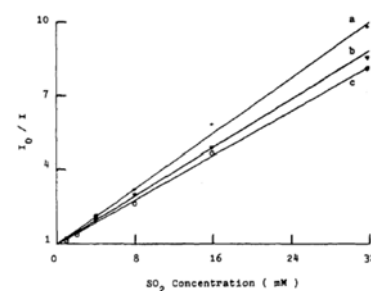
**118. Book Chapter: Fiber Optical Fluorosensors in Analytical and Clinical Chemistry, O. S. Wolfbeis; in: *Molecular Luminescence Spectroscopy: Methods, Applications*, S. G. Schulman (ed.), Wiley, New York, 1988, vol. 2, pp. 129-281. ISBN: 0471636843, 9780471636847**

### 117. Evaluation of Critical Micelle Concentrations Using New Superpolar Lipid Probes, M. Kriechbaum, O. S. Wolfbeis and E. Koller, *Chem. Phys. Lipids* **44**, 89-94 (1987). DOI: 10.1016/0009-3084(87)90003-X

**Abstract.** New fluorescent probes (pyranine long alkyl ethers such as 8-octadecyloxy-pyrene-1,3,6-trisulfonate) are presented for the determination of the critical micelle concentration (CMC) of non-ionic detergents. The probes have excellent photostability and are not quenched by mol. oxygen. Both the fluorescence maximum and intensity of the probes change during the transition from monomeric to micellar solns. The environment of this probe in the micelle had a polarity identical with that of MeOH. Cationic detergents cannot be probed because of efficient fluorescence quenching, and with anionic detergents no interaction was observed at all.

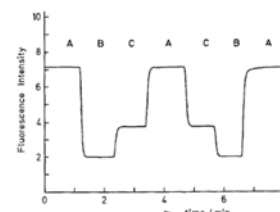
### 116. The Quenching of the Fluorescence of Polycyclic Aromatic Hydrocarbons and Rhodamin 6G by Sulphur Dioxide, A. Sharma & O.S. Wolfbeis; *Spectrochim. Acta* **43A**, 1417-1421 (1987). DOI: 10.1016/S0584-8539(87)80021-1

**Abstract.** The quenching of the fluorescence of polycyclic aromatic hydrocarbons (PAHs) such as fluoranthene, benzo(b)fluoranthene, and pyrene, and that of Rhodamine 6G and Rhodamine B by SO<sub>2</sub> was studied. Stern-Volmer and bimol. diffusion consts. for the quenching process were determined. Fluorescence quenching of SO<sub>2</sub> is efficient, particularly for fluoranthene, pyrene, and benzo(b)fluoranthene, and exclusively dynamic for all PAHs studied. The quenching of the rhodamines is less efficient. The findings are of potential utility for the development of a fiber-optic SO<sub>2</sub> sensor and other methods for its quantitative determination. The Fig. shows Stern-Volmer plots of the quenching of polycyclic aromatic hydrocarbons by sulfur dioxide in methanol at 22 °C. (a) Fluoranthene, (b) pyrene, (c) benzo(h)fluoranthene.



### 115. A New Sensing Material for Optical Oxygen Measurement, O. S. Wolfbeis, M. J. P. Leiner and H. E. Posch, *Microchim. Acta* **90** (1986) 359-366. DOI: 10.1007/BF01199278

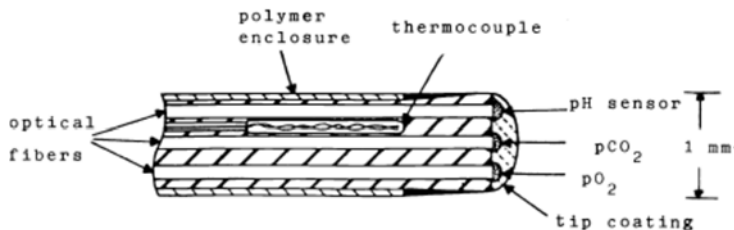
**Abstract.** A new type of oxygen-sensitive material is obtained by preparing an aqueous (or water on silica gel) emulsion of an oxygen-sensitive fluorescent dye – a metal-organic ruthenium complex – in a silicone polymer. The fluorescence of this sensing material strongly depends on oxygen partial pressure, but Stern-Volmer plots deviate from linearity at oxygen tensions above 5 to 10 kPa. The Fig. shows the response of a sensing membrane consisting of the ruthenium indicator on silica gel that was homogeneously mixed into a silicone matrix. A, nitrogen; B, oxygen; C, air. Analytical wavelengths: 470 nm excitation and 610 nm emission.



### 114. Review: Fibre-Optic Sensors in Biomedical Sciences. O. S. Wolfbeis; *Pure Appl. Chem.* **59** (1987) 663-672.

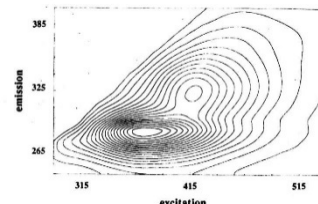
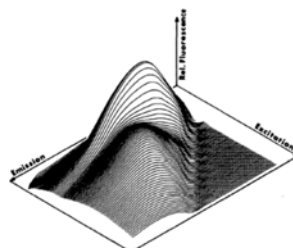
**Abstract.** We review the state of sensor development in biomedical, mainly clinical sciences. The figure shows a respective instrument (left) and a schematic (right) of the tip of a fiber optic triple sensor for continuous and in-vivo determination of pH, oxygen, CO<sub>2</sub> and temperature in blood.





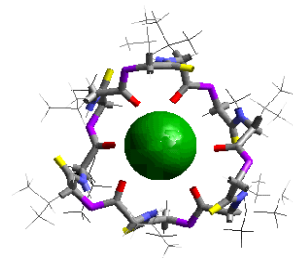
**112. The Total Fluorescence of Human Urine**, M. J. P. Leiner, M. R. Hubmann and O.S. Wolfbeis; *Anal. Chim. Acta* **198**, 13-23 (1987). DOI: 10.1016/S0003-2670(00)85002-3

**Abstract.** The 3-dimensional fluorescence spectra (so-called EEM matrices) of human urine were acquired and an attempt was made to assign the major peaks in the UV and visible. Despite the complexity of the composition of urine, 3-5 distinct fluorescence maxima can be observed. Effects of pH were studied and tentative assignments as to the species responsible for the peaks were made. The UV is dominated by the fluorescences of Tyr and Trp, and the visible by various kinds of metabolic species having similar spectral properties and being present in comparable concentrations. Particularly strong fluorescence is found if vitamin B is administered a few hours before samples are taken. The figure shows a perspective view on the 3D-spectra.



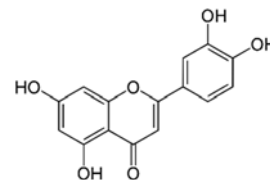
**111. An Ion-selective Optrode for Potassium**, O. S. Wolfbeis and B. P. H. Schaffar, *Anal. Chim. Acta* **198**, 1-12 (1987). DOI: 10.1016/S0003-2670(00)85001-1

**Abstract.** The new type of sensor for continuous determination of electrolytes is based on the ability of certain fluorescent dyes to respond to an electrical potential located at the interface between a lipid phase and an aqueous phase. The potential is created by addition of a neutral ion carrier, its magnitude measured with an appropriate potential-sensitive dye. Specifically, an optosensor for potassium is described. A lipid bilayer is formed on a glass support by applying the Langmuir-Blodgett technique. A lipid-soluble rhodamine dye is incorporated into this layer along with valinomycin as the ion carrier. The sensor responds to potassium over the 0.01 to 10 mM conc. range, with a selectivity factor over sodium varying from 2.5 to 5.0. The figure shows the complex formed between valinomycin and potassium ion.



**110. The Fluorescence Properties of Luteolines**, O. S. Wolfbeis, M. Begum, H. Geiger, *Monatsh. Chem.* **118** (1987) 1403-1411. DOI: 10.1007/BF00810645

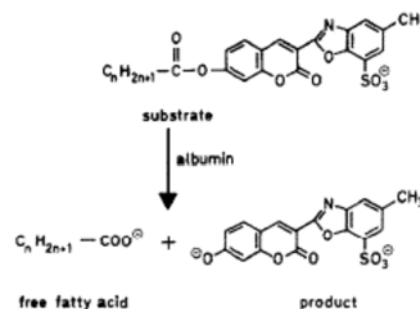
**Abstract.** The fluorescence properties of luteoline and its possible methyl ethers (a representative class of naturally occurring flavonoids) were investigated, together with the effect of diagnostic shift reagents such as sulfuric acid, aluminium trichloride, and borax. The results demonstrate that fluorimetry is a suitable tool for the identification and structure elucidation of minute samples of flavones, in particular if combined with absorption spectrometry. The pKa values of all trimethylethers were determined for the ground and first excited singlet states and related to the effects of basic reagents.



Basic chemical structure of luteolines

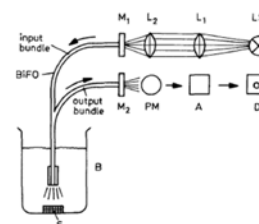
**109. The Effect of Fatty Acid Chain Length on the Rate of Arylesterase Hydrolysis by Various Albumins**, O. S. Wolfbeis and A. Gürakar, *Clin. Chim. Acta* **164**, 329-337 (1987). DOI: 10.1016/0009-8981(87)90308-1

**Abstract.** A series of synthetic chromogenic and fluorogenic substrates for monitoring the aryl esterase-like activity of albumins from various sources was studied. Except for ovalbumin, all displayed enzyme-like activity. The acetate, butyrate, caprylate, laurate, and palmitate esters of a coumarin dye were found to be efficiently hydrolyzed within the pH range 8.8 - 9.8, with the non-enzymic rate being highest for acetate and lowest for laurate. The latter was considered to be the substrate of choice because it was cleaved most quickly by the proteins tested. A considerable increase in hydrolytic activity was obsd. on addn. of detergents, but not of  $\text{Ca}^{2+}$  and  $\text{Mg}^{2+}$ , whereas addn. of lauric acid to bovine serum album resulted in a 30% decrease in its activity. The results were interpreted in terms of the well-known affinity of albumins for long-chain fatty acids and provide the basis for a sensitive detn. of small amts. of albumins.



**108. Kinetic Titration of Sulfide with Heavy Metal Ions Using a Highly Sensitive Fluorescent Indicator**, W. Trettnak, O.S. Wolfbeis; *Fresenius Z. Anal. Chem.* **326**, 547-550 (1987). DOI: 10.1007/BF00468224

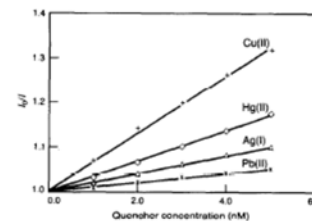
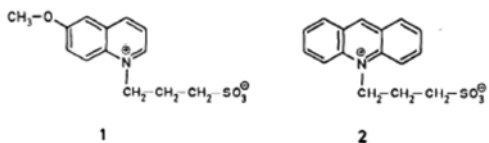
**Abstract.** A new method is presented for the determination of sulfide and is based on a precipitation titration along with fluorometric endpoint detection. The fluorescent indicator 10-(3-sulphonatopropyl)-acridinium (SPA) is efficiently quenched by  $\text{H}_2\text{S}$ . The application of fiber optical light guides makes working within a fluorometer unnecessary and enables online monitoring of the course of a titrn. Sulfide can be detd. at 1 - 10 mM by titration with  $\text{AgNO}_3$  with an av. error of 0.5%.



**107. Fluorescence Quenching of Acridinium and 6-Methoxy-quinolinium Ion by Pb(II), Hg(II), Cu(II), Ag(I) and Hydrogen Sulfide, O. S. Wolfbeis, W. Trettnak, *Spectrochim. Acta* 43A, 405-408 (1987).**

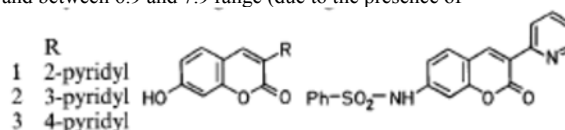
DOI: 10.1016/0584-8539(87)80125-3

*Abstract.* The quenching of the fluorescence of sulfopropyl-quaternized derivatives of 6-methoxyquinoline (SPQ; 1) and of acridine (SPA; 2) by various heavy metal cations and HS<sup>-</sup> were studied. Stern-Volmer constants were determined, and quenching was found to be exclusively dynamic, except for HS<sup>-</sup>, which acts as both a dynamic and static quencher.



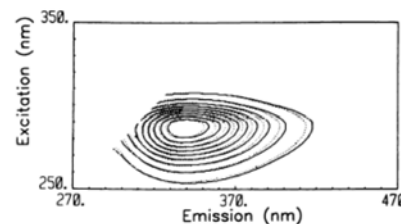
**106. A New Group of Fluorescent pH Indicators for an Extended pH Range, O. S. Wolfbeis, H. Marhold, *Fresenius' Z. Anal. Chem.* 327 (1987) 347-350. DOI: 10.1007/BF00491840**

*Abstract.* We report on the pH versus fluorescence intensity profiles of a series of new pH indicators out of the class of coumarins. They are characterized by two pK<sub>a</sub> values that are located between 3.7 and 4.9 (due to the presence of pyridyl groups) and between 6.9 and 7.9 range (due to the presence of phenol groups and Ph-SO<sub>2</sub>-NH-groups), respectively. The strong change in the intensity of their blue fluorescence with pH allows the determination of pH values over a much wider range (typically 2-9) than with one-step indicators. They are therefore considered to be of potential utility for measurement of pH over the neutral and slightly acidity range which occurs, for instance, in biological fluids such as urine or stomach fluids.



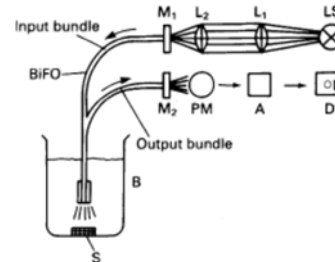
**104. Characteristic Deviations of Tryptophan Fluorescence in Sera of Patients with Gynecological Tumors, M. Leiner, R. J. Schaur, O. S. Wolfbeis and G. Desoye, *Clin. Chem.* 32, 1974 - 1978 (1986). DOI: 10.1093/clinchem/32.10.1974**

*Abstract.* The near-UV region of the total fluorescence (excitation-emission matrix) of human serum reflects essentially the fluorescence of protein-bound tryptophan. In comparison with fluorescence topograms from sera of healthy donors, sera of patients with gynecol. malignancies showed significantly different patterns of tryptophan fluorescence, the major deviations being at 325 and 365 nm. In healthy donors, the tryptophan fluorescence intensity at 365 nm, expressed as percent of the max. fluorescence intensity (i.e., at 337 nm) varied little, but was markedly lower for sera from patients with malignancies. No clear correlation was found between the extent of the fluorescence deviations and the relative concn. of the protein fractions as detd. by electrophoresis. Furthermore, inflammation in tumor patients could be ruled as an explanation for this effect.



**103. Construction and Performance of an Acid-Base Titrator with a Blue LED as a Light Source, O. S. Wolfbeis, B. P. H. Schaffar, E. Kaschnitz, *Analyst* 111 (1986) 1331-1334. DOI: 10.1039/an9861101331**

*Abstract:* An opto-electronic titration unit, which can be used for monitoring the course of acid-base titrations via an optical light-guide, is described. A blue light-emitting diode (LED) is used as a light source and an inexpensive photodiode as a detector to monitor changes in the fluorescence of an added indicator. The instrument is considered to have significant cost advantages over electrode-based titrators. Various kinds of acids and bases have been titrated with excellent precision using the described technique. A voltage change of ca. 100 mV is measured at the end-point. 1-Hydroxypyrene 3,6,8-trisulphonate and fluorescein are used as indicators because of their water solubility and the close overlap of their absorptions with the emission of the blue LED. 7-Hydroxy-3-(4-pyridyl)-coumarin is used as a two-step pH indicator for the titration of phosphoric acid, but this dye can only be excited by the UV light of, e.g., a xenon lamp. The advantages of the method described include simplicity, broad applicability (as demonstrated by the titration of aggressive acids such as hydrofluoric acid), the ease of automation and the possibility of performing assays with sample volumes as small as 0.5 ml.

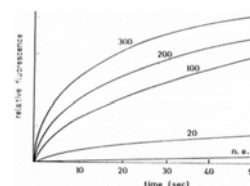


**102. Direct Complexometric Titration of Aluminium(III) with DCTA, O. S. Wolfbeis, B. P. H. Schaffar, R. A. Chalmers, *Talanta* 33 (1986) 867-870. DOI: 10.1016/0039-9140(86)80214-4**

*Abstract:* The end-point of the direct complexometric titration of Al(III) in pH 4.6 solution can be determined by monitoring the fluorescence intensity of the aluminium-morin complex, by use of a bifurcated fibre-optic light guide. The method allows the determination of aluminium in the 1-800 ppm range with good precision. The procedure is applicable even when the solutions are strongly coloured or turbid, but because of the slow complexation kinetics requires a titration time of about 20 min.

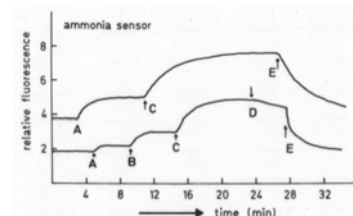
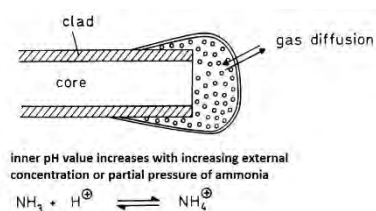
**101. Fiberoptic Probe for Kinetic Determination of Enzyme Activities, O. S. Wolfbeis; *Anal. Chem. (Wash.)* 58, 2874-2878 (1986). DOI: 10.1021/ac00126a065**

*Abstract.* A colorless and nonfluorescent synthetic enzyme substrate was immobilized at the end of an optical fiber. When brought into contact with the appropriate enzyme (in this case a carboxyl esterase) the enzyme hydrolyzes the substrate to produce a colored and strongly fluorescent product whose color (or fluorescence) can be monitored, as a function of time, through the optical fiber. About 20 µg/ml of carboxylic ester hydrolase were detectable with this probe which, however, acts irreversibly because the substrate is consumed.



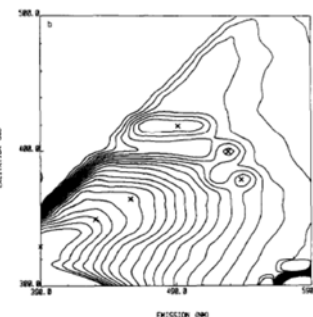
**98. Fiber Optic Fluorescing Sensor for Ammonia, O. S. Wolfbeis und H. E. Posch, *Anal. Chim. Acta* 185, 321-327 (1986). DOI: 10.1016/0003-2670(86)80060-5**

**Abstract.** The fluorescing sensor is based on the change in fluorescence intensity of a buffered pH indicator solution entrapped in silicone rubber. Exposure to ammonia increases the pH of the entrapped solution; this increases fluorescence intensity, which is monitored via an optical fibre bundle. Ammonium chloride in 0.001 M sodium hydroxide, or the indicators themselves, can serve as buffers. Effects of sensor preparation and buffer composition on response time, reversibility and sensitivity are described.



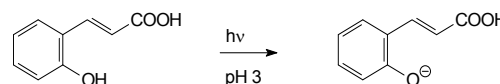
**97. Investigation of Human Plasma Low Density Lipoprotein by 3D Fluorescence Spectroscopy, E. Koller, O. Quehenberger, G. Juergens, O. S. Wolfbeis, H. Esterbauer, *FEBS Lett.* **198** (1986) 229-234. DOI: 10.1016/0014-5793(86)80411-2**

**Abstract:** Human plasma LDL exhibits a diffuse fluorescence (excitation 360 nm) in the 400-600 nm range. Application of three-dimensional fluorescence spectroscopy shows the presence of 7 fluorophores in the lipid and 6 fluorophores in the protein domain. The 430 nm fluorescence in freshly prepared LDL and its apo-B is most likely indicative for remnants of in-vivo lipid peroxidation. The graph shows a contour plot of the fluorescence of total LDL isolated from pooled plasma.



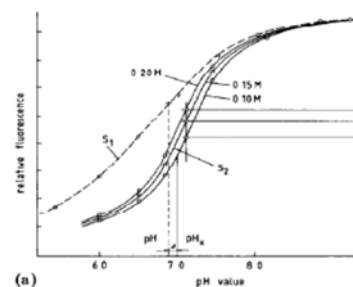
**96. An Unusual Excited State Species of ortho-Hydroxycinnamic Acid, O. S. Wolfbeis, M. Begum & P. Hochmuth, *Photochem. Photobiol.* **44**, 551-554 (1986). DOI: 10.1111/j.1751-1097.1986.tb04707.x**

**Abstract.** The fluorescence of o-hydroxycinnamic acid was studied in aq. soln. at pH = 0-14 and in MeOH. At pH values >9.7, intense anion fluorescence was obsd. At pH 4 - 9, emissions are from both the monoanion (albeit weakly) and from the dianion due to photodissociation. At pH = 0-4, a blue and a green fluorescence was found. It was attributed to emission from the unchanged mol. and from an unusual excited state tautomer. The latter is assumed to be the phenolate anion of cinnamic acid and represents a tautomer with no equiv. in the electronic ground state. It is formed by adiabatic photodissociation during the lifetime of the first excited singlet state.



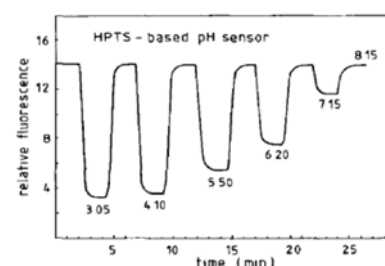
**95. Fluorescence Sensor for Monitoring Ionic Strength and Physiological pH Values, O. S. Wolfbeis and H. Offenbacher, *Sensors Actuators* **9**, 85-91 (1986). DOI: 10.1016/0250-6874(86)80009-9**

**Abstract.** A sensor combination has been developed that measures both pH and ionic strength via two pH determinations. One of the two sensors has an immobilized pH indicator embedded in a micro-environment that makes its dissociation constant highly sensitive towards changes in the ionic strength of the solution. In the second sensor, the indicator is surrounded by charged ammonium groups, which renders the environment of the dye highly charged. Additional changes in ionic strength have practically no adverse effect. The difference in the pH values as displayed by the two sensors can be used to determine ionic strength together with pH in the near-neutral pH range.



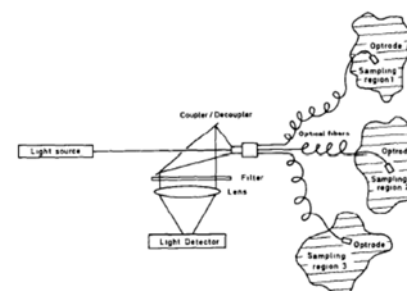
**94. Fluorescence Optical Sensors for Continuous Determination of Near-Neutral pH Values, H. Offenbacher, O. S. Wolfbeis, E. Fuerlinger, *Sensors Actuators* **9**, 73-84 (1986). DOI: 10.1016/0250-6874(86)80008-7**

**Abstract.** The preparation and performance of two types of optical sensors for continuous measurement of near-neutral pH values are described. The sensors are based on glass-immobilized fluorescent pH indicators and allow the determination of pHs in the range 6.4 to 7.7 with a precision of ± 0.01 units. Response times are of the order of 1 min for 99% of the total signal change. Adverse effects of ionic strength are almost completely eliminated by appropriate treatment of the glass surface, thereby creating a well-defined and highly charged environment for the indicator.



**93. Review: Fluorescence Optical Sensors in Analytical Chemistry, O. S. Wolfbeis; *Trends Anal. Chem.* **4** (1985) 184-188. DOI: 10.1016/0165-9936(85)88027-4**

**Abstract.** Recent advances in fluorescence spectroscopy, optical fiber technology, and opto-electronics have led to an exciting new analytical technique called fiber-optical fluorosensing. Optical sensors offer interesting advantages over other sensor types in that they are not subject to electrical interferences, do not require a reference element, and can be quite small. Remote sensing over wide distances is another attractive feature of the method. Working principles and typical fluorosensor representatives are described in some detail. The figure shows the principle of a sensing unit with multiple sensing sites.

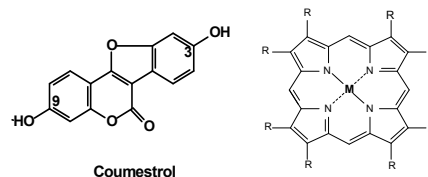




**92. Book Chapter: The Fluorescence of Organic Natural Products, O.**

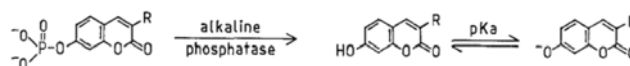
S. Wolfbeis; in: *Molecular Luminescence Spectroscopy: Methods & Applications* (S. G. Schulman, ed.), Wiley & Sons, New York, 1985, vol. 1, chapter 3. ISBN: 0471868485, 9780471868484

Contains chapters on \*Amino acids; \*proteins; \*vitamins and coenzymes; \*oxygen ring compounds, \*alkaloids, \*dyes incl. tetrapyrroles, \*miscellaneous other natural products. Contains numerous spectral and other photophysical data.



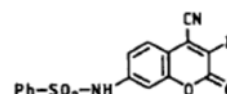
**91. Photometric and Fluorimetric Assay of Alkaline Phosphatase with New Coumarin-Derived Substrates, O. S. Wolfbeis and E. Koller, *Microchim. Acta* 85 (1985) 389-395. DOI: 10.1007/BF01201534**

*Abstract.* Two 7-hydroxycoumarin derivs. were tested as substrates for the detn. of alkaline phosphatase. The optimum pH for assays with both substrates was 9.5. Rates of hydrolysis of the substrates were relatively high (1.5 - 1.8 nmol/min) when detd. by either spectro-photometry or fluorometry, although the sensitivity of the fluorometric assay was higher ( $1 \times 10^{-5}$  units/mL, vs.  $5 \times 10^{-4}$  units/mL for the photometric assay).



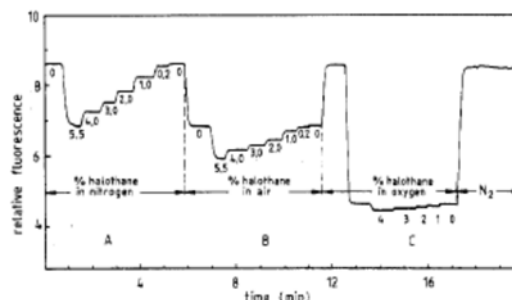
**90. Synthesis and Spectral Properties of 7-(N-Arylsulfonyl)-aminocoumarins, a New Class of Fluorescent pH Indicators, O. S. Wolfbeis and J. H. Baustert, *J. Heterocyclic Chem.* 22, 1215-1218 (1985). DOI: 10.1002/jhet.5570220514**

*Abstract.* Coumarins were prepd. by condensation of benzaldehydes with  $\text{CH}_2$ -active compounds, and oxidative cyanation gave the corresponding 4-cyano derivatives. They showed bright blue fluorescence in org. or acidic aq. soln., which was shifted to green in alkaline solution.



**89. Fiber Optical Fluorosensor for Determination of Halothane and/or Oxygen, O. S. Wolfbeis, H. E. Posch, H. Kroneis, *Anal. Chem. (Wash.)* 57, 2556-2561 (1985). DOI: 10.1021/ac00290a028**

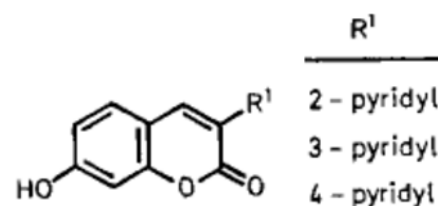
*Abstract.* A fiber optical fluorescence sensor for the inhalation narcotic halothane in the presence of varying concentrations of oxygen is presented. It is based on dynamic fluorescence quenching and consists of a highly halothane-sensitive indicator layer exposed to the sample. Interferences by molecular oxygen are taken into account by a second, poly(tetrafluoroethylene)-covered fluorescent indicator layer highly sensitive toward oxygen. Halothane concentrations can be calculated with the help of an extended Stern-Volmer relation. The two-sensor technique presented here allows the determination of halothane, or oxygen, or both with a precision of  $\pm 5\%$  for halothane and  $\pm 3.5\%$  for oxygen. The probe is practically specific for the two analytes, since other gases present in inhalation gases or blood (including carbon monoxide, dinitrogen monoxide, or fluorans) do not interfere. The graph shows the quenching of the fluorescence of decacyclene in silicone rubber by halothane and oxygen. Range (A): halothane in pure nitrogen; (B): halothane in air; (C): halothane in oxygen.



**88. Syntheses, Absorption and Fluorescence Spectra of 7-Hydroxy-3-pyridylcoumarins, their Esters, Ethers, and Quaternized Derivatives. O.**

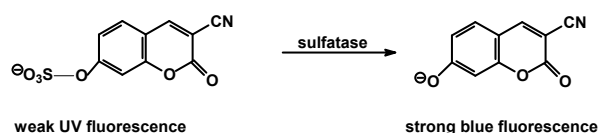
S. Wolfbeis, H. Marhold, *Chem. Ber.* 118 (1985) 3664-3672. DOI: 10.1002/cber.198511809

*Abstract.* The title coumarins were prepd. by condensation of 2-hydroxy-4-methoxybenzaldehyde with pyridylacetic compds. followed by methyl ether cleavage. Its acetates, propionates, and methiodides were also obtained. The absorption and fluorescence spectra in MeOH and water of different pH values were presented, and effects of substituents on spectra and  $\text{pK}_a$  values were discussed.



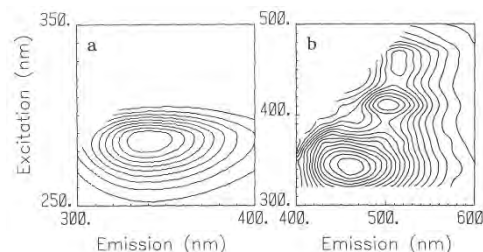
**87. Continuous Kinetic Assay of Arylsulfatases with New Chromogenic and Fluorogenic Substrates, E. Koller, O.S. Wolfbeis; *Anal. Chim. Acta* 170, 73-80 (1985). DOI: 10.1016/S0003-2670(00)81727-4**

*Abstract.* Arylsulfatases can be detd., even in weakly acidic soln., by a direct and continuous kinetic method using new coumarin-derived sulfates as substrates. After enzymic hydrolysis, the substrate dissociates to form intensely colored and strongly fluorescent phenolates, with absorption maxima from 383 - 497 nm and fluorescence emission maxima of 470 - 577 nm.



**86. Mapping of the Total Fluorescence of Human Blood Serum as a New Method for its Characterization, O. S. Wolfbeis, M. Leiner, *Anal. Chim. Acta* 167 (1985) 203-215. DOI: 10.1016/S0003-2670(00)84422-0**

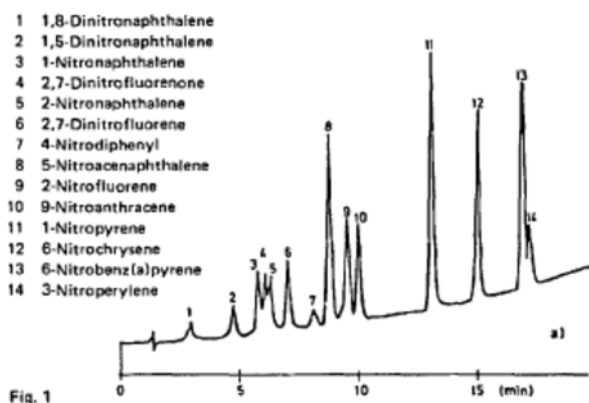
**Abstract.** The total fluorescence spectrum of human serum was acquired at various excitation and emission wavelengths, and is presented in topographic form. The main fluorescent species have tentatively been identified by comparison with literature data as tryptophan, NAD(P)H, pyridoxic acid lactone, pyridoxal phosphate Schiff base, and protein-bound bilirubin. The effect of pH on the fluorescence of the most prominent components and on the pattern of the map is described. Because both the locations of the peaks and their relative intensities are sensitive to deviations from the normal status of human serum, measurement of total fluorescence spectra is considered to be a potentially useful basis for applications of pattern recognition. The graph shows the total fluorescence of serum in the UV (a; excitation from 250 to 350 nm; emission from 300 to 400 nm), and in the visible (b; excitation from 300 to 500 nm; emission from 400 to 600 nm).



**85. Analysis of Nitro-PAHs in Diesel Exhaust Particle Extracts by Multi-Column HPLC,** W. Lindner, W. Posch, O. S. Wolfbeis, P. Tritthart, *Chromatographia* **20** (1985) 213-218. DOI:

10.1007/BF02259689

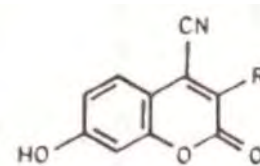
**Abstract:** A method is described for the determination of nitrated polynuclear aromatic hydrocarbons (nitro-PAHs), in particular 1-nitropyrene, in diesel particulate extracts. The method employs a multidimensional HPLC (column switching) technique with final on-line peak identification by UV-VIS spectral comparison with standards. To achieve exceptional chromatographic selectivity for nitro-PAHs, a new pyrene butyric acid amide phase has been prepared which is capable of forming donor-acceptor complexes with them. With this technique it is possible to confirm the presence of 1-nitropyrene in the range 3-100ng/mg on filter-collected diesel soot. Its utility was demonstrated with diesel exhaust extracts spiked with varying levels of 1-nitropyrene and proved to be highly selective.



**84. The Unusually Strong Effect of a 4-Cyano Group on the Electronic Spectra and Dissociation Constants of 3-Substituted 7-Hydroxycoumarins,** O. S. Wolfbeis, E. Koller, P. Hochmuth, *Bull. Chem. Soc. Jpn.* **58** (1985) 731-734. DOI: 10.1246/bcsj.58.731

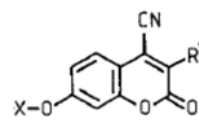
**Abstract:** Synthesis, absorption and fluorescence spectra as well as pKa values of 7-hydroxycoumarins with electron-withdrawing substituents in positions 3 are described. Introduction of a 4-cyano group is achieved by oxidative cyanation of coumarins using potassium cyanide and elemental bromine. 7-Hydroxycoumarins without a 4-cyano group are useful indicators for measuring physiological pH values due to their intense fluorescences, longwave absorptions and emissions, as well as pKa values of around 7.

The presence of a 4-cyano group gives rise to a dramatic longwave shift in absorption (30-40 nm in methanol) and emission (55-80 nm). In water solution, the fluorescence maxima are at around 570-600 nm, with excitation maxima between 410 and 510 nm, depending on whether the phenol or phenolate species is excited. For all coumarins under investigation, fluorescence is from the anion form even in the pH 2-7 range. This phenomenon is interpreted in terms of excited state dissociation according to the Förster model. The interpretation is corroborated by calculations of the excited state pKa values, which show them to be lower by 4.5-6.4 units than those of the ground state.



**83. Synthesis and Spectral Properties of Longwave Absorbing and Fluorescing Substrates for the Direct Kinetic Assay of Carboxylesterases, Phosphatases, and Sulfatases,** E. Koller, O. S. Wolfbeis; *Monatsh. Chem.* **116** (1985) 65-75. DOI: 10.1007/BF00798280

**Abstract.** Syntheses, absorption and fluorescence properties for a series of new enzyme substrates are described, which are derived from 7-hydroxycoumarins possessing electron-withdrawing substituents in position 3. The new substrates are advantageous over existing ones in that they exhibit longwave absorption and fluorescence maxima as well as large Stokes' shifts. In addition, their pKa values, which are usually between 6.0 and 7.0, allow the direct and continuous kinetic assay of hydrolases such as esterases, phosphatases, and sulfatases.



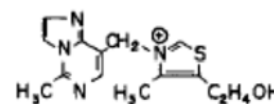
X = fatty acid, sulfate, or phosphate

**82. Acid-Base Titrations Using Fluorescent Indicators and Fiber Optical Light Guides,** O. S. Wolfbeis; *Fresenius' Z. Anal. Chem.* **320** (1985) 271-273. DOI: 10.1007/BF00469585

**Summary.** A report is given on acid-base titrations with fluorescent indicators whose colour changes are followed with the help of fibre optical light guides. Acids as well as bases can be titrated using the almost ideal pH-indicator, 1-hydroxypyrene-3,6,8-trisulphonate. The method offers some principal advantages over electrochemical ones: (a) No reference signals are required; (b) there are no interferences by electrochemical potentials; (c) relatively inexpensive components may be used; (d) solutions harmful to glass electrodes may be titrated as well. The sensitivity of the method towards daylight is a disadvantage, so that titrations have to be performed in diffuse light or, even better, in the dark.

**81. Fluorescence Properties of Ethenothiamine.** O. S. Wolfbeis, G. Uray. *Photochem. Photobiol.* **39** (1984), 111-113. DOI: 10.1111/j.1751-1097.1984.tb03413.x

**Abstract.** The absorption and fluorescence properties of ethenothiamine in neutral and acidic solution are reported, and some are found to be in contradiction to previous findings (Kremer et al.; *Biochemistry* **19** (1980) 5773). It appears that Kremer et al. have measured an optical artifact that results from wavelength-doubling by the grating of the instrument. The low fluorescence quantum yields of ethenothiamine make it a poor substitute for the vitamin in biological systems.

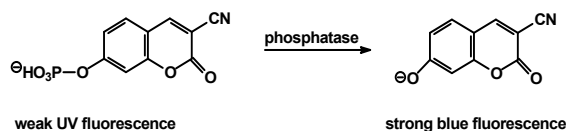


**80. A New Method for the Endpoint Determination in Argentometry Using Halide-Sensitive Fluorescent Indicators and Fiber Optic Light Guides**, O. S. Wolfbeis, P. Hochmuth, *Microchim. Acta* **84** (1984) 129-148. DOI: 10.1007/BF01204164

*Abstract.* Titration of halide solns. with  $\text{AgNO}_3$  in the presence of quinine or acridine in acidic soln. results in a max. in fluorescence intensity at the equiv. point. This effect is due to dynamic fluorescence quenching of the indicators by halide and  $\text{Ag}^+$ , resp. Titrations. of  $\text{Cl}^-$ ,  $\text{Br}^-$ ,  $\text{I}^-$ , and  $\text{SCN}^-$  with  $\text{Ag}^+$ , and of  $\text{Ag(I)}$  with  $\text{Br}^-$  are described, and the effect of varying indicator concentrations is studied.

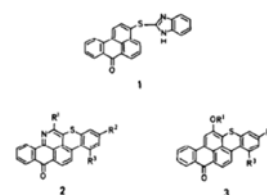
**79. Photometric and Fluorometric Continuous Kinetic Assay of Acid Phosphatases with New Substrates Possessing Longwave Absorption and Emission Maxima**, E. Koller & O.S. Wolfbeis; *Anal. Biochem.* **143**, 146-151 (1984). DOI: 10.1016/0003-2697(84)90569-4

*Abstract.* A direct and continuous kinetic method for the photometric and fluorometric detn. of various acid phosphatases is described. It is based on new coumarin-derived phosphates, which after enzymic hydrolysis undergo disocn. to form intensely colored and strongly fluorescent phenolate anions. The latter have absorption max. of 385- 505 nm, and fluorescence max. of 470-595 nm. The new substrates were compared with respect to their rate of enzymic hydrolysis, optimum pH, and detection limits of acid phosphatase from potato and wheat germ. Detection limits of 0.001 unit/mL were found by photometry, and as low as 0.00006 unit/mL by fluorometry.



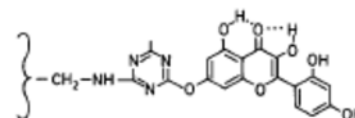
**78. Long Wavelength Fluorescent Indicators for the Determination of Oxygen Partial Pressures**, O. S. Wolfbeis and F. M. Carlini, *Anal. Chim. Acta* **160**, 301-304 (1984). DOI: 10.1016/S0003-2670(00)84535-3

*Abstract.* A series of stable heterocyclic indicators with excitation wavelengths from 469 to 566 and emission wavelengths of 511 to 652 nm allows the fluorometric determination of ca. 1 - 100% partial pressures of oxygen by quenching of fluorescence, especially in toluene solution.



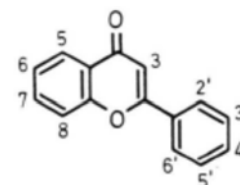
**77. Preconcentration and Semi-Quantitative Determination of Aluminum(III) with Immobilized Morin**, O. S. Wolfbeis and H. Offenbacher, *Fresenius Z. Anal. Chem.* **319**, 282-285 (1984). DOI: 10.1007/BF00487272

*Abstract.* Morin was covalently immobilized onto silica gel via an ether link and other, less suitable methods. The resulting conjugates are able to bind Al ion by both complexation by morin and unspecific cation exchange at active sites of the surface. When these sites are silylated, the conjugates exhibit a "true" binding capacity of 0.5 mg Al ion per g, thus enabling the preconcn. of ppm and sub-ppm solutions of Al(III) ion. Tubes filled with immobilized morin were prepared and are shown to be suitable for the detn. of the ion, as there is a relation between the Al ion concn. of the solution and the length of the fluorescent zone formed.



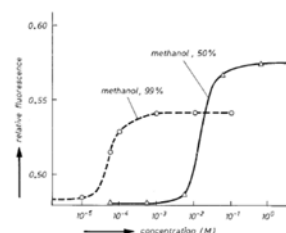
**76. Absorption and Fluorescence Spectra, pK<sub>a</sub>-Values, and Fluorescence Lifetimes of Monohydroxyflavones and Monomethoxyflavones**, O. S. Wolfbeis, M. Leiner, P. Hochmuth, and H. Geiger, *Ber. Bunsenges. Phys. Chem.* **88**, 759-767 (1984).

*Abstract.* The absorption and fluorescence spectra as well as the decay times of all isomeric hydroxyflavones and methoxyflavones, except for the photolabile 3-methoxyflavone, have been measured in org. solvents and in aq. solns. of various acidity. With the exception of 5-hydroxyflavone, all are fluorescent in methanol and water soln. On the other hand, there is virtually no fluorescence observed in cyclohexane soln., a fact that is interpreted in terms of high intersystem crossing rates and the El-Sayed selection rules.



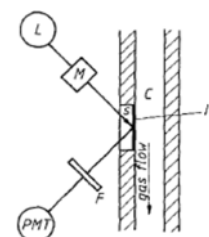
**75. The Effect of Alkali Cation Complexation on the Fluorescence Properties of Crown Ethers**, O. S. Wolfbeis and H. Offenbacher, *Monatsh. Chem.* **115**, 647-654 (1984). DOI: 10.1007/BF00799173

*Abstract.* Alkali metal ion binding leads to changes in the fluorescence intensity along with slight shifts in the spectral maxima of fluorescent crown ethers. The effects are more pronounced in fluorescence than in absorption. Complexation constants were found to strongly depend on the water fraction in the organic solvent.



**74. A Fast Responding Fluorescence Sensor for Oxygen**, O. S. Wolfbeis, H. Offenbacher, H. Kroneis, H. Marsoner, *Microchim. Acta* **82** (1984) 153-158. DOI: 10.1007/BF01202170

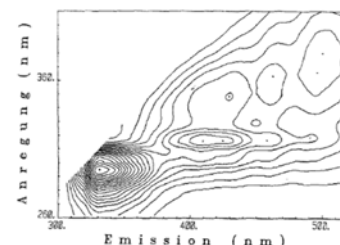
*Abstract.* The sensor is based on the dynamic quenching of the fluorescence of covalently immobilized pyrenebutyric acid. Porous glass in combination with conventional glass is used as a solid support. The main advantages of this sensor include fast response time (<50 ms), a good spectral separation of excitation and emission maxima, and an acceptable long-term stability. The Fig. shows the geometric arrangement of the sensing unit for continuous sensing of oxygen. L, light source; M, monochromator (or optical filter); S, solid glass support; IL, sensing layer with immobilized indicator; F, secondary filter; PMT, photomultiplier tube; C, flow-through cell with gas flow.





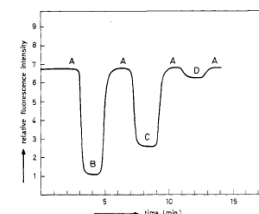
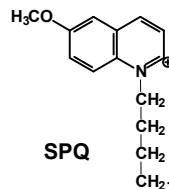
**73. Characterization of Edible Oils via Fluorescence Topography, O. S. Wolfbeis, M. Leiner, *Microchim. Acta* 82 (1984) 221-233. DOI: 10.1007/BF01202914**

*Abstract.* Four types of edible oils were characterized by their total fluorescence which is presented in three-dimensional form and as contour plots ("fluorescence topograms"). The most important contributions to the total emission stem from vitamins E, parinaric acid, and certain chlorophylls. All oils display characteristic topograms, whose curve patterns are distinctly different. In combination with cluster-analytical procedures, the method is thought to be a useful new pattern recognition method in food analysis. It can provide informations on both the type of the oil and the way of its preparation.



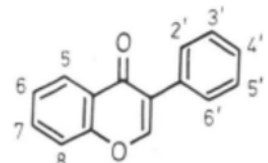
**72. Optical Sensor for Continuous Determination of Halides, E. Urbano, H. Offenbacher, O. S. Wolfbeis; *Anal. Chem. (Wash.)* 56, 427-429 (1984). DOI: 10.1021/ac00267a029**

*Abstract.* The first optical sensor for halides and pseudohalides is based on dynamic fluorescence quenching of acridinium and quinolinium indicators, which were immobilized via spacer groups onto a glass surface. The sensors are capable of indicating the concentration of halides in solution by virtue of the decrease in fluorescence intensity due to the quenching process. The method is increasingly sensitive on going from chloride to bromide to iodide. The left figure shows the chemical formula of the probe sulfoporopyl-quinolinium, and the right figure the signal change, response time, and reproducibility of a sensor to aqueous solutions of (A) pure water, (B) 0.1 M potassium iodide; (C) 0.1 M potassium bromide; (D) 0.1 M potassium chloride.



**71. Absorption and Fluorescence of Isoflavones and the Effect of Shift Reagents, O. S. Wolfbeis, E. Fuerlinger, H. C. Jha, F. Zilliken, *Z. Naturforsch.* 39B (1984) 238-243. DOI: 10.1515/znb-1984-0220**

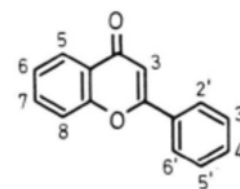
*Abstract.* The absorption and fluorescence maxima of 20 isoflavones have been determined in methanol solution and the effect of addition of water, 50% sulfuric acid, aluminium trichloride, borax, sodium acetate, ammonia and sodium hydroxide has been studied. The following findings may be useful in the structure elucidation of naturally occurring isoflavones: (a) 5-Hydroxyisoflavones have band I absorption maxima around 335 nm. 6-hydroxyisoflavones between 310 and 330 nm, and others below 310 nm. (b) Addition of water produces practically no shift in the absorption spectra, but - unlike other hydroxyisoflavones - can give distinctly longwave shifted new fluorescence bands with 7-hydroxyisoflavones. (c) Addition of sodium acetate gives rise to anion absorption of 7-hydroxyisoflavones and to partial anion absorption of 6-hydroxyisoflavones; the spectral maxima of 5-hydroxyisoflavones remain practically unchanged, (d) Ammonia gives rise to anion absorption of both 6- and 7-hydroxyisoflavones, but not of the 5-hydroxy isomers. (e) Sodium borate is a useful reagent to identify 6,7-dihydroxyisoflavones by virtue of its ability to form a chelate complex with an absorption maximum that is different from the anion absorption, (f) Aluminium trichloride forms complexes with both 5-hydroxy- and 6,7-dihydroxyisoflavones with distinct absorption maxima, (g) 5,7-Dihydroxyisoflavones may be recognized by addition of ammonia, which does not result in a longwave shift, but rather in an intensification of the longwave absorption band, (h) 6-Hydroxyisoflavones can be differentiated from the 7-hydroxy isomers by their longwave shifts (40-60 nm) following addition of ammonia. The respective shifts of the 7-hydroxy isomers are smaller, (i) 5-Hydroxyisoflavones are practically non-fluorescent. while others have fairly strong fluorescences, (j) The absorption and fluorescence maxima of isoflavones give unique combinations which may be useful in their identification, (k) Addition of aluminium chloride makes the non-fluorescent 5-hydroxyisoflavones fluorescent. (l) As in the case of absorption, 6,7-dihydroxyisoflavones form complexes with borate possessing fluorescence bands with maxima different from those of the anion bands.



Chemical Structure of Isoflavone

**70. Fluorescence Properties of Hydroxy- and Methoxyflavones and the Effect of Shift Reagents, O. S. Wolfbeis, M. Begum, H. Geiger, *Z. Naturforsch.* 39B (1984) 231-237. DOI: 10.1515/znb-1984-0219**

*Abstract.* The fluorescence spectra of 42 hydroxy- and methoxyflavones in methanol solution have been investigated. The following findings are considered to be useful in structure elucidation and identification of flavonoids: (a) The maxima of the absorption and fluorescence bands give, in most cases, a unique combination; (b) flavones exhibit exceptionally large Stokes' shifts (6,800 to 10,000 cm<sup>-1</sup>); (c) most flavones fluoresce blue, but flavonols fluoresce yellow or green; the fluorescence of flavonols consists frequently of two bands; (d) fluorescence is zero or very weak for 5-hydroxyflavones; (e) 5-hydroxyflavones become increasingly fluorescent with an increasing number of oxygen functions being present in the molecule; a 3-hydroxy group has a particular beneficial effect; (f) hydroxyflavones fluoresce less intense than the corresponding methoxyflavones; (g) fluorescence intensity is distinctly higher in polar protic than in apolar solvents. The effects of three groups of shift reagents on the spectra has also been investigated. The first group involves water, 10% and 50% sulphuric acid. The second group consists of basic reagents (sodium acetate, sodium hydrogen carbonate and sodium carbonate), and the third group of complexing reagents such as aluminium trichloride, borax and magnesium sulphate. The following generalisations may be made: (a) Water causes a bathochromic shift in emission with 7-hydroxyflavones, but a hypsochromic shift with flavonols; (b) 50% sulphuric acid is able to protonate (and thus to longwave-shift the emission maximum) of all flavones except for the 3-, 5-, and 8-hydroxy isomers; (c) sodium acetate and hydrogen carbonate cause characteristic shifts with 7-hydroxyflavones and, occasionally, with 4'-hydroxyflavones lacking a 7-hydroxy group; (d) aluminum trichloride produces a longwave shift and an enormous increase in fluorescence intensity with flavonols; (e) borax can be used to detect sensitively the presence of a 3',4'-dihydroxy group.



Chemical Structure of Flavone

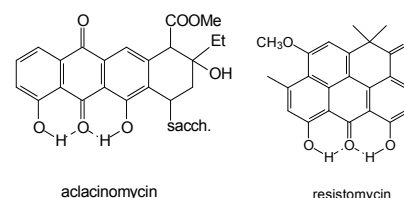
**68. Fluorescence Quenching Method for Determination of Two or Three Components in Solution, O. S. Wolfbeis and E. Urbano, *Anal. Chem.* 55, 1904-1906 (1983). DOI: 10.1021/ac00262a016**

*Abstract.* The Stern-Volmer equation is extended for cases of 2 or more dynamic quenchers in one solution. The determination of  $n$  quenchers requires  $n$  indicators whose Stern-Volmer constants have to be different. The concentration of  $n$  quenchers can be computed by solving an  $n \times n$  matrix. The validity of the equations is shown by the precise fluorometric detection of Cl<sup>-</sup> and Br<sup>-</sup> in an organic material after combustion and by the detection of Cl<sup>-</sup>, Br<sup>-</sup>, and I<sup>-</sup> in a synthetic mixture. The method can be generally applicable for quantifying a variety of dynamic quenchers (ions as well as neutral molecules), if they act independently. Specific indicators are no longer necessary.

$$\begin{pmatrix} \alpha \\ \beta \\ \gamma \end{pmatrix} = \begin{pmatrix} {}^1K_a & {}^2K_a & {}^3K_a \\ {}^1K_b & {}^2K_b & {}^3K_b \\ {}^1K_c & {}^2K_c & {}^3K_c \end{pmatrix} \begin{pmatrix} [Q_1] \\ [Q_2] \\ [Q_3] \end{pmatrix}$$

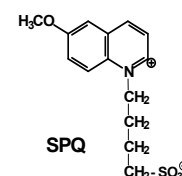
**67. Absorption, Fluorescence, and Fluorimetric Detection Limits of Naturally Occurring Quinoid Antibiotics, O. S. Wolfbeis and E. Furlinger, *Microchim. Acta* 81 (1983) 385-398. DOI: 10.1007/BF01196722**

*Abstract.* Aclacinomycin, cercosporin, chrysomycin A, elsinochrome A, isocercosporine, javanicine, lachnanthocarpon, phleiochrome and resistomycin possess native fluorescence which can be used for their fluorometric assays. Absorption, excitation, and emission max. in org. solvents are reported and the effect of addn. of AlCl<sub>3</sub> is studied. The spectra of some antibiotics were pH-dependent. Detection limits range are 5-200 ng/mL in org. or aq. solns., and 5 - 40 ng in H<sub>2</sub>SO<sub>4</sub>.



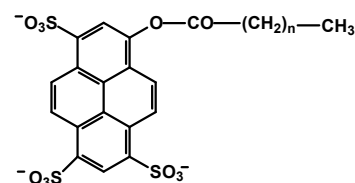
**66. A Fluorimetric Method for Analysis of Chlorine, Bromine and Iodine in Organic Materials, O. S. Wolfbeis und E. Urbano, *Fresenius Z. Anal. Chem.* 314, 577-581 (1983). DOI: 10.1007/BF00474851**

*Abstract.* A fluorometric method for determination of Cl, Br, and I is based on quenching of the fluorescence of certain indicators (quinine, 6-methoxyquinoline, acridine, and their derivatives.). The halide ions, formed by combustion of org. halide-containing material according to Schoeniger's procedure, decrease the fluorescence intensity of the indicator. At low halide concentration the quenching obeys the Stern-Volmer law. The method is increasingly sensitive on going from Cl to I. It is suitable for compds. contg. >1% halide. Advantages of the method include (a) a high sensitivity for Br and, esp. I; (b) the lack of a titrimetric procedure; (c) the possibility for automation. The formula shows the chemical structure of sulfopropyl-6-methoxyquinoline which has experienced considerable interest in the past as a chloride-sensitive bioprobe.



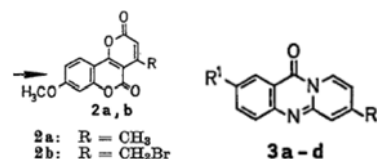
**65. Fluorimetric Assay of Hydrolases at Longwave Excitation and Emission Wavelength with New Substrates Possessing Unique Water Solubility, O. S. Wolfbeis and E. Koller, *Anal. Biochem.* 129, 365-370 (1983). DOI: 10.1016/0003-2697(83)90563-8**

*Abstract.* A direct kinetic fluorometric assay of various hydrolases is described based on new, highly water-sol. substrates. The latter consist of esters of strongly fluorescent 1-hydroxypyrene-3,6,8-trisulfonic acid trisodium salt with acetic, butyric, caprylic, and oleic acids. The K<sub>m</sub> and V<sub>max</sub> values are given for the hydrolytic activity of various esterases, lipases, acylase I, and chymotrypsin. The figure shows the chemical structure of the type of the virtually nonfluorescent enzyme substrates used. They are converted into strongly green fluorescent products by esterases.



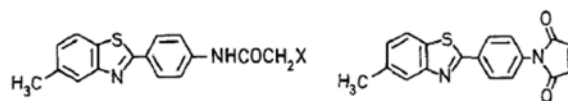
**64. Two New Reagents for the Fluorescence Derivatization of NH- and OH-Containing Compounds, R. Wintersteiger, O. S. Wolfbeis; *Z. Naturforsch.* 38B (1983) 248-250. DOI: 10.1515/znb-1983-0223**

*Abstract:* The synthesis of three new reagents, namely the bromomethyl derivatives of a pyrano-[3,2-c]benzopyran (2b) and of 11H-pyrido[1,2-b]quinazolin-11-one (3b, d) is described. Introduction of the reactive bromomethyl group was accomplished in one case (2 b) by a ring closure reaction using ethyl  $\gamma$ -chloroacetoacetate, and in the other cases (3 b, d) by bromination of a methyl group using N-bromosuccinimide. 2 b is suitable for the derivatization of barbiturates, whilst 3d reacts with oxygen nucleophiles like alcohols, phenols or carboxylates.



**63. Synthesis of New Reagents for the Fluorescence Derivatization of Thiols and Alcohols, O. S. Wolfbeis, H. Marhold, *Monatsh. Chem.* 114 (1983) 599-604. DOI: 10.1007/BF00798615**

*Abstract.* The synthesis of two selective thiol derivatisation reagents is described, starting from readily available 2-(4-aminophenyl)-6-methyl-benzo-thiazole. The respective isocyanate, being a known alcohol derivatisation reagent, is obtained from I in a two step synthesis, in which the usual isocyanate synthesis using phosgen is avoided.

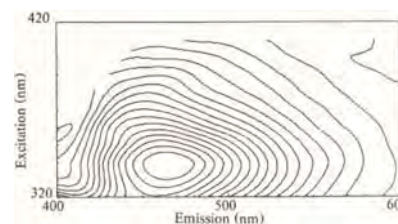


**62. IR-, UV- and Fluorescence Spectroscopic Properties of Flavonoid Complexes (= IR-, UV- und fluoreszenzspektroskopische Eigenschaften von Flavonoid-Komplexen). A. Hiermann, O. S. Wolfbeis, Th. Kartig, M. Begum, *Arch. Pharm. (Weinheim)* 316 (1983) 995-1000. In German. DOI: 10.1002/ardp.19833161205**

*Abstract:* The complexes of Ca(II), Mg(II) and Zn(II) with 3-hydroxy-, 5-hydroxy- and 3',4'-dihydroxyflavone were investigated by means of IR, UV and fluorescence spectroscopy. The infrared spectra of the flavonoids adsorbed onto CaO, MgO and ZnO were found to be identical with those of the respective metal complexes that were obtained synthetically. The effect of pH on the UV and fluorescence spectra also was studied.

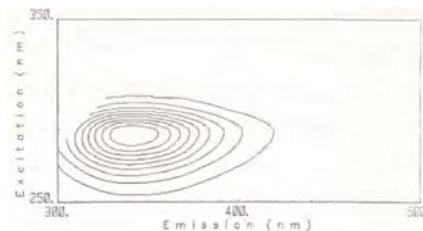
**61. Visible 3D Fluorescence of Rat Sera, and Cluster Analysis of Fluorescence Parameters of Sera of Yoshida Ascites Hepatoma-Bearing Rats, M. Leiner, R. J. Schaur, O. S. Wolfbeis, H. M. Tillian, *IRCS Med. Sci. - Biochem.* 11 (1983) 841-842.**

*Abstract:* In this paper we report on visible fluorescence topograms of serum of healthy rats and on a cluster analysis for the operator-independent differentiation between Yoshida hepatoma-bearing and tumour free rats by means of three UV and visible topogram parameters. Difference spectra of Trp fluorescence of these sera are also shown.



**60. Ultraviolet 3D Fluorescence of Rat Sera, and Decrease of Tryptophan Fluorescence in Yoshida Ascites Hepatoma-Bearing Rats, M. Leiner, O. S. Wolfbeis, R. J. Schaur, H. M. Tillian, *IRCS Med. Sci. - Biochem.* 11 (1983) 675-676.**

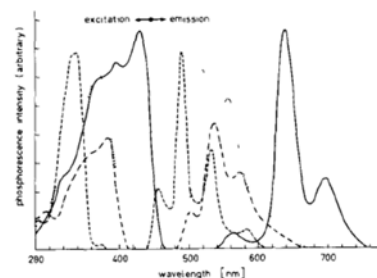
Serum is composed of a variety of substances, but only a few of them contribute to the overall fluorescence emission. In the UV part the emission is almost exclusively due to tryptophan (Trp). Even when tyrosine is electronically excited, fluorescence will be observed from Trp due to intramolecular energy transfer in proteins (1). The total emission of a complex mixture such as serum can be represented best by an excitation-emission-matrix (EEM) (2). Basically, the EEM is the representation of a three-dimensional plot of the emission wavelength  $\lambda_2$ , (usually the x-axis) versus the excitation wavelength  $\lambda_1$  (the y-axis) versus the fluorescence intensity at the given excitation-emission wavelength combination (z-axis). The contour plots are obtained by connecting z-values of the same intensity ("isohypses"). We refer to this kind of representation as a fluorescence topogram. It has been shown by conventional fluorimetry (3), that sera of tumour-bearing rats suffer changes in both fluorescence intensity and emission maximum of Trp. Here we present the total UV fluorescence of a representative series of normal rat sera and the changes thereof as a result of the growth of the rapidly growing Yoshida AH 130 ascites hepatoma. The hypothesis was examined that any deviation of the fluorescence intensity is associated with a change in the albumin concentration, since hypoalbuminemia is a frequent phenomenon in tumour-bearing hosts (4).



**59. Phosphorescence Spectra and Detection Limits of Nitrated Polynuclear Aromatic Hydrocarbons**, O. S. Wolfbeis, W. Posch, G. Guebitz, P. Tritthart, *Anal. Chim. Acta* **147** (1983) 405-410. DOI: 10.1016/0003-2670(83)80113-5

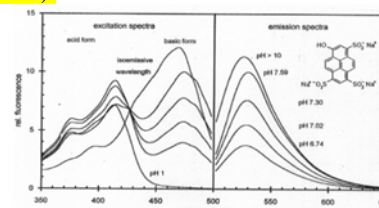
*Abstract.* Nitrated polycyclic aromatic hydrocarbons (NPAHs) can be found in exhaust gases of (diesel) engines and therefore selective detection is needed. It is shown that NPAHs display strong and analytically useful phosphorescence at 77 °C.

The Fig. shows the phosphorescence spectra (excitation and emission) of the four most abundant nitro-PAHs: (---) 1-nitropyrene; (-----) 9-nitroanthracene; (-.-.-.-) 5-nitroacenaphthene; (. . . . .) 1-nitronaphthalene.



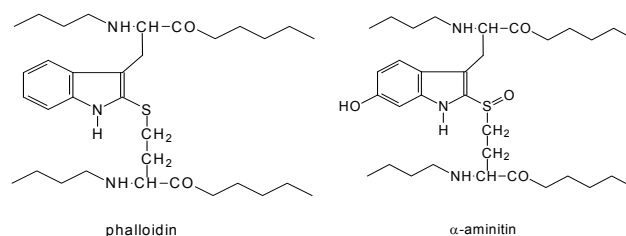
**58. A Study on Fluorescent Indicators for Measuring Near-Neutral ("Physiological") pH Values**, O. S. Wolfbeis, E. Furlinger, H. Kroneis, and H. Marsoner, *Fresenius' Z. Anal. Chem.* **314**, 119-124 (1983). DOI: 0.1007/BF00482235

*Abstract.* Fluorescence max. and  $pK_a$  values of 28 potential indicators are presented in detail, and other data (fluorescence quantum yields, soly., and stability) are given qual. Indicators are divided into groups A and B. Group A compounds exhibit their most long-wave absorption and most intense fluorescence in acidic soln. Group B indicators exhibit their most long-wave absorption and most intense fluorescence in basic soln. As a result of its stability, water solubility, long-wave excitation maximum and large Stokes' shift, HPTS appears to be the pH indicator of choice.



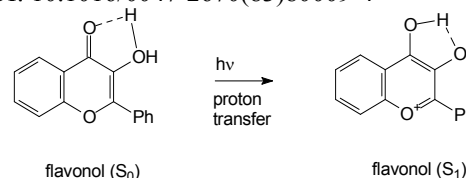
**57. The Absorption, Fluorescence, and Phosphorescence of Phalloidin and alpha-Amanitin**, E. Furlinger & O.S. Wolfbeis; *Biochim. Biophys. Acta* **760**, 411-414 (1983). DOI: 10.1016/0304-4165(83)90382-3

*Abstract.* The peptides phalloidin and amanitin contain two unusual indole-derived chromophores, whose absorption, fluorescence, and phosphorescence in aq. solutions are described. Fluorescence is very weak, but phosphorescence at 77 K is intense. Phalloidin appears to undergo adiabatic photo-dissociation in alkaline solns. and to fluoresce from the indole anion form. In contrast, neither the phenolic nor the indolic protons of amanitin underwent photodissociation.



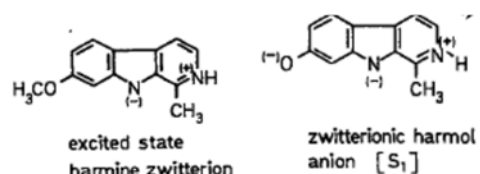
**56. First Excited Singlet State Dissociation Constants, Phototautomerism, and Dual Fluorescence of Flavonol**, O. S. Wolfbeis, A. Knierzinger, and R. Schipfer, *J. Photochem.* **21**, 67-79 (1983). DOI: 10.1016/0047-2670(83)80009-4

*Abstract.* Flavonol fluoresces from four excited state species, the anion A, the neutral mol. N, the cation C and a phototautomer. Two excited state  $pK_a$  values that govern the A-N-C equilibria were established using the Foerster-Weller equation. Fluorescence quantum yields are low, but intersystem crossing was not a major competitive deactivation path for the S1 state owing to the lack of phosphorescence. The long wavelength (green) emission) of flavonol in neutral aq. and org. solvents results from an excited state phototautomer. This conclusion is based on the concn. independence of the relative band intensities, the results of IR studies and the kinetic deuteration effects in neutral and acid solutions.



**55. The pH-Dependence of the Absorption and Fluorescence Spectra of Harmine and Harmol: Drastic Difference in the Tautomeric Equilibria of Ground and First Excited Singlet State**, O. S. Wolfbeis and E. Furlinger, *Z. Phys. Chem., Neue Folge* **129**, 171-183 (1982). DOI: 10.1524/zpch.1982.129.2.171

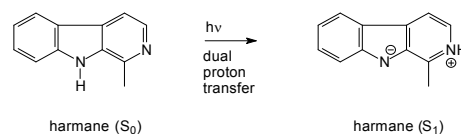
*Abstract.* Three species of the alkaloid harmine are obvious in absorption, and 4 in fluorescence. Three  $pK_a$ 's governing the ground state equil. were determined by spectrophotometry. The excited state  $pK_a$  values were calculated by applying the Förster equation and were compared with the values obtained by fluorescence titration. Harmine is shown by comparison of its spectra with those of model compds. to form an excited state zwitterion by adiabatic proton transfer during the lifetime of the S1-state. Harmol, on the other hand, forms 4 different ground state species depending upon the pH of the solution.



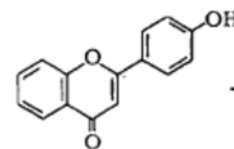


**54. Solvent and pH-Dependence of the Absorption and Fluorescence Spectra of Harmane: Detection of Three Ground State and Four Excited State Species,** O. S. Wolfbeis, E. Furlinger, and R. Wintersteiger, *Monatsh. Chem.* **113**, 509-517 (1982). DOI: 10.1007/BF0079926

*Abstract.* The pH-dependence of the absorption and fluorescence spectra of the alkaloid harmane was investigated. Three species (the cation, the neutral mol. and the anion) were found in absorption, while four species, specifically the cation, the neutral mol., the anion and the zwitterion were detected by fluorimetry. The zwitterion must be formed by a double proton transfer during lifetime of the excited state. Unlike quinine sulfate the fluorescence of harman cation is not quenched by chloride ion, which suggests its use as a standard superior to quinine.

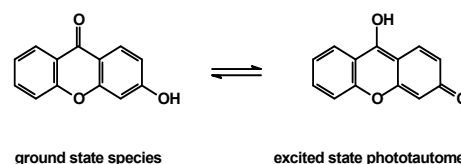


**53. Absorption and Fluorescence Spectra and Dissociations Constants in the Ground State and First Excited Singlet State of 4'-Hydroxyflavone and 4'-Methoxyflavone (= Absorptions und Fluoreszenzspektren sowie Dissoziationskonstanten der Grund- und ersten angeregten Singulettzustände von 4'-Hydroxyflavon und 4'-Methoxyflavon).** O. S. Wolfbeis, R. Schipfer, *Ber. Bunsenges. Phys. Chem.* **86** (1982) 237-241. In German. DOI: 10.1002/bbpc.19820860312



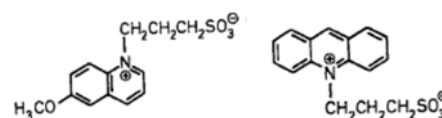
**52. Detection of an Unusual Excited State Species of 3-Hydroxyxanthone.** O. S. Wolfbeis & E. Furlinger, *J. Am. Chem. Soc.* **104**, 4069-4072 (1982). DOI: 10.1021/ja00379a005.

*Abstract.* The solvent and acidity dependence of the absorption and fluorescence spectra of 3-hydroxyxanthone and 3-methoxyxanthone were studied. 3-Hydroxy-xanthone undergoes adiabatic photodissociation in aq. pH 7-2 soln. An unusual species was detected in the pH to H<sub>0</sub> -2 acidity range, which is characterized by its long-wave emission. This species is assumed to be a phototautomer or an exciplex, formed by proton transfer during the lifetime of the excited singlet state.



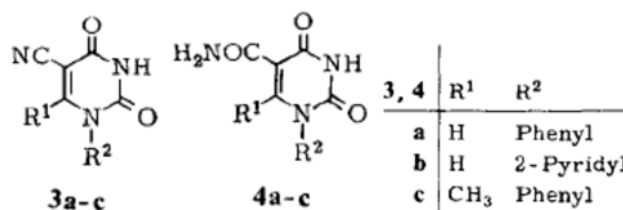
**51. Standards for Fluorescence Measurements in the Near Neutral pH-Range.** O. S. Wolfbeis, E. Urbano, *J. Heterocyclic Chem.* **19** (1982) 841-843. DOI: 10.1002/jhet.5570190427.

*Abstract.* Highly fluorescent cationic indicators were obtained by reaction of heterocyclic nitrogen bases with 1,3-propane sultone. Unlike the fluorescence of quinine or acridine, the fluorescence of sulfopropylquinoline (SPQ) and sulfopropylacridine (SPA) is virtually pH-independent which makes them useful reference fluorophores. Emission wavelengths cover the range from 400 to 530 nm. Lifetimes can be specifically adjusted by adding halides as a quencher.



**50. Synthesis of 1-Substituted 5-Cyanuraciles (= Eine Synthese 1-substituierter 5-Cyanuracile).** O. S. Wolfbeis; *Liebig's Ann. Chem.* **1982** (1982) 182-185. In German. DOI: 10.1002/jlac.198219820118

*Abstract:* Condensation of cyanoacetylurea with aniline and trimethoxymethane affords (3-anilino-2-cyanoacryloyl)urea, which thermally cyclizes to form strongly fluorescent 5-cyano-1-phenyluracil (3a). By using 2-aminopyridine or trimethoxyethane, other uracils (3b, c) are obtained. 3a-c are hydrolyzed to yield the carboxamides 4a-c. UV and fluorescence data are given for compounds 3 and 4.

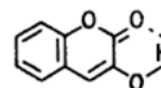


**49. Preparation of Pyrono-condensed Pyrones and Pyridones by Applying the Kappe-Mayer Modification of the von Pechmann-Reaction (= Darstellung pyronokondensierter 2-Pyridone, Cumarine, 2-(1H)-Chinolone mit Hilfe der Kappe-Mayer-Variante der von-Pechmann-Reaktion),** O. S. Wolfbeis; *Monatsh. Chem.* **113** (1982) 365-370. DOI: 10.1007/BF00799563

**48. Method for C-Methylation of cyclic CH-acidic Compounds (= Eine Methode zur C-Methylierung cyclischer CH-acider Verbindungen).** E. Ziegler, O. S. Wolfbeis, I. Trummer, *Z. Naturforsch.* **37B** (1982) 105-107. In German. DOI: 10.1515/znb-1982-0117

**47. Solvent and Acidity Dependence of the Absorption and Fluorescence Spectra of 3-Hydroxycoumarin,** O. S. Wolfbeis; *Z. Phys. Chem., N. F.* **125** (1981) 15-20. DOI: 10.1524/zpch.1981.125.1.015

*Abstract.* Three species of 3-hydroxycoumarin were characterized by their absorption spectra, and two of them (the neutral molecule and the cation) are found to be fluorescent. Ground state pK values were determined for 3-HC (7.16) and its conjugate acid (-3.9). First excited singlet state pK values were calculated using the Förster-Weller equation. The pK values obtained by fluorometry are in complete agreement with ground state data, thus indicating rapid excited state deactivation prior to protolytic



equilibration.

**46. Preparation of Aminomethylene Derivatives of Open-Chain CH<sub>2</sub>-acidic Compounds (= Zur Darstellung von Aminomethylenderivaten offenkettiger CH<sub>2</sub>-acider Verbindungen).** O. S. Wolfbeis; *Chem. Ber.* **114** (1981) 3471-3487. In German. DOI: 10.1002/cber.19811141102

**45. One-Pot Synthesis of 3-Amino-1H-pyrazol-4-carbonitrile (= Eine Eintopfsynthese von 3-Amino-1H-pyrazol-4-carbonitril).** O. S. Wolfbeis; *Monatsh. Chem.* **112** (1981) 875-877. In German. DOI: 10.1007/BF00899789

**44. Chemical Synthesis with Metal Atoms. The Preparation and Structure of (η-5-Cyclo-octa-1,3-dienyl)hydrido-tris(trifluoro-phosphine)-chromium,** J. R. Blackborrow, C. R. Eady, F.-W. Grevels, E. A. Koerner von Gustorf, O. S. Wolfbeis, R. Benn, D. J. Brauer, C. Krueger, P. J. Roberts, and Y.-H. Tsay; *J. Chem. Soc., Dalton Trans.* **1981**, 661-667. DOI: 10.1039/DT9810000661

*Abstract:* The reaction of cyclo-octa-1,5-diene (1,5-cod), PF<sub>3</sub>, and chromium atoms produces [Cr(1,5-cod)(PF<sub>3</sub>)<sub>4</sub>](1) and [Cr(C<sub>8</sub>H<sub>11</sub>)(PF<sub>3</sub>)<sub>3</sub>H](2). The use of 1,3- rather than 1,5-cod produces only (2) under the same conditions. Complex (1) is readily converted into (2) by heating (90 °C, in toluene). The preparation of [Cr(1,5-cod)(CO)<sub>4</sub>](3) from 1,3- or 1,5-cod is also described. The structure of (2) was determined by X-ray crystallography. The compound crystallizes in the orthorhombic space group Pbc<sub>a</sub> with a= 13.452(3), b= 14.419(4), c= 15.268(3)Å, and Z= 8. The final R value was 0.065 9 for 1 699 observed reflections. The structure is retained in solution below -80 °C, but is shown by <sup>13</sup>C and <sup>1</sup>H n.m.r. spectroscopy to become fluxional upon warming. There are two distinct exchange processes; one results in pairwise coalescence of the <sup>13</sup>C and <sup>1</sup>H resonances; the other finally leads to a set of only two <sup>1</sup>H signals with an intensity ratio of 8:4, thus indicating equivalence of the eight ring positions.

**43. An Efficient Synthesis of Aminoalkylidene Derivatives of 5-Membered Active Methylene Compounds (= Eine effiziente Synthese von Aminoalkyliden-Derivaten fünfring-cyclischer methylenaktiver Verbindungen),** O. S. Wolfbeis; *Monatsh. Chem.* **112** (1981) 369-383. In German. DOI: 10.1007/BF00900767

**42. Kinetics of the Formation of Arylaminomethylene Compounds from Triethoxymethane, Arylamines and Methylene-Acidic Compounds in a 3-Component Condensation (= Kinetik der Bildung von Arylaminomethylenverbindungen aus Triethoxymethan, Arylaminen, und methylen-aciden Verbindungen in einer Dreikomponentenkondensation).** G. Uray, O. S. Wolfbeis; *Monatsh. Chem.* **112**(5) (1981) 627-641. In German. DOI: 10.1007/BF00899677

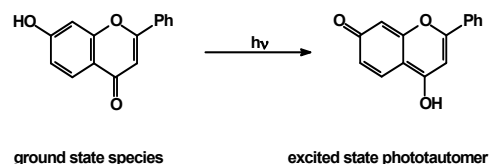
**41. Synthesis of 5-Oxo-5,6,7,8-tetrahydrocoumarins,** I. Trummer, E. Ziegler, O. S. Wolfbeis; *Synthesis* **1981** (03), 225-227. DOI: 10.1055/s-1981-29395

**40. The Rearrangement of Alkoxyethylene- and Aminomethylenehomophthalic Anhydrides to Form Isocoumarines and Isoquinolones (= Über die Umlagerung von Alkoxyethylen- und Aminomethylen-homophthalsäure-anhydriden zu Isocoumarinen bzw. Isochinolonen).** O. S. Wolfbeis; *Liebig's Ann. Chem.* **1981**, 819-827. DOI: 10.1002/jlac.198119810507 In German.

**39. Preparation of 2-Substituted Pyrano(2,3-c)isoquinoline-3,6-diones and Merocyanine Dyes from Homophthalic Acid Imides (= 2-Substituierte Pyrano(2,3-c)isochinolin-3,6-dione und Merocyanin-Farbstoffe aus Homophthalsäure-imiden).** O. S. Wolfbeis, I. Trummer, A. Knierzinger; *Liebig's Ann. Chem.* **1981**, 811-818. In German. DOI: 10.1002/jlac.198119810506.

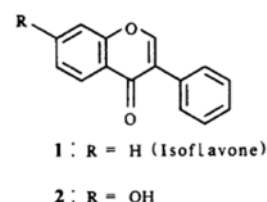
**38. pH-Dependent Fluorescence of Flavone, 7-Hydroxyflavone and 7-Methoxyflavone,** R. Schipfer, O. S. Wolfbeis, A. Knierzinger, *J. Chem. Soc., Perkin Trans. II* **1981**, 1443-1449. DOI: 10.1039/p29810001443.

*Abstract.* The fluorescence of the title flavones was examined as a function of pH. A phototautomer can be identified that has a quite distinct fluorescence emission band with no equivalent in the absorption spectra. Marked D isotope effects on the fluorescence were observed.

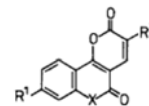


**37. Acidity Dependence of the Absorption and Fluorescence Spectra of Isoflavone and 7-Hydroxyisoflavone,** O. S. Wolfbeis and R. Schipfer, *Photochem. Photobiol.* **34**, 567-571 (1981). DOI: 10.1111/j.1751-1097.1981.tb09043.x

*Abstract.* The dependence of the absorption and fluorescence of isoflavone (formula 1) and 7-hydroxyisoflavone (formula 2) on pH and H<sub>0</sub> values was studied. The pK<sub>a</sub> values of the ground and 1<sup>st</sup> excited-singlet states were detd. spectrophotometrically and fluorimetrically. Excited-state protolytic equilibration processes via a 2<sup>nd</sup>-order reaction are too slow to compete efficiently with fluorescence. However, photodissoc. of hydroxyflavone was faster than its fluorescence decay. It forms a phototautomer or exciplex in the pH 2 to H<sub>0</sub>-1 acidity range, which is characterized by its long-wavelength emission.



36. New 4-Hydroxycoumarins, 4-Hydroxy-2-quinolones, 2H,5H-Pyrano-(3,2-c)-benzopyran-2,5-diones, 2H,5H-Pyrano(3,2-c)-chinolin-2,5-diones, O. S. Wolfbeis, A. Knierzinger, *J. Heterocyclic Chem.* **17** (1980) 225-229. DOI: 10.1002/jhet.5570170204

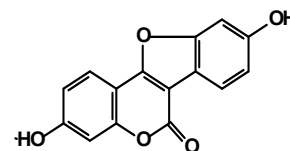


35. A Broadly Applicable Method for the Synthesis of Fluorescent Condensed  $\alpha$ -Pyrone (= Eine breit anwendbare Synthese fluoreszierender kondensierter  $\alpha$ -Pyrone), O. S. Wolfbeis, E. Ziegler, A. Knierzinger, H. Wipfler, I. Trummer, *Monatsh. Chem.* **111** (1980) 93-112. In German. DOI: 10.1007/BF00938720

34. Solvent and Acidity Dependence of the Absorption and Fluorescence of Coumestrol, O. S. Wolfbeis, K. Schaffner, *Photochem. Photobiol.* **32**, 143-148 (1980).

DOI: 10.1111/j.1751-1097.1980.tb04001.x

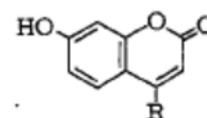
*Abstract.* The UV absorption and fluorescence spectra of the plant estrogen coumestrol are solvent- and pH-dependent. In neutral non-aq. solvent, emission occurred from the uncharged  $1^{st}$  excited singlet state, whereas in aq. soln. 5 species were found. These were characterized by their UV absorption, fluorescence, and ground and excited states pK values, assignments being made by comparison with model compounds.



33. Photochemical Reversible Ring Opening of 4-Phenylumbelliferone, O. S. Wolfbeis, E. Lippert, H. Schwarz, *Ber Bunsenges. Phys. Chem.* **84** (1980) 1115-1119. DOI:

10.1002/bbpc.19800841106

*Abstract.* The title compound (where R = phenyl) undergoes excited state ring opening in aqueous solution, as demonstrated by incorporation of  $^{17}O$  into the compound following irradiation.

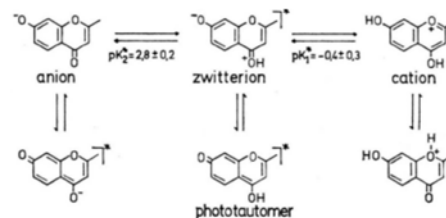


31. Synthesis of Aminomethylen- $\gamma$ -haloacetoacetic Acid Derivatives and Their Ring Closure Reactions to Give 3-hydroxypyrrroles, Pyrido[1,2-a]pyrimidones or 4-quinolones (= Synthesen von Aminomethylen- $\gamma$ -halogenacetessigsäure-Derivaten und deren Ringschluss-Reaktionen zu 3-Hydroxy-pyrrolen, Pyrido(1,2-a)pyrimidonen bzw. 2-Chinolonen). O. S. Wolfbeis, H. Junek; *Monatsh. Chem.* **110** (1979) 1387-1405. In German. DOI: 10.1007/BF00938295

30. Formylation of  $CH_2$ -acidic Compounds via the Anilinomethylene Derivatives, O. S. Wolfbeis, H. Junek; *Z. Naturforsch.* **34B** (1979) 283-289. DOI: 10.1515/znb-1979-0229

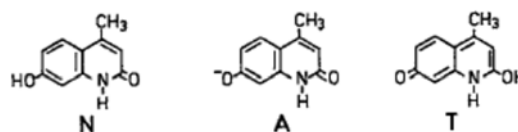
29. pH-Dependent Fluorescence Spectra of Chromone, 2-Methylchromone, and 7-Hydroxy-2-methylchromone, O. S. Wolfbeis & A. Knierzinger, *Z. Naturforsch.* **34A**, 510-515 (1979). DOI:

10.1515/zna-1979-0416 *Abstract.* The absorption and emission spectra of the compounds are studied in the pH 12 to 0 range, and in strong sulfuric acids. Chromone fluoresces from the protonated form and (weakly) from its neutral form. The hydroxychromone fluoresces from the anion, the neutral form, a phototautomer, and from the cation, with strongly varying quantum yields.



23. Multiple Fluorescence of 7-Hydroxylepidone, O. S. Wolfbeis & E. Lippert, *Z. Naturforsch.* **33A**, 238-239 (1978). DOI: 10.1515/zna-1978-0226

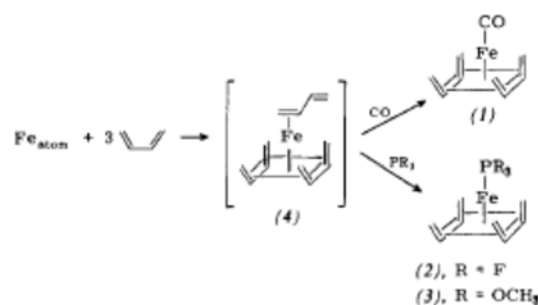
*Abstract.* The title compound (N) undergoes photodissociation in the first excited singlet state to form an anion (A) whose fluorescence is observed even if the undissociated species is excited. At weakly acidic pH values, a phototautomer (T) is formed that has an unusually longwave emission band.



14. Chemical Synthesis with Metal Atoms: The Reaction of Iron with Some Conjugated Dienes. *J. Organomet. Chem.* **111** (1) (1976), pp. C3-C5. DOI:

10.1016/S0022-328X(00)87064-3

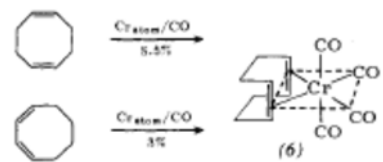
*Abstract:* Complexes have been obtained by the reaction of iron atoms with butadiene or styrene at -196% followed by treatment with ligands such as CO or  $(MeO)_3P$ .





4. **Review: The Laser-Evaporation of Metals and Its Application to Organometallic Synthesis.** E. A. Koerner von Gustorf, O. Jaenicke, O. Wolfbeis, C. R. Eady, *Angew. Chem. Intl. Ed.* **14** (1975) 278-286. DOI: 10.1002/anie.197502781.

*Abstract:* Metal evaporation syntheses of  $[\text{Cr}(\text{C}_7\text{H}_7)(\text{C}_7\text{H}_{10})]$ ,  $[\text{Cr}(\text{C}_7\text{H}_8)(\text{PF}_3)_3]$ , of metal carbonyls, and of some anhydrous metal acetylacetonates are described.



..end